DOCTOR OF SCIENCES

Characterization of the early immune response against intranasal Brucella infection in mice

Demars, Aurore

Award date:
2020

Awarding institution:
University of Namur

Unité de Recherche en Biologie
des Micro-organismes
URBM

Characterization of the early immune response against intranasal *Brucella* infection in mice

Study presented by **Aurore Demars**

In order to obtain the degree of Doctor in Biological Sciences

2020

Jury:

Prof. Arnould T. - University of Namur - Belgium

Dr. Goriely S. - University of Brussels - Belgium

Dr. Gorvel J.-P. - Aix-Marseille University - France

Dr. Romano M. - Sciensano - Belgium

Prof. Van Melderen L. - University of Brussels - Belgium

Promoters:

Prof. De Bolle X. - University of Namur - Belgium

Dr. Muraille E. - University of Brussels - Belgium

« La connaissance des maladies infectieuses enseigne aux hommes qu'ils sont frères et solidaires. Nous sommes frères parce que le même danger nous menace, solidaires parce que la contagion nous vient le plus souvent de nos semblables »

(Charles Nicolle)

« Les moyens à dédier peuvent sembler énormes. Ils sont dérisoires en regard du coût d'une épidémie, voire d'une pandémie. La recherche est le meilleur investissement que nous puissions proposer »

(Philippe Sansonetti)

Summary

Brucellae are alpha-proteobacteria which induce brucellosis, a worldwild zoonotic disease infecting mammals, including humans. *B. melitensis* and *B. abortus* are the species the most often isolated in human brucellosis. Inhalation of airborne agents, ingestion of contaminated products and contact between a contaminated fluid or organ with a cutaneous lesion constitute the main natural routes of transmission. Up to now, no fully efficient prophylactic or therapeutic treatments are available, leading to serious economic losses and public health problems.

Despite recent progress in mouse models of brucellosis, very little is known about the first steps of *Brucella* infection *in vivo*. Here we studied the *Brucella melitensis* 16M strain, that infects goat and sheep, and we investigated the immune response of mice following intraperitoneal (i.p.), intranasal (i.n.) or intradermal (i.d.) infection. The main objectives were to compare (i) the dissemination of bacteria after a primary infection, (2) the immunity required to control a primary infection, (3) the virulence gene essentiality, and (4) the lymphocyte populations indispensable for a secondary infection control. Our results showed that these four parameters are strongly influenced by the route of infection. For example, the dissemination from the local site of infection to the systemic organs is dependent on the amount and the rapidity of bacteria that enter in blood at the same time. The protective immune response after a primary and secondary infections seems dependent on the localization of bacteria (inter- or extra-cellular), the amount of bacteria, and the infected organs. The control of secondary i.p. infection in spleen requires B cells and CD4 T cells, while CD4 T cells or CD8 T cells are sufficient to control a secondary i.n. infection in the same organ. Finally, we showed that *virB*, a virulence gene defined as essential in *in vitro Brucella* model, can be partially dispensable, or even deleterious after i.p or i.d. infections, respectively.

The intranasal model mimics one of the most physiological route of infection. Thus, we chose to deeply study this model. Following intra-nasal infection, the alveolar macrophages are the main (> 95 %) infected cells during the first 48 hours post infection. We used a without a priori approach (RNA sequencing) in order to find new potential genes involved in the early response in alveolar macrophages after *Brucella* infection. Among the 466 genes upregulated in alveolar macrophages, *Acod1* was one of the most interesting candidate. Indeed, itaconate, a Krebs cycle derivate, produced by aconitate decarboxylase1 gene (*Acod1,* also known as *Irg1*), is emerging as a potential immunoregulatory metabolite since few years. This compound, produced mainly

in mitochondria of myeloid cells, is known to have two main roles: an anti-inflammatory one and an anti-bacterial one. In our model of intranasal *Brucella* infection, we observed that the deficiency of *Acod1* does not trigger any inflammation signs in comparison to wild type mice. In contrast, we observed that itaconate inhibits the *in vitro Brucella* growth and that *Acod1* deficiency increase the number of bacteria in the lungs of infected mice. These effects seem *Brucella* isocitrate lyase-dependent in both conditions. The understanding of how itaconate impacts the growth of *Brucella* could allow the development of new therapeutic drug against brucellosis.

List of abbreviations

4-OI	4-octyl itaconate
A.	*Acinetobacter*
Acod1	Aconitate decarboxylase 1
ADEP4	Acyldepsipeptide antibiotic
APC	Antigen presenting cell
ATF	Activating transcription factor
ATG	Autophagy-related protein
B.	*Brucella*
BC	Before Christ
BCR	B cell receptor
BCV	*Brucella*-containing vacuole
BMDM	Bone marrow-derived macrophage
Bta	*Brucella* trimeric autotransporter
CCR	C-C chemokine receptor
CFU	Colony forming units
Clpp	Caseinolytic Mitochondrial Matrix Peptidase Proteolytic
CpG	Cytosine-phosphate-Guanine
CXCL	Chemokine (C-X-C motif) ligand
DAMPs	Damages-associated Molecular Patterns
DETC	Dendritic epidermal T cells
DMI	Dimethyl itaconate
DNA	Deoxyribonucleic acid
E. coli	*Escherichia coli*
EEA1	Early Endosome Antigen 1
ELISA	Enzyme-linked immunosorbent assay
ER	Endoplasmic reticulum
FC	Fold change
FDR	False discovery rate
GALT	Gut-associated lymphoid tissue

GP1	Glycosylphosphatidylinositol
GST	Glutathione
i.d.	Intradermal
i.n.	Intranasal
i.p.	Intraperitoneal
ICL	Isocitrate lyase
IFN	Interferon
Ig	Immunoglobulin
IL	Interleukin
ILC	Innate lymphoid cells
iNOS	Inducible Nitric Oxide Synthase
IRF	Interferon regulatory factors
Irg1	Immunoresponsive gene 1
IκBζ	NFκB inhibitor ζ
JAK	Janus Kinase
KO	Knock-out
L.	*Legionella*
LCV	*Legionella*-containing vacuole
LN	Lymph nodes
LPS	Lipopolysaccharides
M.	*Mycobacterium*
MALT	Mucosa-associated lymphoid tissue
MHC	Major Histocompatibility Complex
mM	Millimolar
MS	Mass spectrometry
MYD88	Myeloid differentiation primary response 88
NF-κB	Nuclear factor κ-light-chain-enhancer of activated B cells
NK	Natural Killer
NLRP3	NOD-like receptor family, pyrin domain containing 3
NO	Nitric oxide
Nrf2 (or NFE2L2)	Nuclear factor (erythroid-derived 2)-like 2

OMP	Outer membrane protein
PAMPs	Pathogen-associated molecular patterns
PD-1	Programmed cell death 1
pH	Potential of hydrogen
PRR	Pattern recognition receptor
PtpA	Serine/threonine-protein phosphatase 2A activator
RNA	Ribonucleic acid
RNA-seq	Ribonucleic acid-sequencing
RNI	Reactive nitrogen intermediates
ROI	Reactive oxygen intermediates
ROS	Reactive oxygen species
S.	*Salmonella*
SDH	Succinate Dehydrogenase
Si	Silencing
SR-A	Scavenger *receptor-A*
STAT	Signal Transducer and Activators of Transcription
T4SS	Type IV secretion system
TAP1	Transporter associated with Antigen Processing 1
T-bet	T-box transcription factor
TCA	Citric acid cycle
TCR	T cell receptor
TGF	*Transforming growth factor*
TH	T helper
TIRAP	Toll-interleukin 1 receptor domain containing adaptor protein
TLR	Toll-like receptor
TNF	Tumor necrosis factor
Tn-seq	Transposon sequencing
Treg	Regulatory T cells
TRSE	Texas Red-*succinimidyl ester*
VirB	Virulence operon
WHO	World Health Organization
Wt	Wild type

Remerciements

Avant de commencer des remerciements plus personnels, j'aimerais évidemment remercier mon jury de thèse : le Pr. T. Arnould, le Dr. S. Goriely, le Dr. J.-P. Gorvel, le Dr. M. Romano, et le Prof. L. Van Melderen pour le temps pris pour lire le manuscrit, pour leurs idées, leurs conseils pour améliorer ce manuscrit, ainsi que pour leur discussion. Un merci supplémentaire pour S. Goriely, M. Romano et L. Van Melderen qui ont également fait partie de mon comité d'accompagnement. Vous avez permis d'aiguiller mon projet de thèse par vos discussions et vos idées.

***

Bien que situées au début de ma thèse, ces quelques lignes sont les dernières que j'écris. Ainsi s'achèvent ces 4 années de thèse, 5 années de travail en URBM, et ces 9 années d'étude à l'UNamur. Quel parcours, que d'émotions et que de souvenirs !

Mes premiers remerciements iront à **Eric**. Merci. A tes côtés j'aurai appris beaucoup de choses, scientifiques bien sûr, mais également à m'organiser, à gérer mon temps, et à aiguiser mon sens critique. Merci pour la liberté que tu m'as laissé, pour ta patience, pour ta grande disponibilité, tes discussions très enrichissantes et le partage de ton expérience. Tu as pour moi de grandes qualités de chef.

Ensuite, merci à toi **Xavier** pour ton accueil au sein de ton équipe, les discussions, ta disponibilité, ton aide et tes conseils. Tes connaissances et ta manière de les transmettre sont une réelle source d'apprentissage. Merci également pour les sorties labos, les soirées URBMiennes à n'en plus finir ! A tous points de vues, Eric et toi aurez été très complémentaires pour m'accompagner tout au long de ma thèse, merci !

Je n'oublie évidemment pas **Jean-Jacques**, mon promoteur de mémoire qui m'aura également suivie les 2 premières années de ma thèse. Je garde de vous de très bons souvenirs de partage et de discussions. Merci pour votre aide, votre grande g***** et votre rire. Vous avez laissé un vide au labo, et je suis très heureuse d'avoir pu travailler avec vous.

Evidemment, mes prochains remerciements sont pour toi **Arnaud** ! J'ai tellement de choses à dire… Merci, merci, merci ! Je suis arrivée en mémoire sans passion particulière pour la

recherche. Je faisais bio pour être prof, et c'est tout. Tes journées déjantées auraient pu me dégouter, mais ça a été tout l'inverse. Je n'ai pas le souvenir de m'être dit une seule fois en me levant « je n'ai pas envie d'aller au labo ». J'ai tout de suite accroché. Merci pour le partage de tes connaissances, pour ta patience, pour ton caractère, pour ton sourire et tes blagues parfois douteuses. Tu as été là pour mes questions, pour partager mes doutes et mes joies. Dans bien des situations tu as eu les bons mots et ce, quand il le fallait. Je te souhaite tout le meilleur dans le présent et le futur, tu le mérites !

Manon, évidemment, ce mémoire n'aurait pas été le même sans toi ! On a formé un joli trio, je n'ai que de bons souvenirs de ces 10 mois partagés. Le BSL-3 était notre deuxième maison, notre repère. Un repère qui heureusement n'est pas équipé de micros… Seules les oreilles de H. auront sifflé. Oups. Ta bonne humeur, ton rire et ta spontanéité sont des éléments qui auront égailler nos journées. Les souris vaches auront été pour moi les plus belles ! Merci pour tout K* !

Merci à toi **Kévin** pour toute ton aide quotidienne, que ça soit pour l'infection de souris, le facs, la gestion de certaines personnes (…) et tout ce dont tu t'es occupé qui ne faisait pas forcément partie de tes attributions. A mes yeux tu seras toujours un URBMien, toujours le premier pour faire la fête !

De mémo tu es passée à collègue. Je suis heureuse d'avoir pu partager ce petit bout de chemin à tes côtés **Eme**. Je sais que tu es capable de grandes choses, il ne te manque plus qu'à y croire aussi. Fais toi confiance ! Je suis sûre que tu géreras ta thèse comme une pro ! Merci pour ton aide précieuse. N'oublie pas de prendre du temps pour toi ;)

Jérôme (Jérôôôôôme), ça a été un réel plaisir de faire un brin de causette chaque matin quand nous étions collègues de bureau, même quand c'était pour parler foot! Merci pour ta bonne humeur, ton optimisme, tes conseils et ton oreille attentive pour les rares fois où j'avais envie de pousser un coup de gueule. Tu es loin d'être le dernier à avoir ta langue dans ta poche, ou à vouloir prolonger une soirée autour d'un (de) verre(ssss). Je te souhaite encore plein de bonnes choses pour la suite, professionnelles et d'ordre privé, avec pourquoi pas un déménagement dans le sud de la France ? PS : n'oublie pas de changer tes protocoles : Caulo doit être centrifugée 3 x 10 min pour un meilleur résultat !

Merci à toute mon équipe d'accueil, la team Xa ! **Pierre**, en tant que seul représentant masculin, tu as le droit aux premiers remerciements. Merci pour ton aide tout au long de ma thèse (surtout informatique !), pour le partage des cookies, pour la découverte du chocolat à la fleur de sel, des mini Marshmallow, des Gayettes et j'en passe ! Des cours prépas à la thèse, en passant par une naissance d'amitié, nous avons encore beaucoup de moments à passer ensemble ! Courage pour la dernière ligne droite ! **Mathilde**, ta gentillesse et ta droiture sont des exemples pour moi ! Tu es une fille en or. Merci pour tout. Par contre, à moi tu ne la feras pas : je sais très bien qu'à minuit le petit démon qui sommeille en toi se réveille, petit démon capable du meilleur comme du pire. J'attends avec impatience nos prochains City Trip et goûters de mamy. **Caro**, qui aurait cru qu'après nos secondaires nous nous serions retrouvées en thèse dans la même équipe ?? Merci pour ton sourire, tes mots toujours justes et ta gentillesse. Je te souhaite le meilleur pour ta thèse et en dehors. Crois-en toi, moi j'y crois ! **Agnès, Angy, Elodie,** merci pour toute l'aide que vous avez pu m'apporter, ainsi que pour les moments de partage passés ensemble. En vous j'ai vu des copains tournesols : toujours face au soleil ! **Vicky**, the last but not least, thank you for everything! I remember at the beginning I did not dare to talk to you. After my internship, I am not sure my English was better, but I discovered a super great girl ! We had the same sense of work, the same motivation and the same crazy schedule. You are an incredibly strong woman, a friend who really cares and I wish you the best ma biche!

Gwen, après nos 5 ans d'étude ensemble, nous voici dans le même labo pour faire notre mémoire. Ton horloge biologique réglée pour tous les vendredis 16h n'aura laissé personne indifférent ! Tu auras mené ta thèse comme une pro. Je ne suis pas sûre que l'étude du cuivre t'aidera lorsque tu travailleras à Pairi Daiza, mais ça c'est une autre histoire… Plus que quelques semaines, courage !

Merci **Pauline** pour la découverte de Just Dance, mais surtout pour les soirées hors labo qui ne s'arrêteront pas avec la thèse, merci **Popo** pour ton aide, ton soutien, ton grain de folie, merci **Patricia** pour tes gentils mots chaque matin, merci **Mathieu** pour la bonne humeur que tu ajoutes à l'URBM et tes coups de gueule toujours bien placés et justes, merci **Françoise** pour le travail dingue que tu fournis pour le labo et donc pour nous tous, et merci à tous les autres !

J'aurai passé 4 années folles et riches en émotion. Je garde d'incroyables souvenirs de ma thèse, tant scientifiques que humains. Les soupers de thèse, les repas de Noël, les fêtes de l'Université,

les beer hours à n'en plus finir, … sont tant d'occasions qui auront soudé nos liens. Vous n'avez pas idée de tous ces bons moments qui resteront gravés en moi. Merci pour tout.

***

Enfin, merci à mes parents qui m'auront permis d'entreprendre des études. Tout ça n'aurait pas été possible sans vous. Merci à ma famille de manière plus générale pour votre soutien. Il y a certaines périodes où ce soutien comptait énormément et aidait beaucoup ! Merci pour votre compréhension quand je ratais certains événements parce que je devais travailler. Merci Papy pour ton intérêt pour la brucellose. Merci aux amis qui se reconnaitront, qui d'une manière ou d'une autre m'auront apporté leur soutien durant ces 4 années !

Finalement, je terminerai par toi **Cédric**. N'étant pas du tout du milieu, tu es la personne qui aurait pu le moins comprendre, et pourtant… Jamais, jamais, jamais (jamais !) tu ne m'as fait de reproches, jamais tu n'as dit quelque chose quand il fallait me conduire au labo à 5h du matin, venir me rechercher à 1h du matin, ou faire un crochet par le labo dès qu'on allait quelque part. Jamais. Tu as été d'un soutien incommensurable, tu n'imagines pas. Merci pour tout !

Table of content

I. General introduction 18

1 Symbiotic relations 18

1.1 The different relationships 18

1.2 Host-pathogen relationship 19

1.3 Anthropozoonosis, when the infection comes from animals 20

2 Host and pathogen defense strategies 20

2.1 The host side: immunity in brief 20

2.1.1 From innate immunity … 20

2.1.2 … to adaptive immunity 24

2.1.3 Until immune memory 29

2.2 The pathogenic agent side: how to escape the immune system? 30

3 *Brucella* and brucellosis 31

3.1 Discovery of brucellosis 31

3.2 Animal brucellosis 33

3.2.1 *Brucella* species and host specificity 33

3.2.2 Natural routes of infection 34

3.2.3 Symptoms 35

3.2.4 Treatment 36

3.3 Human brucellosis 38

3.3.1 Incidence 38

3.3.2 Natural routes of transmission 39

3.3.3 Symptoms 40

3.4 Treatments 41

3.5 Diagnosis 42

3.6 *Brucella* inside the host cells: what do we know? 42

3.6.1 How to invade the cells? - Entry of *Brucella* 42

3.6.2 How to reach the paradise? - Intracellular trafficking 43

3.6.3 How to reproduce? - Replication of *Brucella* 45

3.6.4 How to be a perfect Trojan horse? - Adaptations to the host 46

II. The comparison of the routes of infection 48

1 What is known from the different *in vivo* infection murine models 48
1.1 The intraperitoneal route, the most currently used 48
1.2 The intragastric and oral routes 49
1.3 The intranasal route, a physiological one? 50
1.3.1 Generalities 50
1.3.2 Mucosal immunity 50
1.4 The intradermal route 52
1.4.1 Generalities 52
1.4.2 Skin immunity 53
1.5 Other routes of infection 54
2 Objectives 55
3 Article 56
4 Discussion and perspectives 57
4.1 The different routes of infection: towards a general model 57
4.2 Infection models in mice: critical, but not as much 59
4.3 Lymph nodes: the perfect fortress? 60
4.4 The essentiality of *virB*: questionable 62
III. The role of *Acod1* and itaconate 64
1 Therapeutic strategies against bacterial infection 64
1.1 Host-directed therapy 64
1.2 Bacteria-directed therapies 64
1.3 *Acod1* and itaconate 65
1.3.1 Discover, and brief history 65
1.3.2 Metabolism of itaconate 69
1.3.3 Transport of itaconate 70
1.3.4 Itaconate and its anti-bacterial role 71
1.3.5 Itaconate and its anti-inflammatory role 73
2 Objectives 79
3 Article 80
4 Discussion and perspectives 81
4.1 The type I IFN response in bacterial infections 81
4.2 *Acod1* and inflammation 82

4.3 Itaconate and its alkylation power 84
4.4 *aceA* gene, towards a new potential role? 84
4.5 Role of *Acod1* and itaconate at the cellular level 85
4.6 ACOD1 and its localization 85
4.7 Dimethyl-itaconate, a good substitute? 86
IV. General conclusion 88
V. Personal bibliography 90
1 As first or second author: published articles 90
2 As first author: in preparation 90
3 As associated author : published articles 90
VI. Supplementary material and methods 91
VII. References 114

I. General introduction

1 Symbiotic relations

1.1 The different relationships

Since the apparition of life on Earth, individuals have learned to live together, or at least to survive for some ones. Indeed, the co-habitation, and the co-evolution inter- or intra-species are the consequences of many years of biological interactions. The symbiosis refers to close and prolonged associations between organisms of distinct species. These interactions can be mutualist, commensalist, or parasitic. In the mutualism, all partners benefit from the relation. A remarkable example of mutualism is the interaction between tubeworms (a long marine invertebrate in the phylum of Annelida, living near the hydrothermal vent sites) and different intracellular chemosynthetic bacteria living in their trophosome[1]. Some carbon isotope experiments showed that the worms are dependent on bacteria carbon compounds synthesis for their nutrition. Bacteria use chemosynthesis to gain energy from a chemical reaction and to capture carbon dioxide from seawater. This leads to the synthesis of molecules used by the worms from the carbon dioxide present in vents. In this relation, through the well-adapted body of tubeworms, bacteria found an oasis in this hydrothermal extreme environment (Dimijian 2000). Another example is the presence of bacteria in our digestive system. The intestinal flora benefits of an environment rich in nutrients, favorable to a high rate of proliferation. In exchange, these bacteria help our digestive system to digest some elements such as fibers.

In the commensalism relationship, only one partner benefits of the relation, but this is not to the detriment of the other ones that are unharmed. An example of this relationship is the barnacles, a type of crustacean, which fixe to the whale or turtles body conferring to barnacles a mean of transport, without consequences (either positive or negative) for the whales or turtles.

Another type of biological interaction is the parasitism. In the case where an organism associates to another one to take advantage of its resources (endoparasitism), we will talk about an infection. This relation, most of the time unbalanced, is composed of a “pathogenic agent”

[1] A highly vascularized organ found in some organisms which do not possess digestive system. This organ houses bacteria providing food to their host.

(coming from "*pathos*" meaning "suffering" and "*gēnes*" meaning "producer of") and a "host". The first one will "use" the host to reproduce, and/or to eat, and/or to hide, etc. All of this will be, in a certain way, detrimental to the host, which will adapt to defend and to survive. But in another hand, the host also can find some advantages to this relation as it will allow him to increase its robustness and to control, at long term, the population demography. In terms of evolution, it is more advantageous for the pathogenic agent to do not kill its host. The host-pathogen relationship is a very precise balance between survival of both host and pathogenic agent.

These three types of relationship are not frozen. Indeed, a relation can shift rapidly or gradually in another type of relation. Many pathogens colonize for example their host for all the host's lifetime. But if the disease is asymptomatic, the relationship between the host and the pathogen can somehow be considered as a commensal relationship for at least a certain period of time. At the contrary, commensal bacteria can become pathogenic for immunocompromised people.

1.2 Host-pathogen relationship

Pathogenic agents can be classified into two categories: the facultative ones, and the obligate ones. These latter are fully dependent on the machinery of their host to reproduce. It is the case of all viruses, but also some bacteria such as *Chlamydia*. Some pathogenic agents are able to infect different host species while other have a very small range of hosts (Balloux and van Dorp 2017). Currently, few is known about the genetic changes necessary for a "host jump". Sometimes, only one mutation is sufficient (Viana, Comos et al. 2016). It was the case for example of the human-adapted *Staphylococcus aureus* strain to adapt to rabbit (Viana, Comos et al. 2016). The intracellular pathogenic agents are well adapted to their host: they can manipulate it, defend against it, use its resources, etc. For that, they acquired virulence factors that are often encoded by clusters of genes named pathogenicity islands. As mentioned above, there is no advantage, in the long term, for a microorganism to kill its host. Even if they are able to produce damages to it with toxins for example (tetanus, anthrax, etc), the host damages are often self-inflicted via a too strong or chronic immune response (Balloux and van Dorp 2017).

In a spirit of "co-evolution" and "relationship", how did the host adapt to the pathogenic agents? In the case of humans, even if they co-evolve with certain microbes and suffer of selection pressures since years, few genetic variants are known (Hill 2012). Today, even if some

devastating agents are eradicated or under control, the recent outbreaks of Zika, Ebola, SARS-CoV-2 viruses, and the drug resistance selection highlight the importance to continue research of new vaccines or therapeutic molecules discovery.

1.3 Anthropozoonosis, when the infection comes from animals

A study of 2005 identified more than 1,400 human pathogenic agents, of which 58 % have an animal origin (Woolhouse and Gowtage-Sequeria 2005). When the transmission of these pathogenic agents occurs from animals to humans, the term "anthropozoonosis" is used, coming from greek *ánthrôpos* (human), *zoo* (life), and *nose* (disease). Some anthropozoonoses are dramatically famous all around the world and the pathogenic agent can be either a helminth, a protozoan, a virus or a bacterium. The Plague disease is one historically but terrible famous example of bacterial anthropozoonoses. This pandemic made up to 50 million of victims just in Europe and Mediterranean area, representing around 35-60 % of the European population (Alfani and Murphy 2017). The Malaria is another example of zoonosis in which *Plasmodium*, the parasite responsible for the disease, is transmitted from mosquito to humans. The typical symptoms of Malaria are fever, vomiting, tiredness. In 2018, more than 200 million of cases were reported by the WHO (WHO 2019) resulting in more than 400,000 deaths in the world, mainly children. Finally, the Severe acute respiratory syndrome coronavirus 2 (SARS-CoV-2), known as "Covid19", considerably modified the human behaviors in 2020. The worldwide pandemic started in December 2019, with probably an animal origin as genetic analyses revealed high homology between SARS-CoV-2 and bat or pangolin Coronaviruses. Up to now, the pandemic made up more than 66 million of infection cases, with more than 1.5 million of death, exclusively people of > 60 years old (WHO 2020).

The number of the different reservoirs, of the intermediated hosts, of the different vectors, etc. are some factors leading to a complex understanding of these zoonoses.

2 Host and pathogen defense strategies

2.1 The host side: immunity in brief

2.1.1 From innate immunity …

The innate immunity is more and more seen as an essential partner of the adaptive immunity, both working together with close associations to fight infections. But this is only true for vertebrates, as the adaptive immune system appeared only 500 million years ago (more

precisely in jawed fish) (Martin and Kasahara 2010). This late apparition of the adaptive immune system highlights the efficiency of the innate immunity, alone, to protect all non-vertebrate organisms against infections. The innate immune system is composed of several components: physical/chemical and cellular ones. Indeed, before to meet the cellular components, pathogenic agents have to face the epithelia, mucus, cilia, pH, etc. Then, the cellular components: the granulocytes (neutrophils, eosinophils, mast cells, basophils), the phagocytic cells (monocytes, macrophages, dendritic cells (DCs)), and the Natural Killer cells (NK), each one having a specific role (see Table 1). NK are part of the Innate Lymphoid Cells (ILC) that are cells from innate immunity, even if they derived from a common lymphoid progenitor. These cells secrete signal molecules and are able to activate both innate and adaptive cells. They are mainly located in mucosal environment and play a key role in the homeostasis of tissue. Following lungs infection by viruses or bacteria, ILC, whose NK, secrete IFN-γ and IL-17. After skin damages, ILC are recruited to the injured site, secrete mainly IL-17 to recruit effector cells (Artis and Spits 2015).

Immune cells	Function
Neutrophils	Phagocytes and digest materials. Able to expulse their genetic material to neutralize the pathogen
Eosinophils	Involve in inflammatory reaction and immunity to some parasites. Role also in allergic and athsma reactions
Basophils	Involve in inflammatory reactions with eosinophils
Mast cells	Play a key role in inflammatory reactions
Monocytes	Phagocytes and digest materials
Macrophages	Phagocytes and digest materials. Role as antigen-presenting cells: activate adaptive immunity
Dendritic cells	Role as antigen-presenting cells: activate adaptive immunity
NK cells	Induce apoptosis of infected cells and produce cytokines such as IFN-γ

Table 1: Summary of the different functions of the innate immune system cells

The activation of the innate response is based on (1) the recognition of pathogenic agents molecules and (2) an intracellular signaling cascade leading to the triggering of an early response.

(1) The repertoire of invariant receptors to detect microorganisms is quite limited, as the immune receptors are encoded in the germline in order to produce an immediate response (Akira, Uematsu et al. 2006). The cells mainly expressing these receptors are the Antigen-presenting cells (APC), such as DCs and macrophages. This limited repertoire is counterbalanced by the fact that these receptors (Pattern recognition receptors – PRRs) target pathogenic agent's components that are very widespread and

conserved such as lipopolysaccharide (LPS), lipoproteins, cytosine-phosphate-guanine (CpG) deoxyribonucleic acid (DNA), flagellum's components, etc, called PAMPs (Pathogenic-Associated Molecular Patterns) (Akira, Uematsu et al. 2006). One of the most studied family of PRRs are the TLRs, for Toll-like receptors. Each PAMPs is recognized by specific receptors: LPS by TLR4, lipoproteins by TLR1/2, CpG DNA by TLR9, porins and peptidoglycans by TLR2/6, and flagellin by TLR5 for examples (see Figure 1) (Akira, Uematsu et al. 2006). In total, there are 12 different TLRs that have been identified in mammals (Akira, Uematsu et al. 2006). Adaptor proteins such as Myeloid differentiation primary response 88 (MYD88) and Toll-interleukin 1 receptor (TIR) domain containing adaptor protein (TIRAP) allow the signal transduction after PAMPs detection by TLRs and allow the activation of proteins that control the pro-inflammatory genes transcription such as Nuclear factor κ-light-chain-enhancer of activated B cells (NF-κβ) or Interferon Regulatory Factor 3 (IRF3) (Figure 1) (Kawai and Akira 2007).

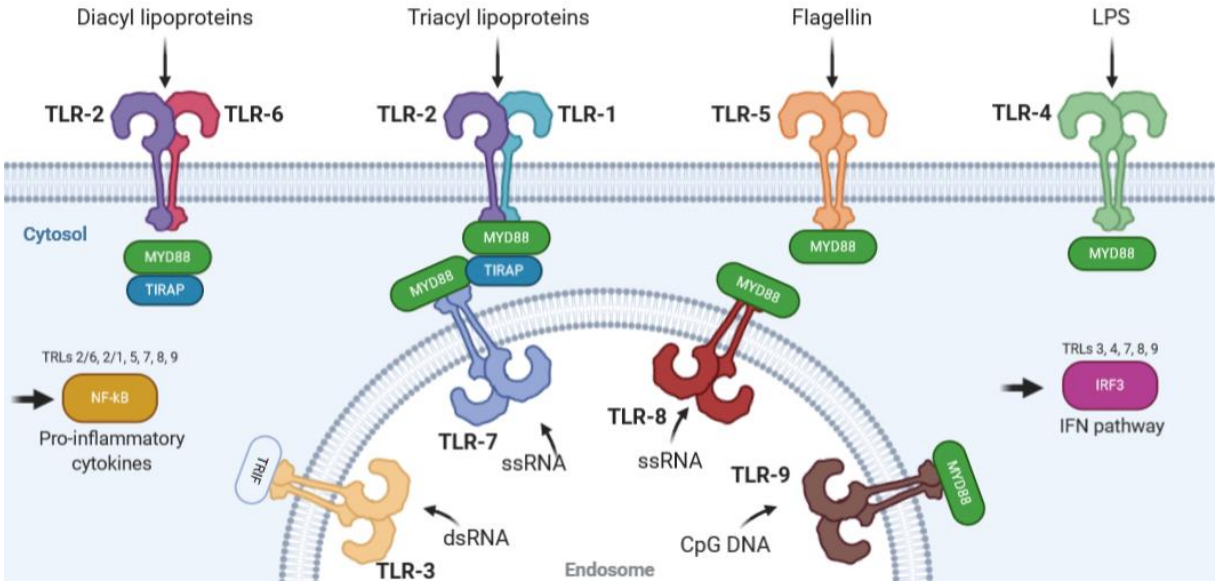

Figure 1: Recognition of bacteria PAMPs by PRRs*. Different TLRs can recognized specific PAMPs of bacteria. For examples, TLR9 recognizes DNA, TLR2 is specific for peptidoglycans and porins, TLR4 for LPS, and TLR5 recognizes flagellin. (Made with BioRender).*

Moreover, the innate immune system can also recognize danger signals (Damage-associated molecular patterns – DAMPs) that are molecules released outside the cell during tissue damages (Rubartelli and Lotze 2007). Some examples of DAMPs are Heat Shock Proteins, fibrinogen, oxidative stress, ATP, or uric acid crystal. These DAMPs

are recognized by TLR2, TLR4, P2X/P2Y receptors, or TLRs 2 and 4, respectively (Frevert, Felgenhauer et al. 2018)

(2) Once the PAMPs/DAMPs detected, signals are presented to the host, triggering pro-inflammatory and anti-microbial responses by activating kinases, transcription factors and other molecules of intracellular signaling pathways (Akira and Takeda 2004). This will be followed by changes in the expression of genes of different proteins such as chemokines, cytokines, receptors, etc that will be involved in the early immune response, such as type I interferon (IFN) for examples. Also, these molecules allow to link innate and adaptive immune responses (see below) (Akira, Uematsu et al. 2006).

The main essential effector mechanisms of the innate immune system are the phagocytosis and the inflammation. The **phagocytosis** is a mechanism that allows the elimination of pathogenic agents or cellular debris by internalizing and digesting them (Rosales and Uribe-Querol 2017). Once internalized, they will be destroyed by different mechanisms such as acid hydrolases from lysosomes, reactive oxygen intermediates (ROI), and reactive nitrogen intermediates (RNI) (Kaufmann and Dorhoi 2016). The macrophages, DCs and neutrophils are cells able to do that. The **inflammation** is induced either after a pathogenic agent invasion or in response to tissue damages. The inflammation has to be a perfect balance between the defense mechanisms and the restoration of the impacted tissue. The inflammation process is mediated by a lot of signals such as chemokines, cytokines, prostaglandins, etc. secreted by the injured cells (Medzhitov 2010).

In addition to this, other elements/mechanisms contribute to the innate mechanisms such as antimicrobial peptides, complement system, autophagy, degranulation (by granulocytes) (Mogensen 2009).

In addition to their role in the innate response, macrophages and DCs, belonging to the APCs, make the link between innate and adaptive immune responses. Indeed, APC and T cells will interact via different receptor-ligand complexes: major histocompatibility complexes (MHC), and CD80/86 of APCs will interact with T cell receptor (TCR), and CD28 of T cells, respectively. This allows to activate, but also to differentiate the T cells (see below) (Ni and O'Neill 1997).

2.1.2 … to adaptive immunity

The apparition of the adaptive system dates of 500 million years ago, but the reason of its selection is debated. In one hand, it is highlighted that the immune system had to adapt to pathogenic agents more and more virulent and furtive. But this would imply that the evolution pressure of microbes would be so strong that no host without adaptive immune system would have survived. On the other hand, it would be possible that the adaptive immune system appeared to reduce the tissue damages made during the chronic infections (Usharauli 2010). Following the first hypothesis, the adaptive response provides another level of protection against pathogenic agents and is in close association with the innate immune response. Indeed, the efficiency of the adaptive immune response will partially depend on the ability of the innate immune system to detect pathogenic agents and to transmit the signals to the adaptive system (Usharauli 2010).

The adaptive immune cells (T and B cells) are composed of two types of receptors: the TCR (for T cells) and the BCR (for B cells). A huge repertoire of these antigen receptors is randomly generated by somatic DNA recombination events during lymphocytes maturation (Schatz, Oettinger et al. 1992). Other mechanisms such as somatic hypermutations (for BCR only) allow to generate a highly diverse repertoire of receptors, with a huge potential to recognize specifically almost every antigenic determinants (Medzhitov 2007). This specificity has a cost: it makes several days to develop. The activation of B and T cells is not only dependent on the antigenic recognition, but also on other signals, termed costimulatory signals, delivered by the innate immune system.

2.1.2.1 The T lymphocytes

The maturation of **T cells** occurs in thymus. The activation of these cells is dependent on the interactions with APCs that will present, via their MHC, the antigens. The T cells possess two main functions, associated to two different phenotypes: one lineage expresses the γδ-CD3 TCR (γδ T cells) and the other one the αβ-CD3 TCR (αβ T cells) (Ciofani and Zuniga-Pflucker 2010).

The γδ T cells are unconventional T cells. Ideally located in epithelia, they act rapidly upon an infection. They secrete cytokines such as IFN-γ, or interleukin (IL)-17, leading to inflammation. They express TLRs and other receptors close to the ones of NK, making them close to innate immune cells. Their activation seems independent on the antigen processing and MHC

presentation of peptide epitopes. Their ligands are today unidentified (Ciofani and Zuniga-Pflucker 2010, Lawand, Dechanet-Merville et al. 2017).

Once differentiated into CD4 or CD8 T cells, expressing the CD4 or CD8 costimulatory molecule (a glycoprotein), respectively, the αβ T cells migrate from the thymus to the secondary lymphoid organs.

1) The **CD8 T cells** are cytotoxic cells. They recognize the infected cells via the presented antigens (Figure 2) and destruct them via the perforin/granzymes axis, leading to the apoptosis (Henkart 1994). The CD8 T cells are activated by cytosolic antigens presented by the MHC-I of DCs. For that, the proteins of intracellular pathogenic agents are degraded by the proteasome in peptides that then enter in the endoplasmic reticulum (ER) via the transporter associated with antigen processing, TAP1. The ER is also the place where MHC-I is formed. The pathogenic peptides bind the MHC-I and are relocated to the cell surface to be presented to the receptor of CD8 T cells (Figure 2) (Kobayashi and van den Elsen 2012). The CD8 T cells are able to secrete cytokines such as IFN-γ and tumor-necrosis factor (TNF)-α, allowing to activate macrophages to kill the infected cells (Tau, Cowan et al. 2001).

2) The **CD4 T cells** activation is dependent on the antigen presentation by APC. Once phagocytosed, the extracellular pathogenic agent is degraded by lysosomal proteases activity. The vesicles containing the new formed peptides fuse with the vesicle containing the MCH-II molecule. The peptides are then presented, via the MHC-II relocated at the APC surface, to T cells (Figure 4) (Kobayashi and van den Elsen 2012). In addition to this first signal of activation, two other signals are required to fully activate and differentiate CD4 T cells: CD80/CD28 interaction (the costimulatory signal) and a cytokine-dependent signal. In function of the cytokines secreted by APCs, the CD4 T cells will differentiate into distinct CD4 T cells subsets, including T Helper (TH) 1, 2, 17, and T regulator (Treg), each one being specialized for particular infections (Zhu, Yamane et al. 2010).

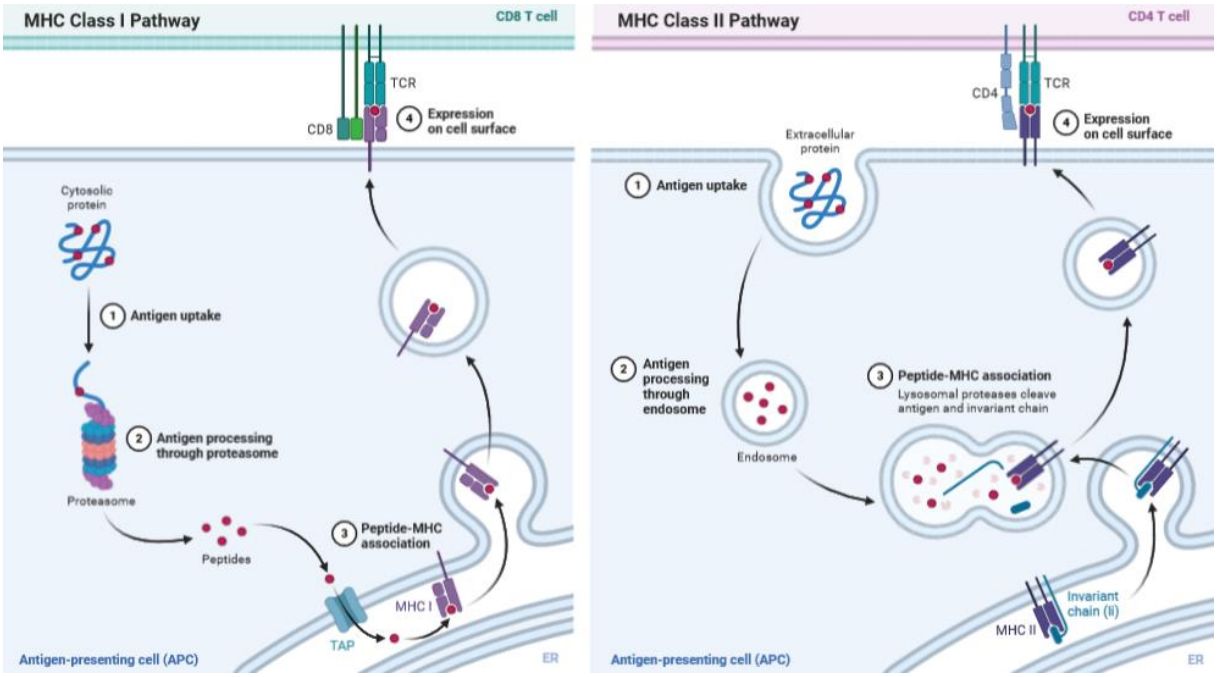

Figure 2: Antigenic presentation. *An intracellular pathogen is presented by MHC-I to CD8 T cells: the proteins of the pathogen are degraded into peptides by the proteasome. Peptides enter in the ER via TAP1 and bind MHC-I. They are presented to CD8 T cells. An extracellular pathogen is presented by MHC-II to CD4 T cells: the proteins of the pathogen are degraded by proteases in endosomes. This vesicle fuses with a vesicle that contains the MHC-II coming from the endoplasmic reticulum where the peptide site was blocked by the invariant (Ii) chain and Corticotropin-like intermediate peptide, CLIP. Once removed, peptides bind the MHCII and are presented to CD4 T cells. (Made with BioRender).*

Briefly, the TH1 response is adapted to eliminate intracellular pathogenic agents. IFN-γ and IL-12 (composed of p40 and p35 proteins) are cytokines produced by DCs and macrophages to differentiate CD4 T cells into TH1 (Figure 3). These cells then secrete mainly IFN-γ via the Signal Transducer and Activators of Transcription (STAT)4/transcription factor T-box expressed in T cells (T-bet) pathway. When IFN-γ binds its receptor (composed of IFN-γR1 and IFN-γR2 sub-units) on macrophages, the signalization is transmitted by Janus Kinases (JAK)/STAT1 pathway, leading to IRF1 expression, a transcriptional factor involved in immune responses and inducible Nitric Oxide Synthase (iNOS) expression. These expressions induce an oxidative burst and the activation of effector cells such as macrophages, leading to a cytolytic activity (Honda, Takaoka et al. 2006, Thieu, Yu et al. 2008).

The TH17 response is induced by IL-6, IL-1β, IL-23, and Transforming Growth Factor (TGF)-β cytokines (Figure 3), and acts against extracellular pathogenic agents and fungi mainly.

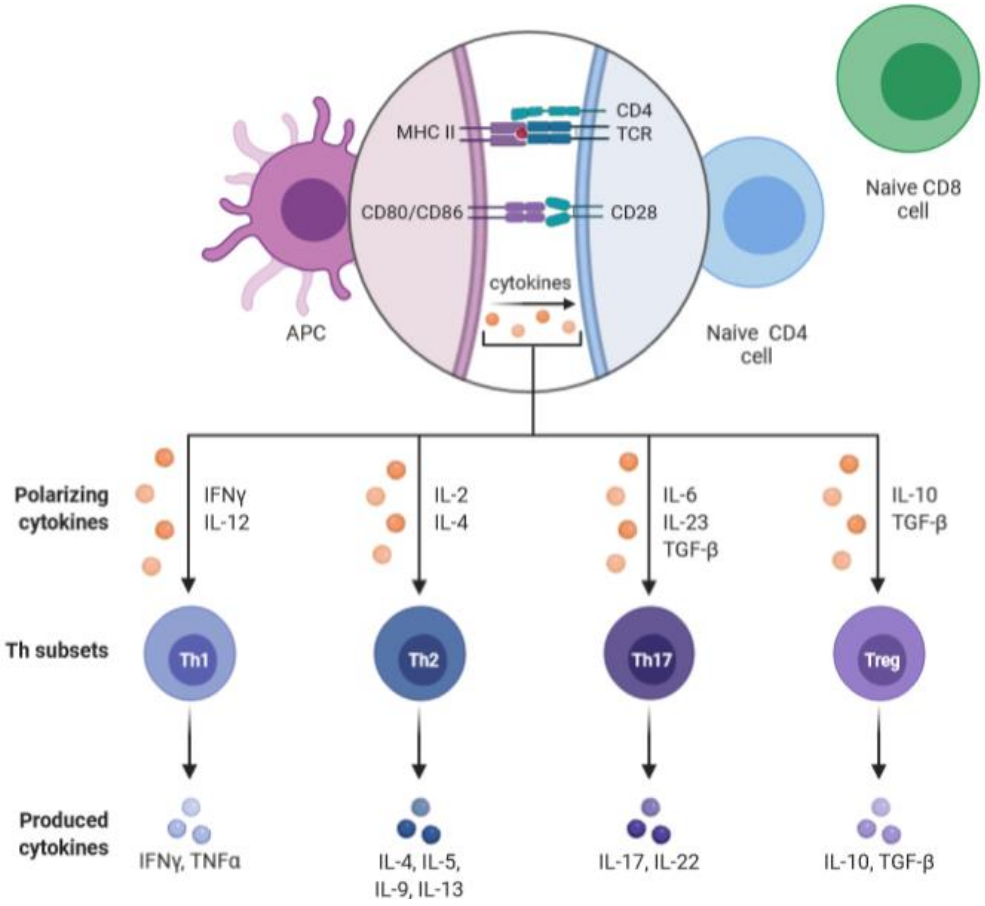

Figure 3: Resume of the different T cells and T Helper subpopulations. *Each T cells possess a CD3-T receptor. But this receptor can be composed of αβ chains or γδ chains. Among the αβ-CD3 T cells, some have a CD8 co-receptor (cytotoxic T cells), other have a CD4 co-receptor (Helper T cells). Those Helper T cells will differentiate into different T subsets in function of the cytokinic signal they will receive. (Made with BioRender).*

Sometimes, the TH17 response, via the IL-21, can also lead to auto-immune diseases. The activated TH17 CD4 T cells secrete IL-17, IL-21, IL-22, and IL-23 (Figure 3), but also chemokines such as the C-X-C motif ligand (CXCL)1 and CXCL2 to recruit neutrophils. The pro-inflammatory role of these cells is mediated by the stimulation of antimicrobial peptides and pro-inflammatory cytokines production by neutrophils, but also by epithelial cells. Indeed, these latter express IL-17 receptors and TLRs, leading to the production of antimicrobial peptides after stimulation by IL-17 and PAMPs, respectively (Kolls, McCray et al. 2010). The IL-17 cytokines also allow the stimulation of some Immunoglobulin (Ig) production by B cells (Ouyang, Kolls et al. 2008, Perez-Lopez, Behnsen et al. 2016).

Finally, the Tregs have a role of suppressor of the immune response by direct cell-to-cell contact, but also through the release of regulatory cytokines such as IL-10 and TGF-β. IL-10 is for example able to negatively impact the TH1 response, modulating TNF-α, IFN-γ, and IL-12 cytokines production (Corsetti, de Almeida et al. 2013).

2.1.2.2 The B lymphocytes

The maturation of **B cells** occurs in the bone marrow, but their activation occurs in secondary lymphoid organs. There, naive B cells scan the environment to the research of microorganism antigens. Once encountered, the antigens activate B cells via their BCR, resulting in B cells proliferation and differentiation. B cells activation requires a second signal, which is dependent or independent of T cells.

1) In the case of **T cells-dependent** activation of B cells (most of the time), two main signals are required: (1) the binding of CD40L (T cells) to CD40 (B cells), and (2) the antigenic peptide presentation from B to T cells. For that, B cells do endocytosis of antigens and degrade them into peptides via the lysosomal proteases. The peptides are then presented at the B cells surface by the MHCII, allowing to activate T cells. Once activated, T cells secrete cytokines to activate B cells, leading to their proliferation. B cells differentiate into "germinal center B cells" and into "short-lived plasma cells" secreting low-affinity IgM and IgG antibodies (MacLennan, Gulbranson-Judge et al. 1997, Bonilla and Oettgen 2010, Takemori 2015, Gaudino 2019). The germinal center B cells form the germinal center and proliferate during the second phase of primary response (Akkaya, Kwak et al. 2020). The germinal center B cells differentiate into memory B cells, and long-lived plasma cells. During its maturation, BCR undergoes somatic hypermutations leading to a better adaptation of BCR to the antigens. Then, they change of phenotype to better adapt to the pathogenic agent via the class-switching, a rearrangement of the heavy chains of antibodies. This process is dependent on cytokines such as IL-4, IL-13, IFN-γ, IL-10 or TGF-β (MacLennan, Gulbranson-Judge et al. 1997, Bonilla and Oettgen 2010).

2) In the **T cells-independent** activation of B cells, the development of active B cells is faster, but the antibodies generated have a lower affinity and are less specific than the ones generated by the T cells-dependent activation. In one case, antigens such as LPS activate B cells via their TLR expressed at their surface. This leads to the production of polyclonal antibodies. The second type of antigens are repetitive structures of bacteria, which will bind and activate a lot of different BCRs, leading to the proliferation, differentiation of B cells, and antibodies production (Mond, Lees et al. 1995, Vos, Lees et al. 2000).

2.1.3 Until immune memory

In 430 before Christ (BC), the immune memory was for the first time briefly mentioned by Thucydides who described that "the same man was never attacked twice - never at least fatally », talking about the plague (Tangye 2015). One characteristic of our immune system is to "remember" previously encountered pathogenic agents. It can come from natural infection, but also from vaccination. The secondary response will be faster and more efficient than the first one. Although it was associated for years with the adaptive immune system, it seems more and more clear that the innate immune system could be also able to "memorize" certain stimuli (Kurtz 2005, Boraschi and Italiani 2018).

B cells develop into memory cells after their activation in a T cells-dependent manner (see above). They will be reactivated following a new contact with the same antigen, and will secrete specific antibodies. In the same way, T cells can also develop in memory T cells upon a first contact with an antigen. Indeed, after a first activation, 90-95 % of activated T cells undergo apoptosis while 5-10 % of T cells differentiate into memory T cells (Valbon, Condotta et al. 2016). Different memory T cells can be distinguished: the tissue effector memory, the central memory and the resident memory T cells (Ratajczak 2018).

- The **central memory T cells** colonize the secondary lymphoid organs such as lymph nodes. These cells are able to proliferate rapidly upon an antigenic stimulation and to activate DCs. However, they do not possess effector functions. The central memory T cells could also regenerate the pool of effector memory T cells (Walzer, Arpin et al. 2001, Ratajczak 2018).
- The **effector memory T cells** are located in the non-lymphoid organs such as lungs, liver, intestine, etc. They circulate between blood and tissues and secrete IL-4, IL-5, IFN, perforin and granzym B, conferring cytotoxic properties to these cells. After a second infection with the same pathogenic agent, the effector memory T cells activate the immune mechanisms, help DCs to migrate to the lymph nodes, and help the CD8 T cells at the infection site. The CD4 effector T cells proliferate less than the CD8 effector T cells (Ratajczak 2018).
- The **resident memory T cells** constitute the first line of defense as they are located in tissues, potentially a "becoming-infectious site" (lungs, brain, skin, reproductive tract, etc). Following a second infection with the same pathogenic agent, their response is the

faster as they are already at the site of infection. The role of the CD4 resident memory T cells is not well known. They secrete IFN-γ, IL-17 and help to the recruitment of cells towards the infectious site. The CD8 resident memory T cells have different roles once activated: they initiate the antimicrobial defenses, help APCs in their functions, rapidly secrete IFN-γ, activate NK, mature DCs, help to recruit T and B cells, etc (Ratajczak 2018).

2.2 The pathogenic agent side: how to escape the immune system?

With years of co-evolution with their hosts, pathogenic agents have acquired different strategies to escape the host immune system. The defense strategies of bacteria can be subdivided in three levels, but with the same objective: avoid or inactivate the immune defenses. **The first level** is the formation of biofilms, thin layer of bacterial populations, stacked to each other and adhering to a surface. The substance that each bacterium secretes extracellularly allows to enclose the populations to protect them from entry of anti-microbial substances (Tremblay, Hathroubi et al. 2014). **The second line** of defense is the external part of bacterium it-self, which is the first thing detected and targeted by the immune system: the cell wall. Some bacteria have acquired a capsule along evolution. This additional external layer allows to bacteria to be protected from phagocytosis, but also allows the production of toxic compound for the host, and the adhesion to the host cells (Reddick and Neal 2014, Zhou, Shi et al. 2015, Bizzell 2018). Other bacteria modified their membrane components, including efflux pumps or LPS to avoid the detection by the immune system or to repel the positively charged host effectors. For example, *E. coli* acylates the lipid A of its LPS to change the charge, becoming positively charged. Finally, another defense strategy is to directly inhibit the host effectors (Raetz, Reynolds et al. 2007). **The third line** consists to secrete effectors playing a role at different levels: the inhibition of the phagocytosis, of the lysosomal fusion, of the DCs maturation, of the T cells activation, etc. For example, when *Mycobacterium tuberculosis* is internalized and follows the endocytic trafficking in macrophages, the acidification of its compartment will trigger the secretion of virulent effectors, like a tyrosine phosphatase called Serine/threonine-protein phosphatase 2A activator (PtpA) which inhibits an ATPase required for the lysosomal fusion and hence its degradation (Reddick and Neal 2014, Zhou, Shi et al. 2015, Bizzell 2018).

An expert in the “not to be detected” mechanisms? *Brucella*!

3 *Brucella* and brucellosis

3.1 Discovery of brucellosis

Brucellosis is not an emerging disease. Indeed, indirect proofs suggest that the first tracks of brucellosis could date from 2.5 millions of years, when *Australoptithecus* started to eat meat (D'Anastasio, Zipfel et al. 2009). Later, specific lesions of brucellosis have been discovered on Egyptian skeleton in 750 BC (Moreno 2014), and an examination of skeletons of humans dead in 79 BC during the Mount Vesuvius eruption has revealed typical bones lesions of brucellosis in more than 17 % of cases (Capasso 2002). This was not really surprising as one of the main sources of food at this moment were goats, sheep and their products (Capasso 2002), meaning one of the main source of contamination as it has been discovered later (Zammit 1905, Eyre 1908). But one of the first direct proof of brucellosis presence dates from 10-13 century, when genetic analyses have revealed *Brucella* DNA on lesions located on human lumbar and thoracic vertebrae (Mutolo 2011). The first "real" description of the disease dates from 1861, and was made by J. Marston (Marston 1861) (see BOX-1 for further explanations).

BOX-1. On the route of *Brucella* discovery. Jeffery Allen Marston, an assistant surgeon of the British Army in the Medical Department, described in the reports of the Army the illness he himself contracted in Malta and which causes fever (Marston 1861). In 1875, Maclean, a professor of military medicine of the Army, published about the "Malta fever". Indeed, he observed soldiers from Malta in bad condition and having distressing fever, what he called the Malta fever (Maclean 1875). The cause of this fever was unknown, but the most frequent characteristics of the disease were the followings: a very long fever (sometimes up to seventy days (Maclean 1875) or even several years (Bruce 1907), the fever does not rise very rapidly and seems to be transient, a headache, an affected spleen, an alteration of the liver functions, a destruction of the lungs, neuralgic and rheumatic pains, and also articular and muscular pains. These last ones seemed to appear after the first weeks of the disease (Maclean 1875).

In 1887, the Surgeon Captain David Bruce of the Royal Army published his notes about the examinations of the bodies of dead soldiers suffering of fever. During these post-mortem examinations, D. Bruce observed that the spleens and other organs like the liver or kidneys were similar to the organs in other diseases involving microorganisms. Based on that, he decided to look for a microorganism which could explain the fever. From spleens of dead British soldier, D. Bruce succeeded to isolate the microorganism responsible for the "Malta

fever", which was negative for the Gram staining (Bruce 1887). At the opposite of Gram positive bacteria, the Gram negative ones have a thinner layer of peptidoglycan but possess an outer membrane composed of LPS. This thin layer of peptidoglycan allows the destaining of Gran negative bacteria with alcohol during Gram staining. The organism was called *Micrococcus melitensis* by D. Bruce in 1893 as the Roman name for Malta was "Melita" meaning "honey-isle" in reference to the unique brand of honey in Malta. Another micro-organism was discovered by Bang in 1895. This Bacillus, called *Bacillus abortus*, was responsible for abortion in cows (Bang 1897) (see BOX-2).

BOX-2. Link between the infectious agent and the zoonotic nature of the disease. In 1895, the veterinary Bernhard L. F. Bang and his assistant Stribolt decided to prove that the abortions of cows that were frequent these years were linked to the bacteria they found in *post-mortem* examinations of cows. They found a "bacillus" that they cultured and injected in the vagina of pregnant cows. After the abortion 2 months later, they concluded that this "bacillus" was responsible for the abortion in the cattle (Bang 1897). The "bacillus" will be called the "Bang's bacillus" or *Bacillus abortus*. It is in 1905, thanks to the experiments of Zammit, that the link between *Micrococcus melitensis* and the goats is done. Indeed, after feeding goats with "bacilli"-containing food, he observed that the goats were susceptible to brucellosis, the "bacilli" were present in the blood, urine and milk of the infected animals, and that people consuming the infected goats milk can become sick (Zammit 1905, Eyre, Durh et al. 1908).

In 1918, an American microbiologist, Alice Evans, suggested in the "Journal of Infectious Disease" that the Bang's bacillus and the Bruce's micrococcus were indistinguishable based on morphological, biochemical and serological studies and were only one and same genus. She proposed that the form of this organism was not a "bacillus" or a "coccus" but a "**coccobacillus**" (Evans 1918). Meyer proposed in 1920 a generic name for the genus: *Brucella* (*B.*), in honor of David Bruce (Meyer and Shaw 1920). This bacterium belongs to the **alpha-proteobacteria** class (E., E. et al. 1990).

3.2 Animal brucellosis

3.2.1 *Brucella* species and host specificity

In the following years, other species of genus *Brucella* were discovered, the most known being: *B. suis*, *B. ovis*, *B. neotomae* (Stoenner and Lackman 1957), *B. canis* (Carmichael and Kenney 1968), *B. ceti* and *B. pinnipedialis* (Foster, Osterman et al. 2007), *B. microti* (Scholz, Hubalek et al. 2008), *B. inopinata* (Scholz, Nockler et al. 2010), *B. papionis* (Whatmore, Davison et al. 2014), and *B. vulpis* (Scholz, Revilla-Fernandez et al. 2016) (Figure 4). The main distinguishable characteristic between these species is the main host they infect. Indeed, even if crossed infections can occur, *B. abortus* has for example a tropism for the livestock, *B. melitensis* for the sheep, *B. canis* for dogs, and *B. suis* for pigs and wild boars (Figure 4) (Bang 1897, Zammit 1905, Carmichael and Kenney 1968). The host specificity is not completely understood yet. Genomic studies between *B. melitensis* and *B. suis* revealed that they have a very similar genome (Paulsen, Seshadri et al. 2002). Indeed, more than 90 % of their genes have 98-100 % of identity at the nucleotide level, but this small variability could explain the variation in host specificity (Viana, Comos et al. 2016). For example, the different genes are coding for outer membrane proteins (OMP), membrane transporters, putative invasins or adhesins, that are probably exposed to the surface (Tsolis 2002). Even if *B. melitensis* and *B. suis* genomes are very close, another study showed that *B. abortus* and *B. melitensis* would be the closest *Brucella* species (Figure 4) (Halling, Peterson-Burch et al. 2005).

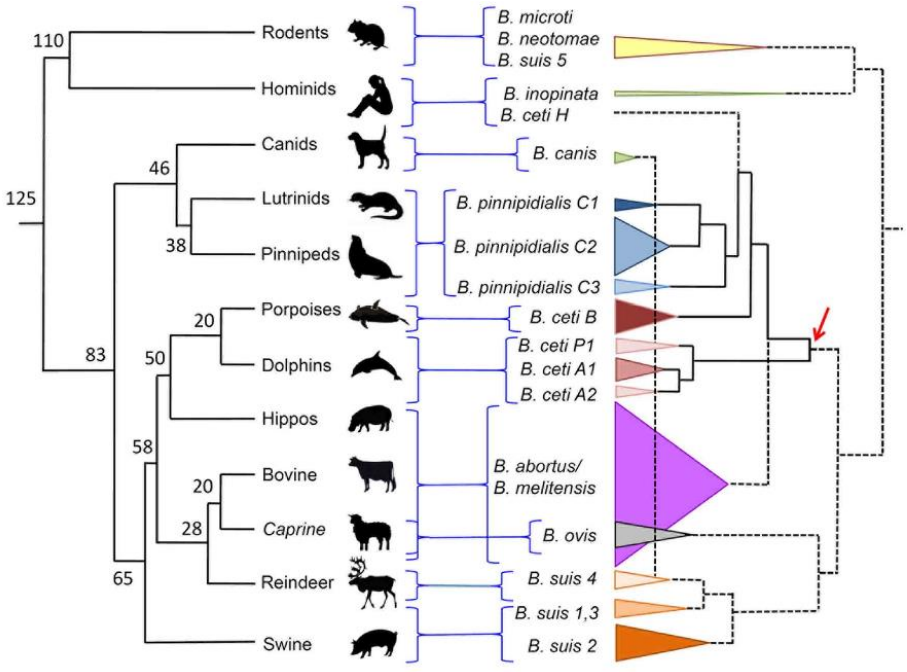

Figure 4: Different species of Brucella in relation with their potential host(s). *Link between the diversity and the phylogeny. The number are in millions of years (Guzman-Verri, Gonzalez-Barrientos et al. 2012).*

3.2.2 Natural routes of infection

The transmission intra-species can occur by different routes, through direct or indirect contacts, in horizontal or vertical manners. **Horizontally**, the contamination by the ingestion of the *Brucella abortus*-infected birthing fluids and tissues (placenta or aborted fetuses for examples) was suggested as possible by Plommet and colleagues in 1973 (Plommet, Fensterbank et al. 1973). The infection by contaminated aerosols produced during abortion that another animal can breathe is a non-negligible route as an infected placenta or aborted fetus can contain up to 10^{14} *B. abortus* (Alexander, Schnurrenberger et al. 1981). The infection via a direct contact of these aborted tissues with a cutaneous lesion or conjunctive tissues is also possible, even if the percentage of this route of infection is difficult to determine. The transmission by blood-sucking insects as vectors is not to be excluded. Indeed, the idea of a transmission via an insect was already reported in 1951 (Wellmann 1951). Finally, it is known that *Brucella* has a tropism for the reproductive tracts (semen, epididymitis, testicles, uterus, vaginal excretions, placenta, etc). Between 100 to 50,000 bacteria / mL can be found in the male semen for example. But despite that, it was suggested that the contamination from one partner to another one during the mating could be rare (Figure 5) (Manthei, DE. et al. 1950, Morgan 1979).

Another direct contamination is the **vertical transmission** from a mother to its offspring that can occur in two ways (Figure 5). First, via the milk sucking as *Brucella* can be isolated from the milk of sheep (*B. melitensis*) (Grillo, Barberan et al. 1997), goats (*B. melitensis*) (Renoux,

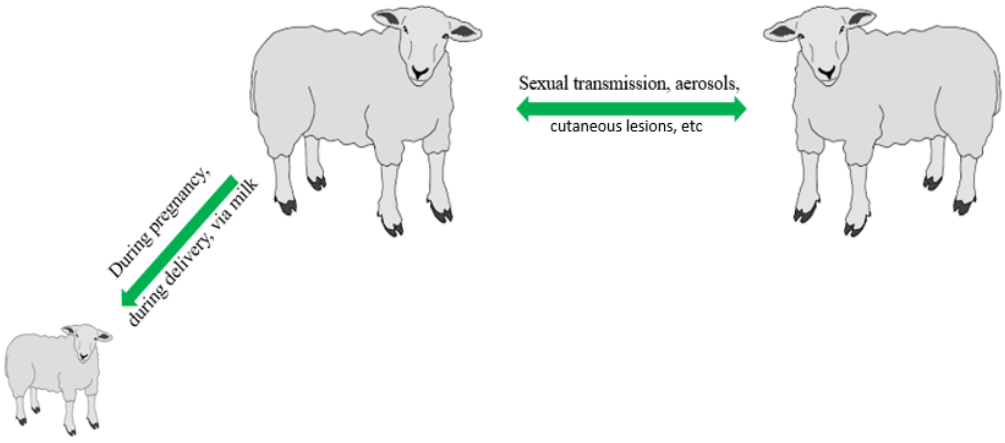

Figure 5: Routes of brucellosis transmission in animals. *The horizontal transmission of Brucella can occur via aerosols, cutaneous lesions, ingestion of contaminated products, and rarely via sexual contacts. The vertical transmission occurs during the pregnancy, the delivery, but also during the milk consumption.*

Alton et al. 1957), cows (*B. abortus*) (Carpenter 1926, Philippon, Renouy et al. 1971) and also mice (*B. melitensis*) (Bosseray and Dufrenoy 1982, Jansen, Demars et al. 2020). Grillo also

suggested that this mode of transmission intra-species could be the main one in animals (Grillo, Barberan et al. 1997). Second, it is known since at least 1962 that *Brucella abortus* preferentially invades the fetal tissues such as the fetal cotyledons, the chorions, or the fetal fluids rather than the adult's ones (Smith, Williams et al. 1962). Plommet and colleagues showed in 1973 that *B. abortus* was transmitted *in utero* in the cattle population. Even if they did not exclude a transmission by the placenta ingestion, via aerosols production or via the colostrum consumption, they concluded that the *in utero* infection was probably the main route of vertical contamination, as they separated the calf from the mothers directly after the birth (Plommet, Fensterbank et al. 1973).

3.2.3 Symptoms

The main consequences of *Brucella* infection in animals are abortion of pregnant females, infertility, orchitis[2], epididymitis, and hygromas[3].

The bacteria, once in the organism, can easily enter the bloodstream to finally reach the uterus. In this organ, *B. abortus* is found in macrophages, but mainly in trophoblasts, cells for which *Brucella* has a tropism (Payne 1959, Anderson and Cheville 1986, Meador and Deyoe 1989), which could be explained by the presence of erythritol, a sugar particularly appreciated by different species of *Brucella* such as *B. abortus*, *B. melitensis*, and *B. suis* (McCullough 1951, Smith, Williams et al. 1962). The abortion could be triggered by the TH1 response established in the uterus in presence of *Brucella*, compromising the homeostasis of uterus (see BOX-3).

BOX-3. *Brucella* and abortion. In 2009, Xavier and colleagues experimentally infected cows with *B. abortus* and studied the lesions caused by the bacteria in the cows and in the fetuses. They showed that the placenta of pregnant cows was full of lesions, necrotic and fibrinous, with a lot of neutrophils (Xavier, Paixa˜o et al. 2009). It has been shown that the immune response triggered by *Brucella* (TH1 / IFN-γ response) leads to damages in trophoblasts tissues and that IFN-γ inhibited the growth hormone secretion, both compromising the survival of the fetus (Smith, Williams et al. 1962, Wegmann, Lin et al. 1993). It is estimated than around 60 to 70

[2] Inflammation of testis

[3] Inflammation of serous bursa in articulations

% of the infected pregnant females abort (Diaz Aparicio 2013). Even if animals stay infected all their entire lives, the pregnant females usually abort only once (Nicoletti 2013).

Orchitis and epididymitis are inflammations of the testis or epididymis, respectively. Complications of these consequences can lead to infertility in infected males (Khan and Zahoor 2018). Finally, hygromas, which is inflammation of synovial bursae, are also consequences of brucellosis, leading to articular pain (Henning 1956, Thienpont, Vandervelden et al. 1961).

3.2.4 Treatment

Once animals are infected, they are usually slaughtered to limit the dissemination of *Brucella* to other animals or humans (Corbel 2006). Consequently, this leads to a huge economic loss. For example, the production loss of milk and meat induces annual economical shortfall of 600 millions of dollars by year in Latin America (Acha and Szyfres 2003). In countries where brucellosis is endemic, prophylactic vaccines can be administrated to animals. Currently, there are 3 main vaccines, all live attenuated vaccines. Briefly, the "S19" (Buck 1930) and "RB51" (Schurig, Roop et al. 1991) vaccines were obtained from *B. abortus* strain, and the "Rev1" (Herzberg and Elberg 1953) vaccine was obtained from *B. melitensis*. However, these vaccines have several main disadvantages such like reversion risks, human infection, diagnostic interference, abortion induction, etc. For now, and despite their limitations, live attenuated vaccines are the most commonly used vaccines to protect animals against brucellosis. The ideal vaccine should (1) induce an efficient TH1 response, (2) be an attenuated strain, stable, with no risk of virulence for humans, (3) confer a long term protection with only one dose and without triggering the abortion, (4) be practical for massive use. Moreover, the ideal vaccine should not produce antibodies that will interfere with diagnosis tests (Dorneles, Sriranganathan et al. 2015).

The S19 strain (from B. *abortus* 2308) is the first vaccine to be extensively used to control bovine brucellosis (Manthei 1960). This attenuated strain was isolated in 1923 by John Buck, after one year spent, accidentally, in cow's milk at room temperature, attenuating its virulence (Buck 1930, Graves 1943). This attenuated strain showed a good protection with 82-95 % of vaccinated cattle that are protected (Dorneles, Sriranganathan et al. 2015). Experimentally, the S19 vaccinated mice develop IFN-γ producing-CD4 T cells and cytotoxic CD8 T cells, but the attenuated S19 strain presents several problems. First of all, the induced antibodies are indistinguishable from the antibodies induced after a natural infection (WHO/EMC/ZDI/98.14

1997). Then, the vaccination of pregnant female can lead to abortion in certain cases (Nicolletti 1981). After a high dose of vaccination (>10^9 CFU), the strain is rapidly cleared of cervical lymph nodes but can sometimes persist and then be extracted in the milk (LA. and CG. 1981). The strain can also cause testis inflammation as a virulent strain of *Brucella.*

Some years later, the attenuated strain ***B. abortus* 2308 RB51** has been developed, via successive passages in a rich medium, by Gerhardt Schurig in 1982 (Schurig, Roop et al. 1991). It is a rough strain, interfering less with the diagnosis tests. But in this case, the medium used for the successive passages was supplemented with antibiotics, Penicillin and Rifampicin. This last one is used as antibiotic treatment against human brucellosis (Schurig, Roop et al. 1991). The Rifampicin acts by binding the RNA polymerase of bacteria, leading to an inhibition of RNA synthesis. The successive passage of RB51 strain in medium with antibiotics leads to a resistance of the RB51 strain to Rifampicin, which is the main problem of this vaccine strain (Ashford, di Pietra et al. 2004). The attenuated RB51 strain is protective, but not as much as than S19 vaccine: around 70 % of the vaccinated bovine are protected (Cheville, Stevens et al. 1993). In addition, the strain is eliminated from the cervical lymph nodes 6 to 10 weeks after the vaccination (Cheville, S.C. et al. 1996). Abortions of vaccinated pregnant females can also occur (Cheville, Stevens et al. 1993).

Finally, the attenuated strain ***B. melitensis* Rev.1** was obtained by reversion of a strain naturally resistant to Streptomycin in the middle of 1950's (Herzberg and Elberg 1953). The virulence attenuation of this strain could be explained by mutations mainly in ABC transporters, as some of them are required for the type IV secretion system in *B. ovis* (Silva, Mol et al. 2014, Issa and Ashhab 2016). *B. melitensis* Rev.1 confers a very good protection against future infections with *B. melitensis* (Lalsiamthara and Lee 2017) but also against *B. ovis* with 90 % of the vaccinated animals which are protected (Fensterbank, Pardon et al. 1982). However, another study revealed that Rev.1 strain, despite the fact that it limits the infection dissemination in 80 % of cases, only protects 35 % of the vaccinated animals (Brinley Morgan, Littlejohn et al. 1966). The vaccination via parenteral route offers a better protection than a vaccination via oral route (Olsen 2013, Olsen, Boggiatto et al. 2017). The rate of abortion is quite high with this strain, but the injection of the vaccinated strain by conjunctive route would reduce this percentage (Jiménez de Bagüés, Marin et al. 1989). As for the RB51 strain, the main problem of this vaccine is its resistance to an antibiotic required to treat brucellosis.

Campaign to vaccinate wild animals like buffalo, reindeer or bison have been tried with the *B. abortus* RB51 strain, via conjunctive or sub-cutaneous routes. However, the efficiency of this vaccination seems to vary a lot (Olsen 2013). The 3 main vaccines present clearly a set of disadvantages such as a not 100 % efficiency (El Idrissi, Benkirane et al. 2001), the possible induction of abortion in vaccinated pregnant animals (Smith and Ficht 1990), the risk of reversion into a virulent strain for humans (Spink, Hall et al. 1962, Thomas, Bracewell et al. 1981, Ashford, di Pietra et al. 2004, Sfeir 2018) or the resistance to antibiotics used to treat human brucellosis such as Rifampicin or Streptomycin. High doses of bacteria (around $5x10^9$) are usually used, in one (or two) injection(s). Moreover, S19 and Rev1 vaccines present an interference with the diagnostic tests as these tests mainly detect LPS epitopes, preventing the distinction between naturally infected and vaccinated animals (Barrio, Grillo et al. 2009, Avila-Calderon, Lopez-Merino et al. 2013). Different researches have been conducted to develop new vaccine approaches: inactivated, recombinant subunit, DNA, and vectored experimental vaccines. But up to now, no alternative has demonstrated a sufficient protection to make it commercially available (Carvalho 2016).

3.3 Human brucellosis

3.3.1 Incidence

Figure 6: Map of the distribution of caprine brucellosis all over the world. *Brucellosis is mainly reported in south of America, Africa, South of Europe, and the Middle-East (Rossetti, Arenas-Gamboa et al. 2017)*

Humans can be infected by different species of *Brucella,* mainly by *B. abortus*, *B. melitensis*, and *B. suis, B. melitensis* being the main species isolated in human population (Corbel 2006).

Humans are considered as accidental hosts as they are not able to transmit the disease to another host. Up to 12,500,000 new cases of brucellosis could be reported each year according to the WHO, with for examples an incidence of 34.9 cases per 100,000 person per year in Chad (South of Africa), 4 to 32 in Greece and 1.4 in Italy (South of Europe), 88 in Kyrgyzstan (Asia) and 12.8 and 25.7 in Argentina and Mexico (Latina America), respectively (Figure 6) (Pappas 2006, Dean 2012).

3.3.2 Natural routes of transmission

In the developed countries, brucellosis is considered as an occupational disease. Indeed, the researchers in laboratories (Ollé-Goig and Canela-Soler 1987, Staszkiewicz, Lewis et al. 1991, Fiori, Mastrandrea et al. 2000) and people working with animals or tissues are the most at risks (vets, butchers, farmers, etc) (Wallach, Samartino et al. 1997). A non-negligible route of transmission is via direct contact between a cutaneous lesion and infected tissues or fluids. This route of transmission is complicated to evaluate due to the rapid suppression of cutaneous manifestations (Berger 1981). The infection by contaminated aerosols is also an important route of infection (Hendricks, Borts et al. 1962). It is estimated that 10 to 100 bacteria are sufficient to infect a human via aerosols (Bossi 2004). In the developing countries, where the consumption of dairy milk products is widespread, or in the traveler population, the contamination by ingestion is also considered as a main route of infection (Figure 7) (Eckman 1975, Young 1975, Turgut, Turgut et al. 2006).

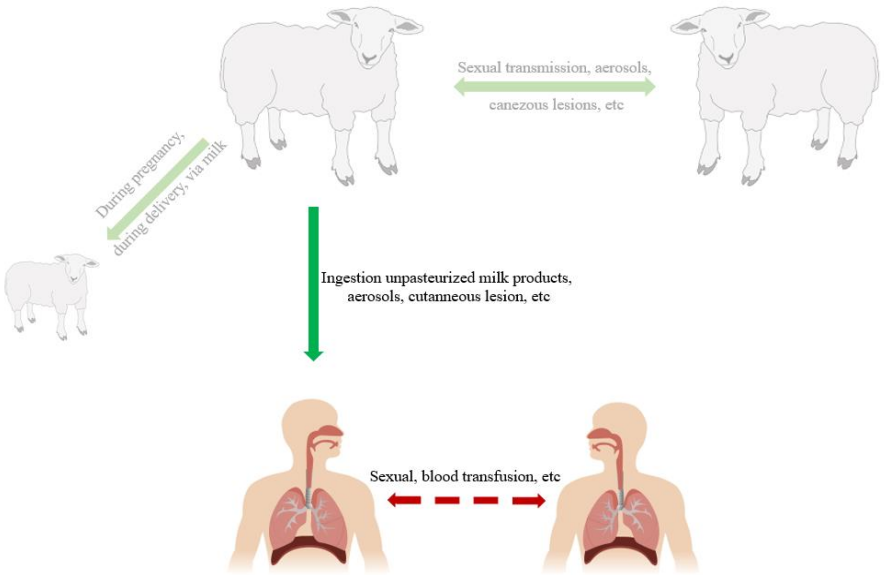

Figure 7: The different modes of human brucellosis transmission. *Humans can be infected by ingestion of unpasteurized milk products, via contaminated aerosols, direct contact between a cutaneous lesion and a contaminated fluid or tissue, etc. The human-to-human transmission is very rare.*

The transmission between humans is very rarely reported and very speculative. Some studies, by elimination, concluded that the sexual transmission was the only possible route of infection (Goossens 1983, Ruben 1991). The infections by blood transfusion (Wood 1955, Doganay 2001) or bone-marrow transplantation have also already been described in rare cases (Naparstek, Block et al. 1982). The vertical transmission from a mother to her child during the pregnancy or delivery is really rare (Figure 7) (Alsaif, Dabelah et al. 2018).

3.3.3 Symptoms

The *Brucella* infection is characterized by two phases; the acute one and the chronic one if the first one is not treated. According to the WHO, the period of incubation can last between 2 and 4 weeks, and in its chronic form, brucellosis can persist several years. Most of the time, human brucellosis is asymptomatic (Zhen, Lu et al. 2013), which is one of the reason of the difficulty to estimate the real burden of the disease. When symptoms are present, they are not specific and very difficult to link to brucellosis, which is another reason of the under estimation of the disease. Among the flu-like symptoms (tiredness, muscular pain, skeletal pain, etc.), the main one and maybe the most characteristic is the undulant fevers, with night sweats. In some cases, a clinical exam can reveal a splenomegaly or hepatomegaly (Memish, Mah et al. 2000, Basappa, Mallanagouda et al. 2006, Zhen, Lu et al. 2013). If brucellosis is not treated, two outcomes can occur: in the first one, the patients spontaneously recover or, in the second one, the disease evolves towards its chronic form. In this case, the subacute focalized form appears as the bacteria reach different organs, and can cause arthritis, spondylitis, meningitis, endocarditis, neurological disorders. Even if the death is rarely observed (less than 2 %), the majority of the death cases are due to cardio-vascular complications (Raju, Solanki et al. 2013). After this subacute phase, the chronic phase appears (until one year after the infection) and can stay for years.

In pregnant women, a first case of abortion was reported in 1908 (Eyre 1908), but since, few reports have been listed (Schreyer, Caspi et al. 1980). The studies were usually made in endemic countries, making the link between brucellosis and abortion difficult to prove (Yousuf Khan, Mah et al. 2001, Karcaaltincaba and Yalvac 2010, Ali, Akhter et al. 2016).

3.4 Treatments

The treatment against human brucellosis had to be initiated rapidly to avoid the establishment of the chronic infection. The WHO recommends a therapy based on the combination of two antibiotics, one from the Tetracyclin family (Doxycyclin) and the other one from either the aminosides family (Streptomycin, or Gentamycin) or Rifamycin family (Rifampicin) (WHO 1986). The duration of the treatment is variable and depends on the disease phase: 6 weeks for a treatment taken just after the infection, more than 3 months for the phase during which *Brucella* is already focalized and less accessible for antibiotics (WHO 1986). Unfortunately, it is too late to treat during the chronic phase. Currently, there is no vaccine for humans due to unacceptable levels of virulence, but the WHO wants to make human vaccine discovery one of its priorities (WHO 1997). The current strategy to avoid human infection and eradicate human brucellosis is to limit the cases of animal brucellosis through veterinary vaccination campaigns. Animals are also tested to identify the infected animals, which will be eliminated if they are positive to avoid the dissemination of brucellosis. However, even if the control of domestic animals is possible, the infected wild animals cannot be tested and identified. The transmission of brucellosis from wild to domestic animals remains possible. The BOX-4 summarizes the situation in Belgium.

BOX-4. And today, brucellosis in Belgium? Thanks to a campaign of eradication of the brucellosis, the disease gradually decreased since 1989 with around 500 cases of bovine brucellosis, to only 2 cases in 1999 (Godefroid 2002). Belgium became a brucellosis-free country in 2003 according to the European Union (Commission Decision 2003/467/EC). Surveys and random controls in farms are made to ensure the brucellosis-free status. Only some strains of *Brucella*, such as *B. suis* biovar[4] 2, are still present in wild animals, in hares and boars, in several countries including Belgium. In 2012, brucellosis has been discovered in farms of the Namur Province (Fretin, Mori et al. 2013). The few human cases now reported in Belgium are certainly imported cases from people coming back from Mediterranean countries, as it is the case in France for example (Mailles, Garin-Bastuji et al. 2016).

[4] Sub-group of a strain that can be differentiate from another biovar based on biochemical modifications

3.5 Diagnosis

Different diagnostic tests, most of the time serodiagnostic tests, can be used to detect *Brucella* in samples. As false-negative, false-positive results, and cross reactions with other infections like *Yersinia enterolitica* O9, *Vibrio cholerae*, and *Francisella tularensis* are frequent, the combination of several tests is often used. The **directs tests** used to detect the *Brucella* in samples are (1) the *polymerase chain reaction* (PCR) test (Fekete, Bantle et al. 1990), resulting in the amplification of the *Brucella* DNA, and (2) the hemoculture test, consisting in the search of *Brucella* in samples of lymph nodes, bone-marrow, etc (Gotuzzo, Carrillo et al. 1986). But the test currently used and recommended by the WHO is the Wright test, an **indirect test**. This test allows to detect the presence of IgM mainly, and consists in the agglutination and precipitation of antibodies-antigens complexes (Wright and Semple 1897).

3.6 *Brucella* inside the host cells: what do we know?

3.6.1 How to invade the cells? - Entry of *Brucella*

Being intracellular bacteria, *Brucellae* will rapidly enter inside cells once in an organism. *In vivo*, the main infected cells are myeloid professional phagocytic cells such as macrophages and DCs (Billard, Cazevieille et al. 2005, Archambaud, Salcedo et al. 2010, Copin, Vitry et al. 2012). But other non-professional phagocytic cells can be infected such as the trophoblast (Payne 1959), or non-phagocytic cells such as erythrocytes (Vitry, Mambres et al. 2014). The entry and the intracellular trafficking of *Brucella* have been described *in vitro* these last years. The internalization of *Brucella* inside the host cell could occur depending on two different mechanisms still little known. The first mechanism of entry could be dependent on the lipid raft and independent of opsonization. A study described that a first contact between the host and the pathogen was essential to induce the phagocytosis. The interaction components between *Brucella* and the plasma membrane of macrophages is still unknown, but different hypotheses are highlighted. It could be an interaction between a class A scavenger receptor (SR-A) of host cells with components of the outer membrane such as LPS for example (Kim, Watarai et al. 2004). Several more recent studies have shown that adhesins from the autotransporter family such as Putative surface-exposed virulence protein BigA (Czibener, Merwaiss et al. 2016), *Brucella* trimeric autotransporter (Bta) E (Ruiz-Ranwez, Posadas et al. 2013), or BtaF (Muñoz González, Sycz et al. 2019) were involved in the adhesion of *Brucella* to extracellular matrix of cells and could be the first contact between *Brucella* and cells. After this first contact,

Brucella was shown to "swim" along the macrophage surface (Watarai, Makino et al. 2002). During this time, the phagosomes transiently form, incorporating components of the plasma membrane lipid rafts (cholesterol, glycosylphosphatidylinositol (GPI)-anchored proteins, and ganglioside GM1) to their membrane with bacterium inside (Naroeni and Porte 2002).

The second mode of entry could be opsonins-dependent: once bacteria are opsonized by IgG, it will be recognized by surface receptors of the host cell, interact, and induce signals transduction to trigger the polymerization of actin at one site and then the phagocytosis (Greenberg, El Khoury et al. 1991).

3.6.2 How to reach the paradise? - Intracellular trafficking

The first steps after the internalization seem independent of the Type 4 Secretion System (T4SS), composed of *virB* genes, placed in operon (see BOX-5) (Comerci, Martinez-Lorenzo et al. 2001, Delrue, Martinez-Lorenzo et al. 2001).

BOX-5. As major actor of the entry and the surviving of *Brucella* inside its host: the *virB* operon. Briefly, the *virB* operon is a type IV secretion system first described in *Agrobacterium tumefaciens* (Ward, Akiyoshi et al. 1988), and then discovered in *Brucella* (O'Callaghan, Cazevieille et al. 1999). It is composed of 11 *virB* genes, and the proteins are assembling together in the envelope to form a transporter of molecules between the bacterium (cytoplasm or periplasm) and the outside (the vacuole or the host cytosol) (O'Callaghan, Cazevieille et al. 1999). It was shown later that *virB* operon is essential for the virulence of *Brucella* in *in vitro* (O'Callaghan, Cazevieille et al. 1999, Foulongne 2000) and *in vivo* (Hong, Tsolis et al. 2000, Sieira 2000) models, injecting its effectors in the host cell cytoplasm to control its intracellular trafficking.

Indeed, both *Brucella*-containing vacuoles (BCV) containing either wild type (wt) or *virB*-mutated strain acquire the markers of early endosomes such as Early Endosome Antigen 1 (EEA1) (Comerci, Martinez-Lorenzo et al. 2001) and transit to the phagocytic pathway (Pizarro-Cerda, Meresse et al. 1998). Around 12-24h post infection, during maturation of the BCV, the compartment with living bacteria has a pH decrease until 4 - 4.5. This acidification is dependent on vacuolar proton ATPases and is important for the bacteria replication (Porte, Liautard et al. 1999). The acidification was shown to be the trigger of the *virB* expression (Boschiroli, Ouahrani-Bettache et al. 2001) and thus indirectly to promote the secretion of

Effectors	Associated function
RicA	Regulation of vesicles trafficking
VceC	Activation of Unfolded Protein Responses
BtpA/B	Inhibition of TLR pathways
BspA/B/F	Inhibition of the secretory pathways
SepA	Inhibition of BCV fusion with the lysosome
VceA	Unknown
BspE/C	Unknown
BPE005/043/275/123	Unknown

***Table 3**: the 15 known effectors secreted by Brucella through its T4SS*

effectors essential for the trafficking of *Brucella* in the macrophages (Figure 8). Up to now, about 15 effector proteins have been identified, most of them without associated function (Ke, Wang et al. 2015), see Table 3. BtpA (or TcpB) is known to interact with MYD88, an adaptor host protein for TLR2 and TLR4. This interaction triggers the degradation of MYD88 and hence so the decrease of the signaling TLR2/4 pathways (Radhakrishnan and Splitter 2010). SepA has been shown to inhibit the fusion with lysosomes by excluding the LAMP1 lysosomal marker (Dhomer, Valguarnera et al. 2014) and RicA to regulate the vesicles trafficking (de Barsy, Jamet et al. 2011, Smith, Cotto-Rosario et al. 2020) (Figure 8). All these effectors are proposed to be used by *Brucella* at a perfect coordinated timing with the key steps of the host intracellular trafficking (Celli 2019). It has also been shown that the fusion between BCV and lysosomes was avoided thanks to another element, the periplasmic cyclic-β1-2 glucan (Arellano-Reynoso, Lapaque et al. 2005).

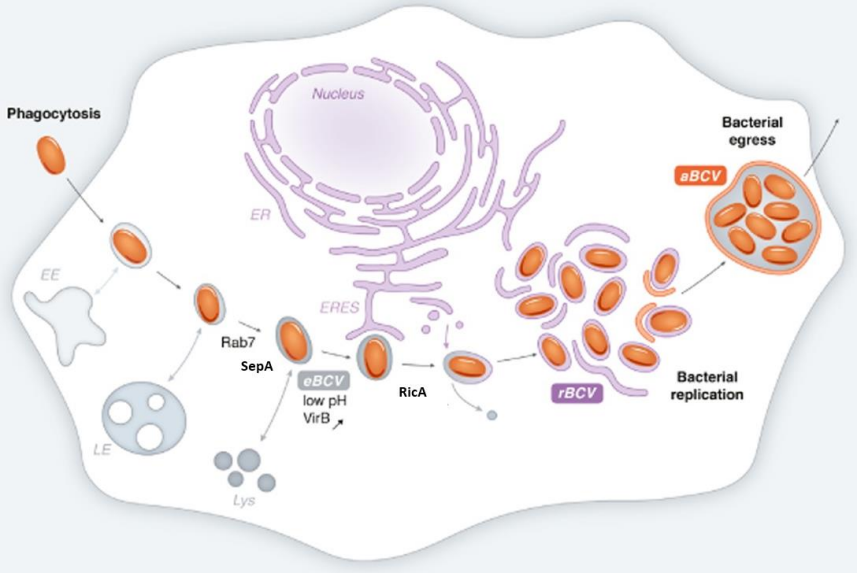

***Figure 8: Intracellular trafficking of Brucella.** After internalization, Brucella is in the BCV, that will interact with the different vesicles of the endocytic pathway of the host. At the same time, the BCV acquires specific markers. After kiss and run with lysosomes, the BCV acidifies, which triggers the expression of virB operon. Different effectors are then secreted and inhibit the complete fusion with lysosomes and promote their trafficking to the ER-like compartment (rBCV). The virB-deficient strain will fuse with lysosomes and, in the end, will be degraded. Modified from (Celli 2015).*

At the contrary of wt strains, the *virB*-mutated strains are unable to escape the fusion with lysosomes, as the BCVs have sustained association with LAMP1 and cathepsin D markers (Comerci, Martinez-Lorenzo et al. 2001, Delrue, Martinez-Lorenzo et al. 2001). The *virB*-mutated strain is thus degraded (usually between 24 and 48 h post-infection) (Figure 8), explaining why these strains are avirulent (Sieira 2000). Once the fusion with lysosomes is avoided, wt *Brucella* will reach an ER-like compartment, their replicative niche *(in vivo* and *in vitro*) (Figure 8) (Anderson, Cheville et al. 1986, Detilleux, Deyoe et al. 1990, Pizarro-Cerda, Meresse et al. 1998, Sedzicki, Tschon et al. 2018). Once in the ER, *Brucella* will trigger its replicative cycle and its growth. The replicative BCV (rBCV) is in interaction with the ER and Golgi apparatus, from which *Brucella* is able to use the resources of the host. More the bacteria replicate inside the replicative niche, more the structure of the ER is modified (Celli, de Chastellier et al. 2003, Celli 2019). Following replication in the ER, the rBCV are transformed into autophagic BCV (aBCV) through a mechanism dependent on the autophagy initiation process, involving Beclin1 and Autophagy-related protein (ATG) proteins and the formation of a double membrane around *Brucella*. This structure will help the egress of bacteria outside the cell, ready to infected new cells and to start a new cycle of replication, at 72 h post infection (Starr, Child et al. 2012, Celli 2015).

3.6.3 How to reproduce? - Replication of *Brucella*

It has been shown that *B. abortus* is blocked in G1 phase, the first step of the replicative cycle, during the first hours post infection in HeLa cells and RAW 264.7 macrophages. *B. melitensis,* such as the other *Brucella* species*,* contains two unique chromosomes of 2.1 and 1.15 millions of base pairs for each chromosome (Michaux, Pailisson et al. 1993). Each chromosome has its own origin of replication and its own segregation system. Chromosomal replication and bacterial growth are two mechanisms taking place at the same time (Figure 9 a). The membrane staining with the Texas Red Succinimidyl Ester (TRSE) allows to study the replication of *Brucella* by labelling the primary amines of its outer membrane (Deghelt, Mullier et al. 2014). Thanks to the polar growth and asymmetric division of *Brucella,* the different phases of division are easily discerned (Figure 9 b). At the beginning of the staining, all bacteria are labelled. Then, after growth and division, the newly formed bacteria lose the TRSE staining, allowing to distinguish the bacteria from the infectious dose (mother bacteria) of the bacteria after growth and division (daughter bacteria) (Figure 9 b). The eFluor^{670} staining works in the same way, but is conjugated to another fluorochrome.

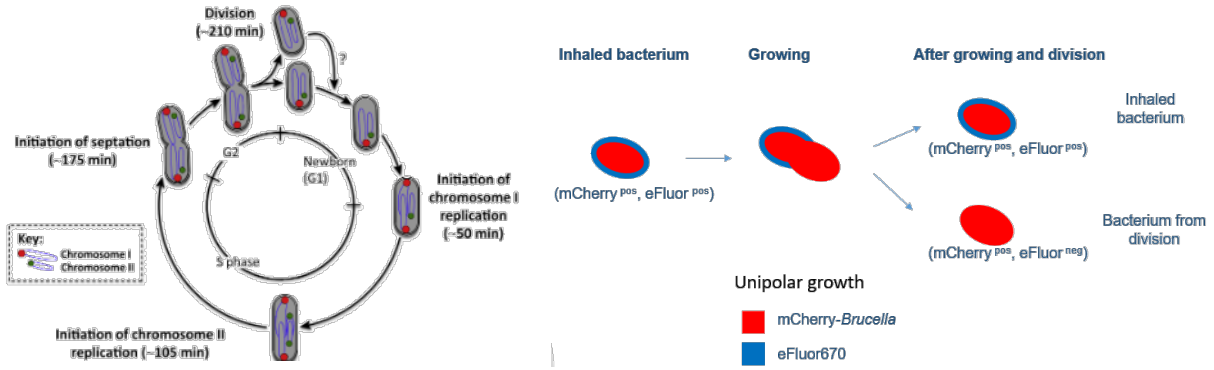

Figure 9: Replication of Brucella chromosomes (a), and labeling of outer membrane proteins to distinguish mother and daughter bacteria (b)*. A. To replicate, Brucella initiates first the replication of its 1st chromosome, followed by initiation of the replication of the 2nd one (during the S phase). At the same time, the bacterium grows. Then, during the G2 phase, the septation is initiated, followed by the division. Each newborn bacterium possesses the two chromosomes, with their own origin of replication. B. Schematization of a modified strain that expresses constitutively the mCherry gene and labelled before use with eFluor670. The "mother bacteria" are positive for both stainings (mCherrry and eFluor670). As Brucella has a unipolar growth, and that primary amines do not move in the outer membrane, the "daughter bacteria" loose the eFluor670 staining after growth and division.*

3.6.4 How to be a perfect Trojan horse? - Adaptations to the host

Both passive and active mechanisms allow to *Brucella* to be almost undetected by the immune system and to have a chance to survive in an austere environment.

As **passive mechanisms**, there is for example the modification or the absence of elements that are normally detected by the host TLRs: the PAMPs. For Example, *Brucella* does not possess pili, fimbriae, or capsules (Moreno and Moriyon 2002). Moreover, its LPS, lipoproteins and flagellin components are poorly detected by the host immunity. Indeed, the Lipid A of the *Brucella* LPS contains a long fatty acids chain of 16-18 carbons (rather than 12-14 in LPS of other bacteria), leading to a poor endotoxicity and a low detection by the immune system (through the MD2-TLR4 complex) (Conde-Alvarez, Arce-Gorvel et al. 2012). In addition, the O-chain of *Brucella* LPS is longer than in other bacteria, leading to a steric hindrance, avoiding the action of complement (Barquero-Calvo, Chaves-Olarte et al. 2007). Finally, as both the Lipid A and the core of *Brucella* LPS present lower number of charged groups leads to a low permeability and so a resistance to cationic peptides action (Martinez de Tejada, Pizarro-Cerda et al. 1995, Barquero-Calvo, Chaves-Olarte et al. 2007). As the LPS is poorly detected, the macrophages are weakly activated and induce low amount of pro-inflammatory cytokines such as TNF-α, IL-1β, IL-6 or IL-10 (Barquero-Calvo, Chaves-Olarte et al. 2007).

As **active mechanisms**, it has been published that *Brucella* was able to decrease the secretion of TNF-α, in an outer membrane protein (OMP)-25 and micro-RNA dependent manner (Billard, Dornand et al. 2007, Luo, Zhang et al. 2018). This leads to a weak maturation of DCs, with only a small increase in the maturation markers C-C chemokine receptor (CCR)7 and CD83. Due to this, the activation of naive T lymphocytes is weakly induced (Billard, Dornand et al. 2007). As already mentioned, *Brucella* is also able to inhibit the TLR4 signaling pathway via its effector molecule TcpB interfering with upstream elements (Sengupta, Koblansky et al. 2010) and to induce IL-10 by Treg cells in order to inhibit TH1 response (Corsetti, de Almeida et al. 2013)

II. The comparison of the routes of infection

1 What is known from the different *in vivo* infection murine models

Despite the fact that natural hosts of *B. abortus*, *B. melitensis*, and *B. suis* are cattle, sheep and goats, and suidae, respectively, the mice are often used as an experimental model to study brucellosis (Grilló, Blasco et al. 2012). To infect mice, different routes of injection have been used, with results sometimes completely different. Here are some examples of used routes.

1.1 The intraperitoneal route, the most currently used

The intraperitoneal (i.p.) route consists in injecting *B. melitensis* in the right side of the peritoneum of the mice. This route of injection allows the use of big volume (500 µl / mouse) limiting the precision errors. However, it is absolutely not physiological as numerous defenses are bypassed such as the mucosal barriers. After this inoculation, the bacteria directly reach the bloodstream and quickly colonize the spleen, only after 10 minutes with a high dose of 10^8 bacteria per mouse (Copin, Vitry et al. 2012). *B. melitensis* can persist in the spleen for more than 50 days (Machelart, Khadrawi et al. 2017). Once the blood and the spleen infected, the colonization of the other organs rapidly expands. It has been shown in this model that the main infected cells in the spleen are the resident macrophages (the red pulp and the marginal zone macrophages), the recruited monocytes, and the inflammatory DCs (Copin, Vitry et al. 2012). In the primary response against *B. melitensis*, the IFN-γ cytokine is crucial to control the infection. IFN-γR-knock-out (KO) mice have an excessive recruitment of neutrophils, and a higher number of granulomas formation than wt mice. These IFN-γR-KO mice die of lack of monocytes and hyper-neutrophilia, demonstrating the importance of an efficient TH1 response in this model. Indeed, the TH1 CD4 T cells are indispensable to control the infection, as infected MHCII- and IL12p35-deficient mice have a higher number of colony forming units (CFU) than wt mice (Vitry, De Trez et al. 2012). Even if CD8 T cells and B cells are also activated, their role is not indispensable (Vitry, De Trez et al. 2012). Granulom formation was observed in the spleen of infected mice. These structures are composed of infected macrophages and DCs, surrounded by T cells and their role is to centralize the bacteria near an arsenal of destruction

(Copin, Vitry et al. 2012). During a second infection, humoral and cellular responses are indispensable. Indeed, MuMT-deficient mice (mice deficient for B cells) are more susceptible to the *B. melitensis* secondary infection than wt mice. In the same study (Vitry, Hanot Mambres et al. 2014), it is suggested that IgM alone seem to be sufficient for the control of the second infection. As the MHCII- and IL12p35-deficient mice have an increase in CFU in comparison to wt mice, that suggests that TH1 CD4 T cells are a key element in the control of secondary infection by *Brucella,* after an i.p. injection (Vitry, Hanot Mambres et al. 2014).

1.2 The intragastric and oral routes

Through the intragastric route, by gavage, a lot of challenges are highlighted: the microbiota, the acidity of the stomach, the epithelial cells, the local immune responses, the bile salts, etc. To successfully infect mice via this route, a high dose of *B. melitensis* (10^{10} bacteria per mouse) is recommended to obtain a systemic infection of mice, especially at early infection stages (Paixao, Roux et al. 2009). The first sites of *Brucella* entry are the small intestine, the Gut-Associated lymphoid tissues (GALT), but also the Peyer's patches and the mesenteric and cervical lymph nodes (Paixao, Roux et al. 2009, von Bargen, Gagnaire et al. 2014). Even if some bacteria also enter by the upper tract, one problem of this route of infection is that a lot of bacteria directly arrive in the stomach, extracellularly, and without food bolus around. This leads to a direct contact with bile salts and acidity that affect bacteria. It has been shown that a neutralization of the acidity leads to a faster and homogenous infection (Pasquali, Rosanna et al. 2003). To survive in these unfavorable conditions, *Brucella* bacteria possesses bile salts hydrolase (Delpino, Marchesini et al. 2007) and urease. *B. abortus* (Sangari, Seoane et al. 2007) and *B. suis* (Bandara, Contreras et al. 2007) seem to have a higher urease activity than *B. melitensis* (Paixao, Roux et al. 2009). One of the main problem of this mouse model is the bypass of the upper digestive tract tissue.

In another more recent model, mice are orally infected with 10 µL of *B. melitensis* suspension in milk, using a micropipette (von Bargen, Gagnaire et al. 2014). In this model, *B. melitensis* could be internalized by DCs that migrate into the cervical lymph nodes *(von Bargen, Gagnaire et al. 2014)*. This site could play a role of filter, but also of reservoir for *Brucella* (von Bargen, Gagnaire et al. 2014). The bacteria which bypass the local immune response of the host could invade the gastrointestinal tract via the M cells of the Peyer's Patches (Nakato, Hase et al. 2012). Following this infection, bacteria are directly in contact with saliva, containing

lysozyme, lactoferrin, peroxidases, and IgA, but also with gingival fluid, containing complement molecules, neutrophils, etc. In the mucosal tissue, the infected cells migrate into the lymph nodes to activate the T cells. Bacteria are found in these lymph nodes for weeks (von Bargen, Gagnaire et al. 2014). This could be the natural entry of *Brucella* after the ingestion of contaminated products, but also a good reservoir (von Bargen, Gagnaire et al. 2014).

1.3 The intranasal route, a physiological one?

1.3.1 Generalities

A more physiological route of infection is certainly the infection by aerosols using an exposure chamber and a nebulizer. Experimentally, the infection by aerosols has been demonstrated in guinea pigs in 1948 with *B. melitensis* and *B. suis* (Elberg and Henderson 1948). Around 240 organisms were sufficient to infect the half of the animals (Elberg and Henderson 1948). The intranasal infection can also require only anesthesia and a micropipette (Mense, Van De Verg et al. 2001). It is not to exclude that conjunctival, or oral mucosal infections occur during this mode of infection (Grillo, Blasco et al. 2012). After an intranasal route of infection, the bacteria are rapidly found in the lungs at almost similar doses than the infectious dose (Hanot Mambres, Machelart et al. 2016). However, bacteria are not found in the bloodstream, at any tested times (Hanot Mambres, Machelart et al. 2016), suggesting why *Brucella* only reaches the spleen and other organs after around 6 days post infection, with a dose of $2x10^4$ bacterial / mouse (Hanot Mambres, Machelart et al. 2016). At the local site of the infection, no alterations are observed: no histopathological lesions, no granuloma, no cells recruitment during the first 48 hours (Hanot Mambres, Machelart et al. 2016).

1.3.2 Mucosal immunity

After intranasal infection, *Brucella* first joins the upper airways, constituted of the oral and nasal cavities, and the larynx. The lower airways are composed of trachea, bronchi, bronchioles and alveoli (Figure 10). The role of bronchioles is mainly to ensure the air conduction from outside to inside. The function of alveoli is to ensure the gaseous exchange. As the functions are different, it is normal that the structure and the immunity of these different parts are different too. The tracheal mucosal barrier is constituted of pseudo-stratified layer composed of ciliated epithelial cells, Goblet cells, and undifferentiated basal cells. This barrier is one of the first ones encountered by *Brucella* after an intranasal infection. It is characterized by the production of mucus, composed of mucin and glycoproteins, by the Goblet cells and the Mucosal-associated

lymphoid tissue (MALT), but also defensins, cytokines, chemokines. The mucus is the first physical barrier that pathogenic agents have to face. The viscosity of the mucus prevents the adhesion of pathogenic agents to the epithelium, traps the pathogenic agents or debris that will be expelled thanks to mechanic movements of cilia and sneezing and coughing. In addition, the mucus contains antimicrobial peptides, lysozyme and surfactant that affect the bacterial membranes (Chairatana and Nolan 2017). The IgA also present in the mucus allow to clutter the bacteria and prevent them to adhere to the epithelium (Chairatana and Nolan 2017). In the case of *Brucella* infections, the humoral response itself does not seem to have an important role (Hanot Mambres, Machelart et al. 2016). The non-lymphoid tissues are composed of different immune cells such as macrophages, DCs, lymphocytes, etc., leading to a good detection of pathogenic agents and a good immune stimulation. As already mentioned, the epithelial cells

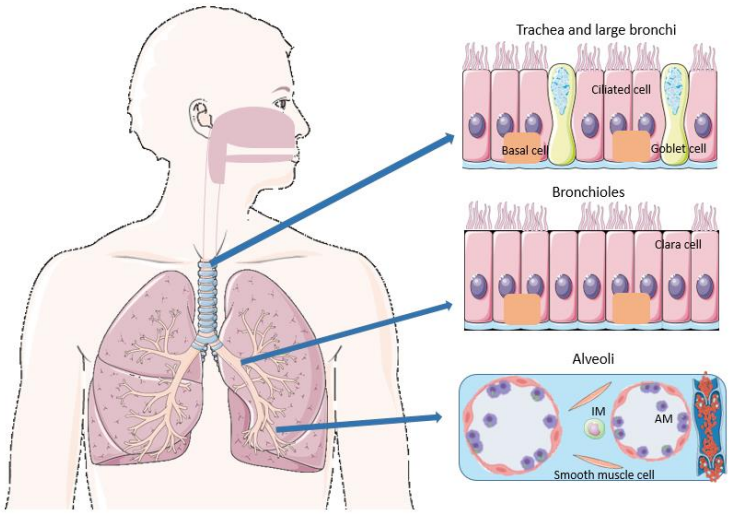

Figure 10: The lower respiratory tract is composed of the trachea and large bronchi (1), the bronchioles (2), and the alveoli (3). *The membrane of trachea and bronchi is mainly composed of ciliated epithelial cells, basal cells, Goblet cells, producing the mucus. The bronchial mucosa is mainly composed of ciliated epithelial cells, and basal cells. Finally, the alveoli are composed of alveolar macrophages, interstitial macrophages, smooth muscle cells, blood vessels.*

express TLRs and are able to secrete cytokines and chemokines in response to pathogenic agents detection. DCs and macrophages are then activated, T cells and neutrophils are recruited. Once infected, APCs (Antigen presenting cells) directly migrate, via the lymphatic vessels, to lymph nodes to activate lymphocytes. If *Brucella* successes to bypass the first barriers, bacteria will reach the alveoli, and infect alveolar macrophages, the first and main infected cells up to 48 h post infection (Figure 10). The alveolar macrophages are specific macrophages from alveoli, and are able to patrol and control in and between alveoli. They have a high efficiency to phagocyte inhaled bacteria as the lungs are in contact with non-sterile air constantly (Neupane, Willson et al. 2020). But then, *Brucella* is able to evade these cells and to disseminate

to other organs such as the spleen, and several lymph nodes such as the mediastinal ones (Archambaud, Salcedo et al. 2010). As the mucosal immunity is in contact with the external environment, the immune response is a precise balance to tolerate the commensal bacteria but fight against the external bacteria. The alveolar macrophages, the DCs, the neutrophils, and the lymphocytes must be highly regulated.

Concerning the primary immune response against *Brucella*, in the lungs of C57BL/6 mice, an IL-17-mediated response associated to γδ T cells is indispensable the first 5 days p.i. (Hanot Mambres, Machelart et al. 2016). Later, at 12 days p.i., IL-12/IFN-γ axis, in association with CD4 T cells, is indispensable in the lungs (Hanot Mambres, Machelart et al. 2016). Finally, in the spleen after 12 days p.i., IFN-γ, produced by CD4 T cells, is essential. However, B cells are dispensable (Hanot Mambres, Machelart et al. 2016). After a secondary infection with *Brucella*, a good protection is observed in the lungs. This protection is associated to T cells (αβ CD3 T cells), suggesting a compensatory role of CD4 and CD8 T cells (Hanot Mambres, Machelart et al. 2016). As either IL-12p35- or IL-17-deficient mice are not susceptible to the infection, this also suggests a compensatory role between TH1 and TH17 responses (Hanot Mambres, Machelart et al. 2016). In contradiction with the i.p. model, B cells are dispensable, even after a secondary infection, suggesting that bacteria could already be intracellular (Hanot Mambres, Machelart et al. 2016). IL-1, via the action of IL-1β and "NOD-like receptor family, pyrin domain containing 3" (NLRP3) inflammasome, could play a role in the control of *Brucella* in the lungs (Hielpos, Fernandez et al. 2018).

1.4 The intradermal route

1.4.1 Generalities

As mentioned above in the general introduction, *Brucella* infection via cutaneous lesion can occur in natural wild life, but also in some work like it is the case for vets or butchers for examples. To mimic this route of infection, an intradermal model with injection in the footpad has been developed. The infection in the footpad has the advantages that the site of infection is drained by an easy take-away lymph node (popliteal one) (Kawashima, Sugimura et al. 1964), and that local and systemic studies are possible (Pardon 1977). The injection being made with a needle in a small place, skin lesion, tissue destruction, and so local inflammation are produced (Gray and Jennings 1955, Kamala 2007). However, this could actually mimic the skin lesion made with a vets or butcher's instrument (knife, scissors, needle, etc.), but also by a bite of

insects. Indeed, an experiment showed that *B. abortus* could persist transiently in the midgut of *Musca autumnalis*, a face fly very abundant in the cattle population (Cheville, Rogers et al. 1989). Taken together, and with the fact that *Brucella* is able to invade erythrocytes of mice (Vitry, Mambres et al. 2014), the contamination with *Brucella* by a bite of insects, through the dermis, is a plausible hypothesis.

After the mice intradermal injection, bacteria are rapidly found in the popliteal lymph node (Pardon 1977), in the blood and in the spleen (Plommet and Plommet 1983).

1.4.2 Skin immunity

The skin constitutes the layer at the interface between outside and inside environments and is composed of three sub-layers: epidermis, dermis and hypodermis. The first one is directly in contact with the environment. Thanks to lamellar bodies and lipids, a hydrophobic barrier is created. The epidermis is a stratified epithelium mainly composed of keratinocytes, which are continually renewed, and Langerhans cells. The dermis is mainly composed of macrophages, DCs, and T cells (Matejuk 2018).

By producing keratin, a fibrous protein, keratinocytes play a role of protection and support. They also produce antimicrobial peptides playing an important role of defense against pathogenic agents invasion. Keratinocytes express TLRs, allowing them to produce IFN-γ upon activation (Lebre, van der Aar et al. 2007, Miller 2008). These cells also express MHCII on their surface. Finally, keratinocytes are able to produce different cytokines (IL-1β, IL-10, etc.) and chemokines (CXCL9, CXCL10, CCL20, etc.) (Lebre, van der Aar et al. 2007). The Langerhans cells are the resident DCs of the skin. Their main role is to capture antigens thanks to their dendrites and they are also able to secrete different cytokines such as TNF-α upon stimulation of their expressed TLRs (Miller 2008).

In the dermis, the dermal DCs are able to stimulate B cells leading to the production of IgM (Dubois, Bridon et al. 1999). As keratinocytes, dermal DCs express TLRs at their surface (Angel, Lala et al. 2007) and are able to produce TNF-α and iNOS. The T lymphocytes (CD4 and CD8) continually circulate and other are recruited at the site of infection when necessary. The lymphocytes role was detailed above in the general introduction. The mast cells, the macrophages and the innate lymphoid cells also play a great role in the skin immunity by secreting different enzymes, cytokines, chemokines to modulate the immune system (Burke,

Issekutz et al. 2008). The mouse skin has the particularity to have a specific population of T cells expressing the γδ-TCR receptor: the dendritic epidermal T cells (DETCs). These cells monitor and recognize the non-self antigens and the stress signals of surrounding cells. Once a stress is detected, the DETC secrete chemokine and cytokines such as IL-17 and IFN-γ, etc. to modulate the skin inflammation (Asarnow, Goodman et al. 1989, Nielsen 2014).

1.5 Other routes of infection

Briefly, the mode of transmission via the milk was suggested by Grillo et al. who showed that one of the targeted organ of *Brucella* could be the lymph nodes of the mammary glands (Grillo, Barberan et al. 1997). However, other sources suggested that there are few *Brucella* in the mammary gland (1 to 10^3) - in a mouse model - and that the successive sucking could proffer a resistance to this bacterium (Bosseray and Dufrenoy 1982) as well as the transfer of protective antibodies (Brambell 1970) leading to a low level of infection via the milk.

Bosseray also showed in a mouse model that 60 % of the offspring was infected at birth probably by vertical transmission, and that the placental barriers, in a same uterus, could have a different efficiency to protect the fetus as all the fetuses from a same uterus were not infected (Bosseray and Dufrenoy 1982).

2 Objectives

Live attenuated vaccines are considered as the most efficient vaccines against intracellular pathogens. They are able to mimic natural infections, to induce a long-term humoral and cellular immunity. The first generations of live attenuated vaccines were produced in an empiric manner, by successive passages in different media, waiting for spontaneous mutations. But this empiric production cannot prevent the risk of reversion to wild type virulence or the risk of disease in immune compromised people or animals. A rational development of live attenuated vaccines should bypass these problems and produce more safety vaccines. In this development, a first step is to better understand the influence of the infection route in the identification of infected cells, virulence genes and the nature of the protective immune response. For that, we decided to compare different parameters in three *in vivo* infection models. After intraperitoneal, intranasal or intradermal mouse infection by *Brucella melitensis*, we will compare the course of the infection in organs, the main cellular reservoirs of infection and the virulence genes involved in the persistence of *B. melitensis*. Another very important parameter is the identification of immune markers of protection, such as the type of T helper response and the lymphoid subpopulations indispensable to have a protective immunity.

3 Article

frontiers in Immunology

ORIGINAL RESEARCH
published: 11 July 2019
doi: 10.3389/fimmu.2019.01589

Route of Infection Strongly Impacts the Host-Pathogen Relationship

*Aurore Demars[1], Aurore Lison[1], Arnaud Machelart[1], Margaux Van Vyve[1], Georges Potemberg[1], Jean-Marie Vanderwinden[2], Xavier De Bolle[1], Jean-Jacques Letesson[1] and Eric Muraille[1,3]**

[1] Unité de Recherche en Biologie des Microorganismes, Laboratoire d'Immunologie et de Microbiologie, NARILIS, Université de Namur, Namur, Belgium, [2] Laboratory of Neurophysiology, Université Libre de Bruxelles, Brussels, Belgium, [3] Laboratoire de Parasitologie, Faculté de Médecine, Université Libre de Bruxelles, Bruxelles, Belgium

Live attenuated vaccines play a key role in the control of many human and animal pathogens. Their rational development is usually helped by identification of the reservoir of infection, the lymphoid subpopulations associated with protective immunity as well as the virulence genes involved in pathogen persistence. Here, we compared the course of *Brucella melitensis* infection in C57BL/6 mice infected via intraperitoneal (i.p.), intranasal (i.n.) and intradermal (i.d.) route and demonstrated that the route of infection strongly impacts all of these parameters. Following i.p. and i.n. infection, most infected cells observed in the spleen or lung were F4/80$^+$ myeloid cells. In striking contrast, infected Ly6G$^+$ neutrophils and CD140a$^+$ fibroblasts were also observed in the skin after i.d. infection. The *virB* operon encoding for the type IV secretion system is considered essential to deflecting vacuolar trafficking in phagocytic cells and allows *Brucella* to multiply and persist. Unexpectedly, the Δ*virB Brucella* strain, which does not persist in the lung after i.n. infection, persists longer in skin tissues than the wild strain after i.d. infection. While the CD4$^+$ T cell-mediated Th1 response is indispensable to controlling the *Brucella* challenge in the i.p. model, it is dispensable for the control of *Brucella* in the i.d. and i.n. models. Similarly, B cells are indispensable in the i.p. and i.d. models but dispensable in the i.n. model. γδ$^+$ T cells appear able to compensate for the absence of αβ$^+$ T cells in the i.d. model but not in the other models. Taken together, our results demonstrate the crucial importance of the route of infection for the host pathogen relationship.

Keywords: *Brucella melitensis*, brucellosis, infection control, live vaccine, virulence genes, reservoir cells

OPEN ACCESS

Edited by:
Maria Isabel Colombo, Universidad Nacional de Cuyo, Argentina

Reviewed by:
Luis Mayorga, CONICET Mendoza, Argentina
Pablo C. Baldi, University of Buenos Aires, Argentina

***Correspondence:**
Eric Muraille
emuraille@hotmail.com

Specialty section:
This article was submitted to Microbial Immunology, a section of the journal Frontiers in Immunology

Received: *01 March 2019*
Accepted: *25 June 2019*
Published: *11 July 2019*

Citation:
Demars A, Lison A, Machelart A, Van Vyve M, Potemberg G, Vanderwinden J-M, De Bolle X, Letesson J-J and Muraille E (2019) Route of Infection Strongly Impacts the Host-Pathogen Relationship. Front. Immunol. 10:1589. doi: 10.3389/fimmu.2019.01589

INTRODUCTION

Live attenuated vaccines (LAVs), composed of live pathogens that are made much less virulent than the pathogenic parental strains, are one of the most cost effective health tools in medical history [for review see (1–3)]. The advantages of LAVs include their mimicry of natural infections, the stimulation of long-term humoral and cellular immunity and their intrinsic adjuvant properties. First generation LAVs relied on empirical and somewhat unpredictable attenuation. In the present regulatory environment, the use of LAVs has been limited by safety concerns, especially due to the risk of reversion to wild-type virulence and the possibility of causing disease in immune compromised individuals. However, advances in immunology, molecular virology and bacteriology have paved the way for the rational design of LAVs while avoiding the unpredictability of empirical attenuation to thus reduce the safety risks.

Rational design of LAVs requires good knowledge of the *in vivo* infection process. In particular, the pathogen's cell cycle, main reservoirs of infection and the virulence genes involved in persistence of the pathogen can be characterized in order to help select the most effective candidate vaccines. However, one of the biggest remaining challenges is the identification of immune markers of protection, such as the type of T helper response and the lymphoid subpopulations associated with protective immunity (4). In the current study, we use the *Brucella* infection in mice as a model to investigate the impact of the route of infection on the identification of these parameters.

Brucella (an alphaproteobacterium) is a facultative intracellular Gram-negative coccobacillus that infects wild and domestic mammals and causes brucellosis. Human brucellosis is among the most common zoonoses (5). The vast majority of cases worldwide are attributed to *B. melitensis* [reviewed in Pappas et al. (6)]. Although it is rarely fatal, *Brucella* can cause a devastating multi-organ disease in humans with serious health complications in the absence of prolonged antibiotic treatment (6, 7). Human brucellosis primarily occurs following mucosal exposure to contaminated aerosols or ingestion of contaminated foods (8–12). However, in some occupational groups, such as cattle dealers, butchers, veterinarians, and farmers, it is well-documented that brucellosis can be acquired directly through contact of broken skin with infected animals (13, 14). The frequency of direct cutaneous infection is difficult to determine and could be underestimated as cutaneous manifestations of brucellosis are known to disappear spontaneously in patients (15).

During infection, *B. melitensis* mainly leads a stealthy intracellular lifestyle (16). Effector proteins secreted by the type IV secretion system (T4SS), which is encoded by the *virB* operon, are involved in the establishment of intracellular replicative niches. *B. melitensis* strains lacking a functional T4SS appear to be highly attenuated in mice and in their natural host, the goat [reviewed in De Jong and Tsolis (17)]. *In vitro* experiments using macrophage cell lines have shown that the T4SS is required for maturation of the *Brucella* phagosome into an endoplasmic reticulum-derived compartment (18).

Although the most frequent natural routes of *Brucella* infection are mucosal or cutaneous, the main experimental model for studying brucellosis in mice is intraperinoneal (i.p.) infection, which bypasses mucosal immune defenses and leads to infection that very rapidly becomes systemic. Over the last decade, our group characterized the phenotype of infected cells and the protective response against *Brucella* in an i.p. model (19, 20) and compared it to a model of intranasal (i.n.) infection (21). Taken together, those studies demonstrated that the lymphocyte populations required to control a *Brucella* challenge in each infectious model differed widely. The $CD4^+$T cell-mediated Th1 response and B cells are indispensable in the i.p. model (20) but appear to be dispensable in the i.n. model (21).

To our knowledge, there is no described experimental model of cutaneous *Brucella* infection in mice. Only one study (22) describes cutaneous injection with *Brucella abortus* in the footpad of guinea pigs and the development of protective memory. Thus, in the present study, we developed and characterized an original intradermal (i.d.) infection model in mice. We compared the dissemination of wild-type and *virB*-deficient strains of *Brucella* and the type of cells infected and the protective immune response in the i.d., i.n., and i.p. models. This approach led us to conclude that the route of infection has unexpected major consequences on the host-pathogen relationship and should definitely be considered when selecting LAVs.

MATERIALS AND METHODS

Ethics Statement

The procedures used in this study and the handling of the mice complied with current European legislation (Directive 86/609/EEC) and the corresponding Belgian law "Arrêté royal relatif à la protection des animaux d'expérience" of 6 April 2010 and published on 14 May 2010. The Animal Welfare Committee of the Université de Namur (UNamur, Belgium) reviewed and approved the complete protocol for *Brucella melitensis* infection (Permit Number: UN-LE-13/195).

Mice and Bacterial Strains

Wild-type C57BL/6 and BALB/c mice were acquired from Harlan (Bicester, UK). TCR-$\delta^{-/-}$, CD3$\varepsilon^{-/-}$, TCR-$\beta^{-/-}$, MuMT$^{-/-}$, CCR2$^{-/-}$, and CCR7$^{-/-}$ C57BL/6 were all purchased from The Jackson Laboratory (Bar Harbor, ME). IFN-γR$^{-/-}$ (23) and IL-12$_{p35}^{-/-}$ C57BL/6 mice (24) were acquired from Dr. B. Ryffel (University of Orleans, France). IL17RA$^{-/-}$ C57BL/6 mice (25) were acquired from Dr. K. Huygen (Belgian Scientific Institute for Public Health, Brussels, Belgium). TNFR1$^{-/-}$ C57BL/6 (26) were acquired from Dr. C. De Trez (Vrije Universiteit Brussel). TAP1$^{-/-}$ C57BL/6 mice (27) and MHCII$^{-/-}$ C57BL/6 mice (28) were acquired from Jörg Reimann (University of Ulm, Ulm, Germany). All wild-type and deficient mice used in this study were bred in the animal facility of the Gosselies campus of the Université Libre de Bruxelles (ULB, Belgium). We used wild-type strains of *Brucella melitensis* 16M. We also used *Brucella melitensis* 16M stably expressing a rapidly maturing variant of the red fluorescent protein DsRed (29), the mCherry protein, under the control of the strong *Brucella* spp. promoter, p_{sojA}. The construction of the mCherry-expressing *Brucella melitensis* (mCherry-*B*) strain has been described previously in detail (30). The Δ*virB* mutant was constructed in the mCherry-*B* strain by triparental mating to introduce the pJQ200 UC1-*virB* plasmid from the *E. coli* DH10B strain [described in Nijskens et al. (31)] into the mCherry-*B* strain using the *E. coli* MT 607 (pro-82 thi-I hsd R17 (r-m+) supE44 recA56 pRK600) strain [described in Casadaban and Cohen (32)], and the allelic replacement was performed as described previously for other gene deletions (33). Deletion of the *virB* operon was checked by PCR using the *virB*-F-check 5′-CGCTCGGCTATTATGACGGC-3′ and *virB*-R-check 5′-CGCCGATCATAACGACAACGG-3′ primers.

Cultures were grown overnight with shaking at 37°C in 2YT liquid medium (Luria-Bertani broth with double quantity of

yeast extract) and were washed twice in RPMI 1640 (Gibco Laboratories; 3,500x g, 10 min) before inoculation of the mice.

Brucella melitensis was always handled under BSL-3 containment according to Council Directive 98/81/EC of 26 October 1998 and a law of the Walloon government of 4 July 2002.

Brucella melitensis Staining With eFluor670

For some experiments, we stained *Brucella melitensis* with eFluor670 labeling. Cultures were grown overnight as indicated above and we then incubated the bacteria for 20 min in the dark with eFluor670 dye at the final concentration of 10 μM. After incubation, the bacteria were washed three times in PBS and once in RPMI before inoculation of the mice.

Measurement of *Brucella melitensis* Multiplication *in vitro*

The growth of *Brucella melitensis* in liquid culture was monitored continuously using the multiwell Bioscreen system (Thermo Fisher, ref. 110001-536). The *B. melitensis* cultures in 2YT medium were centrifuged, washed once with PBS and diluted to an OD_{600} of 0.05 in 2YT to start culture in the Bioscreen system. Each sample (200 μl per well) was cultured at 37°C for 48 h.

Brucella melitensis Infection *in vivo*

We used wild-type or mCherry-expressing *Brucella melitensis* in RPMI [described in Copin et al. (30)]. Control animals were inoculated with the same volume of PBS. The infectious doses were validated by plating serial dilutions of the inoculums. For i.n. infection, mice were anesthetized with a cocktail of Xylasine (9 mg/kg) and Ketamine (36 mg/kg) in PBS before being inoculated with 30 μl of the indicated dose of *Brucella melitensis*. For i.d. infection, mice were anesthetized by inhalation of Isofluran before injecting 20 μl of the indicated dose of *Brucella melitensis*. For i.p. infection, mice were injected with 500 μl intraperitoneally without anesthesia.

Protocol for Secondary Infection With *Brucella melitensis*

C57BL/6 mice were immunized intranasally (i.n.), intradermally (i.d.) or intraperitoneally (i.p.) as indicated, with 2×10^4 CFU of live wild type *B. melitensis*. The infectious doses were validated by plating serial dilutions of inoculums. 28 days after immunization, the mice were given antibiotics for 15 days to clear the infection. This oral treatment was a combination of rifampicin (12 mg/kg) and streptomycin (450 mg/kg; adapted from Vitry et al. (20)] prepared fresh daily and given in the drinking water. To ensure that the antibiotic treatment was effective, some mice in each group were sacrificed 1 week prior to the challenge and the CFU counts were evaluated in the spleen. After resting for an additional 15 days, the mice were challenged i.n., i.d. or i.p., as indicated with 2×10^4 CFU of live mCherry-*B. melitensis* and sacrificed at the indicated times.

Footpad Lesion Monitoring

The thickness of *Brucella melitensis* infected footpads was measured regularly with a metric caliper, and corresponded to the size of the footpad lesions.

Brucella melitensis Counting in Mice

At the selected time post infection, we collected 75 μl of blood from the mice. They were then sacrificed by cervical dislocation. Immediately after sacrifice, the spleen, liver (one lobe), footpad, lung (left), mediastinal lymph node, thymus, muscle (1 square cm of thigh muscle), heart, brain, tail (2 mm), ovary, popliteal lymph node (depending on the experiment) were collected for bacterial counting. Tissues were crushed and transferred to PBS/0.1% X-100 Triton (Sigma-Aldrich). We performed successive serial dilutions in PBS to obtain the most accurate bacterial count and plated them on 2YT agar plates. The CFU were counted after 5 days of culture at 37°C.

Cytofluorometric Analysis

The lungs were harvested and cut into small pieces. As described previously (21), spleens and footpad lesions were harvested, cut into small pieces and incubated for 1 h at 37°C with a mix of 100 μg/ml of DNAse I fraction IX (Sigma-Aldrich) and 1.6 mg/ml of collagenase (400 Mandl U/ml). The cells were then washed and filtered, and incubated with saturating doses of purified 2.4G2 (anti-mouse Fc receptor, ATCC) in 200 μl PBS, 0.2% BSA, 0.02% NaN3 (FACS buffer) for 20 min at 4°C to prevent antibody (Ab) binding to the Fc receptor.

$3–5 \times 10^6$ cells were stained on ice with various fluorescent mAb combinations in FACS buffer. We acquired the following mAbs from BD Biosciences: BV421-coupled T45-2342 (anti-F4/80), BV421-coupled M1/70 (anti-CD11b), fluorescein (FITC)-coupled 145-2C11 (anti-CD3ε), FITC-coupled 30-F11 (anti-CD45), FITC-coupled M1/70 (anti-CD11b), phycoerythrin (PE)-coupled HL3 (anti-CD11c), PE-coupled 1A8 (anti-Ly6G), allophycocyanin (APC)-coupled BM8 (anti-F4/80), biotin-coupled 2G9 (anti-MHCII, I-A/I-E). Biotin-coupled APA5 (anti-CD140a/ PDGFRA) was purchased from eBioscience. The biotin-coupled Abs were incubated with streptavidin-coupled APC for 30 min. The cells were analyzed on a BD FacsVerse flow cytometer. Dead cells and debris were eliminated from the analysis according to size and scatter.

Fluorescence Microscopy of *Brucella melitensis in vitro*

Brucella melitensis strains were observed with a Nikon 80i (objective phase contrast × 100, plan Apo) connected to a Hamamatsu ORCA-ER camera. For the observation of *B. melitensis*, 2 μl of an exponential phase culture was dropped on an agarose pad (solution of 1% agarose in PBS) and sealed with VALAP (1/3 vaseline, 1/3 lanoline and 1/3 paraffin wax). Images were taken manually every 20 min at 32 °C with NIS-Element software (Nikon).

Immunofluorescence Microscopy of Tissue

Spleens and lymph nodes were fixed for 2 h at RT in 2% paraformaldehyde (PFA) (pH 7.4), washed in PBS, and incubated overnight at 4°C in a 20% PBS-sucrose solution. Lungs were fixed for 20 min at RT in 2% PFA. Then, lungs were placed under a vacuum until no air was present in the lungs in 2% PFA for 2 h. After fixation, lungs were incubated overnight at 4°C in a 20% PBS-sucrose solution. Tissues were then embedded in Tissue-Tek OCT compound (Sakura), frozen in liquid nitrogen, and cryostat sections (5 µm) were prepared. For staining, tissue sections were rehydrated in PBS and incubated in a PBS solution containing 1% blocking reagent (Boeringer) (PBS-BR 1%) for 20 min before incubation overnight in PBS-BR 1% containing any of the following mAbs or reagents: DAPI nucleic acid stain Alexa Fluor 350, 488 phalloidin (Molecular Probes), APC-coupled BM8 (anti-F4/80, Abcam), Alexa Fluor 647-coupled M5/114.15.2 (anti-I-A/I-E, MHCII, BioLegend), Alexa Fluor 647-coupled HL3 (anti-CD11c, BD Biosciences), biotin-coupled 1A8 (anti-Ly6G, BioLegend), biotin-coupled APA5 (anti-CD140a/ PDGFRA, eBioscience). The biotin-coupled Ab was incubated with streptavidin-coupled APC for 2 h. Slides were mounted in Fluoro-Gel medium (Electron Microscopy Sciences, Hatfield, PA). Labeled tissue sections were visualized with an Axiovert M200 inverted microscope (Zeiss, Iena, Germany) equipped with a high-resolution monochrome camera (AxioCam HR, Zeiss). Images (1,384 × 1,036 pixels, 0.16 µm/pixel)

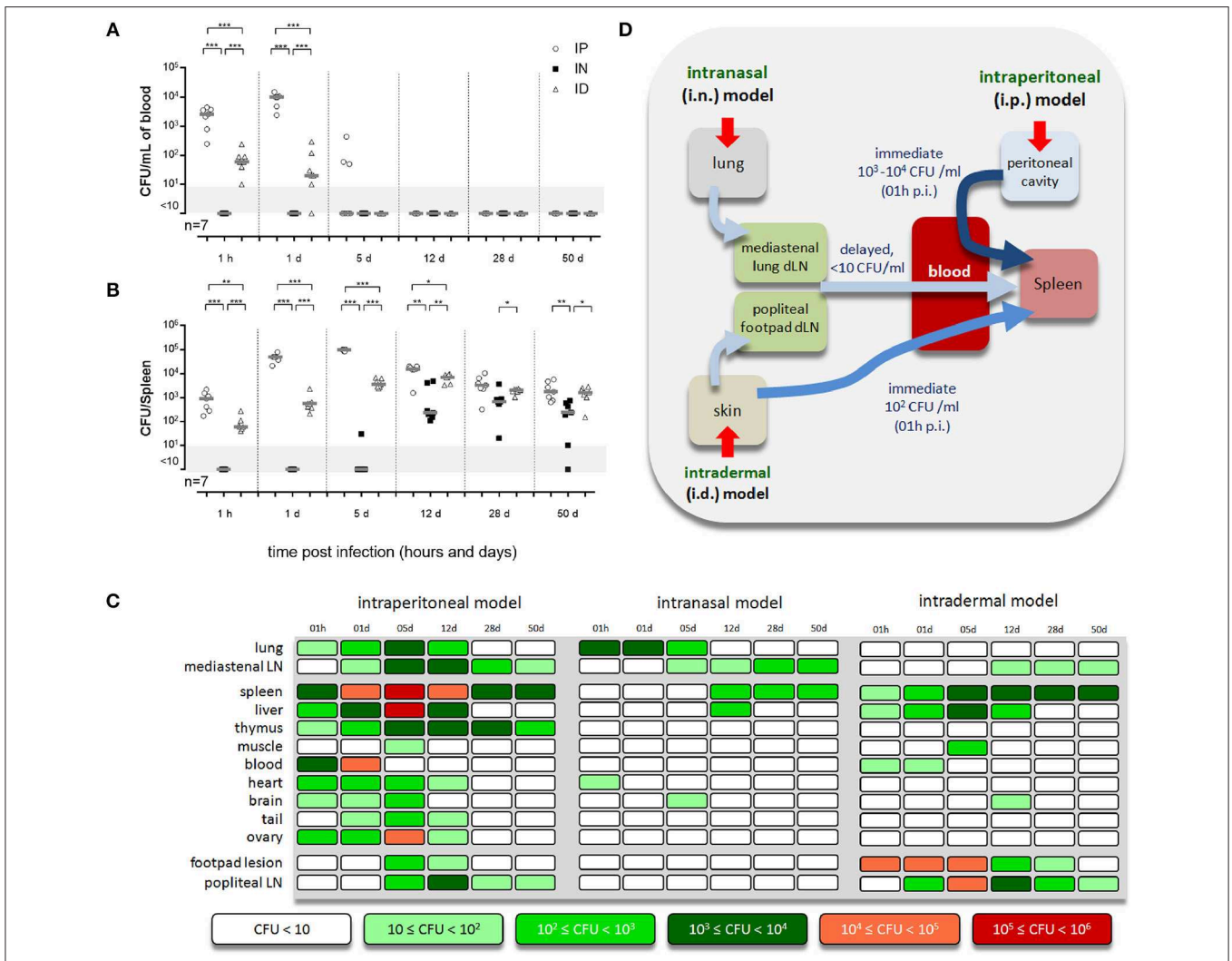

FIGURE 1 | Each route of infection leads to a specific pattern of infected organs. Wild-type C57BL/6 mice were intraperitoneally (i.p.), intranasally (i.n.), or intradermally (i.d.) infected with a dose of 2×10^4 CFU of mCherry-*B. melitensis* and sacrificed at the indicated times. **(A,B)** The data represent the CFU count per ml of blood or per spleen, as indicated. Gray bars represent the median. The significant differences between the indicated groups are marked with asterisks: $^{*}p < 0.1$, $^{**}p < 0.01$, $^{***}p < 0.001$. **(C)** The individual kinetic CFU data are summarized in a matrix giving the median level of CFU ($n = 7$) by tissue according to the route of infection. These results are representative of two independent experiments. h, hours; d, days; LN, lymph node; p.i., post infection; n, number of mice per group. **(D)** Hypothetical model summarizing the spread of *Brucella* from the primary site of infection to the spleen for each route of infection.

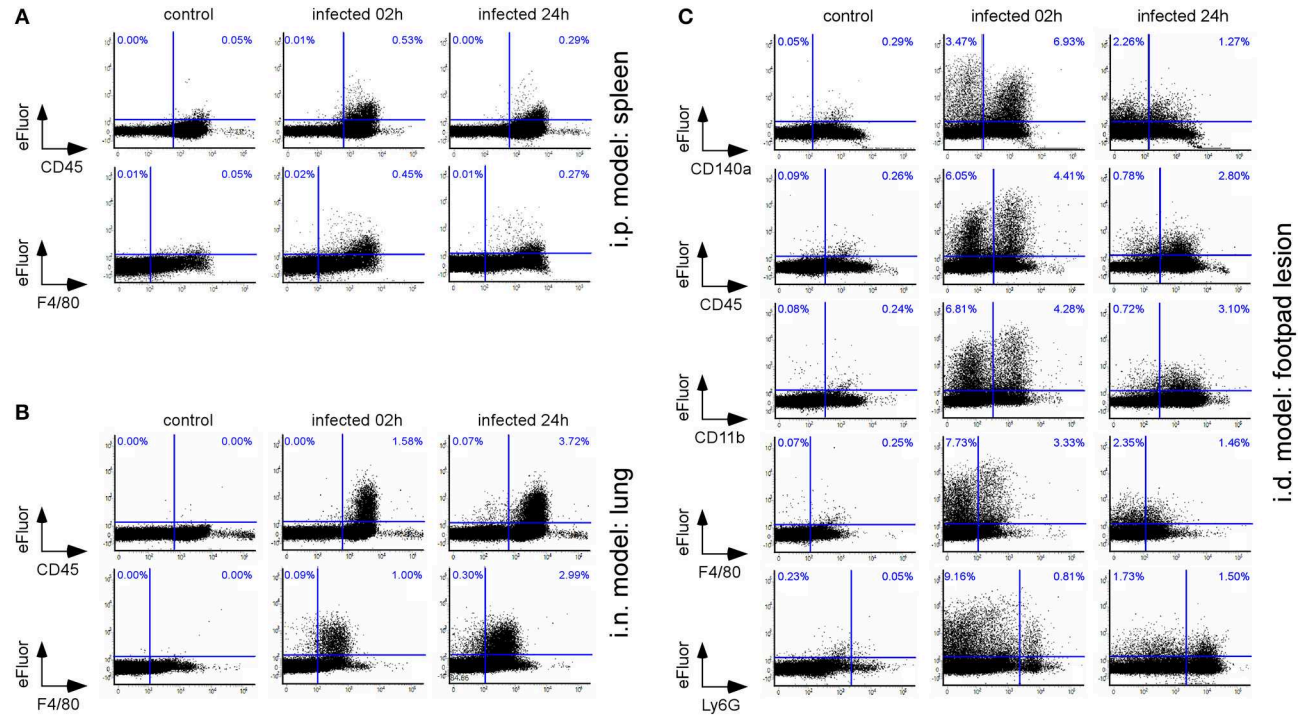

FIGURE 2 | The type of cells infected is dependent on the route of infection. Wild-type C57BL/6 mice ($n = 5$) were infected intraperitoneally (i.p.) **(A)**, intranasally (i.n.) **(B),** or intradermally (i.d.) **(C)** with a dose of 10^8 **(A,B)** or 10^7 **(C)** CFU of eFluor670 labeled *B. melitensis* and sacrificed at 2 and 24 h post infection. The spleen **(A)**, lung **(B),** or footpad lesion **(C)** were harvested and the cells were isolated and then analyzed by flow cytometry for the expression of eFluor670, CD45, F4/80, CD140a, and CD11b as indicated. Numbers in blue indicate the percentage of eFluor670$^+$ cells in each quadrant out of the total cells. These results are representative of three independent experiments.

were acquired sequentially for each fluorochrome with A-Plan 10x/0.25 N.A. and LD-Plan-NeoFluar 63x/0.75 N.A. dry objectives and recorded as eight-bit gray-level *.zvi files. At least 3 slides were analyzed per organ from 3 different animals and the results are representative of 2 independent experiments.

Confocal Microscopy

Confocal analyses were performed using a LSM780 confocal system fitted on an Observer Z 1 inverted microscope equipped with an alpha Plan Apochromat 63x/1.46 NA oil immersion objective (Zeiss, Iena, Germany). DAPI was excited using a 405 nm blue diode, and emission was detected using a band-pass filter (410–480 nm). The 488 nm excitation wavelength of the Argon/2 laser was used in combination with a band-pass emission filter (BP500-535 nm) to detect Alexa Fluor 488 phalloidin. The 543 nm excitation wavelength of the HeNe1 laser and a band-pass emission filter (BP580–640 nm) were used for the red fluorochrome mCherry. The 633 excitation wavelength of the HeNe2 laser and a band-pass emission filter (BP660–695 nm) were used for far-red fluorochromes such as APC. To ensure optimal separation of the fluorochromes, blue & red signals were acquired simultaneously in one track and green & far red signals were acquired in a second track. The electronic zoom factor and stack depth were adjusted to the region of interest while keeping image scaling constant (x-y: 0.066 micron, z: 0.287 micron). A line average of 4 was used and datasets were stored as 8-bit proprietary *.czi files. The images were displayed using Zen2012 software (Zeiss) with linear manual contrast adjustment and exported as 8-bit uncompressed *.TIF images. The figures, representing single optical sections across the region of interest, were prepared using the Canvas program.

Enzyme-Linked Immunosorbent Assay (ELISA)

The presence of *Brucella melitensis* specific murine IgM, IgG1, IgG2a, and IgG3 was determined by ELISA. As already described (17), polystyrene plates (269620; Nunc) were coated with HK *B. melitensis* (10^7 CFU/mL) and incubated overnight at 4°C. The plates were blocked for 2 h at RT with 200 µl/well of PBS-3.65% casein. Then, plates were incubated with 50 µl/well of plasma in serial dilutions in PBS-3.65% casein. The plasma of uninfected mice and PBS were used as negative controls and a 12B12 mAb specific to *Brucella* LPS (34) was used as a positive control. After four washes with PBS, isotype-specific goat anti-mouse HRP conjugated Ab were added (50 µl/well) at appropriated dilutions (anti-IgM from Sigma-Aldrich; LO-MG1-13 HRPO, LO-MG2a-9 HRPO, and LO-MG3-13 HRPO from LOIMEX). After 1 h of incubation at RT, plates were washed four times in PBS and 100 µl/well of substrate solution (BD OptEiA Kit) was added. After 15 min of incubation at RT in the dark, the enzyme reaction was

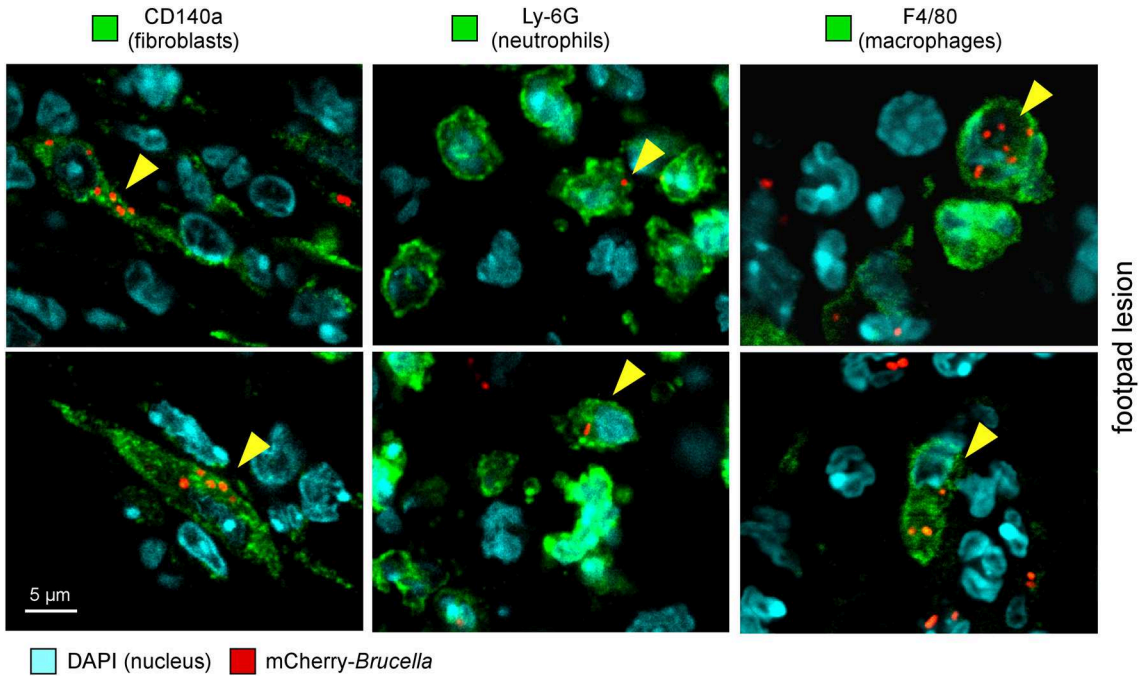

FIGURE 3 | Following intradermal infection with *Brucella melitensis*, fibroblasts, neutrophils, and macrophages were found to be infected in the footpad lesion. Wild-type C57BL/6 mice were infected intradermally with a dose of 10^7 CFU of mCherry-*B. melitensis*. Mice were sacrificed at 24 h post infection and the footpad lesions were collected and analyzed by confocal microscopy for the expression of mCherry and CD140a, LY6G, and F4/80 markers. The panels are color-coded with the text for DAPI, the antigen examined or mCherry-*Brucella*. Scale bar = 5 µm. Yellow arrowheads indicate the cells infected. The data are representative of two independent experiments.

stopped by adding 25 µl/well of 2 N H_2SO_4. The absorbance was measured at 450 nm.

Statistical Analysis

We used a (Wilcoxon-)Mann-Whitney test provided by the GraphPad Prism software to statistically analyse our results. Each group of deficient mice was compared to the wild-type mice. We also compared each group with the other groups and displayed the results when required. Values of $p < 0.05$ were considered to represent a significant difference. *, **, *** denote $p < 0.05$, $p < 0.01$, $p < 0.001$, respectively.

RESULTS

Each Route of *Brucella* Infection Is Associated With a Specific Pattern of Organ Infection

In order to determine the impact of the route of *Brucella* infection on the pattern of infected organs in mice, we administered 2×10^4 CFU of mCherry-*Brucella melitensis* via i.p., i.n. or i.d. route to wild-type C57BL/6 mice. Mice were bled for CFU counting in the blood and then sacrificed at 1 h, 1, 5, 12, 28, and 50 days post infection and a large number of organs and tissues were collected (lung and draining mediastinal lymph node (LN), spleen, liver, thymus, skeletal muscle of the thigh, heart, brain, fragment of the tail, ovary, footpad lesion, and draining popliteal LN) and the CFU count was measured by plating, as described in the Material and Methods.

Our results, presented in **Figures 1A,B** and **Figures S1**, **S2**, showed drastic differences between the pattern of tissues infected via the i.p., i.n., and i.d. routes. A table providing an overview of the individual kinetic CFU data with the average CFU by tissue according to the route of infection is presented in **Figure 1C**. As previously reported by us, CFU are not detectable in blood following i.n. infection (21, 35) but are detectable following i.p. and i.d. infection (**Figure 1A**). However, CFU in blood were 10–100-fold lower following i.d. infection compared to i.p. infection. Despite these differences, which led to very different kinetics and levels of spleen infection in the first 12 days of infection, the spleen appears to be infected at almost comparable levels at 28 days post infection in all three models (**Figure 1B**). Several interesting observations can be made based on **Figure 1C** which summarizes our CFU data. They confirm that i.p. infection can be considered as a systemic model of infection as all tissues collected were found to be infected early and the majority of lymph nodes tested were still infected at 50 days post infection (**Figure S3**). In striking contrast, the i.n infection model produced a very narrow infection pattern: only the mediastinal LN (draining the lung) and spleen were infected persistently. The lung, liver, heart, and brain were infected significantly but only transiently. The i.d. infection model gave an intermediate infection pattern. The skin footpad lesion, popliteal LN (draining the footpad lesion),

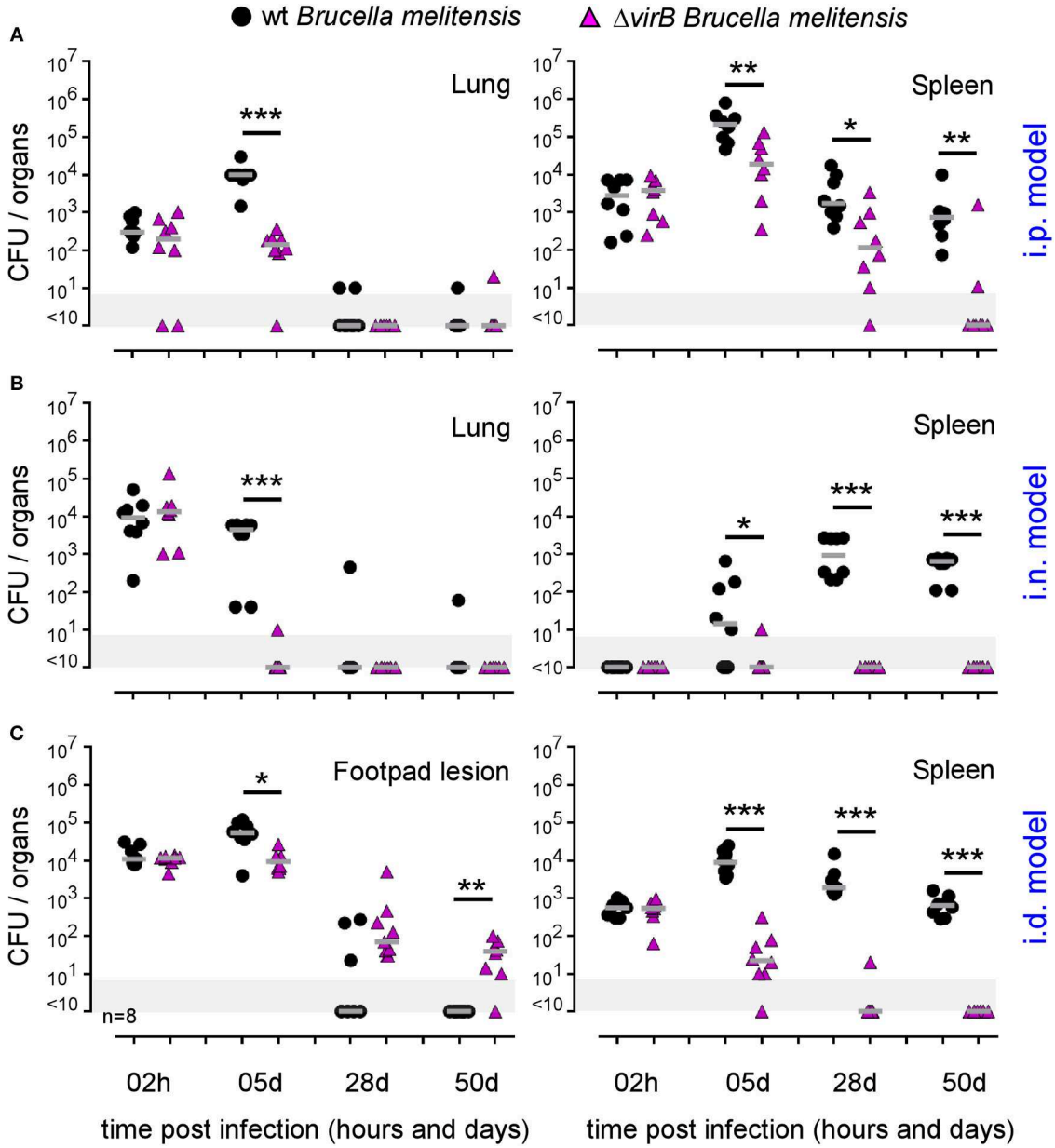

FIGURE 4 | The essentiality of *virB* is dependent on the route of infection and organ. Wild-type C57BL/6 mice were infected intraperitoneally (i.p.) **(A)**, intranasally (i.n.) **(B)** or intradermally (i.d.) **(C),** with a dose of 2×10^4 CFU of mCherry-*B. melitensis* or with mCherry-Δ*virB B. melitensis*. Mice were sacrificed at the indicated times. The data represent the CFU count per lung, spleen, or footpad lesion. Gray bars represent the median. Significant differences between the indicated groups are marked with asterisks: $^*p < 0.1$, $^{**}p < 0.01$, $^{***}p < 0.001$. These results are representative of two independent experiments. h, hours; d, days; n, number.

mediastinal LN, spleen, and liver were infected persistently. Skeletal muscle and the brain were only infected transiently. Importantly, we observed that *Brucella* persists over the long term, until 50 days post infection, mainly in lymphoid tissues, such as the LN and spleen, in all models and in the thymus in the i.p. model. A proposed model for the spread of *Brucella* from the primary site of infection to the spleen in the three models of infection is presented in **Figure 1D**.

The Type of Cells Infected Depends on the Route of Infection

In the past (30, 36), we have used a *Brucella melitensis* 16M strain expressing the mCherry fluorescent tracer to detect and phenotype *Brucella* infected cells *in situ* by fluorescent microscopic analysis. However, this approach is very long and is not appropriate for the quantitative analysis of many organs. Flow cytometry analysis would be more suitable. Unfortunately,

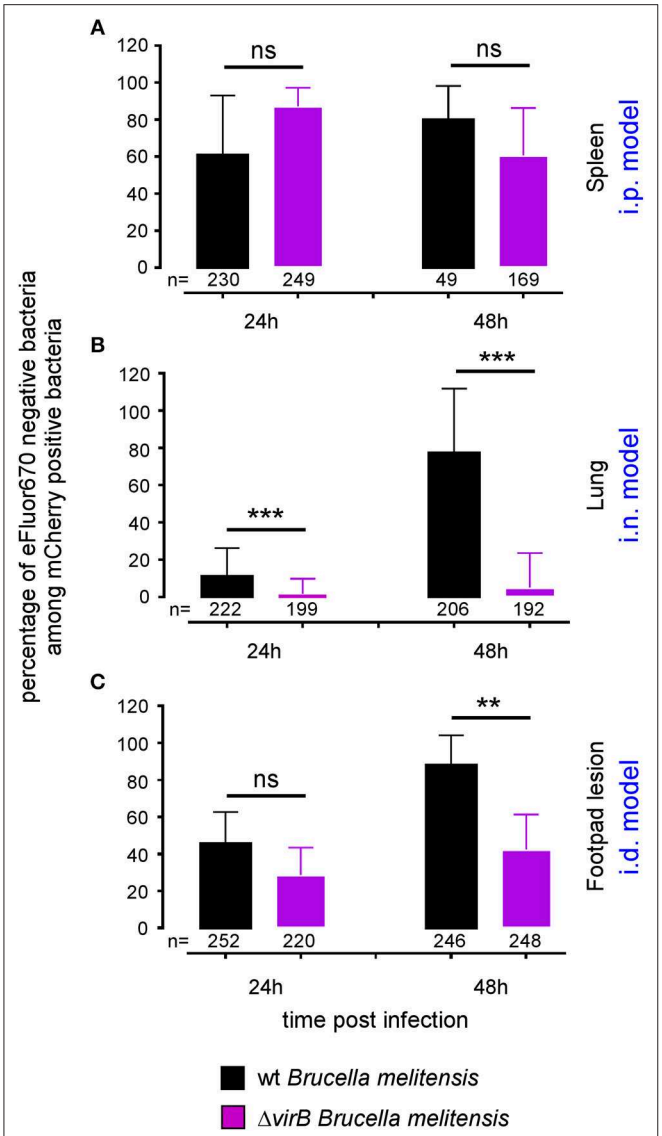

FIGURE 5 | The Δ*virB B. melitensis* strain multiplies differently depending on the tissue. Wild-type C57BL/6 mice were infected intraperitoneally (i.p.) **(A)**, intranasally (i.n.) **(B)** or intradermally (i.d.) **(C)**, with a dose of 10^7 CFU of eFluor670 labeled mCherry-*B. melitensis* or with eFluor670 labeled mCherry-Δ*virB B. melitensis*. Mice were sacrificed at the indicated times and the spleen, lung or footpad was harvested, fixed and analyzed by fluorescent microscopy. The data represent the percentage of eFluor670 negative bacteria among mCherry positive bacteria. Bars represent the standard deviation. Significant differences between the indicated groups are marked with asterisks: $^{**}p < 0.01$, $^{***}p < 0.001$. These results are representative of two independent experiments with 3 mice per condition. h, hours; n, number of bacteria analyzed in each condition.

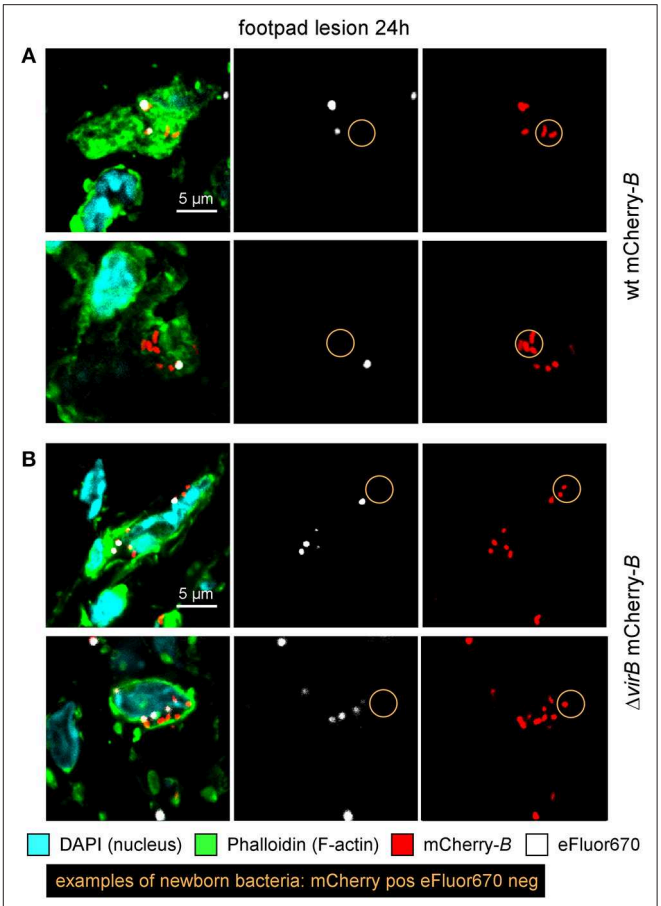

FIGURE 6 | Δ*virB B. melitensis* actively multiplies in the footpad lesion. Wild-type C57BL/6 mice were infected intradermally (i.d.) with a dose of 10^7 CFU of eFluor670 labeled wild-type or Δ*virB* mCherry-*B. melitensis*. Mice were sacrificed at 24 h post infection and the footpad was harvested, fixed, and analyzed by confocal microscopy. **(A,B)** show representative images for wild-type or Δ*virB* mCherry-*B. melitensis*, respectively. The panels are color-coded with the text for DAPI, Phalloidin, mCherry, and eFluor670. Scale bar = 5 µm. pos, positive; neg, negative.

in the absence of an available yellow laser, the fluorescence of the mCherry-*Brucella* strain is too low to permit the direct detection of infected cells by flow cytometry. To avoid this technical problem, we developed a protocol using the dye eFluor™ 670 (eFluor670) that produces intense fluorescent staining of the bacterial cell wall. Brief incubation of bacteria with eFluor670 leads to intense, stable and homogeneous staining of *Brucella* that can be detected by flow cytometry (**Figure S4A**. This staining does not negatively affect *Brucella* growth *in vitro* in a rich medium culture (**Figure S4B**) or in mice in the i.n (**Figure S4C**) and i.p. infection models (**Figure S4D**).

As shown in **Figure 2**, eFluor670 staining allowed for rapid flow cytometric detection and quantification of *Brucella* infected cells present within tissues harvested at 2 and 24 h from infected mice. Our data confirm that, as previously reported by microscopic analysis, infected spleen cells in the i.p. model (30) (**Figure 2A**) and infected lung cells in the i.n. model (37) (**Figure 2B**) are mainly $CD45^+$ $F4/80^+$ myeloid cells, presumably red pulp macrophages and alveolar macrophages, respectively. In striking contrast, the same analysis of footpad lesion cells from the i.d. infection model showed that two clearly distinct cell populations, $CD45^{neg}$ and $CD45^+$, are infected by *Brucella* (37) (**Figure 2C**). Infected $CD45^{neg}$ cells express high levels of the CD140a fibroblast marker

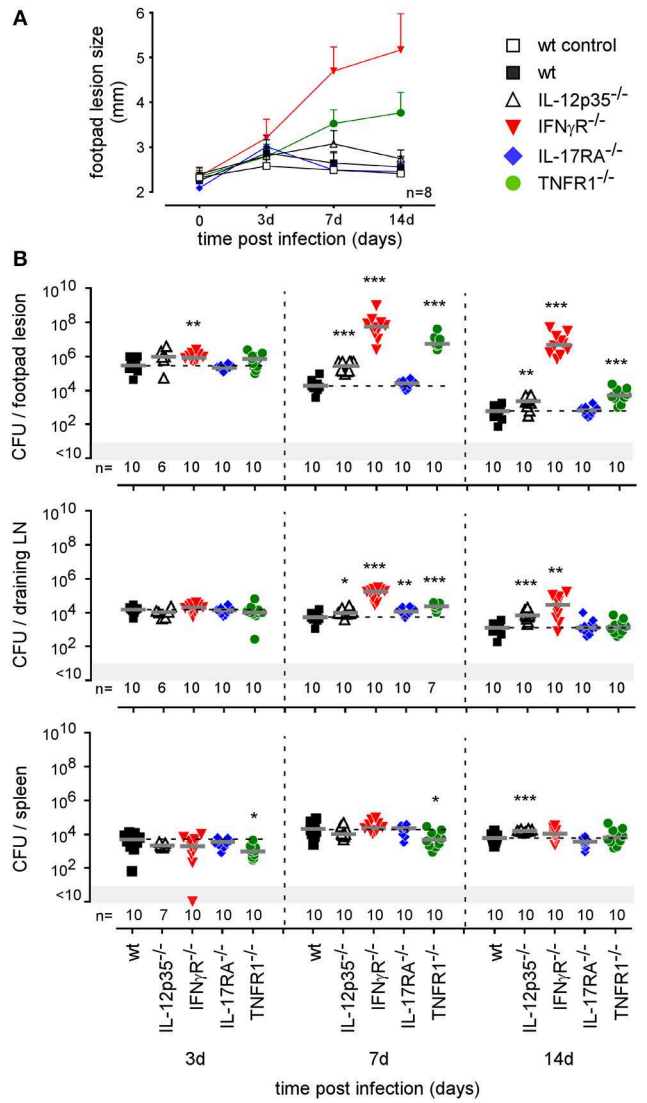

FIGURE 7 | Intradermally infected IFNγR and TNFR1$^{-/-}$ mice display significant footpad swelling and CFU counts. Wild-type, IL12p35$^{-/-}$, IFNγR$^{-/-}$, IL-17RA$^{-/-}$, and TNFR1$^{-/-}$ C57BL/6 mice were infected intradermally with a dose of 2×10^4 CFU of mCherry-*B. melitensis*. **(A)** At the indicated time post infection, the swelling of the lesion was measured for each mouse. The error bars are the SD. **(B)** At the indicated times, mice were sacrificed and the footpad, draining popliteal lymph node, and spleen were harvested. The data represent the CFU count per organ. Gray bars represent the median. The significant differences between the indicated groups are marked with asterisks: $^{**}p < 0.01$, $^{***}p < 0.001$. These data are representative of two different experiments. d, days; n, number; LN, lymph node.

and infected CD45$^+$ cells express CD11b myeloid markers (**Figure S5**), which can be subdivided into CD11b$^+$ F4/80$^+$ Ly6G$^{neg/med}$ and CD11b$^+$ F4/80$^{neg/med}$ Ly6G^{high} (**Figure S6**). Confocal microscopic analysis of footpad samples collected at 24 hours from infected mice demonstrated that CD140$^+$, Ly6G$^+$, and F4/80$^+$ cells are indeed infected and display typical morphology of fibroblasts, neutrophils, and macrophages, respectively (**Figure 3**).

On the whole, these data showed that the type of cells infected by *Brucella* is strongly dependent on the route of infection. Although the infected cells are mainly macrophages in the i.p. and i.n. models, fibroblasts, and neutrophils are also infected in the i.d. model.

Identification of Virulence Factors Is Affected by the Route of Infection and Organ Analyzed

In the rational development of LAVs, it is essential to identify virulence factors allowing for escape from the immune response and persistence in the host. LAVs must be able to establish infection in order to stimulate an adaptive immune response without persisting or disseminating deeply in the host. The most studied virulence factor in *Brucella* is undoubtedly the *virB* T4SS. *In vitro* in RAW 264.7 macrophages, a Δ*virB Brucella* strain is unable to escape the phagolysosome system and appears to be highly attenuated (38).

In order to determine the impact of the route of infection on the type of virulence factors required to establish a successful infection *in vivo*, we compared the course of wild-type and Δ*virB Brucella* strains in wild-type C57BL/6 mice (**Figure 4**). As previously described (39), the Δ*virB Brucella* strain appears attenuated but able to persist for several weeks in the spleen in the i.p infection model (**Figure 4A**). In this model, we observed that the Δ*virB Brucella* strain is also attenuated in the lung. It persists at ∼100 CFU between 2 h and 5 days post infection and is no longer detectable from 28 days. In striking contrast, in the i.n. model (**Figure 4B**), the Δ*virB Brucella* strain appears completely unable to multiply in the lung and reach the spleen. In the lung, the number of CFU drops by 3 log between 2 h and 5 days post infection. A complemented Δ*virB* strain recovers the ability to multiply in the lung, demonstrating that the inability of the Δ*virB* strain to persist in the lung is specific and related to the *virB* deficiency only (**Figure S7**). More surprising, in the i.d. model, the Δ*virB* strain persists longer in the primary footpad lesion than the wild-type *Brucella* strain. At 50 days post infection, the Δ*virB* strain is still present in the footpad while the wild-type strain has already disappeared at 28 days (**Figure 4C**). In the spleen, the Δ*virB* strain remains attenuated (**Figure 4C**).

The differing behavior of the Δ*virB* strain observed depending on the route of infection and the tissue may be due to a difference in the ability to actively multiply or to passively persist (i.e., persistence without multiplication). *Brucella* has been widely described to display atypical unipolar growth (40). Unlabelled daughter cells can be visualized upon the resumption of growth following staining of the bacteria with Texas red conjugated to succinimidyl ester (TRSE) (41). Here, we chose to replace TRSE with eFluor670 staining, which is compatible with the mCherry *Brucella* strain. Thus, newly formed bacteria, called "newborn" bacteria, appear as mCherry$^+$ eFluor670^{neg} (**Figure S8A**). We confirmed by fluorescence microscopy the stability and absence of transfer of eFluor670 staining during *Brucella* growth and division *in vitro* (**Figure S8B**). Using this tool, we tried to quantify multiplication of the wild-type and Δ*virB Brucella* strains *in situ*. Mice were infected by i.p., i.n.

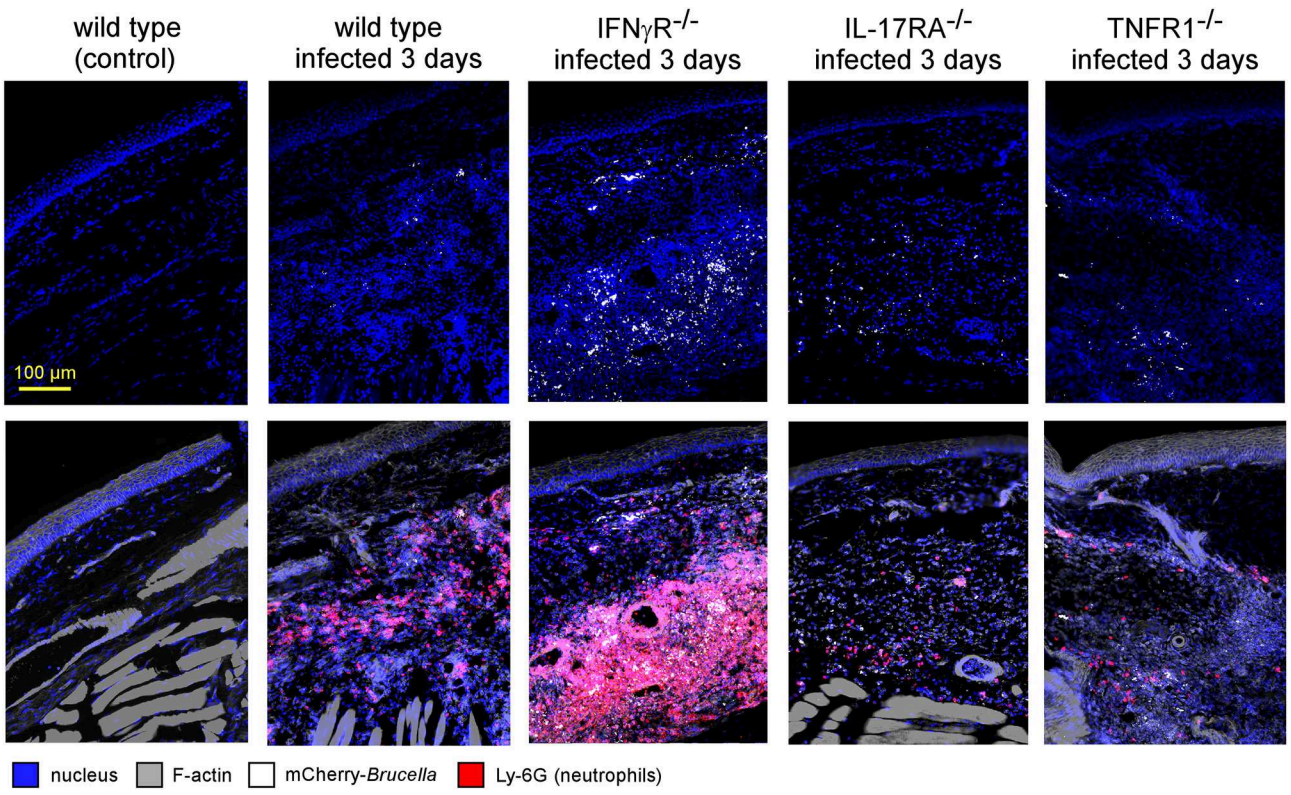

FIGURE 8 | IFNγR deficiency leads to the massive recruitment of neutrophils in dermal tissue. Wild-type, IFNγR$^{-/-}$, IL-17RA$^{-/-}$, and TNFR1$^{-/-}$ C57BL/6 mice were infected intradermally with a dose of 2×10^4 CFU of mCherry-*B. melitensis*. Control wild-type mice were injected with PBS. Mice were sacrificed at 3 days post infection and the footpad was harvested and analyzed by fluorescent microscopy. The panels are color-coded with the text for DAPI, phalloidin, mCherry-*B.melitensis,* and LY-6G. Scale bar = 100 µm. These data are representative of two different experiments.

or i.d. route with eFluor670-stained wild-type mCherry-*B* and Δ*virB* mCherry-expressing *Brucella* strains. 24 and 48 h later, mice were sacrificed and the organs of interest were harvested and analyzed by confocal microscopy. **Figures 5A–C** show the frequencies of mCherry$^+$ eFluor670^{neg} (newborn) bacteria among the mCherry$^+$ bacteria in the spleen, lung and footpad lesion at 24 and 48 h post infection from i.p., i.n., or i.d. infected mice, respectively. **Figure 6** presents representative images from infected footpads. As expected, wild-type *Brucella* appears able to multiply in all tissues analyzed based on the abundant presence of mCherry$^+$ eFluor670^{neg} newborn bacteria at 48 h post infection. The frequency of newborn *Brucella* in the spleen from wild-type and Δ*virB Brucella* infected mice was similar (**Figure 5A**). In contrast, the frequency of newborn *Brucella* in the lung from Δ*virB Brucella* infected mice is strongly reduced (∼15 times) compared to wild-type *Brucella* infected mice (**Figure 5B**). In the footpad lesion, the situation appears to be intermediate. The frequency of newborn *Brucella* from Δ*virB Brucella* infected mice is only reduced by ∼2-fold. These results suggest that the absence of persistence of Δ*virB Brucella* in the lung is due to a reduced ability to multiply and that persistence in the spleen and footpad lesion is associated with active multiplication.

We can conclude that the impact of *virB* deficiency appears vary widely as a function of the route of infection and organ analyzed, suggesting that the identification of virulence factors could be strongly impacted by these parameters.

In the next part of this article, we will focus on the impact of the route of infection on the type of immune response and lymphocyte populations involved in primary and secondary control of *Brucella melitensis* infection.

Th1 Immune Response Is Crucial to Control of the Primary Cutaneous *Brucella* Infection

To our knowledge, the type of immune mechanism underlying cutaneous *Brucella* infection has never been investigated in a mouse model. As reported in i.p. (42) and i.n. (21) infectious models, BALB/c mice appear to be more susceptible to cutaneous *B. melitensis* infection compared to C57BL/6 mice (**Figure S9**). In order to identify the T helper subset of immune response associated with *Brucella* control in skin lesions, we compared the course of *Brucella melitensis* infection in wild-type, IL-12$_{p35}^{-/-}$, IFNγR$^{-/-}$, IL-17RA$^{-/-}$, and TNFR1$^{-/-}$ C57BL/6 mice. We observed that *Brucella* infection in wild-type and IL-17RA$^{-/-}$ mice leads to moderate footpad lesions at 3 days post infection that disappeared spontaneously at 7 days (**Figure 7A**). The lesions persisted longer in IL-12$_{p35}^{-/-}$ mice, but regressed

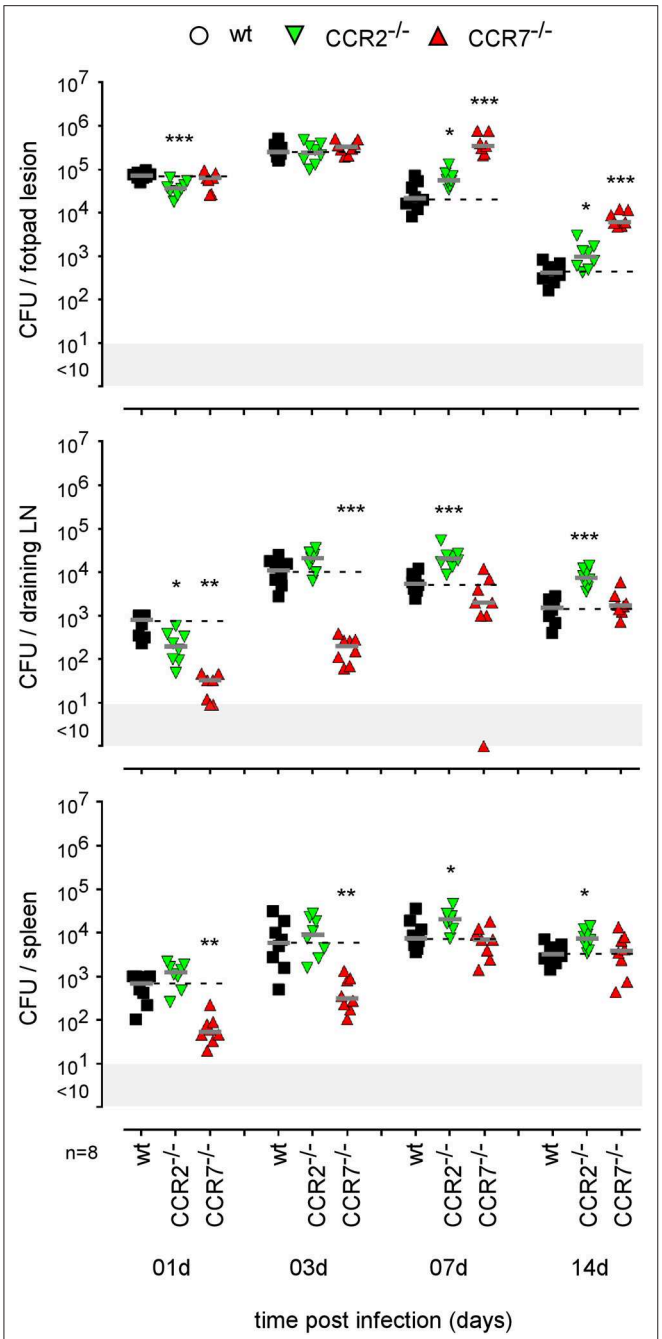

FIGURE 9 | Impact of CCR2 and CCR7 deficiency on the course of intradermal *Brucella* infection. Wild-type, CCR2$^{-/-}$, and CCR7$^{-/-}$ C57BL/6 mice were infected intradermally with a dose of 2×10^4 CFU of *B. melitensis* and sacrificed at the indicated times. The data represent the CFU count per organ. Gray bars represent the median. The significant differences between the indicated groups are marked with asterisks: $^*p < 0.1$, $^{**}p < 0.01$, $^{***}p < 0.001$. These results are representative of three independent experiments. LN, lymph node; d, days; n, number.

spontaneously at 14 days. In striking contrast, lesions in IFNγR$^{-/-}$ and TNFR1$^{-/-}$ mice displayed uncontrolled growth until 14 days (**Figure 7A**) and become necrotic (data not shown). Growth and necrosis of the lesion were higher in IFNγR$^{-/-}$ mice. The severity of the footpad lesion in all groups of mice appeared to be closely correlated with the corresponding CFU level (**Figure 7B**). We have previously reported (21) a dramatic difference between IL-12$_{p35}^{-/-}$ and IFNγR$^{-/-}$ mice in control of a *Brucella* infection in the i.n. infection model. In this model, IFNγR$^{-/-}$ mice, but not IL-12$_{p35}^{-/-}$ mice, display severe neutrophilia and succumb to the infection, suggesting that this lack of control and mortality result from the complete absence of IFN-γ and are not proportional to its level.

Fluorescent microscopic analysis of the footpad lesion at 3 days in wild-type, IL-17RA$^{-/-}$ and TNFR1$^{-/-}$ infected mice showed a moderate presence of neutrophils, identified by Ly-6G staining (**Figure 8**). In contrast, the dermis of the lesion from infected IFNγR$^{-/-}$ mice displayed very intense neutrophil recruitment. This was confirmed by flow cytometric analysis of the footpad lesion (**Figure S10A**). In wild-type mice, *Brucella* infection led to the recruitment of CD11b$^+$ F4/80$^+$ Ly6G^{neg} monocytes that peaked at 7 days post infection with only moderate recruitment of CD11b$^+$ F4/80^{neg} Ly6G$^+$ neutrophils. In infected IFNγR$^{-/-}$ mice, neutrophils constituted the major population in the footpad lesion and the frequency of monocytes appeared to be strongly reduced (**Figure S10B**).

As our microscopic analysis showed that F4/80$^+$ monocytes/macrophages appear to be infected by *Brucella* in the skin of i.d. infected mice (**Figure 3**) and their recruitment is correlated with the control of *Brucella* (**Figure S10B**), we investigated the impact of chemokine receptor CCR2 and CCR7 deficiency on *Brucella* control in our i.d. infection model. Monocyte emigration from bone marrow during bacterial infection requires signals mediated by CCR2 (43) but seems to be dispensable for the maintenance of dermal macrophages and dendritic cells (44). In contrast, CCR7 regulates the migration of inflammatory monocytes (45), and dendritic cells (46) from skin to the draining lymph node under inflammatory conditions. We observed that i.d. infected CCR2$^{-/-}$ mice display delayed monocyte recruitment and a higher rate of neutrophils at 7 days post infection in the footpad lesion (**Figure S10B**) associated with an increased CFU count in the footpad lesion, popliteal draining LNs, and spleen (**Figure 9**), confirming the importance of monocyte recruitment in the local and systemic control of *Brucella* infection. Interestingly, CCR7 deficiency led to retention of *Brucella* in the lesions and seemed to delay its dissemination to the popliteal draining LNs and spleen, suggesting that *Brucella* dissemination is partially dependent on monocyte and dendritic cell migration. In agreement, flow cytometry analysis of footpad lesions and popliteal draining LNs from mice i.d. infected with eFluor670$^+$ bacteria showed that, while the eFluor670$^+$ cells in the lesion are mainly CD11c and MHCII negative, they are mostly positive in the LNs (**Figures 10A–C**). Interestingly, the frequency of CD11c$^+$ MHCII$^+$ infected dendritic cells is drastically reduced in CCR7$^{-/-}$ mice compared to wild-type mice (**Figure 10C**).

Finally, using a battery of genetically-deficient C57BL/6 mice, we investigated the role of lymphoid populations in the control of i.d. *Brucella melitensis* infection. Comparison of the course of

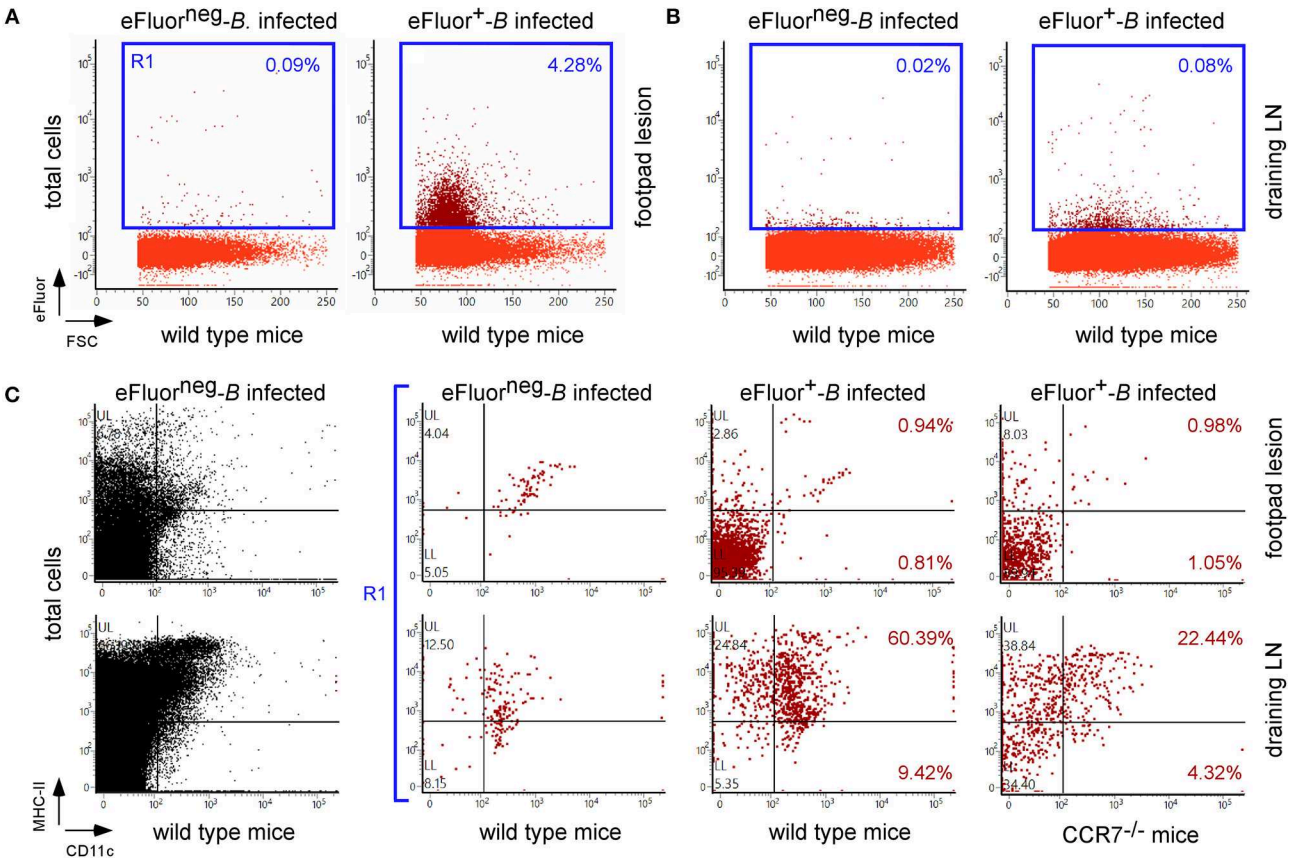

FIGURE 10 | CCR7 deficiency reduced the frequency of infected dendritic cells in popliteal draining lymph nodes. Wild-type and CCR7$^{-/-}$ C57BL/6 mice were infected intradermally with a dose of 10^7 CFU of eFluor670$^+$ labeled *B. melitensis* and sacrificed at 24 h post infection. The footpad lesion and the popliteal draining lymph nodes were harvested and the cells were isolated and then analyzed by flow cytometry for the expression of eFluor670, MHCII, and CD11c as indicated. The data represent the frequency of eFluor670$^+$ cells in cells from footpad lesions **(A)** and popliteal draining lymph nodes **(B)** and the phenotype of eFluor670$^+$ cells in these tissues **(C)**. Percentage indicates the percentage of cells in each quadrant out of the total cells **(A,B)** or of the eFluor670$^+$ cells **(C)**. LN, lymph node. These results are representative of three independent experiments.

Brucella infection in wild-type, CD3$^{-/-}$ (deficient for T cells), TCR-δ$^{-/-}$ (deficient for γδT cells), TCR-β$^{-/-}$ (deficient for both CD4$^+$T and CD8$^+$T cells), MHCII$^{-/-}$ (deficient for CD4$^+$T cells), TAP1$^{-/-}$ (deficient for CD8$^+$Tcells), and MuMT$^{-/-}$ (deficient for B cells) mice showed that CD4$^+$T cells are strictly required for *Brucella* control in the footpad lesion and popliteal draining lymph node (**Figure 11**). Interestingly, CD4$^+$T cells appear to be dispensable in the spleen, as only CD3 and TCR-β deficiency negatively impaired *Brucella* control there. CD8$^+$T cell deficiency significantly favored *Brucella* control in the draining lymph node but not in the lesion or spleen. This may be the consequence of the higher number of CD4$^+$T cells in absence of CD8$^+$T cell in TAP1$^{-/-}$ mice. In a previous study (47), we demonstrated that even though the amounts of IFN-γ produced by CD8$^+$T cells and CD4$^+$T cells are similar, CD8$^+$T cells are unable to replace CD4$^+$T cells in their control of *Brucella* infection, suggesting that CD4$^+$T cells deploy as yet unidentified effector mechanisms that may be independent of IFN-γ. In the i.d. infection model, γδ$^+$T cells appeared to be dispensable for the control of i.d. *Brucella* infection. Despite the detectable humoral response (**Figure S11A**), similar to that observed in the i.p. infection model (**Figure S11B**), B cells also appeared to be dispensable. However, though the finding was not statistically significant, we did observe a repeated tendency of MuMT mice to display increased CFU counts in draining lymph nodes at 50 days post infection (**Figure 11**).

Taken together, our data demonstrate that the control of primary cutaneous *Brucella* infection mainly required an IFN-γ-mediated Th1 response, TNF-α production and CD4$^+$ T cells but not an IL-17RA-mediated Th17 response. They also show that monocyte recruitment plays a crucial role in both the control and dissemination of cutaneous *Brucella* infection.

The Type of Immune Response Controlling Secondary *Brucella* Infection Is Dependent on the Route of Infection

In order to establish the main features of the protective immune response induced by i.d. *Brucella* infection, we started by comparing the course of i.d. mCherry-*B. melitensis* infection in

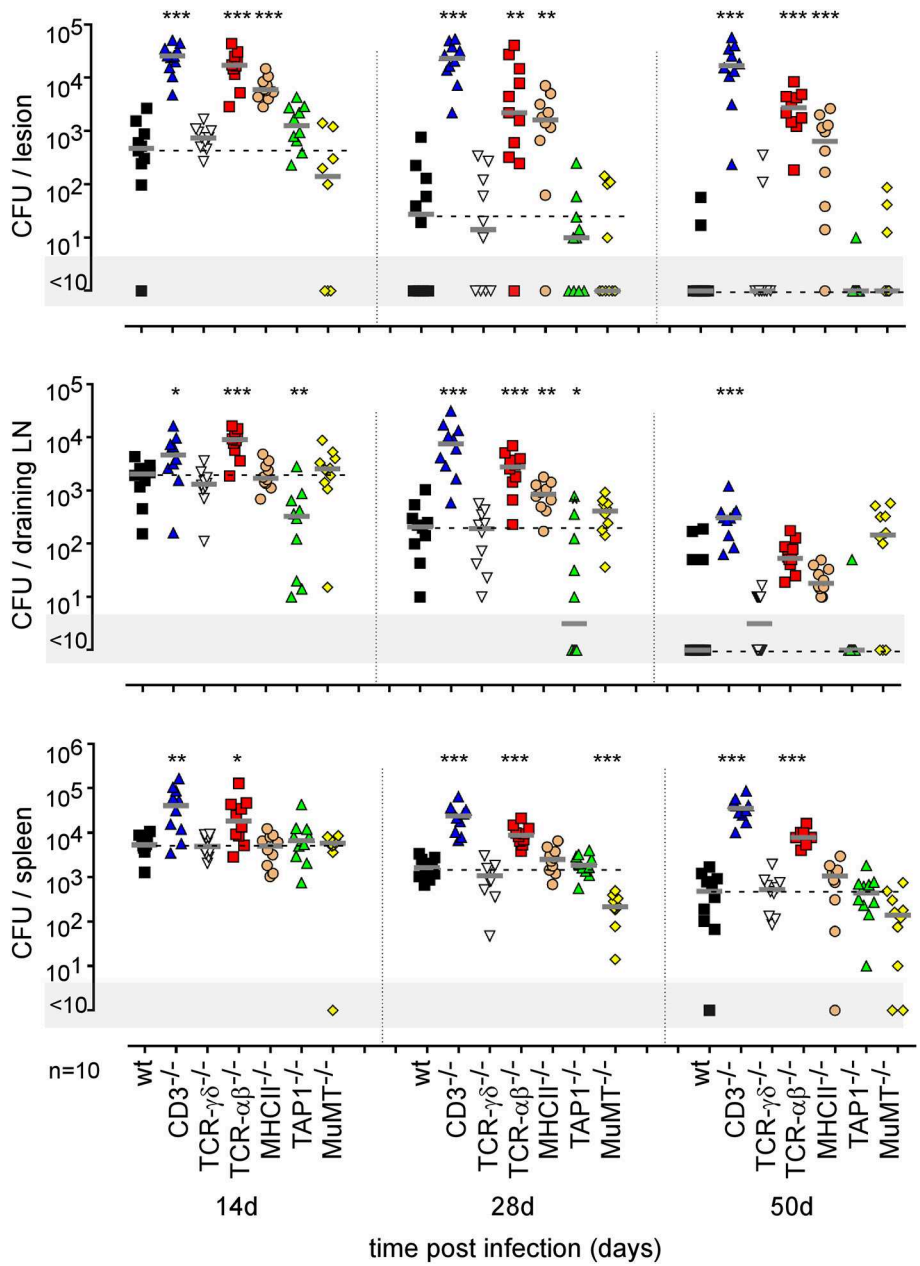

FIGURE 11 | Impact of various lymphocytes deficiencies on the course of intradermal *Brucella* infection. Wild-type, CD3$^{-/-}$, TCRαβ$^{-/-}$, TCRγδ$^{-/-}$, MHCII$^{-/-}$, TAP1$^{-/-}$, and MuMT$^{-/-}$ C57BL/6 mice were infected intradermally with a dose of 2×10^4 CFU of *B. melitensis* and sacrificed at the indicated times. The data represent the CFU count per organ. Gray bars represent the median. The significant differences between the indicated groups are marked with asterisks: $^{*}p < 0.1$, $^{**}p < 0.01$, $^{***}p < 0.001$. These results are representative of three independent experiments. LN, lymph node; d, days; n, number.

naive mice (primary infection group) and in mice previously i.d. infected with wild-type-*B. melitensis* for 28 days and then treated with antibiotics (secondary infection group), as described in the Material and Methods.

Antibiotic treatment is indispensable to the comparison of wild type and genetically deficient mice. It is well known that the persistence of a pathogen generates chronic inflammation and can cause a "Mackaness effect"(48, 49). Without antibiotics, the level of persistence of the vaccine strain would be very different between wild-type mice and mice deficient for key components of the immune response against *Brucella*, which would make our results very difficult to interpret. It has been reported that Rev1 infection in sheep (50, 51) and rams (52) is fully cleared between the second and third month after subcutaneous or conjunctival vaccination. Thus, by eliminating the primary infection at 28 days in our experimental model, we are not so far away from the

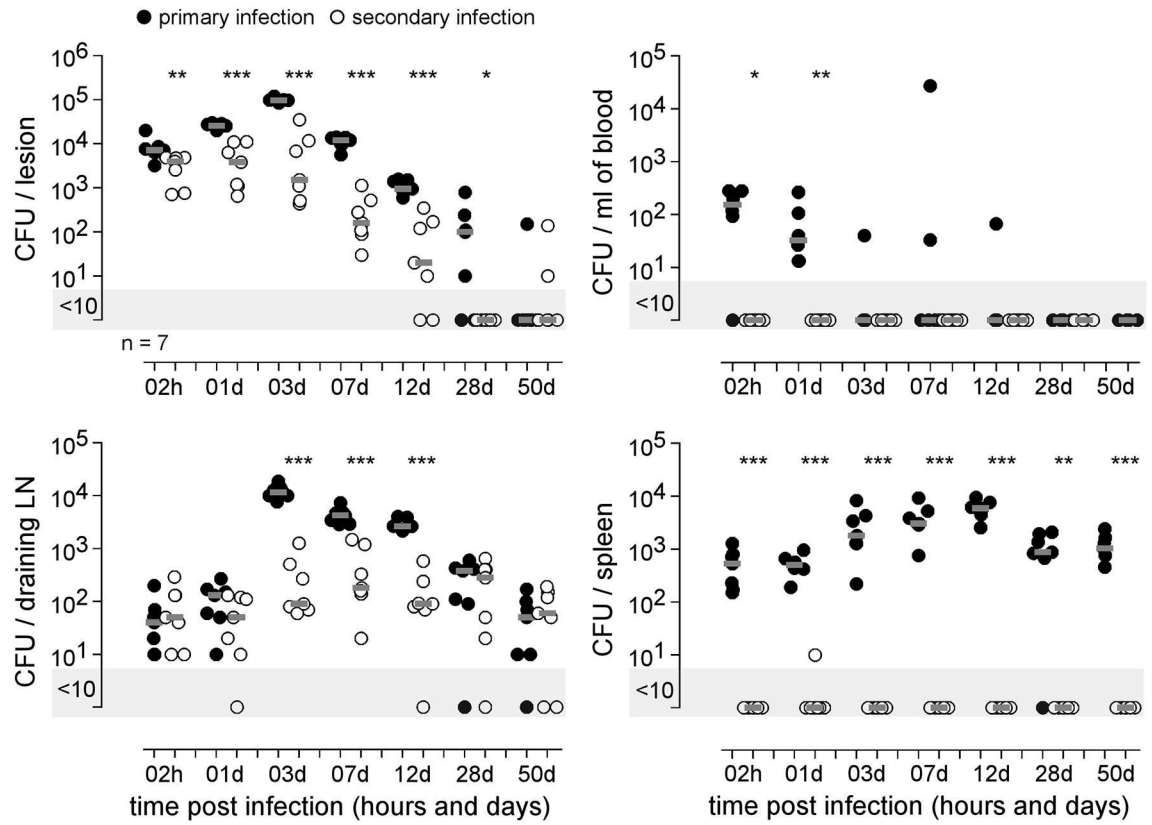

FIGURE 12 | Comparison of protection in control mice and mice previously immunized with live *B. melitensis*. C57BL/6 mice were immunized intradermally (i.d.) with 2×10^4 CFU of live wild type *B. melitensis* and treated with antibiotics, as described in the Materials and Methods. Naive (primary infection group) and immunized (secondary infection group) mice were challenged i.d. with 2×10^4 CFU of live mCherry-*B. melitensis* and sacrificed at the indicated times. The data represent the CFU count per organ or per ml of blood. Gray bars represent the median. Significant differences between the indicated groups are marked with asterisks: $^*p < 0.1$, $^{**}p < 0.01$, $^{***}p < 0.001$. These results are representative of three independent experiments. LN, lymph node; d, days; h, hours; n, number.

conditions of the natural host vaccinated with the reference Rev1 vaccine against *Brucella melitensis*.

Our results (**Figure 12**) demonstrated that i.d. infection leads to the development of an adaptive immune response able to efficiently control secondary i.d. infection in the footpad lesion, blood, popliteal draining lymph node and spleen. It is interesting to note that while *Brucella* is almost completely eliminated in the footpad lesion, blood, and spleen, it nevertheless persists at a significant level in the lymph nodes, suggesting that it may be sheltered from the adaptive immune response at this site.

The type of immune mechanism required for the protective secondary immune response appears to be dramatically dependent on the tissue analyzed. As shown in genetically-deficient mice, effective control in the footpad lesion is dependent on TNFR1 and IL-17RA but not IL-12_{p35} and, in the spleen, is dependent on TNFR1 but not IL-17RA and IL-12_{p35}. In the popliteal lymph node, the absence of IL-12_{p35}, IL-17RA, or TNFR1 does not have a significant impact on the CFU count (**Figure 13**). Similarly, only $CD4^+$T cells, and no other lymphoid populations, are essential to control *Brucella* in the footpad lesion, but $CD4^+$T cells are dispensable in the popliteal draining lymph node and spleen. In the spleen, B cells are strictly required but only the absence of all T cells in $CD3^{-/-}$ mice leads to a significant loss of *Brucella* control, suggesting that the absence of a T cell subpopulation can be compensated for by the other subpopulations in this organ. Unexpectedly, the absence of T cells in $CD3^{-/-}$ mice, and especially of $CD8^+$T cells in $TAP1^{-/-}$ mice, improved the control of *Brucella* in popliteal draining lymph nodes, suggesting that *Brucella* persistence there implicates $CD8^+$T cells (**Figure 14**). Regulatory $CD8^+CD122^+PD\text{-}1^+$T cells, which are located in lymph nodes and act in a non-antigen-specific manner, have been described in persistent viral infection (53, 54). These cells have not been described in a *Brucella* model but could be responsible for this phenomenon.

It would also have been interesting to test the ability of IFN-$\gamma R^{-/-}$ mice to develop a protective memory response against *Brucella*. However, these mice develop highly necrotic footpad lesions and, for ethical reasons, we therefore limited our observations of these mice to 14 days post infection.

Lastly, to summarize the impact of the route of infection on the type of protective immune memory response, we compared the results obtained in the i.d. infection model with those obtained by our group in the i.p. (20) and i.n. (21) infection

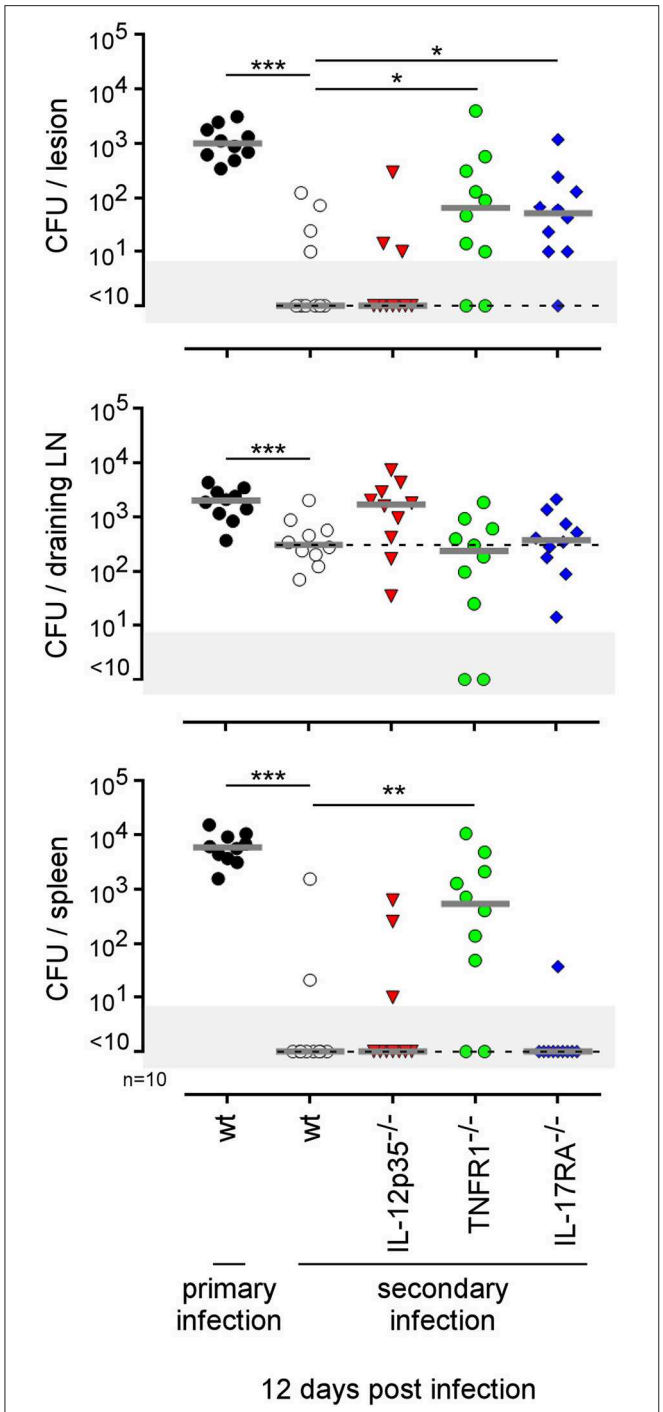

FIGURE 13 | Comparison of protection in wild-type and various deficient mice previously immunized by intradermal route with live *B. melitensis*. Wild-type, IL-12p35$^{-/-}$, TNFR1$^{-/-}$, IL-17RA$^{-/-}$ C57BL/6 mice were immunized intradermally (i.d.) with 2×10^4 CFU of live wild-type *B. melitensis* and treated with antibiotics, as described in the Materials and Methods. Naive (primary infection group) and immunized (secondary infection group) mice were challenged i.d. with 2×10^4 CFU of live mCherry-*B. melitensis* and sacrificed at 12 days post infection. The data represent the CFU count per organ. Gray bars represent the median. The significant differences between the indicated groups are marked with asterisks: $^*p < 0.1$, $^{**}p < 0.01$. These results are representative of three independent experiments. LN, lymph node; n, number.

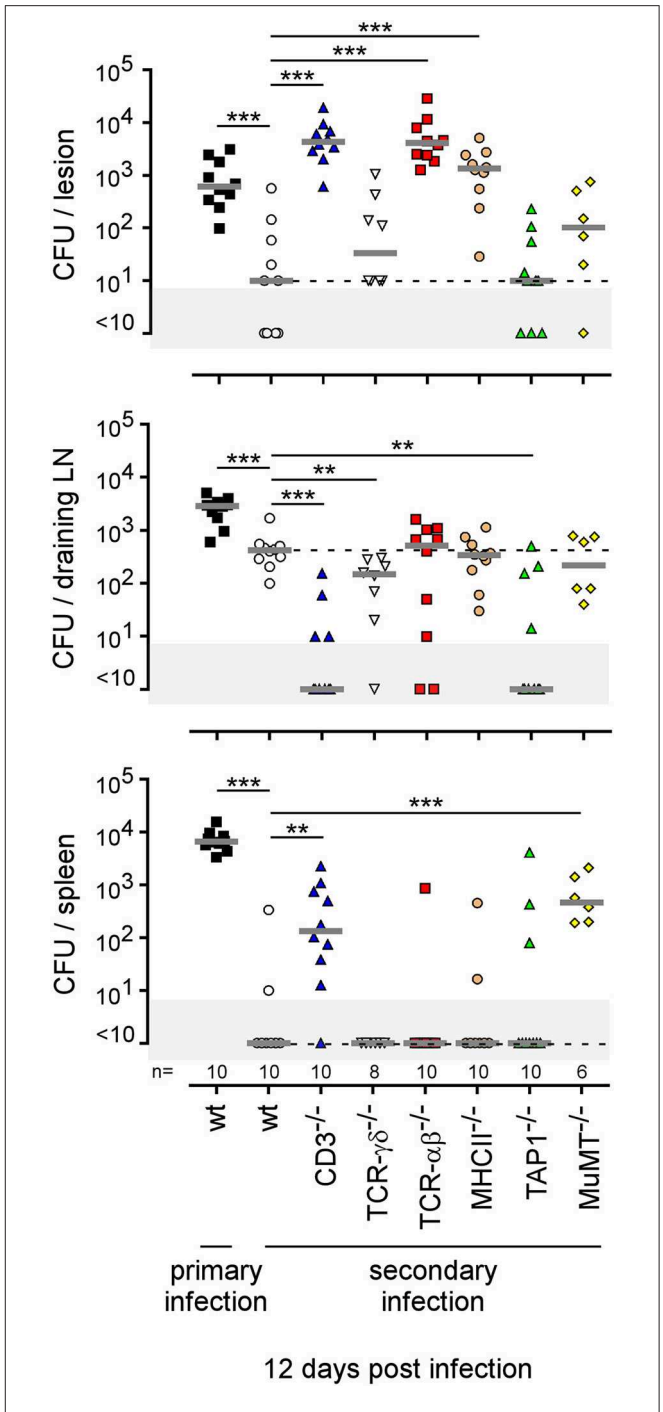

FIGURE 14 | Comparison of protection in wild-type and various lymphocyte-deficient mice previously immunized by intradermal route with live *B. melitensis*. Wild-type, CD3$^{-/-}$, TCR$\alpha\beta^{-/-}$, TCR$\gamma\delta^{-/-}$, MHCII$^{-/-}$, TAP1$^{-/-}$, and MuMT$^{-/-}$ C57BL/6 mice were immunized intradermally (i.d.) with 2×10^4 CFU of live wild-type *B. melitensis* and treated with antibiotics, as described in the Materials and Methods. Naive (primary infection group) and immunized (secondary infection group) mice were challenged i.d. with 2×10^4 CFU of live mCherry-*B. melitensis* and sacrificed at 12 days post infection. The data represent the CFU count per organ. Gray bars represent the median. The significant differences between the indicated groups are marked with asterisks: $^{**}p < 0.01$, $^{***}p < 0.001$. These results are representative of three independent experiments. LN, lymph node; n, number.

models (**Figure 15**). Note that the requirements were completed in the i.p. model to allow for a full comparison with other models (**Figure S12**). **Figure 15** shows clearly that the type of lymphoid cells and T helper response required to control secondary *Brucella* infection is strongly dependent on the route of infection and the tissues infected. For example, $CD4^+$T cells are indispensable in the footpad lesion in the i.d. model and in the spleen in the i.p. model but are dispensable in the spleen level in both the i.d. and i.p. models. B cells are indispensable in the i.d. and i.p. models but dispensable in the i.n. model. The IL-12_{p35} dependent Th1 response is only required in the spleen in the i.p. model and in the footpad lesion in the i.d. model. It is dispensable in the i.d. and i.n. models in the spleen. Thus, we can conclude that the identification of immune markers associated with protection against infection is strongly affected by the route of infection used and the organ analyzed.

DISCUSSION

There are well-documented cases in which generalization of use of a new drug favors, in just a few decades, the development of resistance leading to treatment failure [reviewed in Zur Wiesch et al. (55)]. This problem has become so acute that drug resistance is viewed as one of the major challenges in public health, reinforcing the importance of vaccines in the control of epidemics.

Historically, highly successful global vaccination campaigns have been associated with the administration of live-attenuated vaccines (LAVs) (1). Today, modern vaccination strategies focus mainly on the use of subunit vaccines (SUVs) with an adjuvant (56–58). Compared to LAVs, SUVs offer several advantages: (i) their supposed safety because they exclude all risks of reversion of attenuated pathogens to a virulent form, (ii) their high specificity limiting the risk of autoimmune diseases, and (iii) the ease to produce, conserve, and transport them. But the benefits of SUVs hide some weaknesses. In addition to their classical antigen- or target-specific protective effects, LAVs can induce non-specific protective effects. Epidemiological data suggest that vaccination with smallpox, measles, BCG or oral polio vaccines results in increased overall childhood survival [reviewed and discussed in Benn et al. (59) and de Bree et al. (60)]. These observations can be partially explained by the poly-specificity of antigenic T and B receptors, the Mackaness effect and the induction of innate immune memory (trained immunity) (61). SUVs drive immune responses against a reduced number of dominant antigens and are associated with a modern adjuvant selected for its low inflammatory potential. Because this design reduces the possibilities of TCR and BCR-mediated cross-protection and a short-lived, low level of activation of innate immune response, it limits the possibility of non-specific protection. More importantly, vaccine resistance, although rare, is now well-documented for several SUVs (62). This seems mainly due to single mutational events, suggesting that small variations of pathogens can allow them to escape to sharp antigen selection pressure generated by SUVs. These weaknesses of SUVs, combined with the growth of antibiotic resistance, could in the near future leave us extremely helpless in the face of epidemics.

One solution to this problem is the rational development of second-generation LAVs retaining the efficiency of first-generation LAVS but compatible with current safety standards. This goal is achievable thanks to our better understanding of the genetics of microorganisms. However, we lack a rigorous methodology for selecting candidate vaccines in animal models.

Ideally, an effective and safe LAV should induce strong and adapted mucosal and systemic immunity against the target pathogen, without persisting or disseminating in the host. This requires, in particular, that the natural niche of pathogen persistence, the virulence genes necessary for pathogen persistence and the immune markers associated with the protective memory state be identified. The vast majority of studies attempting to identify these factors in animal experimental models are carried out using a single route of infection. Often, for historical or convenience reasons, a single route of infection is considered as the reference. In the case of studies to select candidate vaccines against *Brucella* in mice models, the reference is the intraperitoneal (i.p.) route (63) that leads to a rapid systemic infection. Rare studies use the more physiological intranasal (i.n.) or oral infection routes. The purpose of the present study was to highlight the impact of the route of infection on the identification of infection niches, virulence genes and immune markers associated with the development of a protective immune memory in the *Brucella* model.

We took advantage of the fact that we have already studied the reservoir of infection and the type of protective immune response in the i.p. (19, 20, 30) and i.n. (21, 36) *Brucella* infection models. In order to include a third model of infection in our comparison, we developed and characterized an original model of intradermal (i.d.) infection in this study. Contamination by cutaneous route is not the most common for *Brucella*, but it is however well-documented in certain occupational groups (13–15). We have chosen to characterize this route, rather than a more common type of *Brucella* contamination such as the oral route, because of its technical simplicity and because a large number of vaccines are given subcutaneously, including some *Brucella* vaccines in animals.

We observed that, following i.d. infection, *Brucella* disseminates immediately into the spleen and liver through the bloodstream and reaches the popliteal draining LNs in 24 h. *Brucella* is detected later in the mediastinal lymph nodes, muscles, and brain. At 50 days post infection, *Brucella* persists only in the spleen and LNs. As expected, control of the primary cutaneous infection requires a functional IL-12_{p35}/IFNγ axis, TNFα, as well as $CD4^+$T cells. $CD8^+$ T cells, $\gamma\delta^+$T cells, B cells and IL-17RA deficiencies appear to be dispensable. Thus, the i.d. model seems to be similar to the i.p. model (19). It differs strongly from the i.n. infection model which requires $\gamma\delta^+$T cells and IL-17RA to control *Brucella* during the early phase of lung infection (21).

The i.d. model is characterized by recruitment of monocytes and neutrophils at sites of skin infection in association with transitory moderate swelling. A deficiency of CCR2 results in a

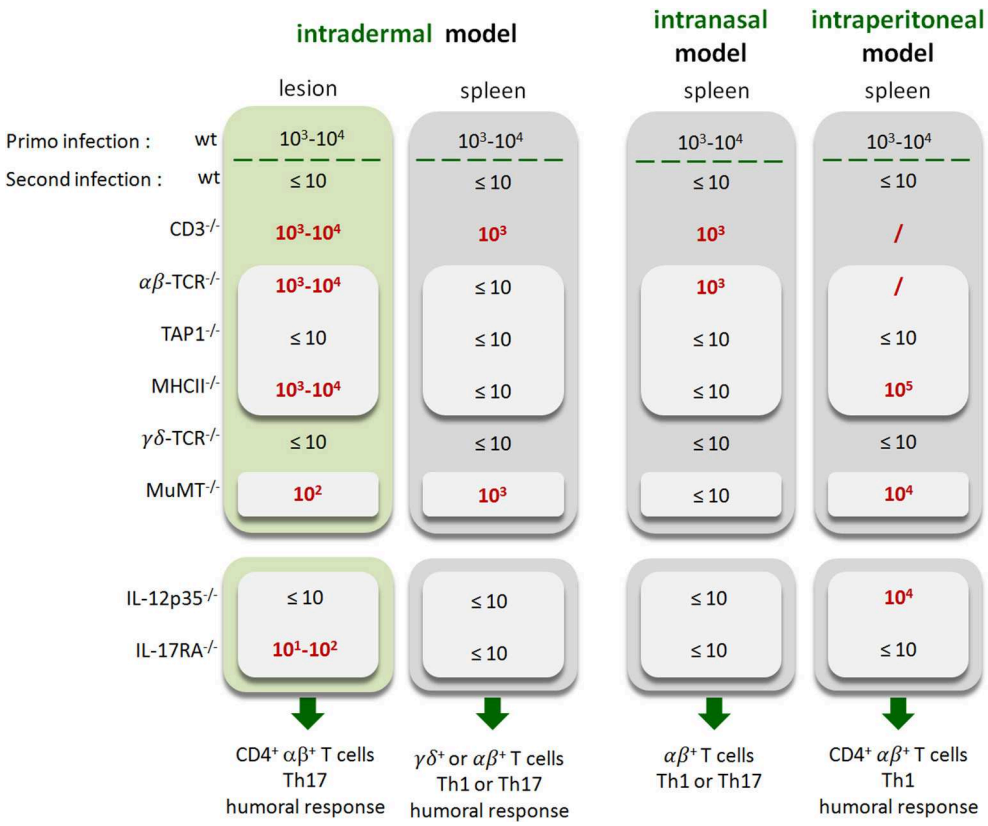

FIGURE 15 | Summary of the immune response components indispensable to the control of secondary *Brucella* infection as a function of the route of infection. Wild-type, CD3$^{-/-}$, TCRαβ$^{-/-}$, TCRγδ$^{-/-}$, MHCII$^{-/-}$, TAP1$^{-/-}$, MuMT$^{-/-}$, IL-12p35$^{-/-}$, and IL-17RA$^{-/-}$ C57BL/6 mice were infected intradermally (i.d.), intranasally (i.n.) or intraperitoneally (i.p.) with 2×10^4 CFU of live wild-type *B. melitensis* and treated with antibiotics, as described in the Materials and Methods. Naive (primary infection group) and immunized (second infection group) mice were challenged i.d., i.n., or i.p. with 2×10^4 CFU of live mCherry-*B. melitensis* and sacrificed at 12 days post infection (for i.d.) or 28 days post infection (for i.n. and i.p.). The data represent a qualitative approximation of the CFU count per organ in the present article (i.d. model and **Figure S8** for i.p. model) or in our group's previous article characterizing the i.p. (20) and i.n. (21) models. The CFU counts of mice which do not control the secondary infection are in red. "/", not tested. Note that "Th1 or Th17" indicates that the Th1 response can compensate for the absence of the Th17 response and vice versa.

delay in the recruitment of monocytes and a transitory lack of *Brucella* control at the cutaneous lesion and popliteal draining LN. IFNγR deficiency also reduces monocyte recruitment and is associated with a strong influx of neutrophils in the footpad lesion, development of necrosis and a high CFU count in the lesion, LN, and spleen. In contrast, as previously reported by us (21), in the i.n. *Brucella* infection model, monocyte and neutrophil recruitment is not observed in the lung and CCR2 deficiency does not affect the control of infection. Interestingly, in the i.d. model, CCR7 deficiency leads to a significant reduction of the spread of *Brucella* from the footpad lesion to the draining LN and the spleen at 1 and 3 days post infection, and an important increase in the number of bacteria in the cutaneous lesion at 7 and 14 days. Taken together, our data suggest that recruited monocytes play a key role in the control of *Brucella* in the i.d. model. They also suggest that dissemination of *Brucella* from the primary lesion to the draining LN and spleen could implicate CCR7-dependent cell migration. In agreement, Archambaud et al. (37) have shown that *Brucella* can migrate from the lung to draining LNs by infecting dendritic cells and alveolar macrophages.

An original and surprising observation in the i.d. infection model is the inability of the protective memory response to prevent establishment of *Brucella* in popliteal draining lymph nodes. The memory response eliminates *Brucella* in the cutaneous lesion, blood, and spleen, but fails to control *Brucella* in the draining LN, suggesting that there is a special reservoir protecting *Brucella* in this tissue. These LN reservoir cells should be better characterized, as von Bargen et al. (64) reported that LNs constitute the first site of *Brucella* infection and multiplication during oral infection in mice and humans. Unfortunately, in our i.d. model, the low CFU counts in LNs at later times of infection did not allow us to analyse the LN reservoir cells by flow cytometry and made it very difficult to visualize them by fluorescence microscopy.

By comparing i.p., i.n., and i.d. models, we observed that the host-pathogen relationship is strongly affected by the route of infection.

First, the pattern of tissue infection appears to vary widely depending on the route of infection. The i.p. route of infection leads to immediate systemic dissemination of *Brucella* to all tissues tested. In contrast, i.n. infection displays a more restricted pattern of infected tissues, including mainly the lung, mediastinal draining LNs and spleen. The i.d. model presents an intermediate pattern, with systemic dissemination to the spleen and liver and localized strong persistence of *Brucella* in the cutaneous lesion and popliteal draining LNs. The impact of the route of infection on the spread of bacteria has already been documented by whole body imaging in mice with radiolabelled or bioluminescent bacteria. However, only high bacteria levels in tissues is detected by this approach. Consequently, high doses of bacteria need to be administered and weakly infected organs are not identified. In the *Francisella* model (65), 2×10^9 radiolabelled bacteria were administrated and their dissemination was only monitored until 20 h post infection. In models using bioluminescent *Brucella melitensis* (66) and *Brucella suis* (67), $1\times$ to 2.5×10^7 bacteria were injected. In the spleen of mice infected with 2.5×10^7 CFU of *B. melitensis*, no bioluminescence was detected despite the detection of 4.8×10^3 CFU by plating (66), confirming the very poor sensitivity of bioluminescence detection. In contrast, though time-consuming, our classical approach based on the plating of select tissues detects up to 10 bacteria per tissue and allows us to use a moderate dose of infection, 2×10^4 CFU per mouse. Our results showed that, at 50 days post infection, *Brucella* persists mainly in lymphoid organs, such as the spleen and LNs in the three models, but also in the thymus in the i.p. model. However, our goal here was not to identify all possible *Brucella* persistence sites in mice and *Brucella* may persist in other tissues, such as the bone marrow as recently described (68).

Second, using eFluor670 labeled *Brucella*, we demonstrated that the type of cells infected first depends on the route of infection. As previously observed, we confirmed that the main cells infected in the lung of i.p. and i.n. infected mice at 2 and 24 h post infection were $F4/80^+$ red pulp macrophages (30) and alveolar macrophages (37), respectively. Surprisingly, we observed that, in addition to $F4/80^+$ monocytes/macrophages, $Ly6G^+$ neutrophils and $CD45^{neg}$ $CD140a^+$ fibroblasts also appear to be infected in the footpad lesion of i.d. infected wild-type mice. *Brucella*-infected neutrophils have been described in pathological conditions (69). To our knowledge, this is the first description of *Brucella*-infected fibroblasts *in vivo* in wild-type mice. Infection by *Brucella* of neutrophil and fibroblasts in the footpad lesions was confirmed by confocal microscopy. The infection of different cell types can have a significant impact on the persistence of *Brucella*. It has been observed *in vitro* that the intracellular trafficking of *Brucella* is dependent on the type of cells infected. For example, *Brucella abortus* replicates in a vacuole derived from the $LAMP1^{neg}$ endoplasmic reticulum in epithelial cells, macrophages and dendritic cells, although in extravillous trophoblasts it replicated within single-membrane acidic $LAMP1^{pos}$ inclusions (70).

Third, we observed that the route of infection affects the identification of a major virulence gene. The Δ*virB Brucella* strain, known to be attenuated in the i.p. infection model but able to persist for several weeks in the spleen (39), is unable to persist beyond 48 h in the lung in the i.n. infection model but, surprisingly, persists longer than the wild-type strain in cutaneous lesions in the i.d. infection model. This unexpected result is probably due in part to the different type of cells infected. It has been reported that ΔwadC (unable to encode LPS core glysosyltransferases) *Brucella abortus* multiplies in bone marrow-derived macrophages, RAW264.7 macrophages or HeLa cells but is killed in bone marrow-derived dendritic cells (71). Microscopic analysis showed that the Δ*virB Brucella melitensis* strain multiplies very weakly in alveolar macrophages, ∼15-fold less than the wild type strain. In striking contrast, it multiplies at the same level as the wild-type strain in splenic macrophages and at an intermediate level in dermal cells, ∼2-fold less than the wild type strain. This slightly lower multiplication rate of the Δ*virB Brucella* strain in the footpad lesion may make *Brucella* more stealthy and thus less detectable by the immune system and able to persist longer than the wild type strain. Taken together, our data lead us to conclude that a bacterial strain can be considered as attenuated or not depending on the route of infection and the tissues analyzed.

Fourth, we demonstrate that the route of infection also affects the identification of immune markers associated with a protective memory response. As summarized in **Figure 15**, which compares the results obtained in this article in the i.d. infection model as well as those obtained previously by us in the i.p. (20) and i.n. (21) infection models, *Brucella* control in the spleen in challenge conditions required different lymphocyte subsets and T helper responses depending on the route of infection. Control in the i.p. model appears to be dependent on $IL\text{-}12_{p35}$, $CD4^+$T cells and B cells (20). In the i.n. model, only $\alpha\beta^+$T cells appear to be strictly required. A deficiency of $CD4^+$T cells, $CD8^+$T cells, B cells or $IL\text{-}12_{p35}$ has no significant impact on *Brucella* control in the spleen. Only the simultaneous deficiency of $IL\text{-}12_{p35}$ and IL17RA leads to a lack of control (21). Finally, in the i.d. infection model, B cells appear to be indispensable, like in the i.p. model, but $CD4^+$T cells are required in the lesion but not in the spleen. More surprisingly, *Brucella* control in the lesion required IL-17RA, whereas it was not necessary for control of the primary infection. And conversely, $IL\text{-}12_{p35}$, which is needed to control the primary infection, is no longer essential to control the challenge in the lesion.

It may seem surprising that, depending on the route of infection, control of *Brucella* in the same organ, the spleen, requires different types of lymphocyte populations and different T helper responses. These different needs may be the consequence of the specific immune conditions prevailing at the primary infection site in the different models. It is well-established that the composition of immune and stromal cells, as well as the phenotype of those cells, the nature of the microenvironment and the isotypes of the antibodies differ in each tissue and affect the ability of the immune system to control both infections and tumor growth [reviewed in Engwerda et al. (72) and Pao et al. (73)]. Therefore, depending on the route of infection and on the primary infection site, the bacterial load reach in the blood and spleen may differ significantly. We observed this in practice when comparing our 3 models (**Figure 1D**). The need for B cells is correlated with the rapid

spread of bacteria in the blood, like in the i.p. and i.n. models. In the i.n. model, B cells are not needed and *Brucella* is not detected in the blood at any time. The same reasoning can be applied to the requirement for IL-12p35. IL-12p35 is indispensable in the spleen only in the i.p. model, where the bacterial load reaching the spleen is the highest. Regardless of the dose reaching the organ over time, *Brucella* could also reach the spleen in different forms depending on the route of infection. During the first 24 h following i.p. infection, *Brucella* is found in the blood in extracellular form (35). In the i.n. model, *Brucella* disseminates from the lung to draining lymph nodes inside dendritic cells and alveolar macrophages (37). Therefore, *Brucella* could reach the spleen by being protected from antibodies within a cell, which would explain that B cells are not necessary.

The route of infection has been reported to impact the nature of the protective immune response in certain other infection models. For example, control of an i.p. *Listeria monocytogenes* challenge strictly requires memory $CD4^+$ and $CD8^+$ $\alpha\beta^+$T cells producing IFNγ (74). But in the oral *L. monocytogenes* infection model, intestinal multifunctional $\gamma\delta^+$T cells able to simultaneously produce IFNγ and IL-17A can provide enhanced protection against infection and even compensate for the absence of $\alpha\beta^+$T cells (75). However, the impact of different routes of infection on the type of protective memory response is rarely compared and should be more systematic in view of its importance.

One of the major interests of our comparison of the i.p., i.n., and i.d. infection routes is that all of our experiments were conducted using the same strains of *Brucella melitensis* 16M and C57BL/6 mice, with the same infectious dose and under the same animal facility conditions. There is a large body of available data on mice infected i.p. or i.n. by *Brucella* in the literature. It is very difficult, however, to truly compare the data from these models because the infectious doses and the strains of *Brucella* and mice are often different. For example, the study of Hielpos et al. (76) showed that *B. abortus* persisted at high levels in the lungs for at least 7 days and was detected in the spleen as early as 24 h p.i., much earlier than in our i.n. model of infection. However, BALB/c mice, that are more susceptible to *Brucella* than the C57BL/6 strain, were used in the Hielpos study and were infected with 10^6 CFU of *B. abortus*, at a dose 50 times higher than our infection dose. Under these experimental conditions, it is therefore quite normal that *Brucella* was detected in the spleen much faster than in our model. Even though the experimental conditions seem similar, it is well-known that, depending on the animal facility conditions, the immunological experience of mice can affect their ability to control an infection non-specifically and that a strain of bacteria can drift in the laboratory and present slightly different virulence. Consequently, comparisons between different models of *in vivo* infections that are not performed under exactly the same experimental conditions are often hazardous.

It is important to point out that, since the mouse is not the natural host of *Brucella melitensis*, we do not consider that one particular route of infection in a mice model is more physiological or informative than another regarding what is happening in the natural host during a *Brucella* infection. This work must be seen as fundamental research work carried out with the aim of improving the methodology for the rational design of LAVs in animal models. However, our comparison of three routes of infection allows us to draw some practical conclusions. We observed that both the humoral response and the cellular response are essential to the control of a challenge in the i.p. and i.d. models, which is not the case in the i.n. model where a humoral response and even αβT cells are dispensable. As discussed previously, this can be explained by the fact that the i.p. and i.d. routes of infection lead to massive dissemination of *Brucella* in the blood, which is not the case for the i.n. route. Likewise, in sheep, inoculation by the subcutaneous route produced wider and more generalized infections than the conjunctival route (50). Thus, the i.p. and i.d. routes lead to systemic infection that therefore appears to be more difficult to control than a mucosal i.n. infection and consequently may be a more demanding test in mice for assessing the protective capacity of a vaccine candidate. If we compare i.p. and i.d. models, the latter display the advantage of being close to the subcutaneous vaccination route conventionally used with the REV1 *B. melitensis* vaccine in small ruminants. The i.d. model of infection in mice also displays a pattern of tissue infection that is quite similar to that described in the goat (77) following subcutaneous infection with a virulent strain of *Brucella melitensis*. Thus, for these reasons, i.d. could constitute a new promising route of delivery for tests of candidate vaccines in a mouse model.

In summary, our study demonstrates that the identification of candidate LAVs and immune protection markers in an animal model can be strongly affected by the route of infection used. We therefore recommend that researchers systematically compare different routes of infection, identified as those closest possible to the natural host infection, and not be limited to the analysis of a single tissue type. As the infectious doses (78) as well as the strain of pathogen analyzed (79) can also strongly affect the type of protective immune response, as has been well-documented in the experimental mouse model of *Leishmania major* infection, we can conclude that the selection process of candidate LAVs is much more complex than expected.

DATA AVAILABILITY

The raw data supporting the conclusions of this manuscript will be made available by the authors, without undue reservation, to any qualified researcher.

ETHICS STATEMENT

The procedures used in this study and the handling of the mice complied with current European legislation (Directive 86/609/EEC) and the corresponding Belgian law Arrêté royal relatif à la protection des animaux d'expérience of 6 April 2010 and published on 14 May 2010. The Animal Welfare Committee of the Université de Namur (UNamur, Belgium) reviewed and approved the complete protocol for Brucella infection (Permit Number: UN-LE-13/195).

AUTHOR CONTRIBUTIONS

AD and EM wrote the article. AD, AL, AM, MV, and J-MV realized experiments. GP, XD, J-JL, and EM provided reagents.

FUNDING

This work was supported by grants from the Fonds National de la Recherche Scientifique (FNRS) (convention FRSM FNRS 1.4.013.16.F and 3.4.600.06.F, Belgium). EM is a Senior Research Associate from the FRS-FNRS (Belgium). AD, AM, and GP hold FRIA PhD grants from the FRS-FNRS (Belgium). AD and GP were supported by Fonds Spécial de Recherche (FSR) PhD grants from the UNamur (Belgium).

ACKNOWLEDGMENTS

The authors thank Katy Poncin, Manon Merckx, Audrey Comein, and Maxime Lagneaux for their helpful contribution.

SUPPLEMENTARY MATERIAL

The Supplementary Material for this article can be found online at: https://www.frontiersin.org/articles/10.3389/fimmu.2019.01589/full#supplementary-material

Figure S1 | Each route of infection leads to a specific pattern of infected organs (part 1). Wild-type C57BL/6 mice were infected intraperitoneally (i.p.), intranasally (i.n.) or intradermally (i.d.) with a dose of 2×10^4 CFU of mCherry-*B. melitensis* and sacrificed at the indicated times. The data represent the CFU count per footpad lesion, popliteal LN, lung, or mediastinal LN. Gray bars represent the median. The significant differences between the indicated groups are marked with asterisks: $*p < 0.1$, $**p < 0.01$, $***p < 0.001$. These results are representative of two independent experiments. LN, lymph node; h, hours; d, days; n, number of mice per group.

Figure S2 | Each route of infection leads to a specific pattern of infected organs (part 2). Wild-type C57BL/6 mice were infected intraperitoneally (i.p.), intranasally (i.n.) or intradermally (i.d.) with a dose of 2×10^4 CFU of mCherry-*B. melitensis* and sacrificed at the indicated times. The data represent the CFU count per skeletal muscle, heart, tail, brain, liver, or ovary. Gray bars represent the median. The significant differences between the indicated groups are marked with asterisks: $*p < 0.1$, $**p < 0.01$, $***p < 0.001$. These results are representative of two independent experiments. h, hours; d, days; n, number of mice per group.

Figure S3 | Intraperitoneal *Brucella* infection leads to infection of a large panel of lymph nodes. Wild-type C57BL/6 mice were infected intraperitoneally (i.p.) with a dose of 2×10^4 CFU of mCherry-*B. melitensis* and sacrificed at 50 days post infection. The data represent the CFU count per lymphoid organs (spleen, right inguinal LN, right axillary LN, mediastinal LN, mesenteric LN, and right popliteal LN). Gray bars represent the median. These results are representative of two independent experiments. LN, lymph node; n, number of mice per group.

Figure S4 | Impact of eFluor670 staining on *Brucella* growth *in vitro* and *in vivo*. **(A)** 4×10^4 CFU/ml of mCherry-*B. melitensis* were prepared from an overnight liquid culture and stained with the eFluor670 fluorochrome. Bacteria were fixed and then analyzed by flow cytometry. **(B)** Comparison by Bioscreen analysis of the growth of mCherry-*B. melitensis* and eFluor670 stained mCherry-*B. melitensis* in rich medium (2YT). These data represent the mean of three independent experiments. **(C)** Wild-type C57BL/6 mice were infected i.n. with a dose of 2×10^4 CFU of mCherry-*B. melitensis* or eFluor670 labeled mCherry-*B. melitensis* and sacrificed at 5 or 12 days post infection. The data represent the CFU count per lung. **(D)** Wild-type C57BL/6 mice were infected i.p. with a dose of 10^5 CFU of mCherry-*B. melitensis* eFluor670 labeled mCherry-*B. melitensis* and sacrificed at 5 or 12 days post infection. The data represent the CFU count per spleen. These results **(C,D)** are representative of two independent experiments. Gray bars represent the median. d, days; n, number. The significant differences between the indicated groups are marked with asterisks: $*p < 0.1$.

Figure S5 | Phenotype of infected footpad lesion cells from wild type mice. Wild-type C57BL/6 mice were infected intradermally with 10^7 CFU of *B. melitensis*. Control wild-type mice were injected with PBS. The footpad lesions were harvested at 2 or 24 h post infection and the cells were analyzed by flow cytometry. The data result from the flow cytometry analysis of eFluor670, CD45, CD140a, and CD11b expression on footpad cells. The data show the representative dot plot from individual mice. These results are representative of three independent experiments.

Figure S6 | Phenotype of infected CD11b-positive footpad lesion cells from wild type mice. Wild-type C57BL/6 mice were infected intradermally with 10^7 CFU of *B. melitensis*. Control wild-type mice were injected with PBS. The footpad lesions were harvested at 2 or 24 h post infection and the cells were analyzed by flow cytometry. The data result from the flow cytometry analysis of eFluor670, F4/80, Ly6G, and CD11b expression on footpad cells. The data show the representative dot plot from individual mice. These results are representative of three independent experiments.

Figure S7 | Complemented Δ*virB* strain growth in the lung. Wild-type C57BL/6 mice were infected i.n. with a dose of 10^5 CFU of wild type mCherry-*B. melitensis*, Δ*virB* mCherry- *B. melitensis* or complemented Δ*virB* mCherry-*B. melitensis* (Δ*virB* mCherry-*B. melitensis* p*virB*). Mice were sacrificed at 5 days post infection and the lung was collected. The data represent the CFU count per lung. Gray bars represent the median. Significant differences between the indicated groups are marked with asterisks: $**p < 0.01$, $***p < 0.001$. These results are representative of two independent experiments. n, number of mice per group.

Figure S8 | eFluor670 labeling identified newborn *Brucella*. mCherry *Brucella melitensis* is labeled with eFluor670. **(A)** Schematic representation of unipolar growth of eFluor670 labeled mCherry-*Brucella*. As eFluor670 does not move in the bacterial membrane, the newly formed bacterium, called the newborn, loses the eFluor670 labeling, allowing its identification by fluorescent microscopy. **(B)** Representative image at 0 and 24 h of eFluor670 labeled mCherry-*Brucella* extracellular growth *in vitro*. The 24 h image shows a division and a newborn cell ($mCherry^+$ $eFluor670^-$). The panels are color-coded with the text for mCherry and eFluor670. Scale bar = 5 μm. h, hours; n, newborn; pos, positive; neg, negative.

Figure S9 | BALB/c mice are more susceptible to cutaneous *Brucella* infection than C57BL/6 mice. Wild-type C57BL/6 and BALB/c mice were infected intradermally with a dose of 2×10^4 CFU of *B. melitensis* and sacrificed at the indicated times. The data represent the CFU count per organ. Gray bars represent the median. The significant differences between the indicated groups are marked with asterisks: $*p < 0.1$, $**p < 0.01$, $***p < 0.001$. These results are representative of two independent experiments. LN, lymph node; d, days; n, number of mice per group.

Figure S10 | Neutrophils constitute the major population in the footpad lesion from infected $IFN\gamma R^{-/-}$ mice. Wild-type, $IFN\gamma R^{-/-}$, and $CCR2^{-/-}$ C57BL/6 mice were infected intradermally with a dose of 2×10^4 CFU of mCherry-*B. melitensis*. Control wild-type mice were injected with PBS. The footpad lesions were harvested at 3 and 7 days post infection and the cells were analyzed by flow cytometry. **(A)** Flow cytometry analysis of CD11b, F4/80, and LY6G expression on footpad cells. The data show the representative dot plot from individual mice. **(B)** Data represent the mean frequency ($n = 4$) of neutrophils and monocytes in the footpad lesion at the indicated time of infection. These results are representative of three independent experiments. Cont, control; d, days.

Figure S11 | Humoral immune response induced by intradermal *Brucella* infection. Wild-type C57BL/6 mice were infected intradermally **(A)** or intraperitoneally **(B)** with a dose of 2×10^4 CFU of mCherry-*B. melitensis*. Serum was collected at the indicated times, and ELISA was performed to determine the isotype distribution of the *Brucella*-specific antibodies. The data represent the means ± SEM of results for 8 mice. These results are representative of three independent experiments. O.D, optical density; d, days.

Figure S12 | Comparison of protection in wild-type and various deficient mice previously immunized by intraperitoneal route with live *B. melitensis*. Wild-type, $TCR\gamma\delta^{-/-}$, $MHCII^{-/-}$, $TAP1^{-/-}$, Il-12p35$^{-/-}$, and IL-17RA$^{-/-}$ C57BL/6 mice

were immunized i.p. with 2×10^4 CFU of live wild-type *B. melitensis* and treated with antibiotics, as described in the Materials and Methods. Naive (primary infection group) and immunized (secondary infection group) mice were challenged i.p. with 2×10^4 CFU of live mCherry-*B. melitensis* and sacrificed at 12 days post infection. The data represent the CFU count per spleen. Gray bars represent the median. The significant differences between the indicated groups are marked with asterisks: $^{**}p < 0.01$. These results are representative of two independent experiments. n, number of mice per groups.

REFERENCES

1. Minor PD. Live attenuated vaccines: historical successes and current challenges. *Virology.* (2015) 479–480:379–92. doi: 10.1016/j.virol.2015.03.032
2. Detmer A, Glenting J. Live bacterial vaccines - a review and identification of potential hazards. *Microb Cell Fact.* (2006) 5:1–12. doi: 10.1186/1475-2859-5-23
3. Lauring AS, Jones JO, Andino R. Rationalizing the development of live attenuated virus vaccines. *Nat Biotechnol.* (2010) 28:573–9. doi: 10.1038/nbt.1635
4. Delany I, Rappuoli R, De Gregorio E. Vaccines for the 21st century. *EMBO Mol Med.* (2014) 6:708–20. doi: 10.1002/emmm.201403876
5. Pappas G, Papadimitriou P, Akritidis N, Christou L, Tsianos E V. The new global map of human brucellosis. *Lancet Infect Dis.* (2006) 6:91–9. doi: 10.1016/S1473-3099(06)70382-6
6. Pappas G, Akritidis N, Bosilkovski M. Brucellosis. *N Engl J Med.* (2005) 352:130–4. doi: 10.1097/SHK.0000000000000692
7. Colmenero JD, Reguera JM, Martos F, Sánchez-De-Mora D, Delgado M, Causse M, et al. Complications associated with *Brucella melitensis* infection: a study of 530 cases. *Medicine.* (1996) 75:195–211. doi: 10.1097/00005792-199607000-00003
8. Godfroid J, Cloeckaert A, Liautard JP, Kohler S, Fretin D, Walravens K, et al. From the discovery of the Malta fever's agent to the discovery of a marine mammal reservoir, brucellosis has continuously been a re-emerging zoonosis. *Vet Res.* (2005) 36:313–26. doi: 10.1051/vetres:2005003
9. Kaufmann AF, Fox MD, Boyce JM, Anderson DC, Potter ME, Martone WJ, et al. Airborne spread of brucellosis. *Ann N Y Acad Sci.* (1980) 353:105–14.
10. Hendricks SL, Borts IH, Heeren RH, Hausler WJ, Held JR. Brucellosis outbreak in an Iowa packing house. *Am J Public Health.* (1962) 52:1166–78.
11. Olle-Goig JE, Canela-Soler J. An outbreak of *Brucella melitensis* infection by airborne transmission among laboratory workers. *Am J Public Health.* (1987) 1987:335. doi: 10.2105/AJPH.77.3.335
12. Wallach JC, Samartino LE, Efron A, Baldi PC. Human infection by *Brucella melitensis*: an outbreak attributed to contact with infected goats. *FEMS Immunol Med Microbiol.* (1997) 1997:98. doi: 10.1016/S0928-8244(97)00098-9
13. Trunnell T, Waisman M, Trunnell T. Contact dermatitis caused by Brucella. *Cutis.* (1985) 35:379–81.
14. Joffee B, Diamond MT. Brucellosis due to self-inoculation. *Ann Intern Med.* (1966) 65:564–5. doi: 10.7326/0003-4819-65-3-564
15. Berger TG, Guill MA, Goette DK. Cutaneous Lesions in Brucellosis. *Arch Dermatol.* (1981) 56:339–40. doi: 10.1001/archderm.1981.01650010046024
16. Martirosyan A, Moreno E, Gorvel JP. An evolutionary strategy for a stealthy intracellular Brucella pathogen. *Immunol Rev.* (2011) 240:211–34. doi: 10.1111/j.1600-065X.2010.00982.x
17. De Jong MF, Tsolis RM. Brucellosis and type IV secretion. *Future Microbiol.* (2012) 1:47–58. doi: 10.2217/fmb.11.136
18. Celli J. The changing nature of the Brucella-containing vacuole. *Cell Microbiol.* (2015) 17:951–8. doi: 10.1111/cmi.12452
19. Vitry M-A, De Trez C, Goriely S, Dumoutier L, Akira S, Ryffel B, et al. Crucial role of gamma interferon-producing CD4+ Th1 cells but dispensable function of CD8+ T cell, B cell, Th2, and Th17 responses in the control of Brucella melitensis infection in mice. *Infect Immun.* (2012) 80:4271–80. doi: 10.1128/IAI.00761-12
20. Vitry M-A, Hanot Mambres D, De Trez C, Akira S, Ryffel B, Letesson J-J, et al. Humoral immunity and CD4+ Th1 cells are both necessary for a fully protective immune response upon secondary infection with *Brucella melitensis*. *J Immunol.* (2014) 192:3740–52. doi: 10.4049/jimmunol.1302561
21. Hanot Mambres D, Machelart A, Potemberg G, De Trez C, Ryffel B, Letesson J-J, et al. Identification of immune effectors essential to the control of primary and secondary intranasal infection with *Brucella melitensis*. in mice. *J Immunol.* (2016) 196:3780–93. doi: 10.4049/jimmunol.1502265
22. Pardon P, Marly J. Resistance of normal or immunized guinea pigs against a subcutaneous challenge of Brucella abortus. *Ann Rech Vét.* (1978) 9:419–25.
23. Huang S, Hendriks W, Althage A, Hemmi S, Bluethmann H, Kamijo R, et al. Immune response in mice that lack the interferon-gamma receptor. *Science.* (1993) 259:1742–5.
24. Carrera L, Gazzinelli RT, Badolato R, Hieny S, Muller W, Kuhn R, et al. Leishmania promastigotes selectively inhibit interleukin 12 induction in bone marrow-derived macrophages from susceptible and resistant mice. *J Exp Med.* (1996) 183:515–26.
25. Nakae S, Komiyama Y, Nambu A, Sudo K, Iwase M, Homma I, et al. Antigen-specific T cell sensitization is impaired in Il-17-deficient mice, causing suppression of allergic cellular and humoral responses. *Immunity.* (2002) 17:375–87. doi: 10.1016/S1074-7613(02)00391-6
26. Rothe J, Lesslauer W, Lötscher H, Lang Y, Koebel P, Köntgen F, et al. Mice lacking the tumour necrosis factor receptor 1 are resistant to TNF-mediated toxicity but highly susceptible to infection by Listeria monocytogenes. *Nature.* (1993) 364:798–802. doi: 10.1038/364798a0
27. Van Kaer L, Ashton-Rickardt PG, Ploegh HL, Tonegawa S. TAP1 mutant mice are deficient in antigen presentation, surface class I molecules, and CD4-8+ T cells. *Cell.* (1992) 71:1205–14.
28. Cosgrove D, Gray D, Dierich A, Kaufman J, Lemeur M, Benoist C, et al. Mice lacking MHC class II molecules. *Cell.* (1991) 66:1051–66. doi: 10.1016/0092-8674(91)90448-8
29. Shaner NC, Campbell RE, Steinbach PA, Giepmans BNG, Palmer AE, Tsien RY. Improved monomeric red, orange and yellow fluorescent proteins derived from Discosoma sp. red fluorescent protein. *Nat Biotechnol.* (2004) 22:1567–1572. doi: 10.1038/nbt1037
30. Copin R, Vitry M-A, Hanot Mambres D, Machelart A, De Trez C, Vanderwinden J-M, et al. *In situ* microscopy analysis reveals local innate immune response developed around Brucella infected cells in resistant and susceptible mice. *PLoS Pathog.* (2012) 8:e1002575. doi: 10.1371/journal.ppat.1002575
31. Nijskens C, Copin R, De Bolle X, Letesson JJ. Intracellular rescuing of a B. melitensis 16M virB mutant by co-infection with a wild type strain. *Microb Pathog.* (2008) 45:134–41. doi: 10.1016/j.micpath.2008.04.005
32. Casadaban MJ, Cohen SN. Analysis of gene control signals by DNA fusion and cloning in *Escherichia coli*. *J Mol Biol.* (1980) 138:179–207.
33. Mignolet J, Van Der Henst C, Nicolas C, Deghelt M, Dotreppe D, Letesson JJ, et al. PdhS, an old-pole-localized histidine kinase, recruits the fumarase FumC in *Brucella abortus*. *J Bacteriol.* (2010) 192:3235–9. doi: 10.1128/JB.00066-10
34. Cl T, Mertens P, Dierick J, Letesson J, Lambert C, De Bolle X. Functional, molecular and structural characterisation of five anti- Brucella LPS mAb. *Mol Immunol.* (2004) 40:1237–47. doi: 10.1016/j.molimm.2003.11.037
35. Vitry M-A, Hanot Mambres D, Deghelt M, Hack K, Machelart A, Lhomme F, et al. *Brucella melitensis* invades murine erythrocytes during infection. *Infect Immun.* (2014) 2014:14. doi: 10.1128/IAI.01779-14
36. Mambres DH, Machelart A, Vanderwinden JM, De Trez C, Ryffel B, Letesson JJ, et al. *In situ* characterization of splenic brucella melitensis reservoir cells during the chronic phase of infection in susceptible mice. *PLoS ONE.* (2015) 10:e137835. doi: 10.1371/journal.pone.0137835
37. Archambaud C, Salcedo SP, Lelouard H, Devilard E, De Bovis B, Van Rooijen N, et al. Contrasting roles of macrophages and dendritic cells in controlling initial pulmonary Brucella infection. *Eur J Immunol.* (2010) 40:3458–71. doi: 10.1002/eji.201040497
38. Lourdes T, Lacerda S, Salcedo SP, Gorvel J. Brucella T4SS : the VIP pass inside host cells. *Curr Opin Microbiol.* (2013) 16:45–51. doi: 10.1016/j.mib.2012.11.005

39. Den Hartigh AB, Sun Y, Sondervan D, Heuvelmans N, Reinders MO, Ficht TA. Differential Requirements for VirB1 and VirB2 during Brucella abortus Infection. *Infect Immun.* (2004) 72:5143–9. doi: 10.1128/IAI.72.9.5143
40. Brown PJB, De Pedro MA, Kysela T, Van Der Henst C, Kim J, De Bolle X, et al. Polar growth in the Alphaproteobacterial order Rhizobiales. *Proc Natl Acad Sci.* (2012) 109:1697–701. doi: 10.1073/pnas.1200309109
41. Deghelt M, Mullier C, Sternon J-F, Francis N, Laloux G, Dotreppe D, et al. G1-arrested newborn cells are the predominant infectious form of the pathogen *Brucella abortus*. *Nat Commun.* (2014) 5:4366. doi: 10.1038/ncomms5366
42. Copin R, De Baetselier P, Carlier Y, Letesson J-J, Muraille E. MyD88-dependent activation of $B220^{-}CD11b^{+}LY\text{-}6C^{+}$ dendritic cells during *Brucella melitensis* infection. *J Immunol.* (2007) 178:5182–91. doi: 10.4049/jimmunol.178.8.5182
43. Serbina NV, Pamer EG. Monocyte emigration from bone marrow during bacterial infection requires signals mediated by chemokine receptor CCR2. *Nat Immunol.* (2006) 7:311–7. doi: 10.1038/ni1309
44. Malissen B, Tamoutounour S, Henri S. The origins and functions of dendritic cells and macrophages in the skin. *Nat Rev Immunol.* (2014) 14:417–28. doi: 10.1038/nri3683
45. Tamoutounour S, Guilliams M, MontananaSanchis F, Liu H, Terhorst D, Malosse C, et al. Origins and functional specialization of macrophages and of conventional and monocyte-derived dendritic cells in mouse skin. *Immunity.* (2013) 39:925–38. doi: 10.1016/j.immuni.2013.10.004
46. Randolph GJ, Angeli V, Swartz MA. Dendritic-cell trafficking to lymph nodes through lymphatic vessels. *Nat Rev Immunol.* (2005) 5:617–28. doi: 10.1038/nri1670
47. Machelart A, Van Vyve M, Potemberg G, Demars A, De Trez C, Tima HG, et al. Trypanosoma infection favors Brucella elimination via IL-12/IFNγ-dependent pathways. *Front Immunol.* (2017) 8:903. doi: 10.3389/fimmu.2017.00903
48. Mackaness GB. The immunological basis of acquired cellular resistance. *J Exp Med.* (1964) 120:105–20.
49. Blanden RV, Lefford MJ, Mackaness GB. The host response to Calmette-Guérin bacillus infection in mice. *J Exp Med.* (1969) 129:1079–107.
50. Guilloteau LA, Laroucau K, Olivier M, Grillo MJ, Marin CM, Verger JM, et al. Residual virulence and immunogenicity of CGV26 and CGV2631 *B. melitensis* Rev. 1 deletion mutant strains in sheep after subcutaneous or conjunctival vaccination. *Vaccine.* (2006) 24:3461–8. doi: 10.1016/j.vaccine.2006.02.007
51. Barrio MB, Grilló MJ, Muñoz PM, Jacques I, González D, de Miguel MJ, et al. Rough mutants defective in core and O-polysaccharide synthesis and export induce antibodies reacting in an indirect ELISA with smooth lipopolysaccharide and are less effective than Rev 1 vaccine against Brucella melitensis infection of sheep. *Vaccine.* (2009) 27:1741–9. doi: 10.1016/j.vaccine.2009.01.025
52. Muñoz PM, de Miguel MJ, Grilló MJ, Marín CM, Barberán M, Blasco JM. Immunopathological responses and kinetics of *Brucella melitensis* Rev 1 infection after subcutaneous or conjunctival vaccination in rams. *Vaccine.* (2008) 26:2562–9. doi: 10.1016/j.vaccine.2008.03.030
53. Molloy MJ, Zhang W, Usherwood EJ, Alerts E. Suppressive CD8+ T cells arise in the absence of CD4 help and compromise control of persistent virus. *J Immunol.* (2011) 186:6218–26. doi: 10.4049/jimmunol.1003812
54. Liu J, Chen D, Nie GD, Dai Z. CD8+CD122+ T-cells: a newly emerging regulator with central memory cell phenotypes. *Front Immunol.* (2015) 6:6–11. doi: 10.3389/fimmu.2015.00494
55. Zur Wiesch PA, Kouyos R, Engelstädter J, Regoes RR, Bonhoeffer S. Population biological principles of drug-resistance evolution in infectious diseases. *Lancet Infect Dis.* (2011) 11:236–47. doi: 10.1016/S1473-3099(10)70264-4
56. Pérez O, Romeu B, Cabrera O, González E, Batista-Duharte A, Labrada A, et al. Adjuvants are key factors for the development of future vaccines: lessons from the finlay adjuvant platform. *Front Immunol.* (2013) 4:407. doi: 10.3389/fimmu.2013.00407
57. Reed SG, Orr MT, Fox CB. Key roles of adjuvants in modern vaccines. *Nat Med.* (2013) 19:1597–608. doi: 10.1038/nm.3409
58. De Gregorio E, Rappuoli R. From empiricism to rational design: a personal perspective of the evolution of vaccine development. *Nat Rev Immunol.* (2014) 14:505–14. doi: 10.1038/nri3694
59. Benn CS, Netea MG, Selin LK, Aaby P. A small jab - a big effect: nonspecific immunomodulation by vaccines. *Trends Immunol.* (2013) 34:431–9. doi: 10.1016/j.it.2013.04.004
60. de Bree CLCJ, Koeken VACM, Joosten LAB, Aaby P, Benn CS, van Crevel R, et al. Non-specific effects of vaccines: current evidence and potential implications. *Semin Immunol.* (2018) 39:35–43. doi: 10.1016/j.smim.2018.06.002
61. Muraille E. The unspecific side of acquired immunity against infectious disease: causes and consequences. *Front Microbiol.* (2016) 6:1525. doi: 10.3389/fmicb.2015.01525
62. Kennedy DA, Read AF. Why does drug resistance readily evolve but vaccine resistance does not? *Proc R Soc B Biol Sci.* (2017) 284:2562. doi: 10.1098/rspb.2016.2562
63. Grilló M, Blasco JM, Gorvel JP, Moriyón I, Moreno E. What have we learned from brucellosis in the mouse model? *Vet Res.* (2012) 43:29.doi: 10.1186/1297-9716-43-29
64. Von Bargen K, Gagnaire A, Arce-Gorvel V, De Bovis B, Baudimont F, Chasson L, et al. Cervical lymph nodes as a selective niche for brucella during oral infections. *PLoS ONE.* (2015) 10:e121790. doi: 10.1371/journal.pone.0121790
65. Ojeda SS, Wang ZJ, Mares CA, Chang TA, Li Q, Morris EG, et al. Rapid dissemination of *Francisella tularensis* and the effect of route of infection. *BMC Microbiol.* (2008) 8:1–15. doi: 10.1186/1471-2180-8-215
66. Rajashekara G, Glover DA, Krepps M, Splitter GA. Temporal analysis of pathogenic events in virulent and avirulent *Brucella melitensis* infections. *Cell Microbiol.* (2005) 7:1459–73. doi: 10.1111/j.1462-5822.2005.00570.x
67. Wang X, Li Z, Li B, Chi H, Li J, Fan H, et al. Bioluminescence imaging of colonization and clearance dynamics of *Brucella Suis* vaccine strain S2 in mice and guinea pigs. *Mol Imaging Biol.* (2016) 18:519–26. doi: 10.1007/s11307-015-0925-6
68. Gutiérrez-jiménez C, Hysenaj L, Alfaro-alarcón A, Mora-cartín R, Arce-gorvel V, Moreno E, et al. Persistence of *Brucella abortus*. in the bone marrow of infected mice. *J Immunol Res.* (2018) 2018:1–8. doi: 10.1155/2018/5370414
69. Machelart A, Potemberg G, Van Maele L, Demars A, Lagneaux M, De Trez C, Sabatel C, et al. Allergic asthma favors brucella growth in the lungs of infected mice. *Front Immunol.* (2018) 9:1–20. doi: 10.3389/fimmu.2018.01856
70. Salcedo SP, Chevrier N, Lacerda TLS, Ben Amara A, Gerart S, Gorvel VA, et al. Pathogenic brucellae replicate in human trophoblasts. *J Infect Dis.* (2013) 207:1075–83. doi: 10.1093/infdis/jit007
71. Arce-gorvel V, Iriarte M, Manc M, Conde-a R, Chaves-olarte E, Martirosyan A, et al. The lipopolysaccharide core of *Brucella abortus* acts as a shield against innate immunity recognition. *PLoS Pathog.* (2012) 8:2675. doi: 10.1371/journal.ppat.1002675
72. Engwerda CR, Kaye PM, Engwerda C, Kaye P. Organ-specific immune responses associated with infectious disease. *Immunol Today.* (2000) 21:73–8. doi: 10.1016/S0167-5699(99)01549-2
73. Pao W, Ooi C, Birzele F, Ruefli-brasse A, Cannarile MA, Reis B, et al. Prospective tissue-specific immunoregulation : a call for better understanding of the "immunostat" in the context of cancer. *Cancer Discov.* (2018) 8:395–402. doi: 10.1158/2159-8290.CD-17-1320
74. Ladel CH, Flesch IE, Arnoldi J, Kaufmann SHE. Studies with MHC-deficient knock-out mice reveal impact of both MHC I- and MHC II-dependent T cell responses on Listeria monocytogenes infection. *J Immunol.* (1994) 1984:784773. doi: 10.3109/07420528.2013.784773
75. Sheridan B, Romagnoli P, Pham QM, Fu HH, Alonzo F, Schubert WD, et al. gd T cells exhibit multifunctional and protective memory in intestinal tissues. *Immunity.* (2013) 39:184–95. doi: 10.1016/j.immuni.2013.06.015
76. Hielpos M, Ferrero M, Fernández A, Falivene J, Vanzulli S, Comerci D, et al. Btp proteins from *Brucella abortus* Modulate the lung innate immune response to infection by the respiratory route. *Front Immunol.* (2017) 8:1011. doi: 10.3389/fimmu.2017.01011
77. Higgins JL, Gonzalez-Juarrero M, Bowen RA. Evaluation of shedding, tissue burdens, and humoral immune response in goats after experimental challenge with the virulent Brucella melitensis strain 16M and the

reduced virulence vaccine strain Rev. 1. *PLoS ONE.* (2017) 12:e185823. doi: 10.1371/journal.pone.0185823

78. Belkaid Y, Von Stebut E, Mendez S, Lira R, Caler E, Bertholet S, et al. CD8+ T cells are required for primary immunity in C57BL/6 mice following low-dose, intradermal challenge with leishmania major. *J Immunol.* (2002) 168:3992–4000. doi: 10.4049/jimmunol.168.8.3992
79. Noben-Trauth N, Paul WE, Sacks DL. IL-4- and IL-4 receptor-deficient BALB/c mice reveal differences in susceptibility to Leishmania major parasite substrains. *J Immunol.* (1999) 162:6132–40.

Conflict of Interest Statement: The authors declare that the research was conducted in the absence of any commercial or financial relationships that could be construed as a potential conflict of interest.

Supplementary figures

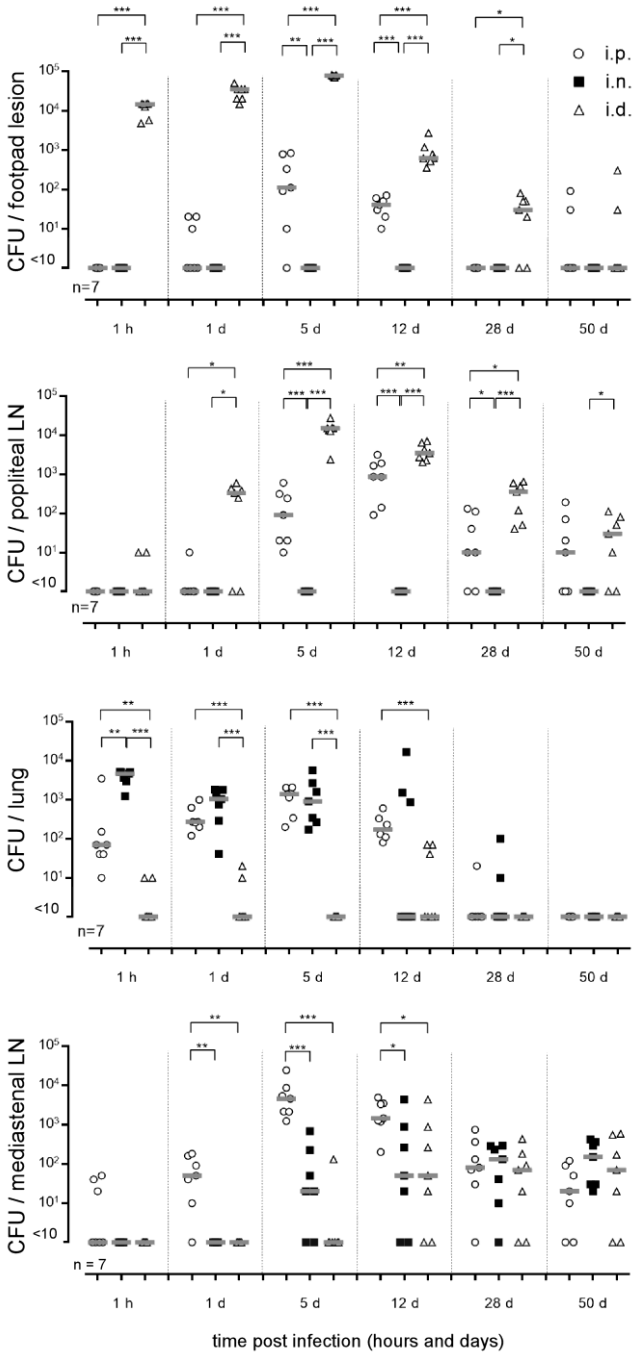

Figure S1

Figure S1. Each route of infection leads to a specific pattern of infected organs (part 1). Wild-type C57BL/6 mice were infected intraperitoneally (i.p.), intranasally (i.n.) or intradermally (i.d.) with a dose of 2×10^4 CFU of mCherry-*B. melitensis* and sacrificed at the indicated times. The data represent the CFU count per footpad lesion, popliteal LN, lung, or mediastinal LN. Gray bars represent the median. The significant differences between the indicated groups are marked with asterisks: $^{*}p < 0.1$, $^{**}p < 0.01$, $^{***}p < 0.001$. These results are representative of two independent experiments. LN, lymph node; h, hours; d, days; n, number of mice per group.

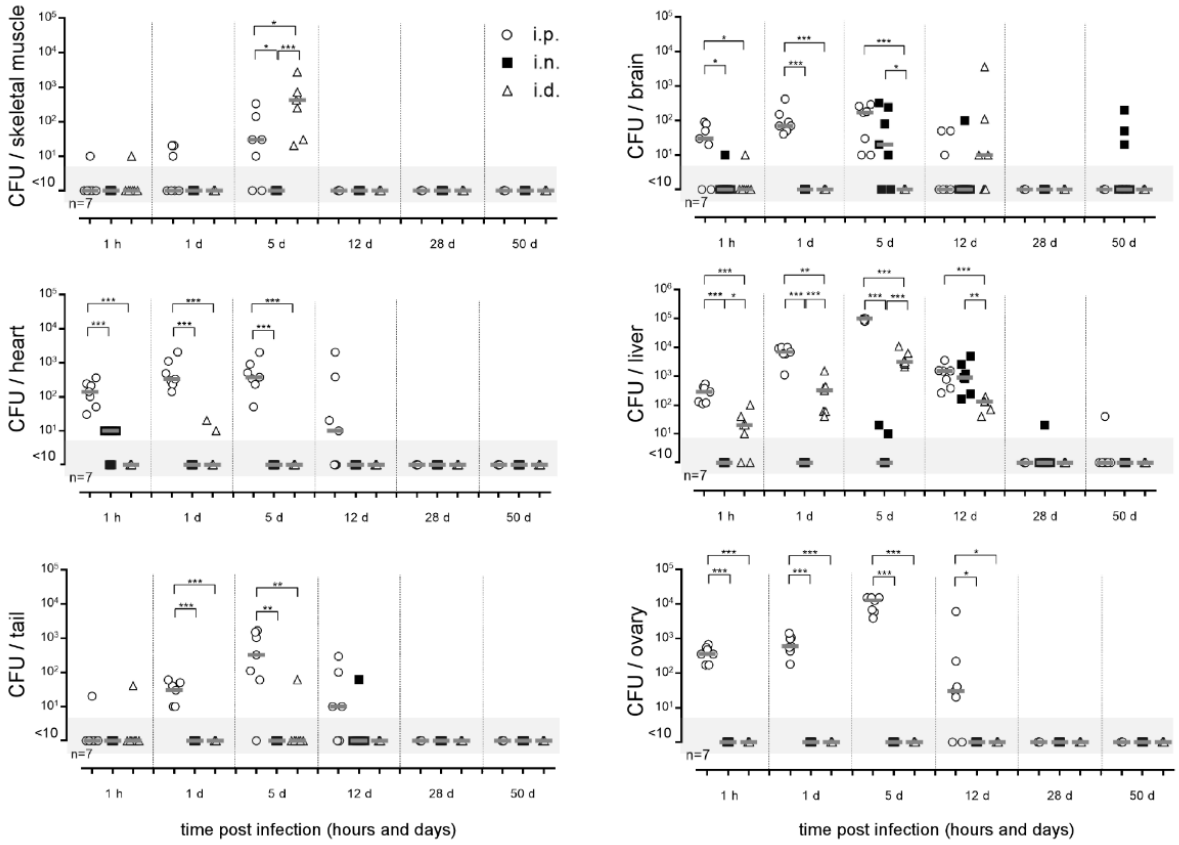

Figure S2

Figure S2. Each route of infection leads to a specific pattern of infected organs (part 2). Wild-type C57BL/6 mice were infected intraperitoneally (i.p.), intranasally (i.n.) or intradermally (i.d.) with a dose of 2×10^4 CFU of mCherry-*B. melitensis* and sacrificed at the indicated times. The data represent the CFU count per skeletal muscle, heart, tail, brain, liver, or ovary. Gray bars represent the median. The significant differences between the indicated groups are marked with asterisks: $^{*}p < 0.1$, $^{**}p < 0.01$, $^{***}p < 0.001$. These results are representative of two independent experiments. h, hours; d, days; n, number of mice per group.

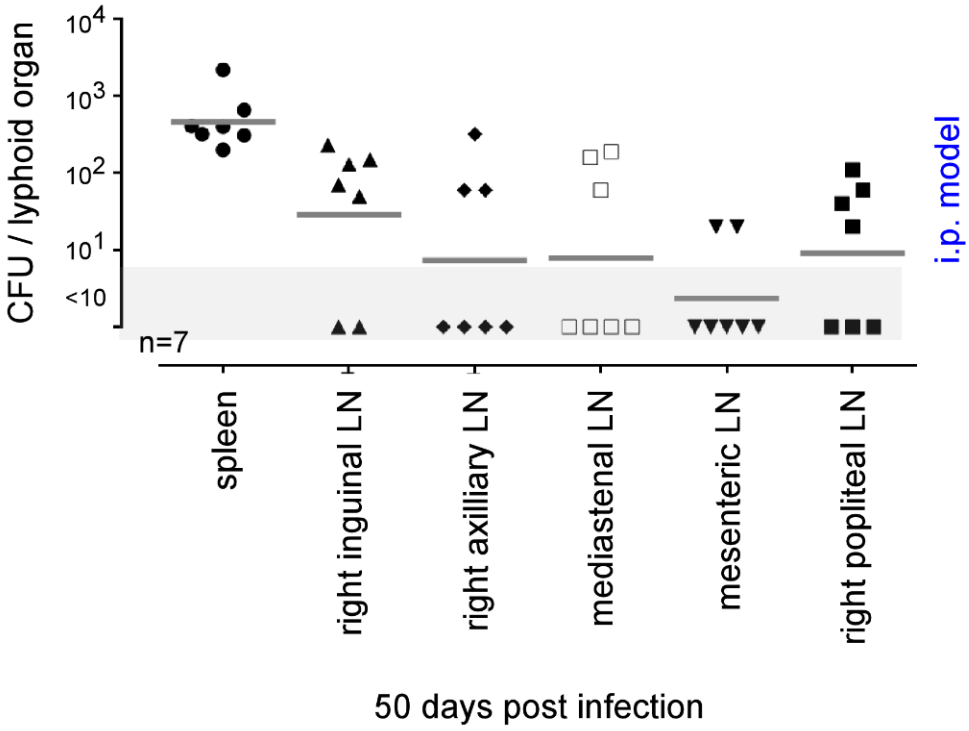

Figure S3

Figure S3. Intraperitoneal *Brucella* infection leads to infection of a large panel of lymph nodes. Wild-type C57BL/6 mice were infected intraperitoneally (i.p.) with a dose of 2 × 10^4 CFU of mCherry-*B. melitensis* and sacrificed at 50 days post infection. The data represent the CFU count per lymphoid organs (spleen, right inguinal LN, right axillary LN, mediastinal LN, mesenteric LN, and right popliteal LN). Gray bars represent the median. These results are representative of two independent experiments. LN, lymph node; n, number of mice per group.

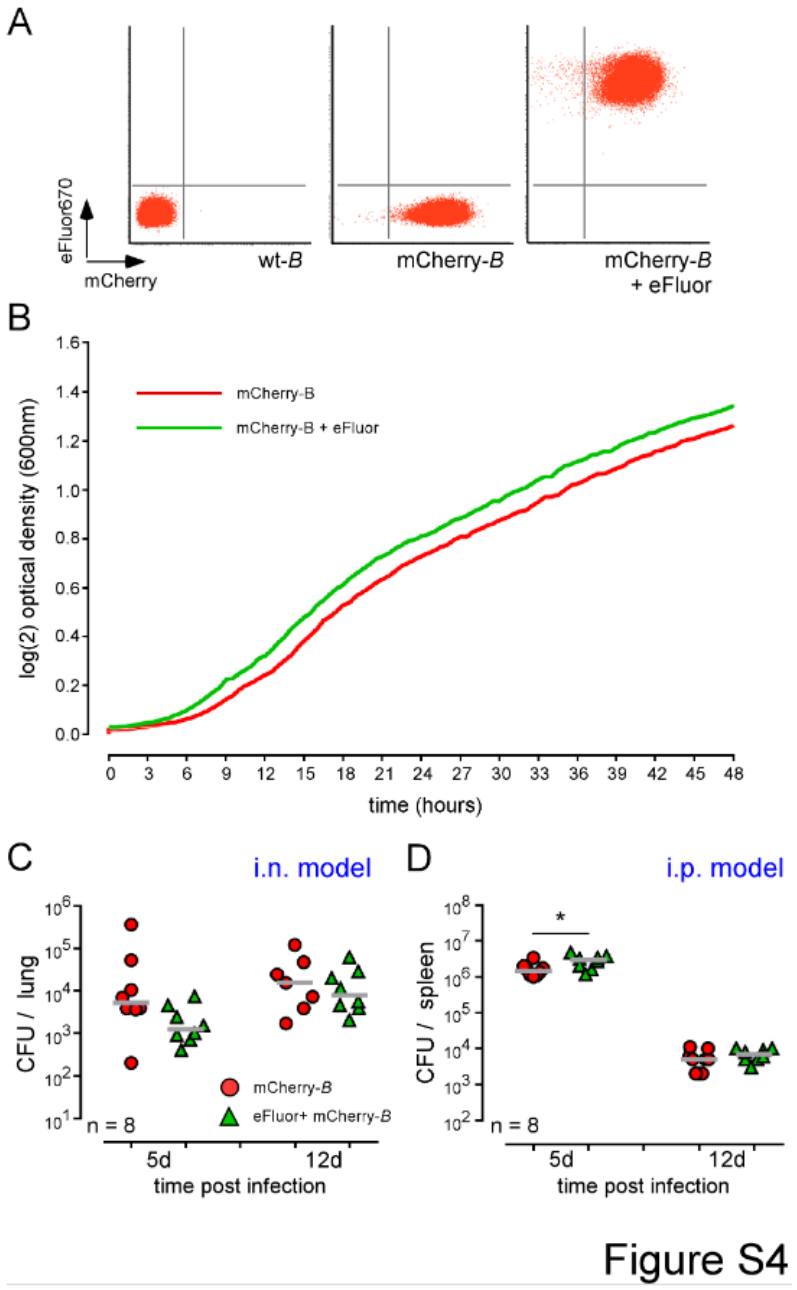

Figure S4. Impact of eFluor670 staining on *Brucella* growth *in vitro* and *in vivo*. **(A)** 4 × 10^4 CFU/ml of mCherry-*B. melitensis* were prepared from an overnight liquid culture and stained with the eFluor670 fluorochrome. Bacteria were fixed and then analyzed by flow cytometry. **(B)** Comparison by Bioscreen analysis of the growth of mCherry-*B. melitensis* and eFluor670 stained mCherry-*B. melitensis* in rich medium (2YT). These data represent the mean of three independent experiments. **(C)** Wild-type C57BL/6 mice were infected i.n. with a dose of 2 × 10^4 CFU of mCherry-*B. melitensis* or eFluor670 labeled mCherry-*B. melitensis* and sacrificed at 5 or 12 days post infection. The data represent the CFU count per lung. **(D)** Wild-type C57BL/6 mice were infected i.p. with a dose of 10^5 CFU of mCherry-*B. melitensis* eFluor670 labeled mCherry-*B. melitensis* and sacrificed at 5 or 12 days post infection. The data represent the CFU count per spleen. These results **(C,D)** are representative of two independent experiments. Gray bars represent the median. d, days; n, number. The significant differences between the indicated groups are marked with asterisks: $^*p < 0.1$.

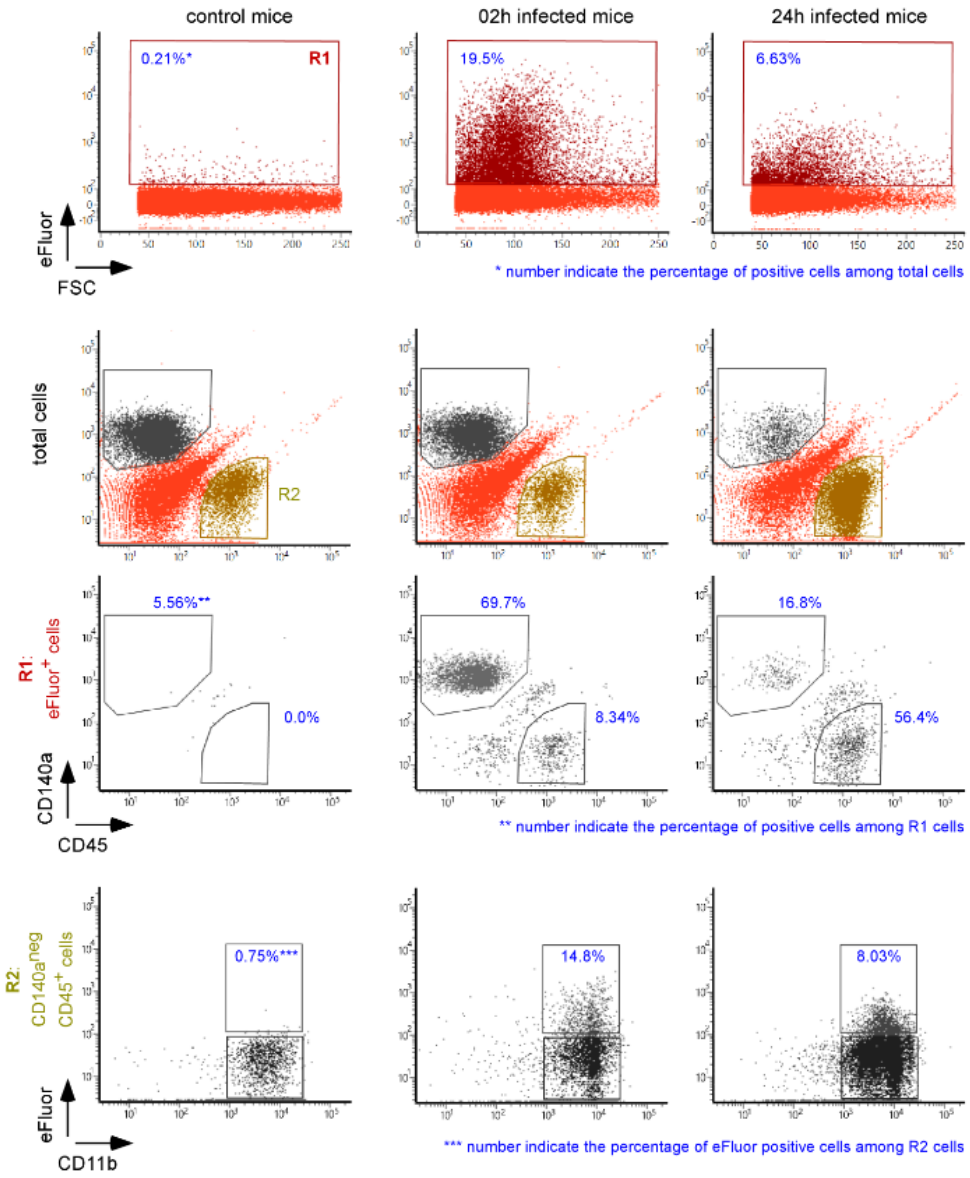

Figure S5

Figure S5. Phenotype of infected footpad lesion cells from wild type mice. Wild-type C57BL/6 mice were infected intradermally with 10^7 CFU of *B. melitensis*. Control wild-type mice were injected with PBS. The footpad lesions were harvested at 2 or 24 h post infection and the cells were analyzed by flow cytometry. The data result from the flow cytometry analysis of eFluor670, CD45, CD140a, and CD11b expression on footpad cells. The data show the representative dot plot from individual mice. These results are representative of three independent experiments.

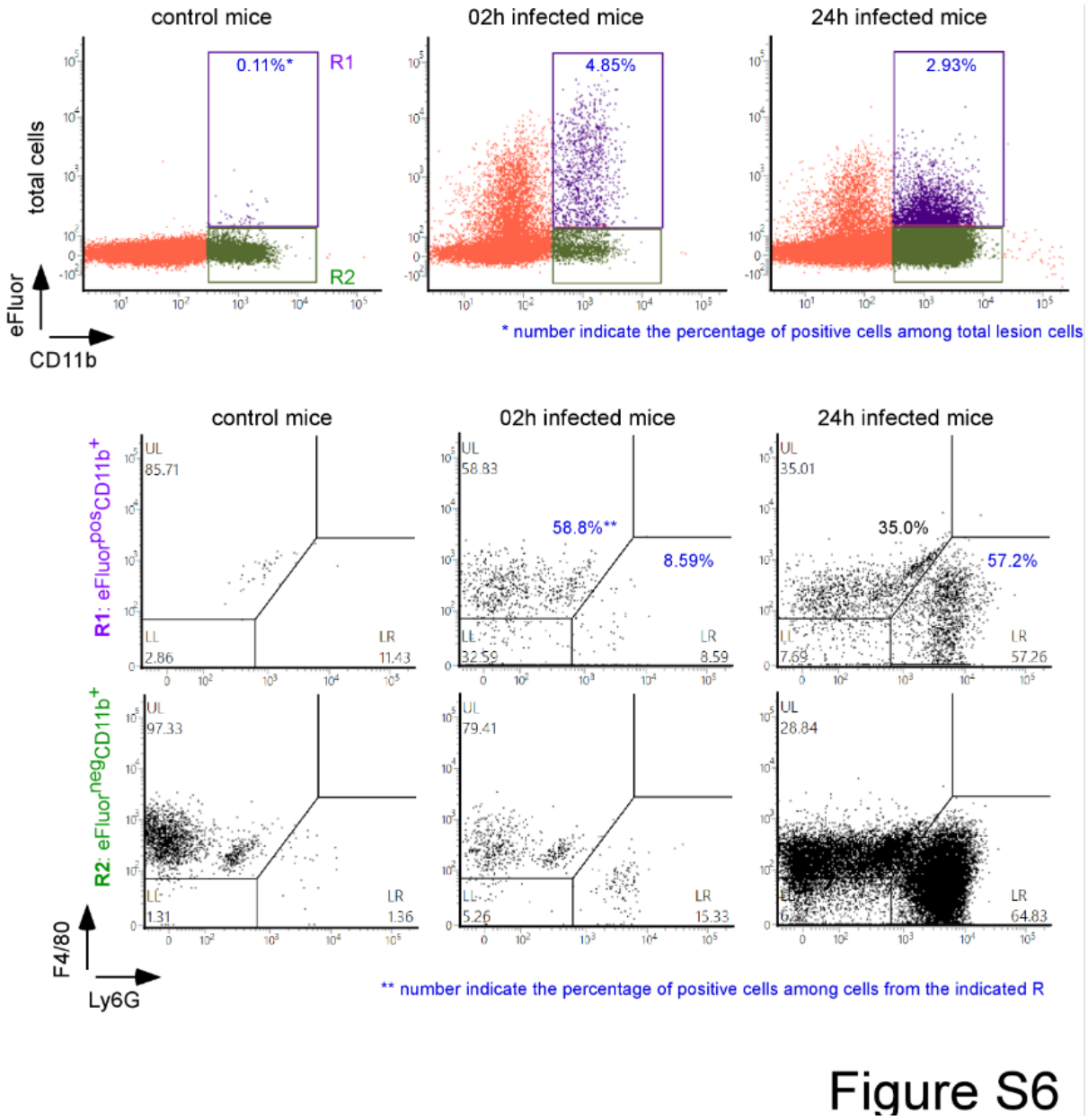

Figure S6

Figure S6. Phenotype of infected CD11b-positive footpad lesion cells from wild type mice. Wild-type C57BL/6 mice were infected intradermally with 10^7 CFU of *B. melitensis*. Control wild-type mice were injected with PBS. The footpad lesions were harvested at 2 or 24 h post infection and the cells were analyzed by flow cytometry. The data result from the flow cytometry analysis of eFluor670, F4/80, Ly6G, and CD11b expression on footpad cells. The data show the representative dot plot from individual mice. These results are representative of three independent experiments.

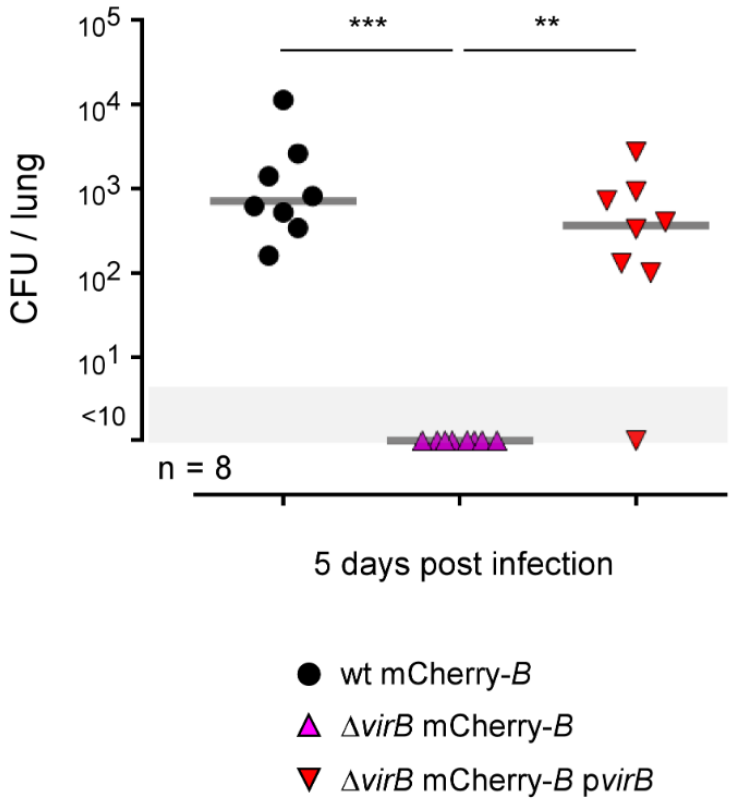

Figure S7

Figure S7. Complemented Δ*virB* strain growth in the lung. Wild-type C57BL/6 mice were infected i.n. with a dose of 10^5 CFU of wild type mCherry-*B. melitensis*, Δ*virB* mCherry- *B. melitensis* or complemented Δ*virB* mCherry-*B. melitensis* (Δ*virB* mCherry-*B. melitensis* p*virB*). Mice were sacrificed at 5 days post infection and the lung was collected. The data represent the CFU count per lung. Gray bars represent the median. Significant differences between the indicated groups are marked with asterisks: $^{**}p < 0.01$, $^{***}p < 0.001$. These results are representative of two independent experiments. n, number of mice per group.

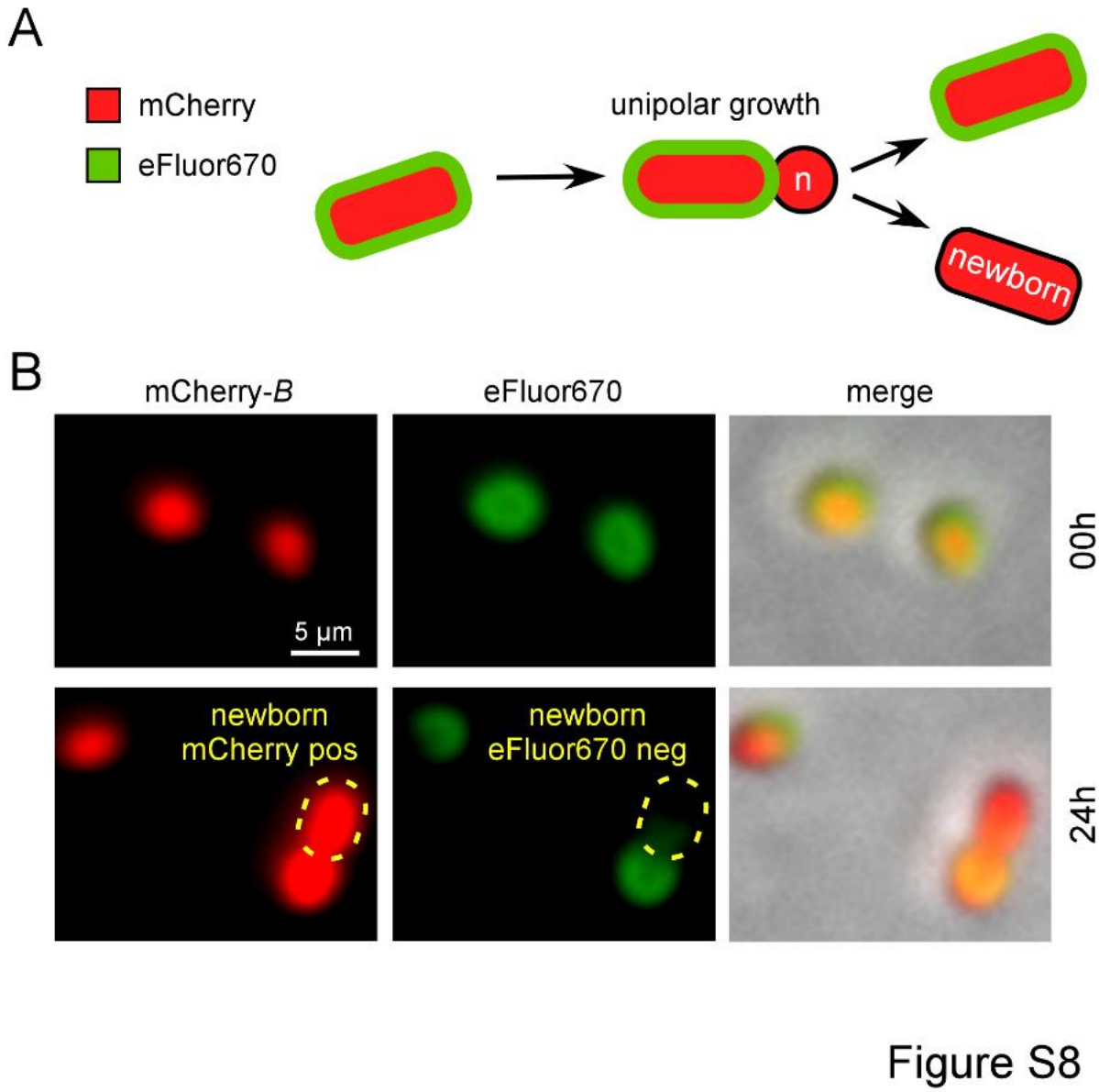

Figure S8

Figure S8. eFluor670 labeling identified newborn *Brucella*. mCherry *Brucella melitensis* is labeled with eFluor670. **(A)** Schematic representation of unipolar growth of eFluor670 labeled mCherry-*Brucella*. As eFluor670 does not move in the bacterial membrane, the newly formed bacterium, called the newborn, loses the eFluor670 labeling, allowing its identification by fluorescent microscopy. **(B)** Representative image at 0 and 24 h of eFluor670 labeled mCherry-*Brucella* extracellular growth *in vitro*. The 24 h image shows a division and a newborn cell ($mCherry^{+}$ $eFluor670^{-}$). The panels are color-coded with the text for mCherry and eFluor670. Scale bar = 5 µm. h, hours; n, newborn; pos, positive; neg, negative.

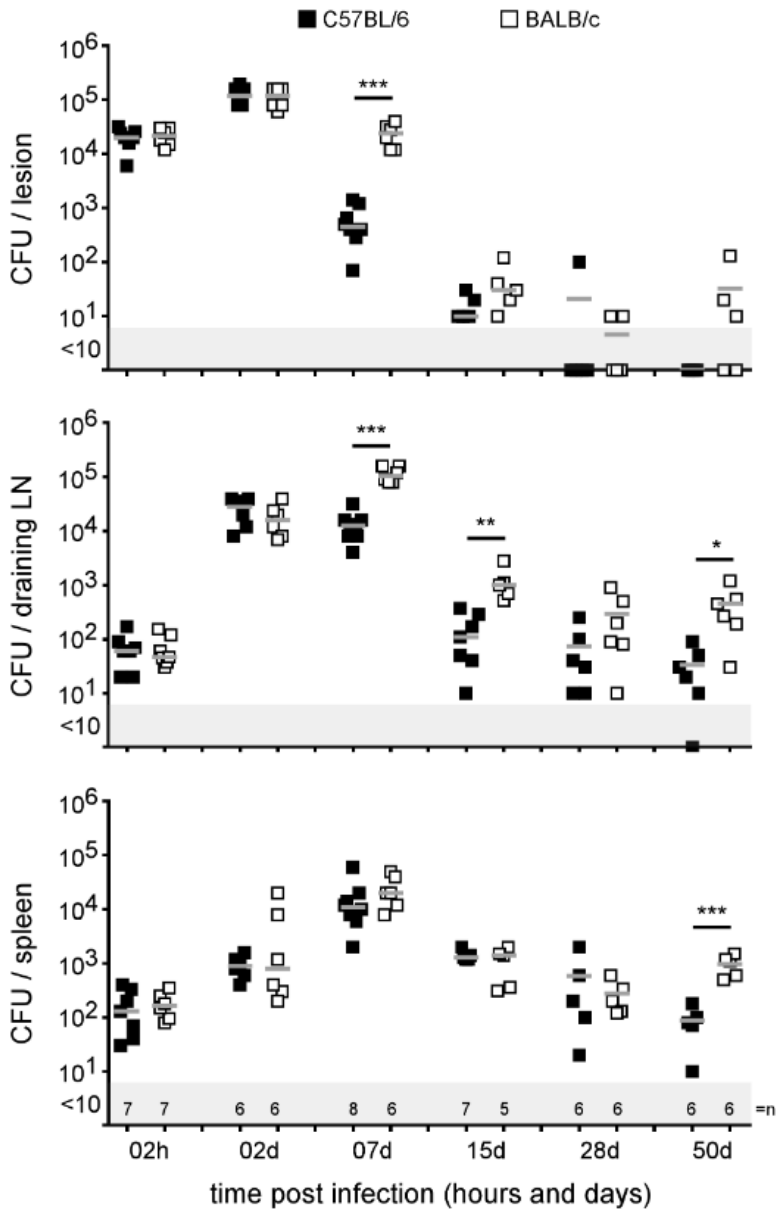

Figure S9

Figure S9. BALB/c mice are more susceptible to cutaneous *Brucella* infection than C57BL/6 mice. Wild-type C57BL/6 and BALB/c mice were infected intradermally with a dose of 2×10^4 CFU of *B. melitensis* and sacrificed at the indicated times. The data represent the CFU count per organ. Gray bars represent the median. The significant differences between the indicated groups are marked with asterisks: $^{*}p < 0.1$, $^{**}p < 0.01$, $^{***}p < 0.001$. These results are representative of two independent experiments. LN, lymph node; d, days; n, number of mice per group.

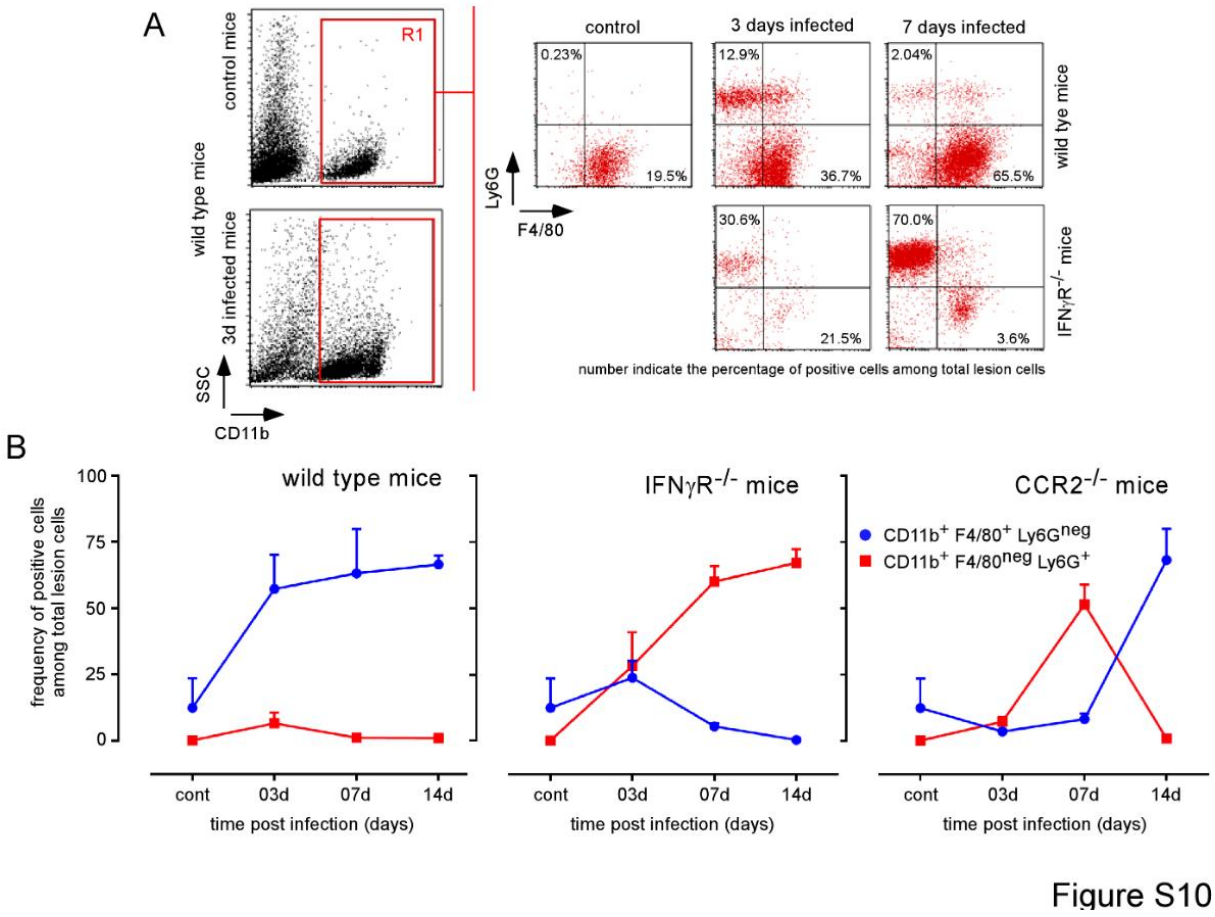

Figure S10

Figure S10. Neutrophils constitute the major population in the footpad lesion from infected IFNγR$^{-/-}$ mice. Wild-type, IFNγR$^{-/-}$, and CCR2$^{-/-}$ C57BL/6 mice were infected intradermally with a dose of 2×10^4 CFU of mCherry-*B. melitensis*. Control wild-type mice were injected with PBS. The footpad lesions were harvested at 3 and 7 days post infection and the cells were analyzed by flow cytometry. **(A)** Flow cytometry analysis of CD11b, F4/80, and LY6G expression on footpad cells. The data show the representative dot plot from individual mice. **(B)** Data represent the mean frequency (n = 4) of neutrophils and monocytes in the footpad lesion at the indicated time of infection. These results are representative of three independent experiments. Cont, control; d, days.

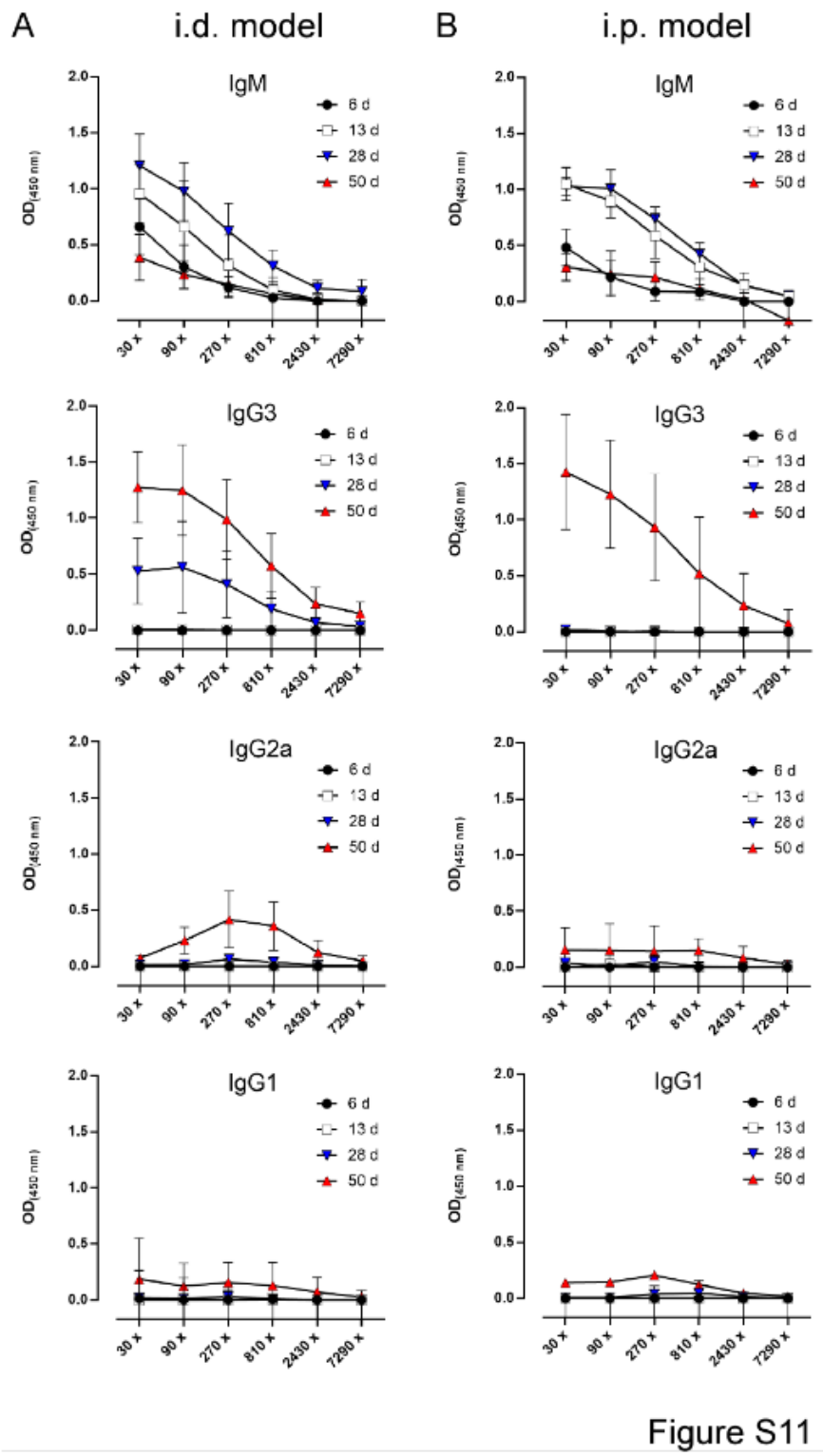

Figure S11. Humoral immune response induced by intradermal *Brucella* infection. Wild-type C57BL/6 mice were infected intradermally **(A)** or intraperitoneally **(B)** with a dose of 2×10^4 CFU of mCherry-*B. melitensis*. Serum was collected at the indicated times, and ELISA was performed to determine the isotype distribution of the *Brucella*-specific antibodies. The data represent the means ± SEM of results for 8 mice. These results are representative of three independent experiments. O.D, optical density; d, days.

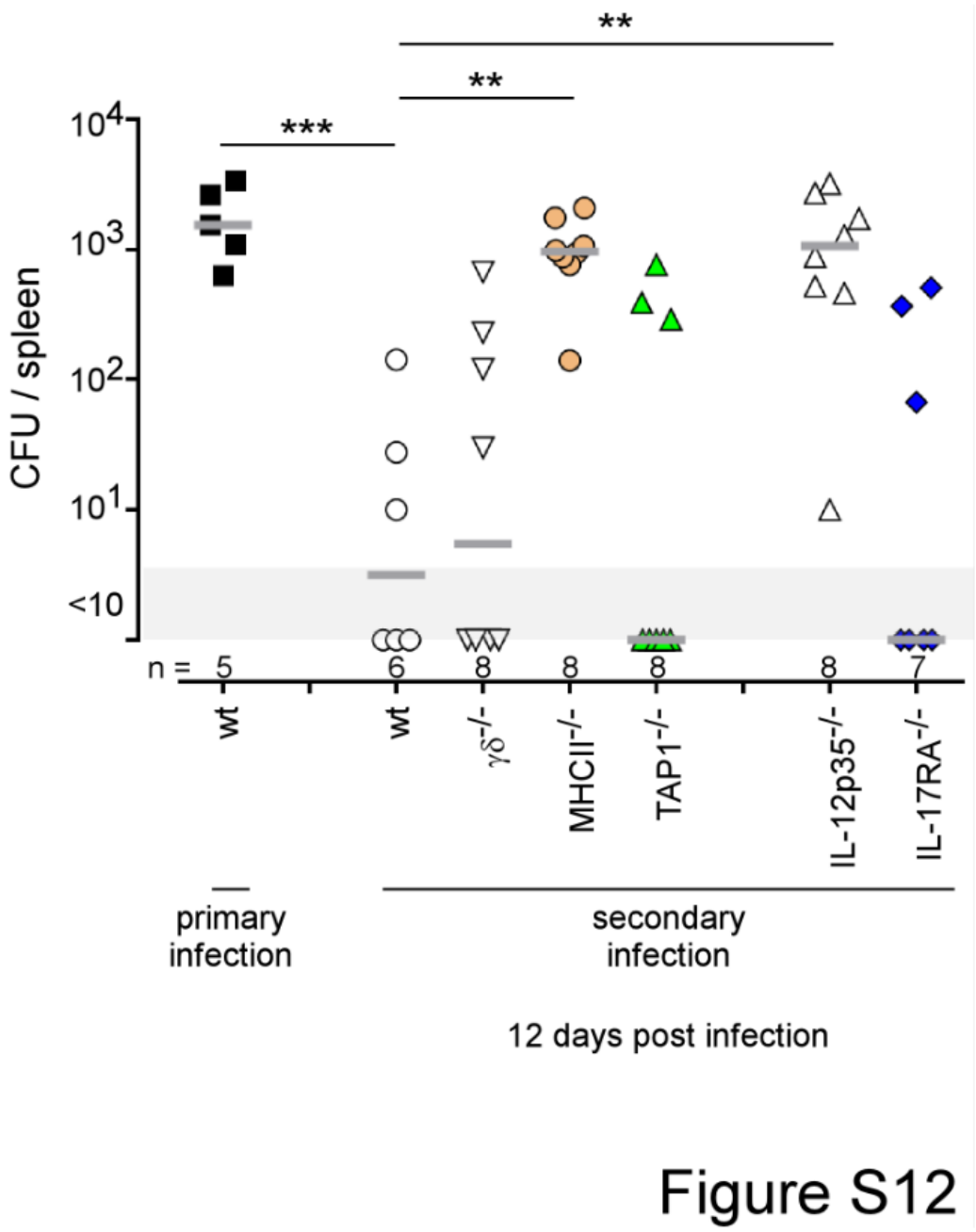

Figure S12

Figure S12. Comparison of protection in wild-type and various deficient mice previously immunized by intraperitoneal route with live *B. melitensis*. Wild-type, TCRγδ$^{-/-}$, MHCII$^{-/-}$, TAP1$^{-/-}$, Il-12p35$^{-/-}$, and IL-17RA$^{-/-}$ C57BL/6 mice were immunized i.p. with 2 × 10^4 CFU of live wild-type *B. melitensis* and treated with antibiotics, as described in the Materials and Methods. Naive (primary infection group) and immunized (secondary infection group) mice were challenged i.p. with 2 × 10^4 CFU of live mCherry-*B. melitensis* and sacrificed at 12 days post infection. The data represent the CFU count per spleen. Gray bars represent the median. The significant differences between the indicated groups are marked with asterisks: $^{**}p < 0.01$. These results are representative of two independent experiments. n, number of mice per groups.

4 Discussion and perspectives

In this work, we compared the impact of the infectious route on different parameters such as the dissemination of bacteria in mice body, the reservoir cells, the nature of the lymphoid populations indispensable after a secondary infection, or one example of the virulence gene importance. To our knowledge, no previous study has answered to this very general question using a same strain of bacterium, a same infectious dose, a same protocol and mice hosted in a same environment and fed with a same food.

4.1 The different routes of infection: towards a general model

The dissemination of *B. melitensis* and the nature of infected organs should logically depend on the route of infection used. Indeed, after intraperitoneal (i.p.), intranasal (i.n.), or intradermal (i.d.) infections, the barriers encounter by *B. melitensis* are different, but also the paths taken from the infectious site to the systemic organs.

The non-physiological i.p. route allows a rapid and massive entry of bacteria, directly inside the peritoneal cavity (Vitry, Hanot Mambres et al. 2014). One of the main role of the peritoneal cavity is to support and protect the organs of abdominopelvic cavity. The cavity is a high vascularized place. Because of that, the i.p. route leads to a rapid entry of extracellular bacteria in the blood circulation and so a rapid systemic dissemination (Figure 11). Indeed, all tested organs are infected at least at one point of infection. After a primary i.p. injection, CD4 T cells are indispensable to control the infection in spleen, with a crucial role of IFN-γ and iNOS (Copin, De Baetselier et al. 2007, Copin, Vitry et al. 2012). However, following a secondary infection, CD4 T cells but also B cells appear indispensable to fully control and eliminate bacteria (Hanot Mambres, Machelart et al. 2016)

By contrast, after an i.n. infection, the bacteria are rapidly internalized by alveolar macrophages in lungs ((Archambaud, Salcedo et al. 2010) G. Potemberg, A. Demars, not published). The mesenteric lymph nodes start to be infected after 5 days of infection. And the spleen is only infected between 5 and 12 days p.i., suggesting a very slow dissemination from the lungs to the systemic circulation. Moreover, no bacteria have been found in the blood at any tested times in this infectious model. The absence of detection of bacteria in the blood and the late dissemination to the spleen suggest that bacteria disseminate very slowly and intracellularly. The passage from the lungs to the spleen is still unknown, even it is thought via the blood. We

think that in this model it is the homing of the infected cells that determine the dissemination of *Brucella* (Figure 11*)*. After a primary i.n. infection, γδ T cells depending-IL-17 plays an indispensable role at 5 days post infection, and IFN-γ produced by CD4 T cells is indispensable later in the lungs (Vitry, Hanot Mambres et al. 2014, Hanot Mambres, Machelart et al. 2016). However, after a secondary infection, αβ T cells (CD4 and CD8 T cells) are indispensable to control the infection. In this model, the humoral response appears not indispensable (Hanot Mambres, Machelart et al. 2016).

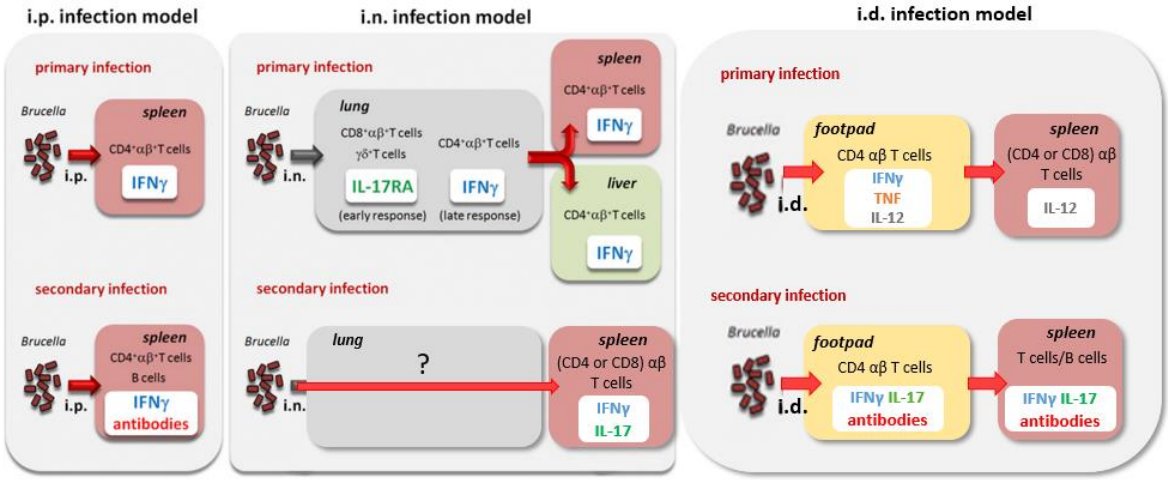

Figure 11: *Models of dissemination and immune response consequences depending on the route of infection. Adapted from (Hanot Mambres, Machelart et al. 2016)*

Finally, after an i.d. infection, the situation is probably intermediate between i.p. and i.n. models. Indeed, some extracellular bacteria should directly enter in the blood stream as the swelling of the footpad during the injection destructs the tissue and opens the access to the capillaries (Figure 11). But other bacteria should be internalized by APCs and follow a "classical" route from the local site of infection to the spleen, via infected cells and the lymph nodes (Figure 11). The control of *Brucella* at local site of infection seems required a TH1 immune response, with CD4 T cells producing IFN-γ, probably because bacteria are intracellular and that microbicide functions of myeloid cells must be activated to eliminate the bacteria. In this model, IFN-γ could also play a role of myelopoiesis modulator, allowing the recruitment and differentiation of monocytes (MacNamara, Oduro et al. 2011). Indeed, the deficiency of IFN-γ leads to an increase in neutrophils recruitment in the footpad and to a necrosis. As in i.p. and i.n. models, B cells are dispensable to control the primary i.d. infection. However, we detected IgM at 6 days post infection and IgG1 at 50 days post infection. After a secondary i.d. infection, footpads and spleen are protected, notably via CD4 T cells action. As after i.p., B cells are crucial for a good protection. The fact that some extracellular bacteria

directly pass through the blood could explain why the B cells and probably antibodies are required in this model too (Figure 11).

By comparing the 3 models, it seems that the rapid and massive entry of bacteria could be the reason why specific cellular and humoral responses are necessary. Indeed, probably that (1) the arsenal of responses should be deployed to fight a so high quantity of bacteria in the same time, and (2) the bacteria probably stay extracellular a certain time, making possible the action of memory B cells, "ready" for this second infection. The fact to block rapidly *Brucella* is crucial to avoid the establishment of bacteria in reservoir cells such as splenic macrophages, where their detection is probably less efficient because protected into splenic cells.

A general model could be that 1) antibodies are never required during a primary infection as B cells do not have the time to develop, 2) antibodies are indispensable after secondary infections only if there is a massive passage of *Brucella* in the blood circulation, when cellular immune response is saturated and that bacteria are extracellular, and 3) more the bacteria arrive massively in an organ or are inside reservoir cells, more a TH1 cellular response is required (Figure 11).

If the hypothesis that "massive entry of bacteria in blood is required to need humoral response after a secondary infection" is correct, maybe that an intranasal infection with a very high dose of *Brucella* will lead to a massive passage of bacteria in blood and a requirement of a very specific immune response with involvement of CD4 T cells and B cells. Thinking in terms of vaccine research, challenge in i.p. mouse model is finally interesting because it requires that the vaccine induces both a TH1-type humoral and cellular immune response to control *Brucella*.

4.2 Infection models in mice: critical, but not as much

The models we used to mimic natural infections are of course objectionable. Indeed, the infection via aerosols is in fact replaced by an injection of liquid containing *Brucella* in the nostrils of mice. In addition, this technique requires a deep anesthesia of animals (see Materials and methods). It also has been shown that the volume used to infect animals can modify the results (Miller, Stabenow et al. 2012). Systems to induce aerosols exist, such as whole-body exposure chamber or nose-only inhalation exposure system (Tsenova, Moreira et al. 1997, Schwebach, Chen et al. 2002, Belser, Gustin et al. 2015). But these systems present several

disadvantages like the requirement of anesthesia of mice, the use of restraint tubes and/or the training of mice, the need of a specific hood for the system, etc. (Belser, Gustin et al. 2015). The reproducibility between inoculations procedures, but also intra- and inter-groups is also debatable (Lucci, Tan et al. 2020). System to induce aerosols directly in trachea of mice also exist, via a syringe connected to a folded straw in which the liquid is expulsed and passes through an atomizer (Kunda, Price et al. 2018). This system could be interesting to test, as it would create aerosols, but it also requires anesthesia of mice as in our mode of infection and is not more physiological as the aerosols are directly injected in the trachea. In addition, studies comparing aerosolization and intranasal infection of viruses show no difference in terms of lethality, toxicity or level of infection between the two techniques (Belser, Gustin et al. 2015). After i.d. infection, tissue destruction during the infection is inevitable in our model. It could be seen as a negative point of the route of infection, but it can also be seen as a very good imitation of cutaneous lesions occurring when a vet, or butcher, or scientific hurts with a sharp object such as needle, scissors, or knife. It can also mimic the hurt of an animal in a meadow with barbed wires, making this mode of infection a good model of what happens naturally.

4.3 Lymph nodes: the perfect fortress?

The only organs staying infected at 50 days p.i. after a primary infection, independently of the route of infection, are the secondary lymphoid organs, meaning the spleen and the lymph nodes. What is very surprising is that, after a secondary infection, *Brucella* still persists in lymph nodes while the spleen of mice is highly protected. A hypothesis is that some specific cells or specific structures like granulomas allow the long-term persistence of *Brucella* in lymph nodes via the presence of nutritive resources and/or the ability to hide from the immune system. A such persistence in lymph nodes has already been observed in other infections. Indeed, it has been shown in an *in vivo* model of cynomolgus and rhesus macaques infected with *M. tuberculosis* that granulomas formation in thoracic lymph nodes allows the persistence of bacteria (Ganchua, Cadena et al. 2018). The authors showed that the high bacterial burden in the thoracic lymph nodes of rhesus macaques was associated to granulomas (Ganchua, Cadena et al. 2018). Indeed, granulomas are structures composed of infected macrophages surrounded by lymphocytes, developing after infections in lungs, liver, or skin for examples. The function of these structures is to kill the microorganisms by assembling in a same place the arsenal of destruction of a pathogenic agent, by increasing the NO presence or cytokines in the center of

the structure, and by decreasing the oxygen presence (Jamaati, Mortaz et al. 2017, Pagan and Ramakrishnan 2018). However, in this study, the lymph nodes granulomas in rhesus macaques are a bit different than the "classical" granulomas: the T cells seem push out, being replaced by CD11c CD68 macrophages (Ganchua, Cadena et al. 2018). Moreover, the blood vessels are disrupted and necrotic lesions are visible. Finally, the cytokinic production is reduced in comparison to a "classical" granulomas. All these events seem allow the increase in *M. tuberculosis* persistence in these lymph nodes (Ganchua, Cadena et al. 2018). It could be possible that this kind of structures exist in lymph nodes where *Brucella* persists at long term, even after secondary i.d. infection. Unfortunately, the low bacterial burden in infected lymph nodes prevents immunohistology studies of these organs to detect the presence of granulomas.

Another explanation for the persistence of *Brucella* in lymph nodes could be the existence of a specific cell population in these organs. To maintain a perfect balance between reactivity to fight aggressions and inhibition of abnormal responses, it is necessary that the immune system differentiates between self- and non-self-antigens. A failure in this mechanism can lead to auto-immune responses, allergies (if self-antigens are recognized by the immune system) or at the contrary to infections with huge consequences (Sakaguchi, Toda et al. 1996). A population of CD8 T regulatory cells has been identified in 1970 (Gershon and Kondo 1970). In function of the presence of not of programmed cell death (PD)-1 at their cell surface, the $CD8^+$ $CD122^+$ T cells can be distinguished in memory T cells ($CD8^+$ $CD122^+$ $PD\text{-}1^-$) or in regulatory T cells ($CD8^+$ $CD122^+$ $PD\text{-}1^+$) (Dai, Wan et al. 2010). The Treg have been shown to inhibit the immune response to pathogens by different mechanisms. For examples, CD8 Treg are able to secrete IL-10 and TGF-β that are inhibitory cytokines (Dai, Wan et al. 2010, Liu, Chen et al. 2015, Yu, Ma et al. 2018). Activated CD4 T cells can also be inhibited by CD8 Treg via the downregulation of costimulatory molecules such as CD86 and CD80, leading to a decrease in pro-inflammatory cytokines like IL-17 (Liu, Chen et al. 2015, Yu, Ma et al. 2018). CD8 Treg cells also secrete IFN-γ that will activate DC to produce NO (Liu, Chen et al. 2015, Yu, Ma et al. 2018). The Qa-1 protein, a non-classical MHC molecule, is essential for immune regulation and is linked to immune response suppression. In mice deficient for Qa-1 protein, CD8 Treg cells have a reduced activity, suggesting a link between Qa-1 and the regulatory CD8 T cells. Qa-1 protein recognizes MHCI on CD8 and inhibits the development of auto-immune disease. However, in absence of Qa-1 protein, CD8 Treg loss their activity and CD4 T cells show a better response (Hu, Ikizawa et al. 2004). A population of regulatory CD8 CD122 PD-1 T cells, located in the lymph nodes, has been described and involved in the persistence of γ-

Herpesviruses by suppressing the immune control via IL-10 secretion (Molloy, Zhang et al. 2011). A such type of cells could explain the persistence of *Brucella* in lymph nodes, even after a secondary infection, as defense strategies are inhibited in lymph nodes in presence of CD8 Treg cells. An interesting experiment to do could be to infect Qa-1-deficient mice following a secondary infection protocol and evaluate the bacterial load in lymph nodes (CFU) or to do flow cytometry on lymph nodes cells in order to study the cells present in these organs, using CD8, CD122, and PD-1 markers. The presence of CD8 Treg could explain the persistence of *Brucella* in lymph nodes after primary and secondary i.d. infections.

4.4 The essentiality of *virB*: questionable

virB operon is known *in vitro* but also in some *in vivo* models to be one of the most important and indispensable virulence gene in *Brucella* infection (O'Callaghan, Cazevieille et al. 1999, Hong, Tsolis et al. 2000). However, in some models, *virB* genes appear dispensable. It is the case for example *in vitro* in specific JEG-3 trophoblasts, where *B. abortus* Δ*virB9* is able to replicate, albeit a bit less than the wt strain (Salcedo, Chevrier et al. 2013). *In vivo*, we showed that the persistence of *B. melitensis* Δ*virB* strain is dependent on the route of infection and on the infected organ. For example, *virB* is dispensable in the spleen of intraperitoneally infected mice up to 4 weeks after infection (Demars, Lison et al. 2019). What is surprising in our model, is that after i.d. infection, not only *virB* is dispensable, but it seems deleterious in the footpad at 28 and 50 days p.i.. This could be linked to specific cells that are infected. We observed that both strains of *B. melitensis* (wt and Δ*virB*) can invade fibroblasts in footpad after i.d. infection at early time points. To our knowledge, it was the first time that fibroblasts were shown to be infected by *Brucella in vivo*. It would be interesting to compare the reservoir of both strains at later times points to study the difference of replication between the two strains, but we did not study this in this thesis as the level of persisting bacteria is too low to study the *Brucella* reservoir by immunohistology. Another explanation of this surprising result could be that it exists a redundant system to *virB* operon which is not yet discovered, but which will be efficient only in specific cellular conditions. To investigate this point, it would be interesting to do a Transposon-sequencing (Tn-seq) analysis in the conditions where *virB* is not required or with a Δ*virB-Brucella* strain coming from infected mice organs. However, this would explain why the mutant persists in lesion, but not why it persists better than the wt.

III. The role of *Acod1* and itaconate

1 Therapeutic strategies against bacterial infection

The discovery of synthetic antibiotics started in the 1932s with the sulfamides class (Aver, Mottin et al. 2017). However, only 4 years later, the first cases of resistance appeared. And each time a new class of antibiotic was discovered, resistance appears few years after. Moreover, since 1960s, few innovations in terms of antibiotic therapy were made, leading to the urgent need of therapeutic alternative to treat bacterial infections. Two main axes are possible: a host-directed therapy, or a bacteria-directed therapy and here are general examples for each of them.

1.1 Host-directed therapy

The host can be targeted by therapeutic molecules at different levels, trying to boost its immune defenses, or to eliminate a bacterial niche for examples. As described above in the introduction, macrophages are cells at the first line of defense and are often infected by intracellular bacteria such as *Mycobacterium* or *Brucella*. One strategy consists to target the uptake of bacteria by these cells. Imatinib is a molecule which inhibits tyrosine-kinases, including the ones involved in the entry of *Mycobacterium* in macrophages (Napier, Rafi et al. 2011). One major problem of this strategy, in addition to all side effects on the cells due to the mechanisms of action, is that the entry receptors are usually multiple, and this approach requires the identification and the inhibition all of them. When intracellular bacteria follow the intracellular trafficking of the host, it is possible to modulate the maturation of phagosomes in order to increase the direct bacterial killing, or to modulate the acidification of phagosomes (Bruns, Stegelmann et al. 2012). Also, the IFN-γ is a key cytokine of the immune system as it allows to increase nitric oxide (NO), autophagy, cells activation, etc. (see general introduction above). In 2009, patients with pulmonary tuberculosis treated with nebulization of IFN-γ showed a reduced inflammation in lungs, an increase in STAT-1 and IRF-1 cytokines, a recruitment of lymphocytes and a reduction of neutrophils inflammation (Dawson, Condos et al. 2009).

1.2 Bacteria-directed therapies

On the other hand, the bacteria themselves can be targeted by drugs in order to weaken them and so to support the immune system. For example, some drugs can decrease or stop the

bacterial virulence until the immune system succeed to kill them. For that, toxins and secretion system are good targets. For example, Chir-1 (chitinase-related protein 1), which targets the T4SS of *Helicobacter pylori*, is currently a molecule in pre-clinical phase (Hilleringmann, Pansegrau et al. 2006). The T4SS inhibition blocks the virulent effectors that are usually secreted through this (Hilleringmann, Pansegrau et al. 2006). In the case of bacteria making biofilms, these last structures are good targets as their degradation make bacteria more sensitive to antibiotics. For that, the components allowing the quorum sensing can be targeted for example. In 2013, Conlon et al. published that the acyldepsipeptide antibiotic (ADEP4) activates the ClpP (Caseinolytic Mitochondrial Matrix Peptidase Proteolytic Subunit) protease leading to the degradation of around 400 proteins, resulting in the eradication of *Staphylococcus aureus* biofilms (Conlon, Nakayasu et al. 2013). Another example is the use of bacteriophages to kill pathogenic bacteria. In a model of antibiotic-resistant *Pseudomonas aeruginosa* in chronic otitis, bacteriophage therapy has been tested in a clinical phase on 24 patients suffering of ear infection. In this study, after being treated with a bacteriophage preparation with a single dose, the phage-treated group shows an improvement in comparison to the placebo group (Wright, Hawkins et al. 2009).

1.3 *Acod1* and itaconate

1.3.1 Discover, and brief history

As new therapeutic agent, itaconate (or itaconic acid) is more and more cited (Lampropoulou, Sergushichev et al. 2016, Naujoks, Tabeling et al. 2016, Meiser, Kraemer et al. 2018, Mills, Ryan et al. 2018). This compound has been identified for the first time in 1836 by a chemist during citric acid distillation (Baup 1836). Five years later, in 1841, Turner identified that itaconate synthesis is produced during the decarboxylation of cis-aconitate, an intermediate of Krebs cycle (Turner 1841). Then, it has been reported for the first time in 1931 by Kinoshita that itaconate was produced by *Aspergillus itaconicus* when growing on Czapek's agar solution containing sucrose (Kinoshita 1931). It was suggested that itaconate production starts with sugar, with citric and cis-aconitic acids as intermediates (Kinoshita 1931). It was then mentioned that itaconate can be produced by other species of *Aspergillus,* such as *A. terreus* (Calam, Oxford et al. 1939). It seems that *Aspergillus* would be able to synthetize itaconate from glucose only when the environment modifies from neutral to acid conditions, suggesting that acidity would be necessary to synthetize enzyme essential to this conversion (Larsen and Eimhjellen 1955). For a long time, itaconate was used exclusively in industry (see BOX-6), but

it becomes more and more interesting in the biology field as its importance in mammalian immunity slowly started to be discovered.

BOX-6. Itaconate use. Itaconate compound was first produced by citric acid distillation (Kinoshita 1931), but then by fermentation of *Aspergillus terreus* (Pfeifer, Vojnovich et al. 1952). It is used for the production of synthetic resins, fibers, for plastic, artificial glass, etc, and used in large range of sectors (agriculture, pharmacy, dental-care, etc). As the demand of itaconate production increases over the years, industries try to adapt (strain modification, primary substance replacement, etc) by decreasing the economic cost of production. Indeed, glucose as substrate being quite expensive, it is now replaced by starch, molasses, corn syrup for examples, that are cheaper but also less pure. In 2009, the annual production of itaconate in China was estimated to be 30,000 tons (Okabe, Lies et al. 2009). For a complete review, see (Okabe, Lies et al. 2009).

Almost 30 years after the discovery of itaconate metabolite in *Aspergillus*, the itaconate metabolism was studied in 1961 in some bacteria and it was shown that *Salmonella* and *Pseudomonas* possess the enzymes for the itaconate metabolism (Martin, Frigan et al. 1961). Despite the fact that it is known since 1957 that exogenous itaconate can be catabolized by rats and guinea pigs liver mitochondria (Alder, Wang et al. 1957), it is only in 2010 that itaconate was identified in metabolic analyses of mammalian tissues (Wibom, Surowiec et al. 2010). But at this time, the itaconate origin was unknown: from the mammals cells themselves, the microbiota or a contaminant? (Wibom, Surowiec et al. 2010). In 2011, different articles showed that itaconate is produced in different contexts. First, Strelko et al. concluded that, *in vitro*, only macrophage lineage cells produced itaconate, at a concentration of 1.33 mM, and that this production was increased after *ex vivo* stimulation of peritoneal macrophages with *E. coli*.-LPS and IFN-γ, suggesting a role in the control of bacterial infections (Strelko, Lu et al. 2011). Second, after treatment of RAW 264.7 macrophages with *E. coli*.-LPS during 22 hours and after the study of the extracellular metabolites released in the culture medium, Sugimoto and colleagues showed that itaconate was one of the most increased metabolite (Sugimoto, Sakagami et al. 2011). And finally, Shin realized *in vivo* metabolomics studies and found that rats infected with *M. tuberculosis* showed more metabolic changes in comparison to uninfected rats and that these changes mainly concerned precursors of different metabolites, including itaconate (Shin, Yang et al. 2011).

In 1995, Lee et al. showed after stimulation of RAW 264.7 macrophages with *E. coli*.-LPS that *irg1* (*immune responsive gene-1*) - now called *Acod1* for *aconitate decarboxylase 1* - was one of the genes the most upregulated.

The induction of *Acod1* gene is mainly related to TLRs stimulation by PAMPs (Figure 12). For examples, it was shown that the TLR4 and its stimulation by *E. coli*.-LPS or Lipid A is required for the expression of *Acod1* mRNA in DCs, BMDM and murine peritoneal macrophages. *Acod1* gene expression can also be induced by TLR2 in RAW264.7 macrophages and in BMDM (Wu, Chen et al. 2020). The detection of CpG-DNA by TLR9 is also able to lead to *Acod1* gene expression in BMDM. It has been shown that the deletion of TLR2 or TLR4 blocks the induction of *Acod1* gene expression, and that the overexpression of TLR4 increases the *Acod1* mRNA expression in ovine macrophages (Wu, Chen et al. 2020). MYD88 could be the adaptor protein recruited at the TLRs to induce the signaling cascade after TLRs stimulation. Indeed, in DC deficient for MYD88 (MYD88$^{-/-}$ DCs), the induction of *Acod1* gene expression via TLR9 decreases, suggesting a TLR9/MYD88/ACOD1 axis. However, it was not the case for TLR2 induced by *E. coli*.-LPS, suggesting the existence of another pathway after TLR2 stimulation. In *Mycobacterium*, the induction of *Acod1* gene is independent of TLR4 and MYD88 or TIRAP,

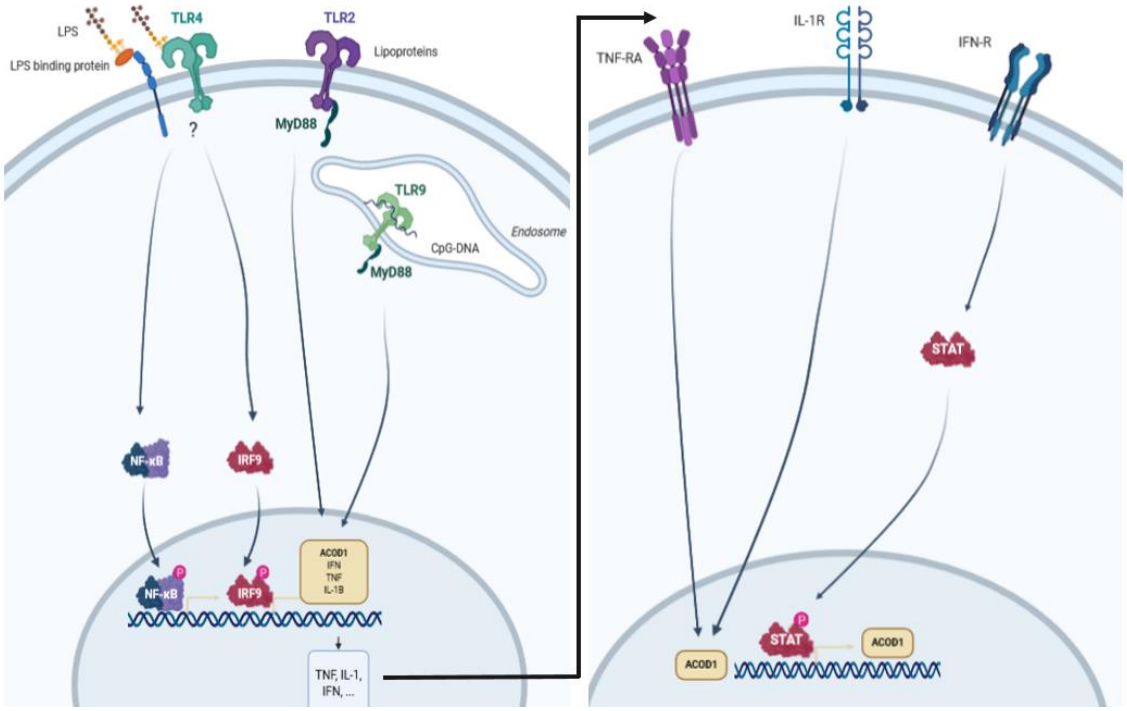

Figure 12: Cascade of signalization leading to the induction of Acod1 gene. TLR can be stimulated by PAMPs, leading to the activation of NFκβ or IRF depending on the host cells and on the level of inflammation. MYD88 could be one of the adaptor protein, but it seems not required after TLR4 stimulation. A synergic effect between PAMPs and pro-inflammatory cytokines allows a strong induction of *Acod1* mRNA.

another adaptor protein. It seems that the induction of *Acod1* gene in this model is IRF dependent. In addition to the stimulation of *Acod1* after PAMPs detection, the pro-inflammatory cytokines produced following the same signalization cascade (such as IL-1β, IFN-β TNF-α cytokines) also increase the expression of *Acod1* mRNA (Figure 12). Depending on the conditions, it seems that the signalization cascade could be dependent on STAT proteins. This suggests a synergic effect of PAMPs and cytokines to induce *Acod1* gene during infection (Wu, Chen et al. 2020).

The function of *Acod1* was unknown until 2013 as this gene had no identity with other known genes (Lee, Jenkins et al. 1995). In 2013, a team found the link between *Acod1* and itaconate. Indeed, Michelucci and colleagues used the siRNA technique to silence *Acod1* gene in *E. coli*.-LPS activated RAW 264.7 macrophages and found that, among the 260 impaired metabolites, itaconate was the most affected, with 60 % of decrease in comparison to macrophages transfected with the si-control (Michelucci, Cordes et al. 2013). In the same model of cells, they found that the intracellular concentration of itaconate is close to 8 mM, leading to the idea that a such high concentration of a metabolite could be linked to immunological function (Michelucci, Cordes et al. 2013). They confirmed *in vivo* that mice treated with *E. coli*.-LPS have an increase in *Acod1* mRNA and a correlated high concentration of itaconate in their peritoneal macrophages, in comparison to mice treated with saline buffer (Michelucci, Cordes et al. 2013).

The main roles of itaconate will be discussed later, but briefly, itaconate was already shown in 1949 to inhibit the succinate dehydrogenase (SDH) in an enzymatic test (Ackermann and Potter 1949) and in 1971 to inhibit the isocitrate lyase (ICL) of *Pseudomonas indigofera* (Williams, Roche et al. 1971, Rittenhouse and McFadden 1974, McFadden and Purohit 1977), but the metabolite was not considered as enough interesting at this time as it was not really involved in the Krebs cycle. It is only years later that its anti-bacterial and anti-inflammatory roles were investigated in infection models.

1.3.2 Metabolism of itaconate

In mice, the formation of itaconate was shown to occur in two steps inside mitochondria: the citric acid from Krebs cycle is first dehydrated by an aconitase enzyme to cis-aconitate, with formation of a double bond between two carbons; then the cis-aconitate is decarboxylated by the cis-aconitate decarboxylase (ACOD1) to itaconate (Figure 13) (Kinoshita 1931, Bentley and Thiessen 1955, Bentley and Thiessen 1957, Bentley and Thiessen 1957, Bentley and Thiessen 1957).

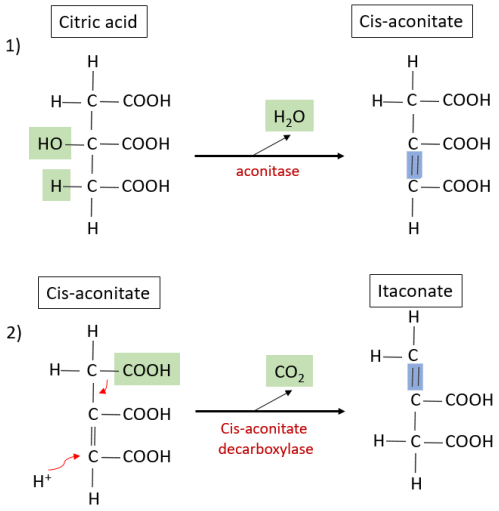

Figure 13: Synthesis of itaconate, from citric acid, with cis-aconitate as intermediate. *The citric acid is dehydrated by an aconitase in cis-aconitate, that will be decarboxylated in itaconate by the cis-aconitate decarboxylase enzyme (ACOD1).*

If itaconate can be produced in mammalian's mitochondria after *E. coli*.-LPS and IFN-γ stimulation, it can also be metabolized into pyruvate and acetyl-CoA in a 3 steps reactions (Figure 14). First, itaconate is activated into itaconyl-CoA by a succinate activating enzyme (Succinyl-CoA synthetase), then the itaconyl-CoA is hydrated into citramalyl-CoA by a itaconyl-CoA hydratase, and finally the citramalyl-CoA is cleaved into pyruvate and acetyl-CoA by a citramalyl-CoA lyase (Alder, Wang et al. 1957, Wang, Adler et al. 1961). This itaconate catabolism pathway is also used by some bacteria as resistance mechanism to itaconate. It is for example the case of *Yersinia pestis and Pseudomonas aeruginosa*, which used itaconate-CoA transferase as first enzyme of this 3-steps reaction (Figure 14) (Sasikaran, Ziemski et al. 2014).

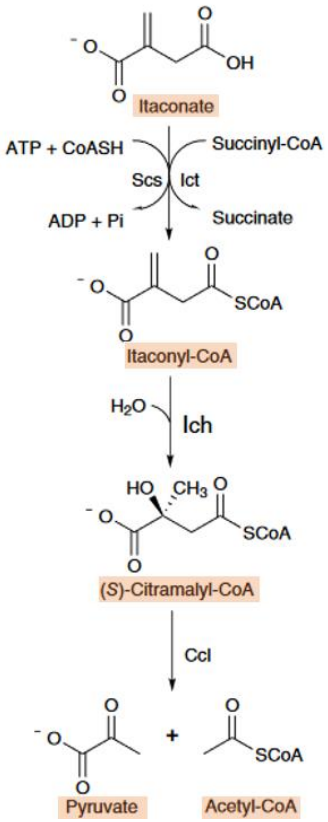

***Figure 14**: **Three-steps reaction of itaconate metabolization into pyruvate and acetyl-CoA.** Itaconate is first activated into itaconyl-CoA via a succinyl-CoA synthetase (Scs). Itaconyl-CoA is then hydrated into citramalyl-CoA via an itaconyl-CoA hydratase (Ich), and the citramalyl-CoA is cleaved into pyruvate and acetyl-CoA via a citramalyl-CoA lyase (Ccl). Adapted from (Sasikaran, Ziemski et al. 2014).*

1.3.3 Transport of itaconate

As mentioned above, itaconate is produced in some fungi, bacteria, and mammals. ACOD1 is present in mitochondria and allowed the production of itaconate inside mitochondria. But in 1995, itaconate was found in the cytosol of eukaryotic cells, suggesting a possible transport of itaconate from mitochondria to cytosol (Horton, Park et al. 2006). As malate and itaconate are structurally very close to each other, Mills et al. hypothesized and showed that itaconate should be transported through the mitochondrial membranes via the same transporters than malate: via dicarboxylated, citrate and/or oxoglutarate carriers (Mills, Ryan et al. 2018). In another context, it was hypothesized that cells were able to release extracellularly itaconate as the it was found in the culture medium of RAW264.7 (Strelko, Lu et al. 2011). This was however not confirmed by another team which concluded later that the extracellular itaconate was the result of cell content released during cell apoptosis or eliminated at the end of the lysosomal pathway (Meiser, Kraemer et al. 2018). Indeed, as the itaconate is a charged molecule, it hardly crosses

the cell membrane, leading to the hypothesis that this compound acts locally (Meiser, Kraemer et al. 2018). For now, the mechanism of itaconate entry in bacteria is not known.

1.3.4 Itaconate and its anti-bacterial role

In 1971, Williams showed that itaconate was able to inhibit the purified isocitrate lyase (ICL) of *Pseudomonas indigofera* in an uncompetitive way, at a succinate-specific site (Williams, Roche et al. 1971). ICL is a key enzyme of the glyoxylate shunt (Figure 15), an anabolic variant of the Krebs cycle, mainly present in plants, nematodes, and microorganisms (Kornberg and

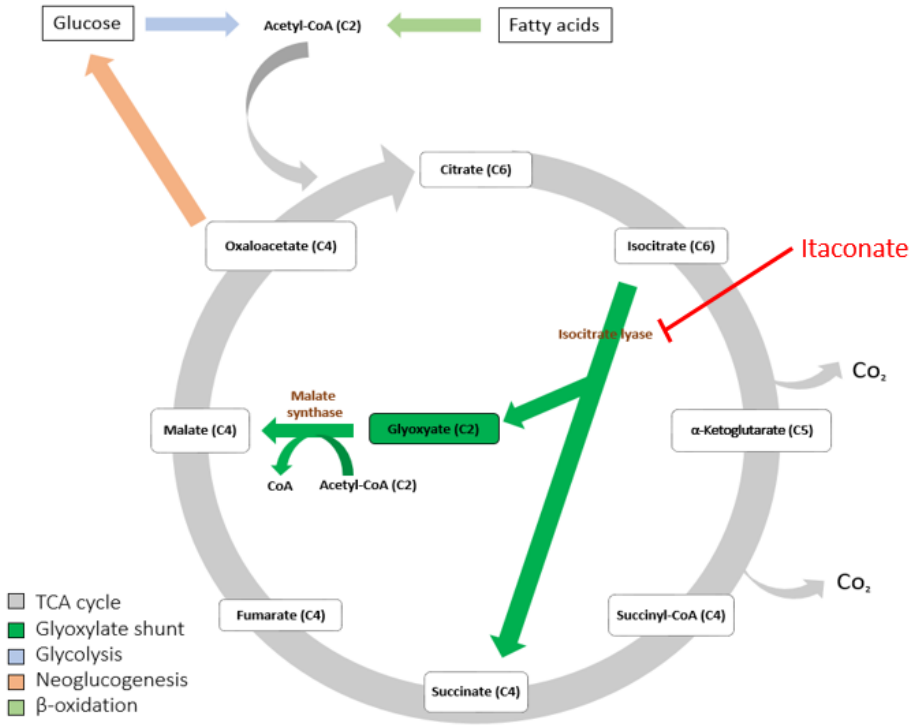

Figure 15: The glyoxylate shunt. *The glyoxylate shunt is an alternative pathway that certain microorganisms possess. It allows them to bypass the loss of carbons during the classical Krebs cycle in stressful nutritional conditions. Only two enzymes are involved in this pathway: the isocitrate lyase and the malate synthase.*

Krebs 1957). In microorganisms, this pathway is used to survive in low-glucose environment like in phagolysosomes for example (Uribe-Querol and Rosales 2017). Indeed, this alternative pathway allows to bypass the loss of two CO_2 molecules which occurs in Krebs cycle (Figure 15). In this low-glucose context, acetyl-CoA, generated by fatty acids β-oxidation, is the only source of carbon available, but the molecule only contains two carbons. To remedy this, the glyoxylate shunt bypasses two decarboxylation steps of the Krebs cycle by first hydrolyzing the isocitrate to succinate and glyoxylate, by the ICL. The succinate enters in the Krebs cycle and the glyoxylate (plus acetyl-CoA) synthetizes malate via the malate synthase (MS). The malate molecule enters at its turn in the Krebs cycle to produce glucose by neoglucogenesis

(Figure 15) (Kornberg and Krebs 1957). If in some bacteria, the MS is usually constitutive, the ICL is only active when two-carbon molecules are available. As there are exceptions, *Pseudomonas* for example possesses high concentration of ICL, even when the glyoxylate shunt is not required (McFadden and Purohit 1977). The ICL (and thus the glyoxylate shunt) was afterwards reported as essential for latent infection in different models. First, in *Mycobacterium avium*, Sturgill discovered a protein present in *Mycobacterium* after phagocytosis in macrophages *in vitro* by a two-dimensional gel analysis. This protein was shown later to be ICL (Sturgill-Koszycki, Haddix et al. 1997). Two years later, *icl* gene was confirmed to be one of the most upregulated gene in *Mycobacterium tuberculosis* during phagocytosis by human macrophages (Graham and Clark-Curtiss 1999). The same year, Honer demonstrated that in *Mycobacterium*, a second gene encodes for another protein with an isocitrate activity: *aceA/icl2*. But it seems to have a subordinate role, when the concentration of isocitrate is too high (Höner, Kerstin et al. 1999). Even if *Mycobacterium* ICL seems dispensable for growth during the acute phase, it seems crucial for long term persistence and virulence in mouse models. Indeed, a mutation in *M. tuberculosis icl* supported a role for the glyoxylate shunt in pathogenesis (McKinney, Honer zu Bentrup et al. 2000). In fungi, enzymes of the glyoxylate shunt (ICL and MS) are also required for the virulence in mice. Indeed, *Saccharomyces cerevisiae*, and *Candida albicans* show an upregulation of the expression of these genes when they are in contact with phagolysosomes during mouse infection, as suggested by genomic expression profile analyses (Lorenz and Fink 2001). The anti-bacterial role of itaconate, via the ICL inhibition, has been confirmed in *Mycobacterium, Pseudomonas and Salmonella in vitro* models (Rittenhouse and McFadden 1974, McFadden and Purohit 1977, Michelucci, Cordes et al. 2013).

In infected mammal cells, a proximity between mitochondria (where itaconate is produced) and microorganisms has been reported several times: in 1999 for *Chlamydia* (Matsumoto, Bessho et al. 1991), in 2011 for *Toxoplasma gondii* (Sinai and Joiner 2001) and more recently in 2016 and 2018 for *Legionella* (Naujoks, Tabeling et al. 2016) and *Brucella* (Lobet, Willemart et al. 2018), respectively. Even if more investigations are needed, this proximity could be either an advantage for the host which will recruit somehow the microorganism-containing vacuole to bring it closer of the itaconate production center, or an advantage for the microorganism itself to be closer of the energetic central of the cell. *Brucella* possesses ICL and MS enzymes, but does not seem to use the glyoxylate shunt. Indeed, a study showed that *B. abortus* grows *in vitro* with 6 or 5-carbons sugars, compensated by amino acids, but without an important role of

glyoxylate shunt (Zuniga-Ripa, Barbier et al. 2014). Moreover, the deletion of *aceA* gene (coding for ICL enzyme) has no impact on the *in vitro* growth in rich medium, and no impact *in vivo*, after an i.p. *B. abortus* infection (Zuniga-Ripa, Barbier et al. 2014).

1.3.5 Itaconate and its anti-inflammatory role

In 2018, Nair and colleagues tested the hypothesis that itaconate could inhibit the ICL of *Mycobacterium* to decrease the infection rate. For that they first intranasally infected wt and *Acod1*-KO mice with a wt *M. tuberculosis* strain (Nair, Huynh et al. 2018). They observed that 75 % of *Acod1*-KO mice died at 30 days post infection, contrary to wt mice that survived up to 80 days post infection (Nair, Huynh et al. 2018). This highlights the importance of *Acod1* and thus itaconate in the control of *M. tuberculosis in vivo* infection. Then they infected intranasally wt and *Acod1*-KO mice with *M. tuberculosis* wt or deficient for ICL (*icl1*). They observed that all the wt mice survived to the infection and all *Acod1*-KO mice died from the infection. However, in the *Acod1*-KO mice, the CFU of *icl*-deficient strain was higher than the CFU of wt strain, suggesting that even if itaconate was important in this model to control the infection, it was independent of the ICL, suggesting another mechanism of action of itaconate *in vivo*. As the *Acod1*-KO mice died with a phenotype close of IFN-γ-KO mice, Nair and his team hypothesized that maybe itaconate was linked to the inflammation (Nair, Huynh et al. 2018).

1.3.5.1 Itaconate and IFN-dependent genes

Pretreatment of Bone Marrow-Derived Macrophages (BMDM) with *E. coli*.-LPS and IFN-β increases the expression of *Acod1* and the production of itaconate (Mills, Ryan et al. 2018). This increase, in part via type I IFNs, promotes the SDH inhibition, the Nuclear factor erythroid 2-related factor 2 (Nrf2) activation (that will be discussed in the next two points), but also its own production via a negative feedback loop on IFN genes. The addition of 4 octyl-itaconate (4OI), a derivative of physiological itaconate, - see BOX-7) to activate BMDM decreases type I IFN-dependent genes, suggesting a link between itaconate and IFN response (Mills, Ryan et al. 2018).

BOX-7. The different derivatives of itaconate (Hooftman and O'Neill 2019).

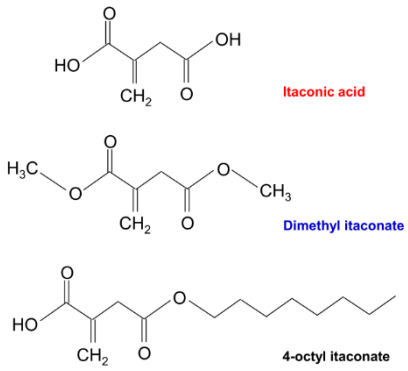

Physiological itaconate needs derivatives for studies as it is not sure yet if/how this molecule is transported inside bacteria as it is a negatively charged non permeable form.

The dimethyl-itaconate (DMI): the esterification of one carboxyl group of physiological itaconate allows a decrease in the negative charge of the molecule and provides a better membrane permeability. However, this modification leads to some negative impacts: the electrophilicity is increased and maybe lead to other effects of the molecule. Another problem is that the DMI is not metabolized to itaconate inside the cell, but instead could boost the biosynthesis of physiological itaconate. The DMI is able to inactivate the glutathione and to activate Nrf2 as the physiological itaconate.

The 4-octyl-itaconate (4OI): the physiological itaconate has been modified by esterification to add an octyl ester to the double carbon-carbon bond responsible of the thiol reaction. The 4OI can be hydrolyzed to itaconate inside the cell, even if in murine macrophages, stimulation by LPS is required. 4OI is able to modify the same cysteine on certain enzymes than physiological itaconate, but not on all enzymes.

The same year, Naujoks studied the itaconate-IFN link on a *Legionella in vivo* model (Naujoks, Tabeling et al. 2016). In this study, the authors compared the genes expression in infected or control lungs mice and showed that more than 1,500 genes were up regulated after the infection. Among these genes, type I (mainly) and type II IFN were shown to be important for the control of *Legionella* infection (Naujoks, Tabeling et al. 2016). To know by which pathways IFN genes led to a better control of *Legionella* infection, they compared the proteomics of *Legionella*-containing vacuole (LCV) in resting macrophages and in IFN-activated macrophages at 2 hours post infection. As the activation of macrophages with IFN did not change the markers of LCV and lysosomes, they concluded that IFN genes do not control the infection by inhibiting the establishment of the LCV or by triggering the fusion of the LCV with lysosomes (Naujoks, Tabeling et al. 2016). After having silenced IFN-dependent genes, they found that *Acod1* expression was impacted, leading to a better replication of *Legionella* in BMDM. By contrast, when BMDM were stimulated with IFN or infected with *Legionella*, *Acod1* was upregulated in

both situations. By Gas Chromatography Mass Spectrometry, they found that IFN stimulation or *Legionella* infection increase itaconate production in host cells. In *vivo* also, *Acod1* gene was upregulated in lungs of mice after infection, and the presence of its metabolite itaconate was also increased, in an IFN-dependent manner (Naujoks, Tabeling et al. 2016).

1.3.5.2 Itaconate and the inhibition of the SDH

Different studies link itaconate to the inflammation by different mechanisms. Among others, it was shown that an activation of macrophages *in vitro* with *E. coli*.-LPS leads to the accumulation of succinate, this latter affecting a lot of different pathways by controlling the Reactive Oxygen Species (ROS) production, IL-1β and Hypoxia-Inducible Factor-1 (Kelly and O'Neill 2015). Itaconate was shown to inhibit SDH in 1949 (Ackermann and Potter 1949), but at this moment, as no effect on the Krebs cycle itself was observed, it did not raise interest of the scientific community. In 2016, Lampropoulou showed that after activation of BMDM with *E. coli*.-LPS, an increase in *Acod1* gene expression and itaconate production was observed (Lampropoulou, Sergushichev et al. 2016). The authors also observed that addition of dimethyl-itaconate (DMI), a permeable form of itaconate (BOX-7), to pre-treated BMDM with *E. coli*.-LPS or IFN+ *E. coli*.-LPS decreases the production of iNOS, IL-6 and IL-12p70, leading to a weaker activation of pro-inflammatory macrophages. These decreases are not completely dependent on the nuclear factor-kappa β (NFκB) signaling as the authors did not observe any change in TNF-α production. To study the pathway impacted by itaconate, the authors did a RNAseq, comparing *E. coli*.-LPS activated BMDM with or without addition of DMI. In the activated BMDM treated with DMI, a decrease of pro-inflammatory transcript was observed, with the decrease of IL-6, IL-12 for examples (Lampropoulou, Sergushichev et al. 2016). The production of IL-1β was also decreased, which is normally induced under NLRP3-activating conditions. After a *Salmonella* infection of BMDM treated with DMI, they also observed a decrease of IL-1β, IL-6 and NO production in comparison to infected BMDM without DMI treatment (Lampropoulou, Sergushichev et al. 2016). Moreover, no difference in the number of bacteria per cell was observed between both conditions. Based on that, they concluded that itaconate does not have a direct bactericidal impact, but rather that an immune-regulatory role. To elucidate that, they did a computational analysis to link inflammation and metabolism in presence of itaconate, and they found that in presence of itaconate, the SDH was inhibited. This inhibition probably occurs via a competitive way, as the structure of itaconate is very close of the one of malonate, a known inhibitor of SDH (Lampropoulou, Sergushichev et al. 2016).

Since the prediction in 1949 made by Ackermann and Poter, it is the first direct evidence in an inflammation model that itaconate could inhibit SDH. After purification of SDH in the presence or absence of itaconate, authors showed that the SDH activity was inhibited in presence of itaconate, and they observed an accumulation of succinate, the substrate of this enzyme. *In vivo* also Lampropoulou showed that DMI was able to inhibit SDH, impacting the ROS production, and so the ROS-dependent cytokines such as IL1-β. Indeed, SDH, in addition to being part of Krebs cycle, is also the second complex of the respiratory chain of electron (Lampropoulou, Sergushichev et al. 2016).

1.3.5.3 Itaconate and the activation of Nrf2

Another explanation of the decrease in IL-1β in presence of itaconate could be the activation of Nrf2, a transcriptional factor protecting against the oxidative stresses (Mills, Ryan et al. 2018). In unstressed conditions, Nrf2 is sequestered by Kelch-like ECH-associated protein 1 (KEAP1), an adapter protein of an ubiquitin ligase. It has been shown that 4OI, another permeable form of itaconate (BOX-7), modifies a cysteine on KEAP1 by alkylation, leading to its inactivation and hence so the activation of Nrf2 (Itoh, Wakabayashi et al. 1999). The DMI could also activates Nrf2 as DMI, being a Michael acceptor (see BOX-8), could have properties close of dimethyl-fumarate (DMF), which is known to activate Nrf2 (Brennan, Matos et al. 2015).

BOX-8. Michael reaction of itaconate and cysteine (modified from (Bambouskova, Gorvel et al. 2018)). The Michael reaction is a reaction allowing mainly the link between two carbons. It consists in the addition of a carbanion (negative organic compound) to an α,β-unsaturated carbonyl compound. Itaconate contains an electrophilic α,β-unsaturated carboxylic acid and could alkylate other proteins on their cysteine residues, leading to the formation of 2,3-dicarboxypropyl adducts.

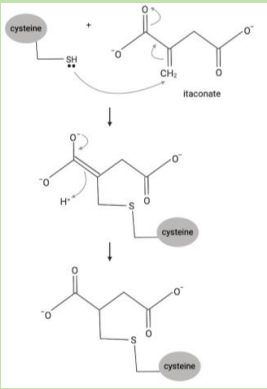

Once activated, Nrf2 is then able to modulate different anti-oxidant like glutathione (Itoh, Wakabayashi et al. 1999) and eliminate the ROS production via those different intermediates. Usually, ROS production leads to the formation of NLRP3-inflammasome and so to the activation of caspase-1. This last one cleaves the pro-IL-1β and pro-IL-6 into their mature forms. But in the presence of activated Nrf2, the elimination of ROS will lead to an indirect decrease in IL-1β and IL-6 (Martinon, Burns et al. 2002, Cruz, Rinna et al. 2007). Moreover, Nrf2 could also have a direct impact on IL-1β production inhibition by binding DNA close to IL-1β and IL-6 genes, leading to the inhibition of the transcription of these genes (Kobayashi, Suzuki et al. 2016). Both DMI and 4OI activate Nrf2 and decreases IL-1β levels. *In vivo*, Mills showed that injection of 4OI by i.p. increases the survival of mice previously injected with *E. coli*.-LPS, by increasing Nrf2, and hence so by decreasing some pro-inflammatory cytokines such as IL-1β production (Mills, Ryan et al. 2018).

1.3.5.4 Itaconate and the ATF3/IκBζ axis

It was already discussed above that DMI treatment of BMDM showed an increase in electrophilic stresses. The electrophilic stresses are able to inhibit NFκB inhibitor ζ (IκBζ) protein induction at a transcriptional level in a Nrf2-independent manner. As the Nrf2-deficient BMDM did not lead to the IκBζ and IL-6 inhibition, Bambouskova and its team did a RNA-seq in Nrf2-deficient and wt BMDM in the presence of itaconate in order to identify the inhibitor of IκBζ (Bambouskova, Gorvel et al. 2018). Among the differentially expressed genes, Activating transcription factor 3 (ATF3) was a good candidate as it is known to be a negative regulator of TLR4 (Gilchrist, Thorsson et al. 2006) and that IκBζ is one of the main transcriptional factor regulating TLRs stimulation after infection or *E. coli*.-LPS stimulation. In the presence of itaconate, this transcriptional factor and its associated genes (such as IL-12β and IL-6) were shown to be inhibited (Bambouskova, Gorvel et al. 2018). The authors found a great overlap between genes regulated by itaconate and those regulated by ATF3. In ATF3-deficient BMDM, the levels of IκBζ and IL-6 were restored in presence of DMI, suggesting that ATF3 could mediate the action of DMI. So, DMI could negatively impact the expression of IL-6, IL-12 genes, dependent on IκBζ transcriptional factor, in a ATF3-dependent manner.

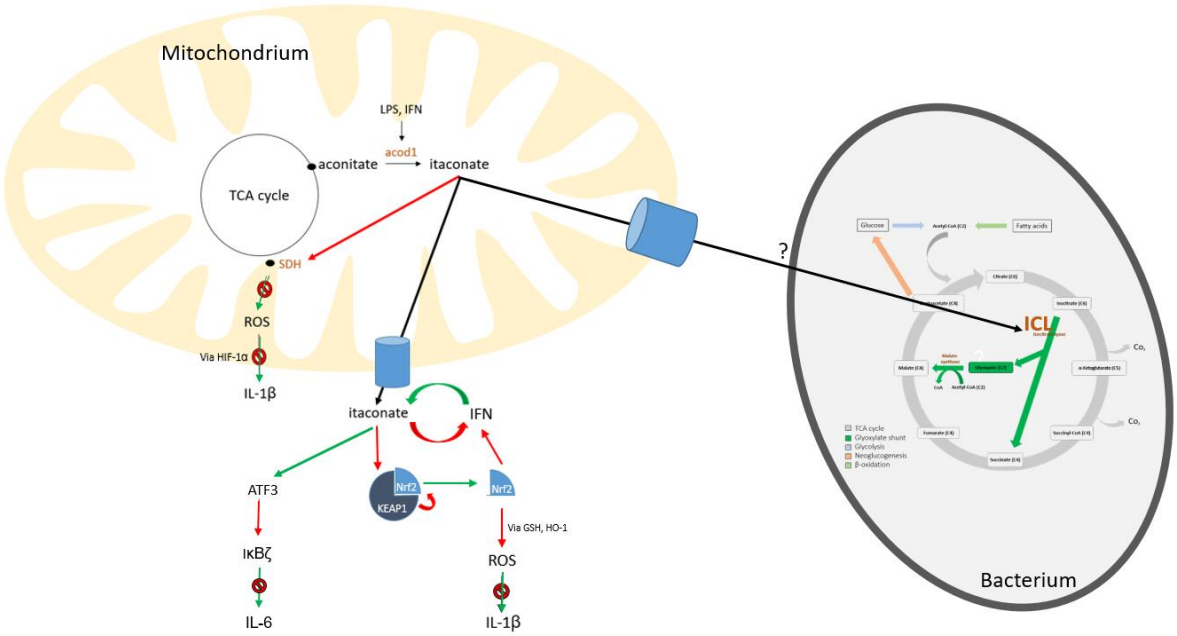

Figure 16: Summarize of the different roles of itaconate. *Itaconate, synthetized from cis-aconitate, has two main roles: an immune-regulator one, and an anti-bacterial one. In the first one, itaconate is able (1) to decrease the level of IL-1β via the inactivation of the succinate dehydrogenase (SDH), and via the activation of Nrf2, (2) to decrease the level of IL-6 via the activation of ATF3. In its anti-bacterial role, itaconate was shown to inhibit the isocitrate lyase (ICL) of some bacteria, leading to an inhibition of the bacterial growth, in a glyoxylate shunt-dependent manner.*

2 Objectives

One of the most physiological routes of infection to study *Brucella* infection in a mouse model is the intranasal infection. This route of infection confronts *Brucella* with the mucosal immune system. *Brucella* must escape from it to be able to reach the lymph nodes and the spleen. The immune effector mechanisms controlling *Brucella* in lungs remain still largely unknown. At 5 and 12 days post infection, comparison of wild type and genetically deficient mice demonstrates that IL-17-dependent TH17 and IFN-γ-dependent TH1 responses, respectively, are indispensable to control infection. However, due to the stealth feature of *Brucella*, inflammation is weakly induced, which makes the analysis of the earlier immune response complicated. Following *Brucella* inoculation, alveolar macrophages are the main infected cells in lungs during the first 48 hours of infection. It is why we wanted to use a without a priori approach (RNA-sequencing) in order to identify upregulated genes in alveolar macrophages following *Brucella* intranasal infection of mice. This approach should allow us to identify candidate genes participating in the early control of *Brucella* growth in alveolar macrophages.

3 Article

Aconitate decarboxylase 1 participates to the early control of pulmonary *Brucella* infection in mice

[1]Aurore Demars, [1]Armelle Vitali, [1]Audrey Comein, [2]Abdulkader Azouz, [2]Stanislas Goriely, [3]Eik Hoffmann, [3]Arnaud Machelart, [3]Pricille Brodin, [1,*]Xavier De Bolle, [4,1,*]Eric Muraille

[1] Unité de Recherche en Biologie des Microorganismes (URBM) - Laboratoire d'Immunologie et de Microbiologie, NARILIS, University of Namur, Rue de Bruxelles 61, 5000 Namur, Belgium.

[2] Université Libre de Bruxelles, Institute for Medical Immunology, and ULB Center for Research in Immunology (U-CRI), Gosselies, Belgium.

[3] Université de Lille, CNRS, INSERM, CHU Lille, Institut Pasteur de Lille, U1019 - UMR 8204 - CIIL - Center for Infection and Immunity of Lille, F-59000 Lille, France

[4] Université Libre de Bruxelles, Laboratoire de Parasitologie, and ULB Center for Research in Immunology (U-CRI), Gosselies, Belgium.

* These authors should be considered as equal last authors.

Corresponding author (*) : Eric Muraille. Mailing address: Laboratoire de Parasitologie. Faculté de médecine. Route de Lennik 808, 1070 Bruxelles. Université Libre de Bruxelles. Belgium. Email: emuraille@hotmail.com

Running title: Role of *Acod1* in *Brucella* infections

Grant support: This work was supported by grants from the Fonds National de la Recherche Scientifique (FNRS) (convention FRSM FNRS 1.4.013.16.F and 3.4.600.06.F to E.M. and PDR-T.0060.15 to X.D.B., Belgium). E.M. is a Senior Research Associate from the FRS-FNRS (Belgium). A.D., and A.M. hold FRIA PhD grants from the FRS-FNRS (Belgium). A.D. was supported by Fonds Spécial de Recherche (FSR) PhD grants from the UNamur (Belgium).

ABSTRACT

Brucellosis is one of the most widespread bacterial zoonoses worldwide. Here, our aim was to identify the effector mechanisms controlling the early stages of intranasal infection by *Brucella* in C57BL/6 mice. During the first 48 hours of infection, alveolar macrophages (AMs) are the main infected cells in the lungs. Using RNA sequencing, we identified the aconitate decarboxylase 1 gene (*Acod1*; also known as Immune responsive gene 1, *Irg1*), as one of the most upregulated genes in murine AMs in response to *B. melitensis* infection at 24h post-infection. Upregulation of *Acod1*was confirmed by RT-qPCR in lungs infected by *B. melitensis* and *B. abortus*. We observed that *Acod1*$^{-/-}$ C57BL/6 mice display a higher bacterial load in their lungs than wild type (wt) mice following *B. melitensis* or *B. abortus* infection, demonstrating that *Acod1* participates to the early control of pulmonary *Brucella* infection. The ACOD1 enzyme is mostly produced in mitochondria of macrophages, and converts cis-aconitate, a metabolite from the Krebs cycle, into itaconate. Dimethyl-itaconate (DMI), a chemically modified membrane permeable form of itaconate, has a dose-dependent inhibitory effect on *B. melitensis* and *B. abortus* growth *in vitro*. Interestingly, DMI does not inhibit multiplication of the isocitrate lyase deletion mutant Δ*aceA B. abortus in vitro*. Finally, we observed that, unlike the wild type strain, Δ*aceA B. abortus* strain multiplies similarly in wt and *Acod1*$^{-/-}$ C57BL/6 mice. These data suggest that bacterial isocitrate lyase might be a target of itaconate in AMs.

INTRODUCTION

Brucellae are facultative intracellular Gram-negative coccobacilli that infect mammals and cause brucellosis (reviewed in (1)(2)(3)(4)). Human brucellosis is a zoonotic infection that is mainly transmitted through ingestion of food contaminated with *Brucella*. Aerosols contamination is also common during abortions or in butcher's shops. Without prolonged antibiotics treatment, brucellosis causes a severe and debilitating chronic disease (1)(5).

The mouse is the experimental animal model the most commonly used to study *Brucella* infection (6). Following intranasal infection, *B. melitensis* multiplies in the lungs for several days before spreading to draining lymph nodes and then to the spleen where they persist for months (7). Chronically *B. melitensis* infected mice develop a protective memory response able to efficiently control a secondary *Brucella* infection (8). However, this response is not able to eliminate bacteria that has settled in $CD11c^+$ splenic reservoir cells during primary infection (9), suggesting that splenic reservoir cells constitute a niche that hides *Brucella* from IFN-γ mediated protective immune response (10)(11). Thus, in order to develop new therapeutic strategies against brucellosis, it would be very useful to identify the early-acting mechanisms against *Brucella* in the lungs before it has established its niche in the spleen.

Over the course of evolution, *Brucella* has acquired specific stealth strategies that allow it to reduce or interfere with its recognition by the immune system and neutralize immune effector mechanisms (reviewed in (3)(12)). Consequently, the inflammatory response against *Brucella* is particularly weak and difficult to detect. We previously showed that TCR-δ, TAP1, and IL-17RA deficiencies affect the early control of *B. melitensis* in the lungs (5 days post infection) (8). At high dose of infection, IL-1R and inflammasomes appear involved in early immune protective mechanisms against respiratory *B. abortus* infection (7 days post infection)

(13). However, the precise effector immune mechanisms involved in early control of *Brucella* remain largely unknown.

Alveolar macrophages (AMs) are well-known to act as first line pulmonary immune sentinels and constitute the dominant immune cells in lungs at the steady state (14). In the first days of intranasal infection, $CD11c^+$ $F4/80^+$ AMs constitute the main pulmonary cells infected by *Brucella* (15)(7). Their elimination increases the spread of *B. abortus* to the draining lymph nodes (15), suggesting that they display an ability to partially control *Brucella* multiplication. AMs perform a critical homeostatic role by clearing inhaled material from the airways and by recycling pulmonary surfactant (14). Due to these steady-state functions, AMs express unique transcriptional and epigenetic profiles that are highly distinct from those of other tissue-resident macrophages (16). It is therefore not surprising that *Brucella* was shown to induce *in vitro* weak IL-1β, IL-6, and TNF-α production in lungs alveolar macrophages compared with peritoneal macrophages (17).

In the present study, to identify the mechanisms involved in *Brucella* control by AMs, we have chosen to use an unbiased approach by RNA sequencing (RNAseq) on whole lungs and purified AMs samples from mice infected by the intranasal route with *B. melitensis*. We observed that *Acod1/Irg1* gene, coding for a cis-aconitate decarboxylase (18), is among the most overexpressed genes in response to infection and we demonstrate that *Acod1* participates to the direct control of *Brucella* multiplication in AMs via itaconate production.

RESULTS

Acod1 is one of the most upregulated gene in alveolar macrophages from *B. melitensis* infected mice.

In order to identify the immune effector mechanisms controlling the early multiplication of *Brucella* in the lung, we compared gene expression in the lungs of *Brucella*-infected and PBS-treated wild type C57BL/6 mice. Mice were infected with 10^7 CFU of *B. melitensis* and sacrificed 24 hours later. Lungs were harvested and analyzed by RNA sequencing. The results of this analysis are presented **Figure S1**. A volcano plot representation of these data shows that only a very low number of genes is significantly upregulated by infection (**Figure S2**). Among them, Lipocalin-2 (*Lcn2*) is involved in innate immune response against bacteria by sequestering iron (19). *Klf2* (Krüppel-like Factor 2), Irx1 (Iroquois homeobox 1) and *Cebpd* (CCAAT enhancer binding protein delta) are transcription factors. This contrasts sharply with the increase in the expression of 1526 genes observed in the lungs of wild type C57BL/6 mice after intranasal infection of 10^6 CFU of *Legionella pneumophilia* (20). However, the very weak immune response induced by *Brucella* in lung is not really surprising given the well-known *Brucella*'s stealth strategy (12).

We hypothesize that the early immune response against *Brucella* is not systemic in lung and should be sought at the cellular level, in the first cells infected with *Brucella*. Following intranasal infection, alveolar macrophages (AMs) constitute the main pulmonary cells infected by *Brucella* between 2 and 24 hours (15)(7). In order to confirm this in our experimental model, we intranasally infected wild type C57BL/6 mice with 10^7 CFU of mCherry-*B. melitensis* stained with the fluorescent tracer eFluor670. The latter makes it possible to visualize by flow cytometry the cells infected with *Brucella* (7). We confirm that the main infected cells at 24

hours post infection express the CD11c and Siglec-F markers (89.9 % of total infected cells) and are therefore indeed AMs (**Figure S3**). Then, we purified under biosafety condition 3 the low-density lung cells expressing the CD11c marker in mice infected for 24 hours with 10^7 CFU of eFluor670 stained mCherry-*B. melitensis*. This cell fraction is highly enriched in infected cells of the AM type and contains 73 % of $CD11c^+$ $eFluor^+$ cells (**Figure S3.B**).

We compared gene expression in AMs enriched fraction purified from the lungs of *Brucella*-infected and PBS-treated wild type C57BL/6 mice. The results of this analysis are presented **Figure S4**. A volcano plot representation of these data shown that 466 genes (R1 genes) are significantly upregulated in infected mice (**Figure 1.A**). We used the Metascape platform to perform a pathway enrichment analyze of these genes. The first signature identified is the response to interferon-beta (**Figure 1.B**). The genes associated with this signature (R2 genes) were represented on a heatmap to see the expression of each gene of this pathway (**Figure 1.C**). Among them, some genes are described to play an effector role in the innate immune response against intracellular pathogen. *Igtp* (IFN-gamma-inducible GTP-binding protein) participate to disruption of *Toxoplasma gondii* vacuoles (21). *Gbp3* and *Gbp6* regulate the cell-autonomous immunity in macrophages by coordinating a potent oxidative and vesicular trafficking program to protect the host from intracellular bacteria (22). The implication of Gbp proteins in the STING-dependent type I interferon response against *B. abortus* has already been described (23). A very interesting candidate is the *Acod1*/*Irg1* gene which has been described to play a role of direct effector against intracellular bacteria but also a role of regulator of the inflammatory response (reviewed in (24)). The involvement of this gene in the control of *Brucella* infection has never been studied to our knowledge.

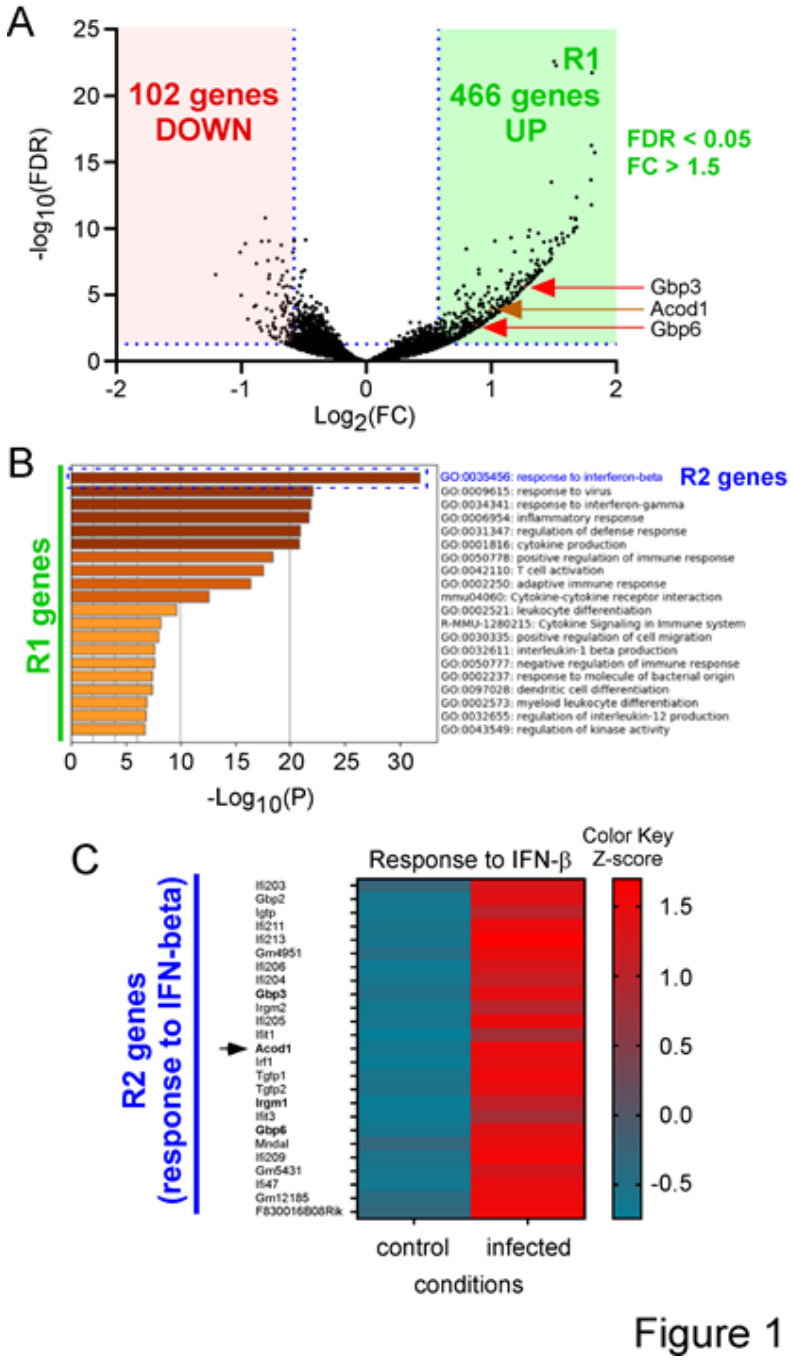

Figure 1

Figure 1. *Acod1* is one of the most upregulated gene in alveolar macrophages from *B. melitensis* infected mice. Wild type C57BL/6 mice were intranasally infected with 10^7 CFU of wild type *B. melitensis* 16M. Lung were harvested at 24 hours post infection, alveolar macrophages purified and the RNA extracted and sequenced. Naïve mice receiving intranasally PBS were used as control. **(A)** Volcano plot of RNA-seq data from naïve versus infected alveolar macrophages shows the adjusted P-value (false discovery rate, FDR -log10) versus fold change (log2). The 466 genes with a FDR < 0,05 and FC > 1,5 are shown in the R1 green square. *Acod1* is the 178th most upregulated gene. **(B)** The R1 genes have been copy-paste in Metascape (https://metascape.org) to perform a pathway enrichment analyze. **(C)** The R2 genes from the first pathway coming out from Metascape analyze were represented on a heatmap to see the expression of each gene of this pathway. The color scale indicates the Z score. RNAseq was performed at least two times and each sample was generated from a pool of at least 3 mice.

***Acod1* deficiency induces a lack of *Brucella* control in lungs.**

To formally determine whether *Acod1* participates to the control of *Brucella* infection or not, we compared the CFU count of bacteria in lungs and spleen from wild type and *Acod1*$^{-/-}$ C57BL/6 mice intranasally infected with 10^7 CFU of wild type *B. melitensis* or *B. abortus* (**Figure 2.A**). We observed that *Acod1*$^{-/-}$ mice infected with *B. melitensis* displayed significantly enhanced CFU only at 9 days post infection in lungs, when compared to wild type mice. In contrast, CFU count are significantly enhanced at 2, 5- and 9-days post infection in *Acod1*$^{-/-}$ mice infected with *B. abortus.* This difference may be the consequence of the lower induction of *Acod1* in response to infection with *B. melitensis* (**Figure 2.B**). In agreement, *Acod1* deficiency has only minimal impact on the course of *B. melitensis* and *B. abortus* in spleen where no *Acod1* expression is detected (**Figure 2.B**).

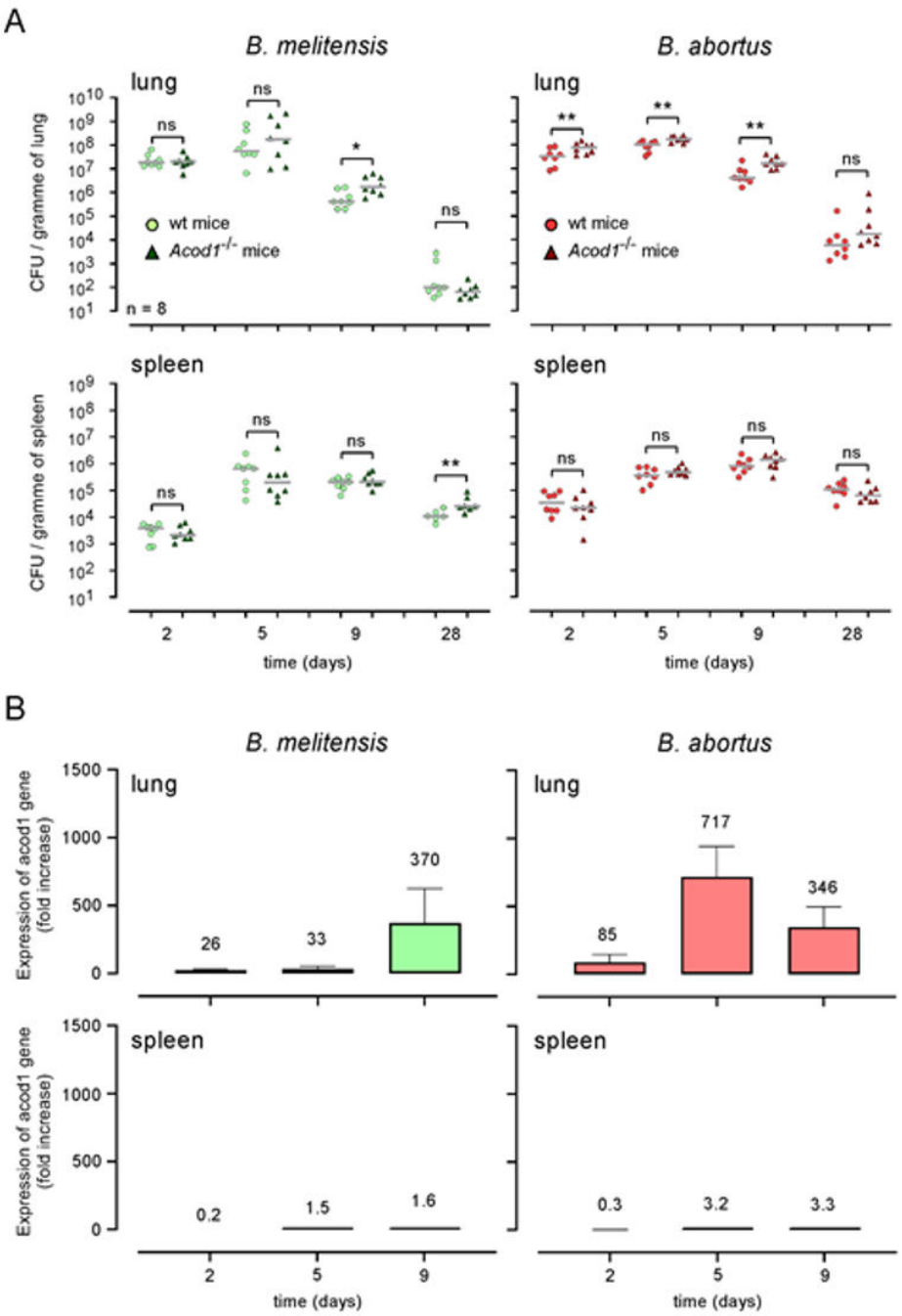

Figure 2

Figure 2. ***Acod1*** **gene expression is correlated to** ***Brucella*** **control in lungs. (A)** wild type and *Acod1*$^{-/-}$ C57BL/6 mice were intranasally infected with 10^7 CFU of wild type *B. melitensis* 16M or *B. abortus* 2308, as indicated. At 2, 5, 9- and 28-days post infection, lungs and spleen were harvested and CFU were counted. Each point represents one mouse. n= number of mice used. Grey bar represents the mean. Significant differences between the indicated groups are marked with asterisks: $^{*}p < 0.1$, $^{**}p < 0.01$. ns= non-significant. Data are representative of at least 3 independent experiments. **(B)** wild type C57BL/6 wt mice were intranasally infected with 10^7 CFU of wild type *B. melitensis* 16M or *B. abortus* 2308, as indicated. At 2, 5- and 9-days post infection, lungs and spleen were harvested and RNA was extracted. After reverse-transcription into cDNA, qRT-PCR were done with *Acod1* primers. At least 6 mice were pooled for each condition. The data are representative of 3 independent experiments. The fold change number is indicated on the bars.

Enhanced susceptibility of *Brucella* infected *Acod1*$^{-/-}$ mice is not associated to higher inflammation in lungs.

Acod1 deficiency has been associated to a lack of inflammatory control in several model of viral (25) and bacterial (26) infection in mice. For example, *Acod1*$^{-/-}$ but not wild type C57BL/6 mice, intranasally infected with *Mycobacterium tuberculosis,* succumbed rapidly, and mortality was associated with increased infection, neutrophilia and production of inflammatory cytokines (26). Depletion of neutrophils enhances survival of *M. tuberculosis*-infected *Acod1*$^{-/-}$ mice.

In order to determine whether *Acod1* tempers *Brucella*-induced inflammation in our experimental model or not, we analyzed the cellular recruitment induced by *B. abortus* in the lungs of infected mice. Wild type and *Acod1*$^{-/-}$ C57BL/6 mice were infected with 10^7 CFU of *B. abortus* and sacrificed 9 days post infection. The lungs were removed and analyzed by flow cytometry and fluorescence microscopy. The cytometric analysis shows that the infection induces an increase in the total number of cells in the lungs, with a significant increase in the number of neutrophils and B and T lymphocytes (**Figure 3.A**). However, this increase is not significantly different between wild type and *Acod1*$^{-/-}$ mice. Histological analysis shows no clusters of neutrophils (GR1$^+$ cells) around cells infected with *Brucella* in the lungs. (**Figure 3.B**). Finally, a measurement of the expression of the proinflammatory cytokines TNF-α, IL-1β and IL-6 in these mice by RT-qPCR shows that these cytokines are indeed induced by the infection but are not significantly more expressed in the *Acod1*$^{-/-}$ mice than in wild type mice (**Figure 4**). On the whole, our data show that *Acod1* deficiency does not lead to a detectable increase in inflammation in mice infected with *Brucella abortus*.

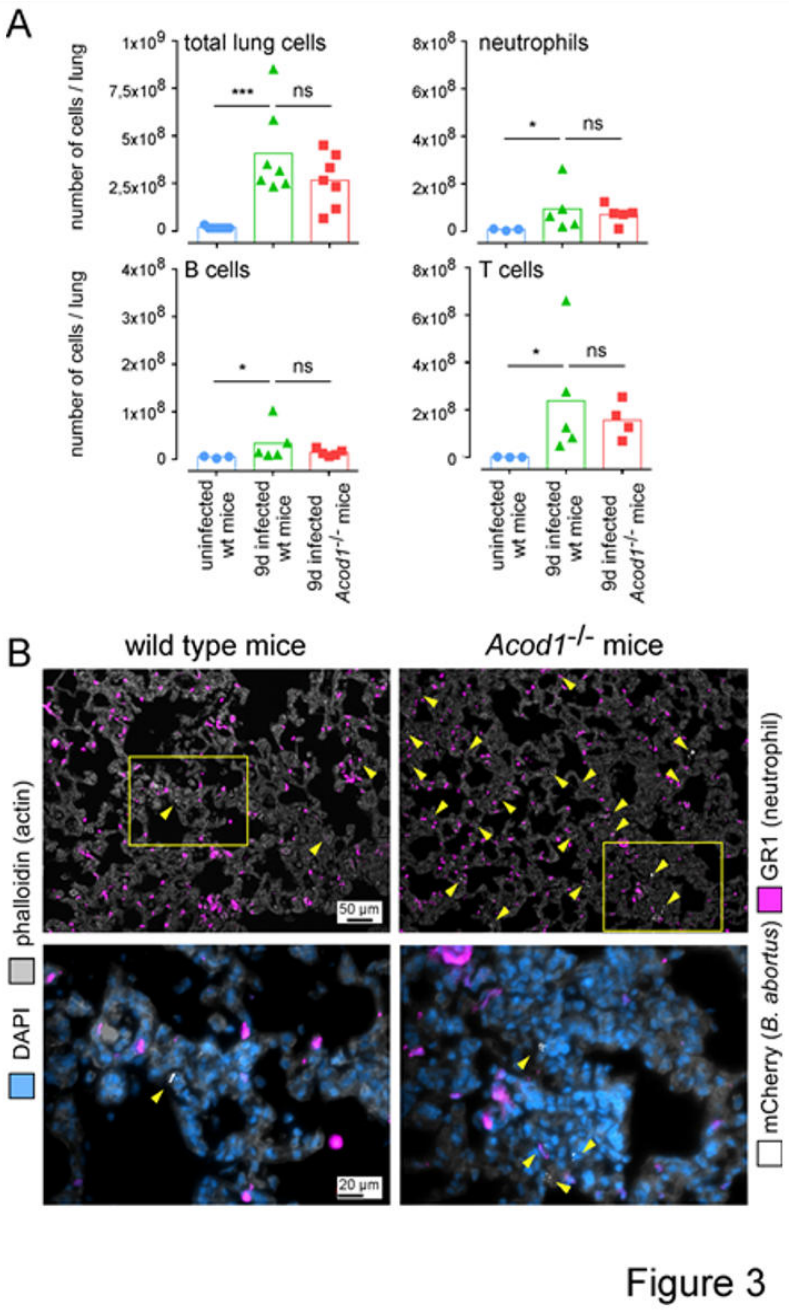

Figure 3

Figure 3. Enhanced susceptibility of *B. abortus* infected *Acod1*$^{-/-}$ mice is not associated to higher cell recruitment in lungs. Wild type and *Acod1*$^{-/-}$ C57BL/6 mice were intranasally infected with 10^7 CFU of wild type mCherry expressing *B. abortus* 2308. At 9 days post-infection, mice were sacrificed and lung harvested. **(A)** Lungs cells were isolated and then analyzed by flow cytometry for FSC and the expression of CD3, F4/80, and B220 markers. Uninfected mice served as control. Significant differences between the indicated groups are marked with asterisks: $^{*}p < 0.1$, $^{***}p < 0.001$. ns= non-significant. The cells were counted from the total cell number by organ. Data represent the number of total cells, neutrophils (F4/80^{neg} Ly6G^{+}), B cells (CD3^{neg} B220^{+}) and T cells (CD3^{+} B220^{neg}) per lung from individual mice. 3 and 6 mice have been used for the control or the infected condition, respectively. These data are representative of at least 2 independent experiments. **(B)**. Lungs were fixed, embedded. Slides of 5 µm were made with a cryostat. Slides were stained and analyzed by fluorescent microscopy for the expression of DAPI, phalloidin, mCherry and GR1 marker. These images are representative of at least 2 independent experiments of at least 3 mice per group.

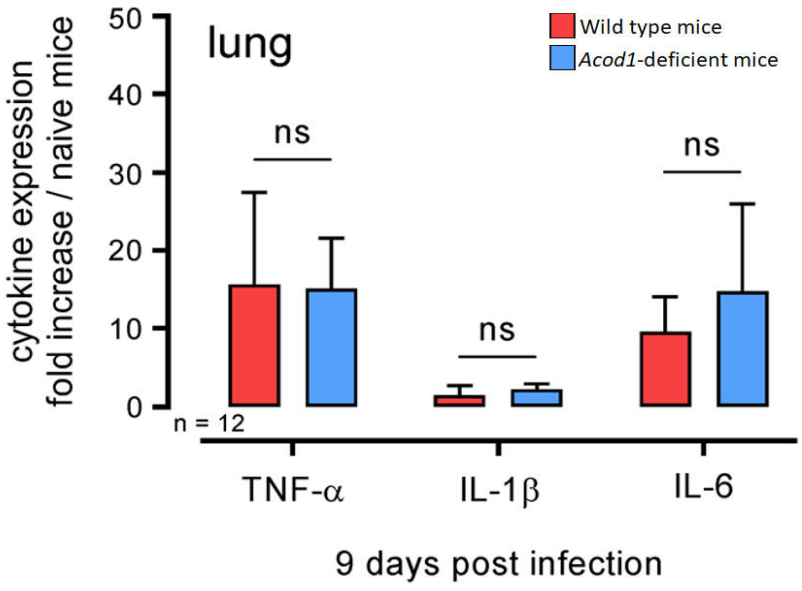

Figure 4

Figure 4. **Enhanced susceptibility of *B. abortus* infected *Acod1*$^{-/-}$ mice is not associated to higher pro-inflammatory cytokines expression in lung**. Wild type (red) and *Acod1*$^{-/-}$ (blue) C57BL/6 mice were intranasally infected with 10^7 CFU of wild type mCherry expressing *B. abortus* 2308. At 9 days post infection, mice were sacrificed, lungs collected, RNA extracted and qRT-PCR performed. TNF-α, IL-1β, and IL-6 expression levels were analyzed. *Tbp* gene was used as negative control, and RNA from naïve mice was used as standard condition. Data shown the fold increase of RNA expression for indicated cytokine from infected mice compared to control mice. At least 6 mice were pooled for each condition. The data are representative of 3 independent experiments. ns=non-significant.

In neutral pH condition, dimethyl-itaconate and 4-octyl-itaconate, but not itaconate, inhibit *Brucella* growth in culture.

Acod1 gene codes for a cis-aconitate decarboxylase that converts the cis-aconitate into itaconate (18). Itaconate concentration reached 5 mM in mouse Bone Marrow-Derived Macrophages after LPS stimulation (27). It has been reported that itaconate could directly inhibit the *in vitro* multiplication of numerous bacteria such as *S. enterica*, *M. tuberculosis* (18), *L. pneumophila*, *S. aureus* and *A. baumannii* (20). As expected, we found that physiologically relevant concentrations of itaconate (8-12 mM) completely inhibits the *in vitro* growth of *B.*

melitensis and *B. abortus* in rich acidic medium (2YT, pH~3.5) (**Figure S5.A**). Surprisingly, at neutral pH in 2YT, itaconate does not seem to have any significant effect on *Brucella* multiplication in *vitro*, regardless of the species (**Figure S5.B**). This could be due to the inability of the itaconate to cross the bacterial membrane because of its charged nature. *In vivo*, after phagocytosis, *Brucella* is supposedly being at acid pH in the phagolysosome of the host cell, increasing the possibility of an increased membrane permeability. Thus, itaconate might be able to enter in *Brucella* in physiological *in vivo* conditions and exert its potentially inhibitory effect. To validate this hypothesis, we tested *in vitro* at neutral pH the impact of different concentrations of dimethyl-itaconate (DMI) (28), a membrane-permeable non-ionic form of itaconate, on the multiplication of *B. melitensis* and *B. abortus*. We observed that DMI inhibits, in a concentration-dependent manner, the growth of both *Brucella* species in rich medium (2YT) (**Figure 5.A**), suggesting that itaconate is able to specifically affect *Brucella* when it can cross its membrane. Similar results were obtained with 4-octyl-itaconate (27), another membrane-permeable non-ionic form of itaconate (**Figure S6**).

B. abortus bacteria incubated for 24 hours in the presence of 10 mM of DMI in 2YT, washed and then cultured again in the absence of DMI show 100 times less CFU than control bacteria, not treated with DMI (data not shown), which demonstrates that the DMI is bactericidal for *Brucella*.

Inhibition of *Brucella* growth in culture by dimethyl-itaconate is isocitrate lyase-dependent.

Itaconate has been described to bind the bacterial enzyme isocitrate lyase (ICL) (18) which is part of the glyoxylate shunt that is exclusively found in prokaryotes, lower eukaryotes, and plants. This alternative shunt is activated in response to nutrient deprivation, a condition

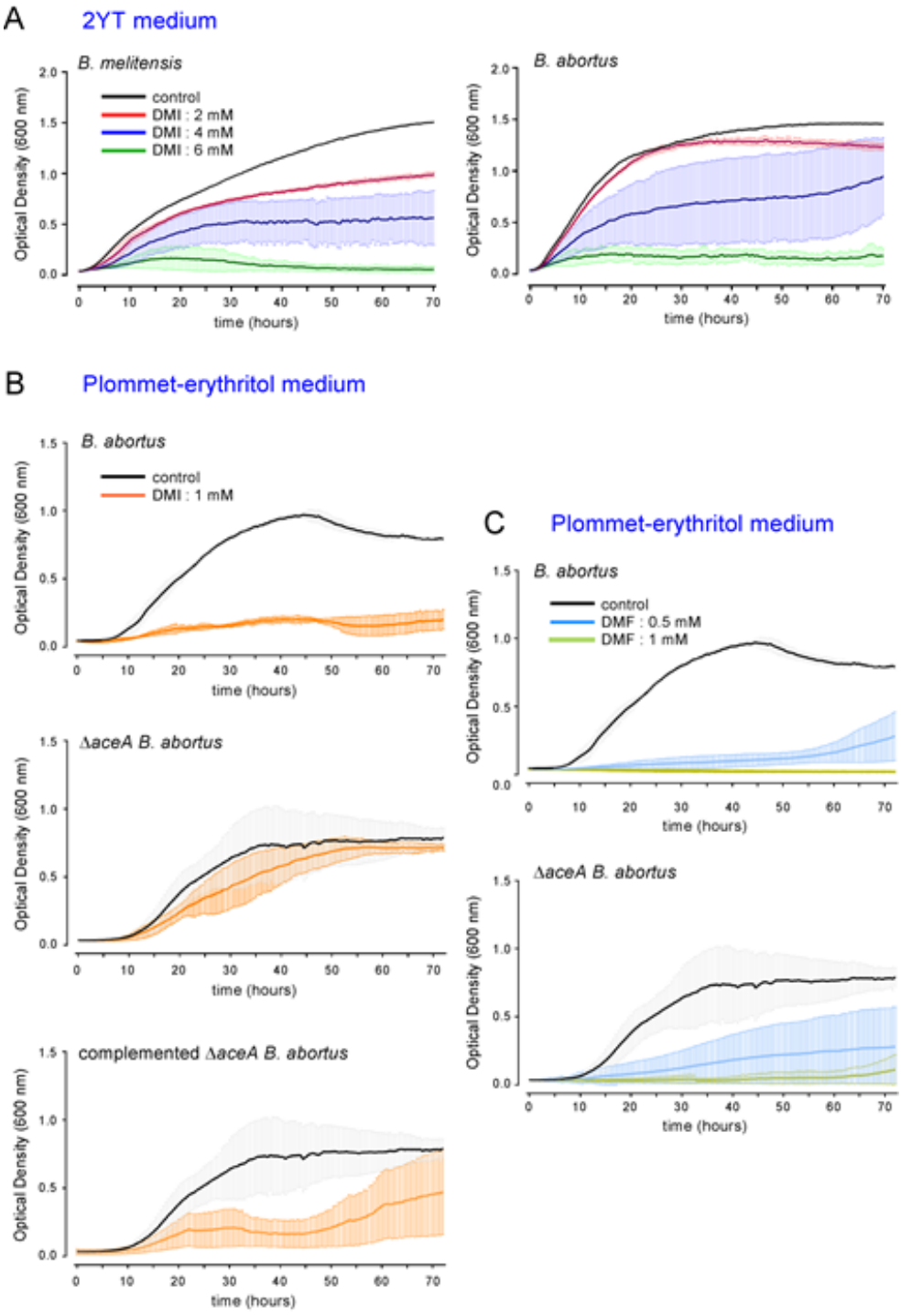

Figure 5

Figure 5. **The multiplication of *Brucella in vitro* is inhibited by dimethyl-itaconate via an isocitrate lyase-dependent mechanism. (A)** Comparison of the impact of different concentrations of dimethyl-itaconate (DMI) on the growth of wild type *B. melitensis* (left panel) or *B. abortus* (right panel) in rich medium (2YT). **(B)** Comparison of the impact of 1 mM of DMI on the growth of wild type, Δ*aceA* and Δ*aceA*-complemented *B. abortus* in poor medium (Plommet-Erythritol). (**C**) Dimethyl-fumarate (DMF) has been used as control, in the same conditions than (B). The bacteria grew during 72h at 37 °C, the OD was measured every 30 min in a Bioscreen system. The standard deviation represents the mean of three independent experiments.

encountered by bacteria in phagolysosomes (29). We compared the effect of DMI on the growth of a wild-type strain and an ICL deficient strain (Δ*aceA*) of *B abortus* in a defined minimal medium for *Brucella*, the Plommet-erythrytol medium (30). We observed that the growth of the Δ*aceA* strain was much less affected by DMI than the growth of the wild type strain (**Figure 5.B**). Complementation of the Δ*aceA* mutant with a plasmid encoding the isocitrate lyase renders it sensitive to DMI, which demonstrates that itaconate acts via ICL to inhibit the multiplication of *Brucella* under our experimental conditions. In contrast, dimethyl-fumarate (DMF), that is described to inhibit the growth of *E. coli* (31), reduce similarly the growth of wild type and Δ*aceA B. abortus* (**Figure 5.C**), suggesting that DMI is specifically responsible for the ICL-dependent inhibition of *B. abortus* growth.

DMI treatment induces significant morphological changes in *Brucella*. Transmission electron microscopy (TEM) analysis shows that wild type *B. abortus* treated for 24 hours with 1 mM DMI present significant thickening of the envelope (**Figure S7**). However, these alterations are also observed with DMI-treated Δ*aceA B. abortus*, demonstrating that these envelope defects do not correlate with the growth inhibition effect of DMI.

***Acod1* deficiency does not affect the growth of *ΔaceA B. abortus in vivo*.**

Finally, to determine whether *Acod1*-dependent control of *Brucella* infection *in vivo* is acting via bacterial ICL, wild type and *Acod1*$^{-/-}$ C57BL/6 mice we intranasally infected with 10^7 CFU of wild type or Δ*aceA B. abortus* and sacrificed 9 days post infection. In striking contrast with wild type strain of *B. abortus*, CFU analysis of lungs from infected mice showed that growth of Δ*aceA* strain is not affected by *Acod1* deficiency (**Figure 6**), demonstrating that *Acod1*-independent control of *Brucella* in lungs is well dependent on the expression of ICL by *Brucella*.

In addition, the fact that the CFU of *Acod1*$^{-/-}$ mice infected with wild type and Δ*aceA B. abortus* are comparable is consistent with the proposal that ICL is the main target of *Acod*1.

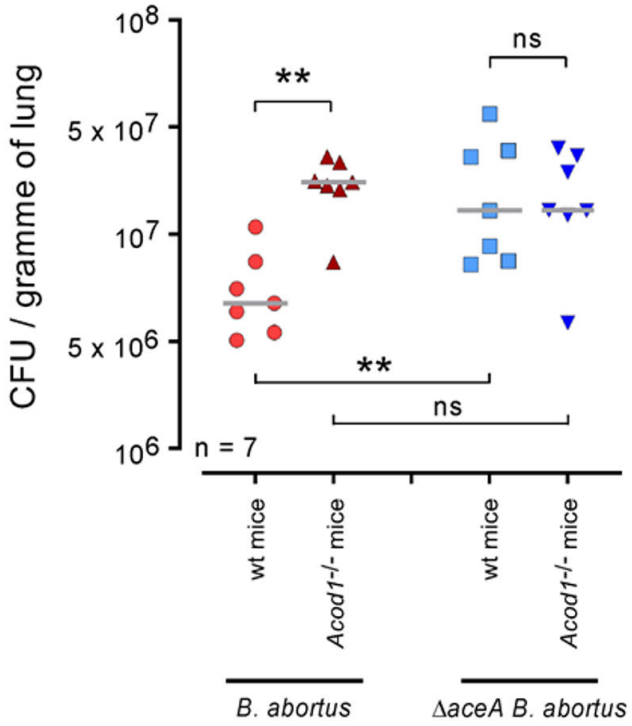

Figure 6

Figure 6. *Acod1* deficiency does not affect the growth of Δ*aceA B. abortus in vivo*. Wild type and *Acod1*$^{-/-}$ C57BL/6 wt mice were intranasally infected with 10^7 CFU of wild type or Δ*aceA* mCherry expressing *B. abortus* 2308, as indicated. At 9 days post infection, mice were sacrificed, lungs harvested and CFU counted. Each point represents one mouse, n = number of mice used for each condition. Grey bar represents the mean. Significant differences between the indicated groups are marked with asterisks: $^{**}p < 0.01$. ns= non-significant. The data are representative of at least 3 independent experiments.

DISCUSSION

Mucosal surfaces are portals of entry for the vast majority of pathogens. In the case of brucellosis, natural infections take place mainly via the intestinal (32) and respiratory tracts (33). Despite this, little is known about the immune mechanisms controlling *Brucella* at mucosal level. We have previously shown that the early multiplication of *B. melitensis* in the lungs of infected mice is controlled by the immune system. The comparison of mice genetically deficient for key elements of the innate and adaptive immune response demonstrated that γδ T lymphocytes, CD8 T lymphocytes as well as pathways dependent on the IL-17RA receptor were involved (34). However, the precise mechanisms directly controlling the proliferation of *Brucella* in the lungs remain largely unknown. In order to identify them, we used a without a priori approach by performing RNA sequencing of the whole lungs as well as the main cells infected by *Brucella*, the alveolar macrophages.

Intranasal *B. melitensis* infection does not appear to induce any detectable systemic response in the lungs at 24 hours post infection, even at a dose of 10^7 CFU, which fits well with its stealth pathogen profile (3)(35). In striking contrast, analysis of the RNA profile of purified alveolar macrophages allowed us to identify 466 genes whose expression is significantly increased compared to uninfected controls. Clustering analysis carried out using Metascape led us to select several genes involved in the anti-bacterial immune responses induced by type 1 interferon, such as *Igtp*, *Gbp3*, *Gbp6* and *Acod1*. Among these, *Acod1* is described to play dual roles in immunity and diseases (for a review see (24)) and has never been associated with the control of *Brucella* infection. We therefore chose to explore its role in the pulmonary immune response against *Brucella*.

Acod1 gene was originally identified in 1995 as a 2.3-kb cDNA from a library synthesized from mRNA isolated from a murine macrophage cell line after LPS stimulation (36). It is markedly upregulated in response to pathogen associated molecular patterns, such as LPS and CpG and inflammatory cytokines, such as type I interferon and tumor necrosis factor. ACOD1 enzyme catalyzes itaconate metabolite production by cis-aconitate decarboxylation and is mainly found in mitochondria of myeloid cells.

Itaconate is well described to downregulate pro-inflammatory cytokine and reactive oxygen species productions by multiple mechanisms (24). It has been reported that *Acod1* expression tempers inflammation and prevent immunopathology during *Mycobacterium tuberculosis* (26) and Respiratory Syncytial Virus (25) infections in mice. In striking contrast, in our *Brucella* infection model, we showed that the absence of *Acod1* does not significantly increase proinflammatory cytokines production or neutrophil recruitments in lungs from infected mice, despite a significant increase in the bacterial load in the lungs. Again, this must be the consequence of the stealth pathogen profile of *Brucella*.

Itaconate is also known for its ability to inhibit the multiplication of several bacteria *in vitro* (18) and *in vivo* (20). We have shown that two membrane-permeable forms of itaconate, DMI and 4OI, fully inhibit *Brucella* multiplication *in vitro*. *B. melitensis* and *B. abortus* display the same sensitivity to DMI and 4OI. However, in mice, *Acod1* deficiency increases susceptibility to *B. abortus* much more than to *B. melitensis*. This difference can be correlated to the earlier and stronger induction of *Acod1* expression in the lungs by *B. abortus* than by *B. melitensis* following intranasal infection. This could be explained by the higher CFU level of *B. abortus*, comparatively to *B. melitensis*, in the lungs of wild type mice.

Itaconate inhibits bacteria multiplication via isocitrate lyase (ICL), the key enzyme of the glyoxylate shunt, a two-step metabolic pathway that serves as an alternative shunt to the tricarboxylic acid cycle and is essential for bacterial growth under specific conditions. In *Mycobacterium tuberculosis*, ICL also exhibits additional methyl-isocitrate lyase activity. This later is required for the detoxification of propionyl-CoA through the 2-methylcitrate cycle (18). No attenuation of ICL deficient *B. abortus* strain, Δ*aceA*, was reported in BALB/c mice (37). We showed that Δ*aceA B. abortus* is more resistant to itaconate inhibition *in vitro* than wild type bacterial strain and displays similar multiplication in wild type and *Acod1*$^{-/-}$ mice. On the whole, our results support a model in which ACOD1 enzyme restricts *Brucella* replication in murine alveolar macrophages through a bacterial ICL dependent mechanism. However, *aceA* deficiency does not prevent or reduce *Brucella* multiplication in lungs, demonstrating that ICL is not essential to *Brucella* multiplication in this condition. This suggests that *Acod1*-mediated ICL-dependent inhibition of *Brucella* multiplication in our murine infection model is not explained by a simple blockage of the glyoxylate shunt or by the toxic accumulation of propionyl-CoA. The precise mechanism of *Brucella* growth inhibition by itaconate therefore remains to be elucidated. It is interesting to remark that DMI induced also, independently of ICL, a massive disorganization of the bacterial envelope. One possible mechanism for this effect could be the inhibition of several L,D-transpeptidases, which are enzymes crosslinking peptide stems of the peptidoglycan. Indeed, these enzymes have a cysteine in their active site and itaconate is known to alkylate this residue.

Our results demonstrate that *Acod1* plays very different roles depending on the bacterial species. Its ability to regulate inflammation does not seem to be exercised against stealthy bacteria such as *Brucella*, although it is essential for the control of neutrophil-mediated immunopathology during *M. tuberculosis* infection (26). The capacity of itaconate to inhibit

bacterial multiplication can occur through a variety of pathways, which might be reflective of metabolic differences between bacteria species.

In summary, our study provides for the first-time evidences showing a role of *Acod1* cis-aconitate decarboxylase enzyme producing itaconate in pulmonary control of *Brucella* infection in mouse model. We also demonstrate that this control is exerted at a cellular level, in alveolar macrophages, and acts via the bacterial enzyme isocitrate lyase. However, due to the moderate effect of *Acod1* deficiency on *Brucella* multiplication *in vivo*, we hypothesize that ACOD1 acts in concert with other antibacterial factors, such as GBP proteins whose expression is also found increased in *Brucella* infected alveolar macrophages and which have been described as participating in the control of *Brucella in vitro* and *in vivo* (23). As mouse ACOD1 enzyme is ∼80% identical in amino acid sequence to human ACOD1 with all five predicted cis-aconitate decarboxylase domains fully conserved (18), the development of pharmacological agents that enhance ACOD1 function or promote itaconate production might help to control early stages of pulmonary *Brucella* infection.

MATERIAL AND METHODS

Ethics statement

The procedures used in this study and the handling of the mice complied with current European legislation (Directive 86/609/EEC). The Animal Welfare Committee of the Université de Namur (UNamur, Belgium) reviewed and approved the complete protocol for *Brucella melitensis* and *B. abortus* infection (Permit Number: UN-LE-18/309).

Mice, bacterial strains and reagent

Wild type C57BL/6 mice were acquired from Harlan (Bicester, UK). *Acod*1$^{-/-}$ C57BL/6 mice (49) were acquired from Dr Eik Hoffmann (University of Lille, France). All wild type and deficient mice used in this study were bred in the animal facility of the Gosselies campus of the Université Libre de Bruxelles (ULB, Belgium).

The wild type *B. melitensis* 16M strain used here is a *B. melitensis* 16M stably expressing a rapidly maturing variant of the red fluorescent protein DsRed (55), the mCherry protein, under the control of the strong *Brucella* spp. promoter, p_{sojA}. The construction of the mCherry-producing *Brucella* strain has been described previously in details (38). We also used mCherry-wild type *B. abortus* 2308 (39) and mCherry-Δ*aceA* (isocitrate lyase) *B. abortus* (37) and the complemented strain. *Brucella abortus* 2308 Δ*aceA* was complemented with the pMR10Ω*aceA* plasmid. Briefly, the *aceA* gene and its promoter was amplified with the Q5 High-Fidelity DNA polymerase (New England Biolabs) with the following forward and reverse primers 5'-CGC GGATCC ATT TCC ACC AGT TCC TGA TC -3' and 5'-AAAA CTGCAG GGA TTG TTC TTC TGC TCT TTC-3'. PCR products were purified (Macherey-Nagel Clean-up kit) and cloned into the *EcoRV* site of the pGemT in *E. coli* DH10B. The *aceA* gene was then subcloned into the pMR10 plasmid

(a kind gift from C.D. Mohr and R.C. Roberts, Stanford University) with the restriction enzymes *BamHI* and *PstI*. The resulting plasmid was introduced into *E. coli* S17.1 strain (40) and into *B. abortus* 2308 Δ*aceA* by mating. *Brucella* strains were always handled under BSL-3 containment according to Council Directive 98/81/EC of 26 October 1998 and a law of the Walloon government of 4 July 2002.

Itaconate (Sigma-Aldrich) as well as dimethyl itaconate (DMI) (Sigma-Aldrich) were diluted in bidistilled water, whereas 4-octyl-itaconate (4OI) (Sigma-Aldrich) was diluted in DMSO. After filtration, the solutions were stored at 4 °C.

Intranasal Brucella infection

Brucella cultures were grown overnight with shaking at 37°C in 2YT liquid medium (Luria-Bertani broth with double quantity of yeast extract) and were washed twice in RPMI 1640 (Gibco Laboratories) (2000xg, 10 min) before inoculation of the mice.

Mice were anesthetized with a cocktail of Xylasine (9 mg/kg) and Ketamine (36 mg/kg) in PBS before being inoculated by intranasal injection of the indicated dose of *Brucella* in 30 µl of RPMI. Control animals were inoculated with the same volume of RPMI. The infectious doses were validated by plating serial dilutions of the inoculums. At the selected time after infection, mice were sacrificed by cervical dislocation. Immediately after sacrifice, lungs and spleen were collected for bacterial count, flow cytometry, qRT-PCR, MAs purification and/or microscopic analyses.

Bacterial counting

Organs were homogenized into PBS/0.1% X-100 Triton (Sigma-Aldrich). We performed successive serial dilutions in PBS to obtain the most accurate bacterial count and plated them on 2YT medium. The CFU were counted after 4 days of incubation at 37°C.

RNA extraction

RNA from whole lungs and spleen was extract with the Tripure/Chloroform method. Briefly, lungs and spleen were harvested from mice, cut in small piece and homogenized in 1 mL of Tripure (Tripure Isolation Reagent – Roche). After 5 min of incubation at RT, 200 µL of chloroform was added, and the tube was mixed vigorously during 15 seconds, then incubated 10 min at RT. After a centrifugation of 15 min (12,000xg at 4 °C), the aqueous phase was collected and placed in a new tube. 500 µL of isopropanol was added. The tube was mixed by inversion and centrifuged for 10 min (12,000xg at 4 °C). The pellet was washed twice with 75 % ethanol (7,500xg for 5 mi at 4 °C), suspended in 50 µL of water, and incubated for 10 min at 55 °C to completely resuspend the RNA pellet. RNA from purified AMs was extracted with the RNeasy Mini kit (Qiagen).

RNA sequencing and analyze

After DNAse I, RNAse-free treatment (Thermo Scientific), the RNA samples were then transform into cDNA, and the library was prepared. The Novaseq 6000 Trueseq SBS reagents (25 millions reads paired-end) and Trueseq stranded RNA library preparation were used for the Illumina sequencing.

Genes with no raw read count were filtered out with an R script. Raw read counts were normalized and a differential expression analysis was performed with DESeq2 by applying an adjusted p-value < 0.05 and absolute log2-ratio larger than 0.5849.

qRT-PCR analysis

RNA was treated with the DNAse I- RNAse-free kit (Thermo Scientific). Briefly, 2 µg of RNA was treated 30 min with DNAse I at 37 °C followed by DNAse I inactivation with 50 mM of EDTA for 10 min at 65 °C. The RNA was then reverse transcribed with Superscript II reverse transcriptase (Invitrogen) with hexamer random primers as described by the manufacturer. A condition without reverse transcriptase was also conducted in parallel as a negative control. cDNA was then mixed with SybrGreen mix (FastStart universal SYBR Green Master (Rox); Roche) and the appropriate primers sets and subjected to qRT-PCR in a LightCtcle96 (Roche). The forward and reverse primers used were 5'-GGC ACA GAA GTG TTC CAT AAA GT-3' and 5'-GAG GCA GGG CTT CCG ATA G-3' for *Acod1*, 5'-GCG AAC AAA GCC AGA TGC AA-3' and 5'-CCC CTT TCC TCC CAA ACC AA-3' for TNF, 5'-CGC ATG TTC CTG GGG AGA TT-3' and 5'-TGG GAT GCA ACA TGG CTC TT-3' for IL-1, 5'-GGC TTG CCC CAC TAC TTA GG-3' and 5'-GCG AAC AAA GCC AGA TGC AA-3' for IL-6. TATA binding protein (*Tbp*, forward 5'-GTT GGG GTG GCA TTT TCT GTG-3', reverse 5'-GGC CTC TGC ATG TGT TCT CAT-3') mRNA was used as the reference housekeeping gene for normalization. A total of 45 three-step cycles were performed as follows: 95 °C for 10 sec, 60 °C for 10 sec, and 92 °C for 10 sec. Melting curves were then performed to assess primer specificity. Target mRNA fold change was calculated based on the $2^{-\Delta\Delta Ct}$ formula, where *Tbp* gene was used as the reference gene, and RNA from naïve mice was used as standard condition. At least 6 biological replicates and 3 technical replicates were performed for each tested gene.

Bioscreen analysis

Overnight cultures were prepared in 2YT rich medium the day before in order to obtain an $OD_{600\,nm}$ between 0.2 – 0.5 the day after. Cultures were washed twice in PBS (2000xg during 10 min at RT), and there suspended in 2 YT rich medium or Plommet-Erythritol defined minimal

medium (30) in order to obtain an $OD_{600\ nm}$ = 0.05 in a final volume of 700 µL. We used the Bioscreen system (Thermo Fisher) to measure the growth of *Brucella* at 37 °C during 72 hours.

Brucella melitensis staining with eFluor^{670}

For some histological and flow cytometry experiments, we stained *B. melitensis* with eFluor^{670} labelling. Cultures (10 ml) were grown overnight as indicated above, bacteria of 1 ml of culture were centrifuged (2 min, 7500xg, RT) and the pellets washed 3 times with 1 ml of PBS, then the bacteria were incubated for 20 min at RT in the dark with eFluor^{670} dye at the final concentration of 10 µM in 1 mL of PBS. After incubation, the bacteria were washed three times in 1 mL of PBS and once diluted in PBS in order to obtain the precise infectious dose before inoculation of the mice.

Cytofluorometric analysis

The lungs were harvested and cut into small pieces and incubated for 1 hour at 37°C with a mix of 100 µg/ml of DNAse I fraction IX (Sigma-Aldrich) and 1.6 mg/ml of collagenase (400 Mandl U/ml), as described previously (6). The cells were then washed, filtered and incubated with saturating doses of purified 2.4G2 (anti-mouse Fc receptor, ATCC) in 200 µl PBS, 0.2% BSA, 0.02% NaN3 (FACS buffer) for 20 min at 4°C to prevent antibody (Ab) binding to the Fc receptor.

3–5x10^6 cells were stained on ice with various fluorescent mAb combinations in FACS buffer. We acquired the following mAbs and reagents from BD Biosciences: BV421-coupled E50-2440 (anti-Siglec-F), BV421-coupled 1A8 (anti-Ly-6G), fluorescein (FITC)-coupled HL3 (anti-CD11c), FITC-coupled 145-2C11 (anti CD3ε), Alexa Fluor 647-coupled T45-2342 (anti-F4/80), APC-coupled RA3-6B2 (anti-CD45R/B220). The cells were analyzed on a BD FacsVerse flow

cytometer. Dead cells and debris were eliminated from the analysis according to size and scatter.

Immunofluorescence microscopy of lung

Lungs were fixed for 20 minutes at RT in 2% paraformaldehyde (PFA). Then, lungs, still in 2% PFA, were placed under a vacuum until no air was present in the lungs for 2 hours. After PFA fixation and two washes in PBS, lungs were incubated overnight at 4°C in a 20% PBS-sucrose solution. Tissues were then embedded in Tissue-Tek OCT compound (Sakura), frozen in liquid nitrogen, and cryostat sections (5 µm) were prepared. For staining, tissue sections were rehydrated in PBS and incubated in a PBS solution containing 1 % blocking reagent (Boeringer) (PBS-BR 1%) for 20 min before incubation overnight in PBS-BR 1% containing the following: DAPI nucleic acid stain Alexa Fluor 350, 488 phalloidin (Molecular Probes) and Alexa Fluor 647–coupled RB6-8C5 anti-Ly6G/Ly6C (Gr1) (Biolegend). Slides were mounted in Fluoro-Gel medium (Electron Microscopy Sciences, Hatfield, PA). Labelled tissue sections were visualized with an Axiovert M200 inverted microscope (Zeiss, Iena, Germany) equipped with a high-resolution monochrome camera (AxioCam HR, Zeiss). Images (1384x1036 pixels, 0.16 µm/pixel) were acquired sequentially for each fluorochrome with A-Plan 10x/0.25 N.A. and LD-Plan-NeoFluar 63x/0.75 N.A. dry objectives and recorded as eight-bit grey-level *.zvi files. At least 3 slides were analyzed per organ from 3 different animals and the results are representative of 2 independent experiments.

Purification and transmission electron microcopy analysis of alveolar macrophage.

Pulmonary alveolar macrophages were obtained by homogenization and filtration of lungs, density gradient centrifugation (5 ml of 1.085 g/cm^3 nycodenz were mixed to the cells, then 5 mL of cold RPMI was delicately added above the nycodenz, and the tube was

centrifuged, 1700xg during 30 min, with minimum braking). A CD11c specific Magnetic associated cell sorting (MACS) was performed on the collected low-density cells at the interface between nycodenz and RPMI by using MiniMACS, MS column and CD11c+ magnetic beads (Miltenyl Biotec).

Purified alveolar macrophages were fixed 2 hours in 2,5% glutaraldehyde in cacodylate buffer 0,1 M at 4 °C, wash 3 times (4000xg, 5 min) with cacodylate buffer 0,2 M then postfixed in 2% osmium tetroxide in cacodylate buffer 0,1 M during 1 hour at RT. After 3 washes, samples were serially dehydrated in ethanol (EtOH 30 % first 5min, followed by 10 min – the same for EtOH 50 %, 70 %, 85 %, 100%). Propylene oxide was then added 4x5 min at RT and the pellet was progressively embedded in epoxy resin (Agar 100 resin; Agar Scientific, United Kingdom) (75:25, 50:50 and then 25:75 % of propylene oxide/resin). Ultrathin 50-nm sections were obtained, mounted on copper-Formvar-carbon grids (EMS, United Kingdom), and stained with uranyl acetate and lead citrate by standard procedures. Observations were made on a Tecnai 10 electron microscope (FEI, Eindhoven, The Netherlands), and images were captured with a Veleta charge-coupled-device (CCD) camera and processed using the AnalySIS and Adobe Photoshop software programs.

Statistical analysis

We used a (Wilcoxon-)Mann-Whitney test provided by the GraphPad Prism software to statistically analyze our results. Each group of deficient mice was compared to the wild type mice. We also compared each group with the other groups and displayed the results when required. Values of $p < 0.05$ were considered to represent a significant difference. *, ** denote $p < 0.05$, $p < 0.01$, respectively.

Acknowledgements

We thank the Plateforme Technologique Morphologie – Imagerie, University of Namur for performing transmission electron microscopy analysis and Angéline Reboul for expert technical assistance.

References

1. Corbel MJ. Brucellosis: An Overview. *Emerg Infect Dis* (1997) **3**:213–221.

2. Godfroid J, Cloeckaert A, Liautard JP, Kohler S, Fretin D, Walravens K, Garin-Bastuji B, Letesson JJ. From the discovery of the Malta fever's agent to the discovery of a marine mammal reservoir, brucellosis has continuously been a re-emerging zoonosis. *Vet Res* (2005) **36**:313–326.

3. Martirosyan A, Moreno E, Gorvel JP. An evolutionary strategy for a stealthy intracellular Brucella pathogen. *Immunol Rev* (2011) **240**:211–234.

4. Moreno E. Retrospective and prospective perspectives on zoonotic brucellosis. *Front Microbiol* (2014) **5**:1–18. doi:10.3389/fmicb.2014.00213

5. Colmenero JD, Reguera JM, Martos F, Sánchez-De-Mora D, Delgado M, Causse M, Martín-Farfán A, Juárez C. Complications associated with Brucella melitensis infection: a study of 530 cases. (1996). doi:10.1097/00005792-199607000-00003

6. Santos RL, Silva TMA, Costa EA, Paixo TA, Tsolis RM. Laboratory animal models for brucellosis research. *J Biomed Biotechnol* (2011) **2011**:

7. Demars A, Lison A, Machelart A, Vyve M Van, Potemberg G, Vanderwinden J, De Bolle X. Route of Infection Strongly Impacts the Host-Pathogen Relationship. *Front Immunol* (2019) **10**:1589. doi:10.3389/fimmu.2019.01589

8. Mambres DH, MacHelart A, Potemberg G, De Trez C, Ryffel B, Letesson J-J, Muraille E. Identification of immune effectors essential to the control of primary and secondary intranasal infection with brucella melitensis in mice. *J Immunol* (2016) **196**: doi:10.4049/jimmunol.1502265

9. Machelart A, Van Vyve M, Potemberg G, Demars A, De Trez C, Tima HG, Vanwalleghem G, Romano M, Truyens C, Letesson J-J, et al. Trypanosoma infection favors Brucella elimination via IL-12/IFNγ-dependent pathways. *Front Immunol* (2017) **8**: doi:10.3389/fimmu.2017.00903

10. Vitry M-A, De Trez C, Goriely S, Dumoutier L, Akira S, Ryffel B, Carlier Y, Letesson J-J, Muraille E. Crucial role of gamma interferon-producing CD4+ Th1 cells but dispensable function of CD8+ T cell, B cell, Th2, and Th17 responses in the control of Brucella melitensis infection in mice. *Infect Immun* (2012) **80**:4271–80. doi:10.1128/IAI.00761-12

11. Vitry M-A, Hanot Mambres D, De Trez C, Akira S, Ryffel B, Letesson J-J, Muraille E. Humoral Immunity and CD4+ Th1 Cells Are Both Necessary for a Fully Protective Immune Response upon Secondary Infection with Brucella melitensis. *J Immunol* (2014) **192**:3740–52. doi:10.4049/jimmunol.1302561

12. Charbit A, Gavrilin MA, Zughaier SM, Liu Z-F, Ahmed W, Zheng K. Establishment of Chronic Infection: Brucella's Stealth Strategy. *Front Cell Infect Microbiol* (2016) **6**:303389–30. doi:10.3389/fcimb.2016.00030

13. Hielpos MS, Fernández AG, Falivene J, Campos PC, Vieira AT, Oliveira SC, Baldi PC. IL-1R and Inflammasomes Mediate Early Pulmonary Protective Mechanisms in Respiratory

Brucella Abortus Infection. *Front Cell Infect Microbiol* (2018) **8**:391. doi:10.3389/fcimb.2018.00391

14. Allard B, Panariti A, Martin JG, Martin JG. Alveolar Macrophages in the Resolution of Inflammation , Tissue Repair , and Tolerance to Infection. *Front Immunol* (2018) **9**:1–7. doi:10.3389/fimmu.2018.01777

15. Archambaud C, Salcedo SP, Lelouard H, Devilard E, De Bovis B, Van Rooijen N, Gorvel JP, Malissen B. Contrasting roles of macrophages and dendritic cells in controlling initial pulmonary Brucella infection. *Eur J Immunol* (2010) **40**:3458–3471.

16. Enhancer TM, Lavin Y, Winter D, Blecher-gonen R, David E, Keren-shaul H, Merad M. Tissue-resident macrophage enhancer landscapes are shaped by the local microenvironment. *Cell* (2014) **159**:1312–1326. doi:10.1016/j.cell.2014.11.018

17. Ferrero MC, Hielpos MS, Carvalho NB, Barrionuevo P, Corsetti PP, Giambartolomei GH, Oliveira SC, Baldia PC. Key role of toll-like receptor 2 in the inflammatory response and major histocompatibility complex class ii downregulation in brucella abortus-infected alveolar macrophages. *Infect Immun* (2014) **82**:626–639.

18. Michelucci A, Cordes T, Ghel J, Pailot A, Reiling N, Goldmann O. Immune-responsive gene 1 protein links metabolism to immunity by catalyzing itaconic acid production. *Proc Natl Acad Sci U S A* (2013) **110**:7820–7825. doi:10.1073/pnas.1218599110

19. Flo TH, Smith KD, Sato S, Rodriguez DJ, Holmes MA, Strong RK, Akira S, Aderem A. Lipocalin 2 mediates an innate immune response to bacterial infection by sequestrating iron. *Nature* (2004) **432**:917–921. doi:10.1038/nature03021.Published

20. Naujoks J, Tabeling C, Dill BD, Hoffmann C, Brown S, Kunze M, Kempa S, Peter A, Mollenkopf H, Dorhoi A, et al. IFNs Modify the Proteome of Legionella - Containing Vacuoles and Restrict Infection Via IRG1-Derived Itaconic Acid. *PLOS Pathog* (2016) **12**:e1005408. doi:10.1371/journal.ppat.1005408

21. Melzer T, Duffy A, Weiss LM, Halonen SK. The Gamma Interferon (IFN-g)-Inducible GTP-Binding Protein IGTP Is Necessary for Toxoplasma Vacuolar Disruption and Induces Parasite Egression in IFN-g-Stimulated Astrocytes. *Infect Immun* (2008) **76**:4883–4894. doi:10.1128/IAI.01288-07

22. Kim B-H, Shenoy AR, Kumar P, Das R, Tiwari S, MackMicking JD. A family of IFN-γ-inducible 65-kD GTPases protects against bacterial infection. *Science (80-)* (2011) **332**:717–721.

23. Franco MMC, Marim F, Erika S, Assis NRG, Cerqueira DM, Harms J, Splitter G, Smith J, Kanneganti T, Queiroz NMGP De, et al. Brucella abortus Triggers a cGAS-Independent STING Pathway To Induce Host Protection That Involves Guanylate-Binding Proteins and Inflammasome Activation. *J Immunol* (2017) **200**:607-622. doi:10.4049/jimmunol.1700725

24. Wu R, Chen F, Wang N, Tang D, Kang R. ACOD1 in immunometabolism and disease. *Cell Mol Immunol* (2020) **17**:1–12. doi:10.1038/s41423-020-0489-5

25. Ren K, Lv Y, Zhuo Y, Chen C, Shi H, Guo L, Yang G, Hou Y, Tan X. Suppression of IRG-1 Reduces Inflammatory Cell Infiltration and Lung Injury in Respiratory Syncytial Virus

Infection by Reducing. *J Virol* (2016) **90**:7313–7322. doi:10.1128/JVI.00563-16.Editor

26. Nair S, Huynh JP, Lampropoulou V, Loginicheva E, Esaulova E, Gounder AP, Boon ACM, Schwarzkopf EA, Bradstreet TR, Edelson BT, et al. Irg1 expression in myeloid cells prevents immunopathology during M . tuberculosis infection. *J Exp Med* (2018) **2015**:1–10.

27. Mills EL, Ryan DG, Prag HA, Dikovskaya D, Menon D, Zaslona Z, Costa ASH, Higgins M, Hams E, Szpyt J, et al. Itaconate is an anti-inflammatory metabolite that activates Nrf2 via alkylation of KEAP1. *Nature* (2018) **556**:113–117. doi:10.1038/nature25986

28. Lampropoulou V, Sergushichev A, Bambouskova M, Diwan A, Diamond MS, Artyomov MN, Lampropoulou V, Sergushichev A, Bambouskova M, Nair S, et al. Itaconate Links Inhibition of Succinate Dehydrogenase with Macrophage Metabolic Remodeling and Regulation of Inflammation. *Cell Metab* (2016) **24**:1–9. doi:10.1016/j.cmet.2016.06.004

29. Lorenz MC, Fink GR. Life and Death in a Macrophage : Role of the Glyoxylate Cycle in Virulence. *Eukaryot Cell* (2002) **1**:657–662. doi:10.1128/EC.1.5.657

30. Plommet M. Minimal Requirements for Growth of Brucella suis and Other Brucella Species. *Zentralbl Bakteriol* (1991) **275**:436–450. doi:10.1016/S0934-8840(11)80165-9

31. Wang H, Sun D, Kuang R. Inhibition of Escherichia coli by dimethyl fumarate. *Int J Food Microbiol* (2001) **65**:125–130.

32. Chomel BB, Debess EE, Mangiamele DM, Reilly KF, Farver TB, Sun RK, Barrett LR. Changing Trends in the Epidemiology of Human Brucellosis in California from 1973 to 1992 : A Shift toward Foodborne Transmission. *J Infect Dis* (1992) **170**:1216–1223.

33. Kaufmann AF, Fox MD, Boyce JM, Anderson DC, Potter ME, Martone WJ, Patton CM. Airborne spread of brucellosis. *Ann N Y Acad Sci* (1980) **353**:105–114.

34. Hanot Mambres D, Machelart A, Potemberg G, De Trez C, Ryffel B, Letesson J-J, Muraille E. Identification of Immune Effectors Essential to the Control of Primary and Secondary Intranasal Infection with Brucella melitensis in Mice. *J Immunol* (2016) **196**:3780–3793. doi:10.4049/jimmunol.1502265

35. Ben-tekaya H, Gorvel J, Dehio C. Bartonella and Brucella—Weapons and Strategies for Stealth Attack. *Cold Spring Harb Perspect Med* (2013) **3**:a010231.

36. Copeland NG, Brien WEO. Cloning and analysis of gene regulation of a novel LPS-inducible cDNA. *Immunogenetics* (1995) **41**:263–270.

37. Zúñiga-Ripa A, Barbier T, Conde-Álvarez R, Martínez-Gómez E, Palacios-Chaves L, Gil-Ramírez Y, Grilló MJ, Letesson J-J, Iriarte M, Moriyón I. Brucella abortus depends on pyruvate phosphate dikinase and malic enzyme but not on Fbp and GlpX fructose-1,6-bisphosphatases for full virulence in laboratory models. *J Bacteriol* (2014) **196**:3045–57. doi:10.1128/JB.01663-14

38. Copin R, Vitry M-A, Hanot Mambres D, Machelart A, De Trez C, Vanderwinden J-M, Magez S, Akira S, Ryffel B, Carlier Y, et al. In situ microscopy analysis reveals local innate immune response developed around Brucella infected cells in resistant and susceptible mice. *PLoS Pathog* (2012) **8**:e1002575. doi:10.1371/journal.ppat.1002575

39. Suárez-esquivel M, Ruiz-villalobos N, Castillo-zeledón A, Jiménez-rojas C, Ii RMR, Comerci DJ, Barquero-calvo E, Chacón-díaz C, Caswell CC, Baker KS, et al. Brucella abortus Strain 2308 Wisconsin Genome : Importance of the Definition of Reference Strains. *Front Microbiol* (2016) **7**:1–6. doi:10.3389/fmicb.2016.01557

40. Simon R, Priefer U, Pühler A. A Broad Host Range Mobilization System for In Vivo Genetic Engineering: Transposon Mutagenesis in Gram Negative Bacteria. *Nat Biotechnol* (1983) **1**:784–791.

Supplementary figures

	A	B	C
1	**Gene name**	**Log2FC**	**FDR**
2	Cebpd	1,144995623	0,00015015
3	Klf2	1,001194194	0,00012002
4	Lcn2	0,984581891	0,00015015
5	Timp1	0,898657729	0,19507953
6	Cxcl1	0,87452506	0,25523031
7	Irx1	0,845783037	0,00962058
8	Acod1	0,837543548	0,25734869
9	Gsta2	0,833623767	0,25523031
10	Cxcl10	0,83280235	0,22586363
11	Snord14e	0,823004261	0,26884027
12	Gm3776	0,818837429	0,25734869
13	Cxcl2	0,781389937	0,28217813
14	Lrg1	0,778192545	0,19507953
15	Gpx2	0,736750491	0,25523031
16	Cbr3	0,733794176	0,25523031
17	Sertad1	0,732039234	0,22398369
18	Saa3	0,729058594	0,25523031
19	Ces1g	0,72721975	0,25523031
20	Cxcl5	0,713101926	0,28481361
21	Cxcl3	0,707234525	0,28481361
22	Il1b	0,705591134	0,22586363
23	Tnfrsf25	0,701638096	0,25523031
24	Areg	0,698372527	0,28399988
25	Nr4a1	0,698113522	0,17399122
26	Esd	0,695820765	0,19507953
27	Hlx	0,692572476	0,11994722
28	Dusp1	0,691631188	0,17399122

Suppl Figure 1. RNAseq data of whole lungs from infected versus naïve mice. Wild type C57BL/6 mice intranasally infected with 10^7 CFU of wild type *B. melitensis* (n=3), or receiving the same volume of PBS (naïve group) (n=3), have been sacrificed at 24 h post infection. Lungs were harvested and RNA extracted. RNAseq was performed with Illumina system and Deseq2 analyze as described in material and methods. Data represent the list of genes associated to their fold change (FC) (Log_2) and adjusted P value - log10 (false discovery rate, FDR). Data are representative of two independent experiments.

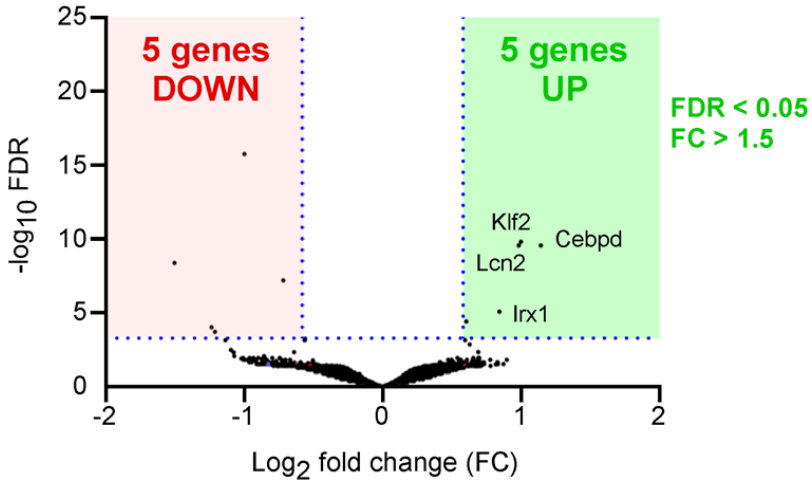

Supplementary Figure 2

Suppl. Figure 2. Few genes are upregulated following intranasal *B. melitensis* infection in whole lungs. Wild type C57BL/6 mice were intranasally infected with 10^7 CFU of wild type *B. melitensis* 16M. Lungs were harvested at 24 hours post infection and the RNA was extracted and sequenced. Naïve mice receiving intranasally PBS were used as control. Volcano plot of RNA-seq data from naïve versus infected lung shows the adjusted P-value (false discovery rate, FDR -log10) versus fold change (FC) (log2). The four genes with an FDR < 0.05 and FC > 1.5 are shown in the R1 green square. RNAseq was performed at least two times and each sample was generated from a pool of at least 3 mice.

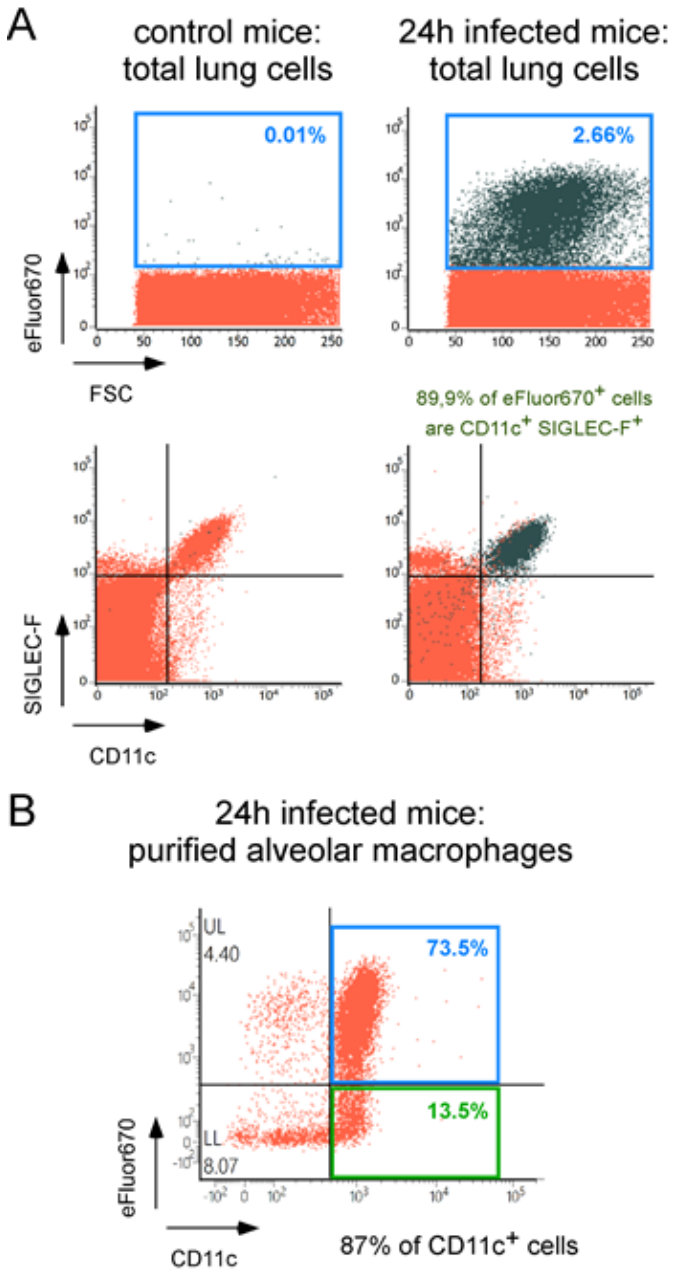

Supplementary Figure 3

Suppl. Figure 3. Alveolar macrophages are the main *B. melitensis* infected cells in lung. Wild type C57BL/6 wt mice (n = 5) received intranasally PBS (control mice) or $5x10^6$ CFU of mCherry-expressing *B. melitensis* labelled with eFluor^{670}. Mice were sacrificed at 24 hours post infection. The lungs were harvested, and the cells were isolated and then analyzed by flow cytometry for the FSC and the expression of eFluor^{670}, mCherry, CD11c, and Siglec-F as indicated. (**A)** Gating strategy. Numbers indicate the percentage of eFluor^{670+} cells among total cells (high panels) and the percentage of eFluor670^{+} cells that are also positive for CD11c and Siglec-F markers (low panels) in naïve mice (left panels) or infected mice (right panels). **B.** Same strategies of gating, but with previously purified alveolar macrophages. These results are representative of three independent experiments.

	A	B	C
1	**GeneName**	**Log2FC**	**FDR**
2	Rai14	2,356159409	8,35E-22
3	Csf1	2,155582586	5,44E-19
4	Slamf8	2,143705453	5,19E-18
5	Serpina3f	2,089392006	4,79E-17
6	Adcy6	1,830504917	1,79E-16
7	Nr4a3	1,807466684	1,85E-22
8	Fscn1	1,80420745	5,25E-17
9	Cd40	1,802952654	1,67E-12
10	Cacnb3	1,799314791	2,11E-14
11	Socs1	1,683404534	7,73E-11
12	Il7r	1,683286885	4,33E-13
13	Slamf7	1,675799962	2,08E-11
14	Oasl2	1,675239233	1,65E-11
15	Slc4a8	1,661655955	9,41E-11
16	Papss2	1,659252526	1,63E-10
17	Gbp5	1,638121961	1,60E-11
18	Mx1	1,613739701	3,38E-10
19	Ccl17	1,577987863	1,09E-09
20	Sema7a	1,573353485	5,35E-10
21	Serpina3g	1,566274167	2,19E-10
22	Mir6381	1,53910938	1,47E-09
23	Pla2g7	1,520895661	4,83E-10
24	Ifi47	1,520120936	6,72E-10
25	Ccl22	1,519702251	5,21E-23
26	Il4i1	1,503665652	2,60E-23
27	Arap3	1,482397618	7,46E-09
28	Slfn5	1,481472027	3,11E-14

Suppl Figure 4. RNAseq data of alveolar macrophages from infected versus naïve mice. Wild type C57BL/6 mice intranasally infected with 10^7 CFU of wild type *B. melitensis* (n=3), or receiving the same volume of PBS (naïve group) (n=3), were sacrificed at 24 h post infection. Lungs were harvested, alveolar macrophages purified and RNA extracted. RNAseq was performed with Illumina system and Deseq2 analysis as described in material and methods. Data represent the list of genes associated to their fold change (FC) (Log_2) and adjusted P value - log10 (false discovery rate, FDR). Data are representative of two independent experiments.

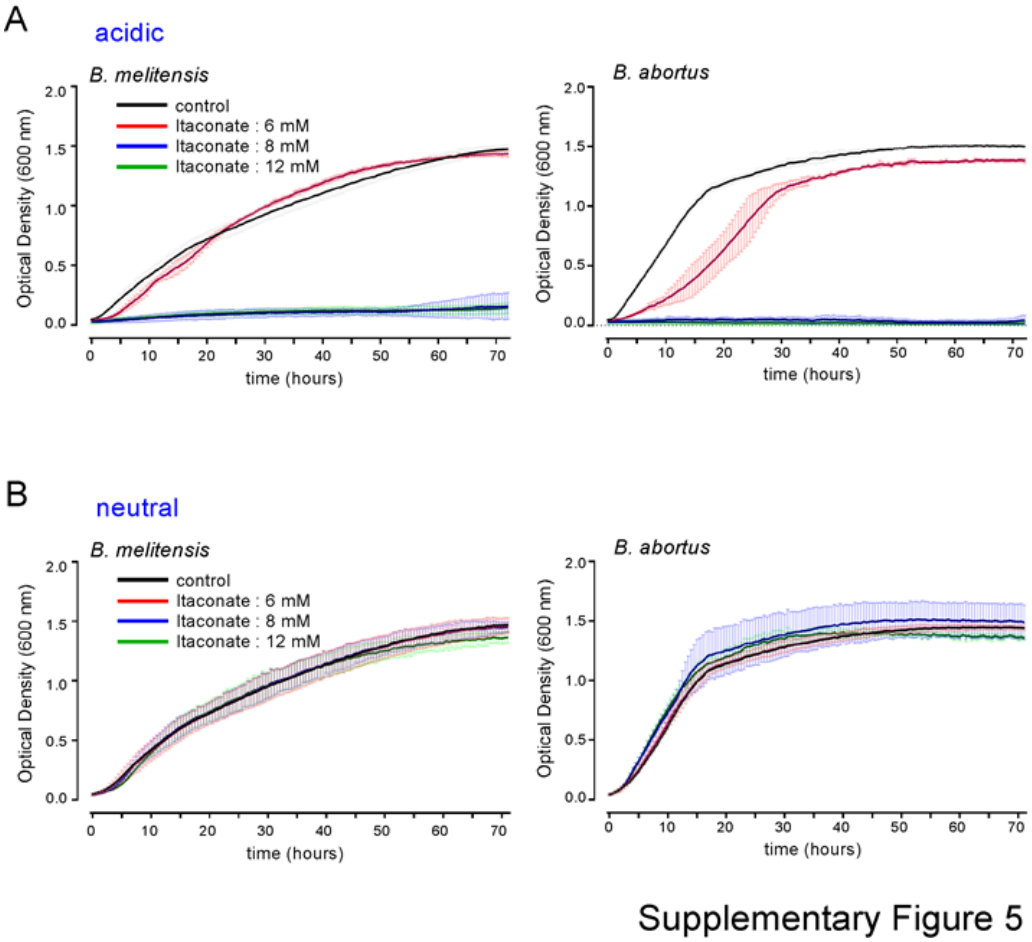

Suppl. figure 5. At neutral pH, itaconate does not inhibit *Brucella* growth *in vitro*. Comparison of the impact of different concentrations of itaconate on the growth of wild type *B. melitensis* (left panel) or *B. abortus* (right panel) in rich medium (2YT). **A** acidic itaconate (pH ≃ 3.6). **B**. neutralized itaconate solution (pH = 7.0). The bacteria grown during 72h at 37 °C, the OD was measured every 30 min in a Bioscreen system. The standard deviation was obtained from three independent experiments.

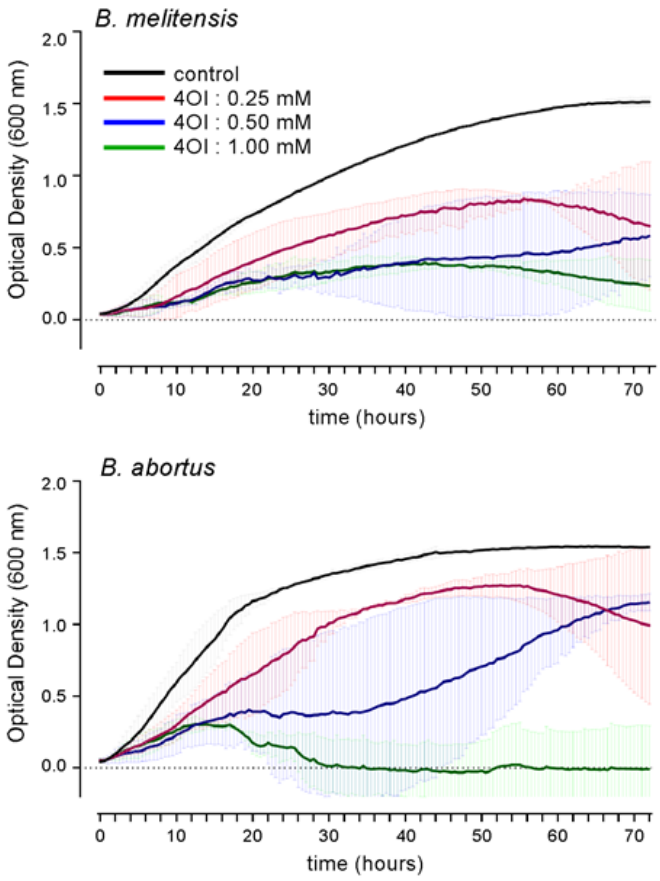

Supplementary Figure 6

Suppl. figure 6. 4-octyl-itaconate inhibit *Brucella* growth *in vitro*. Comparison of the impact of different concentrations of 4-octyl-itaconate on the growth of wild type *B. melitensis* or *B. abortus* in rich medium (2YT). The bacteria grown during 72h at 37 °C, the OD was measured every 30 min in a Bioscreen system. The standard deviation was obtained from three independent experiments.

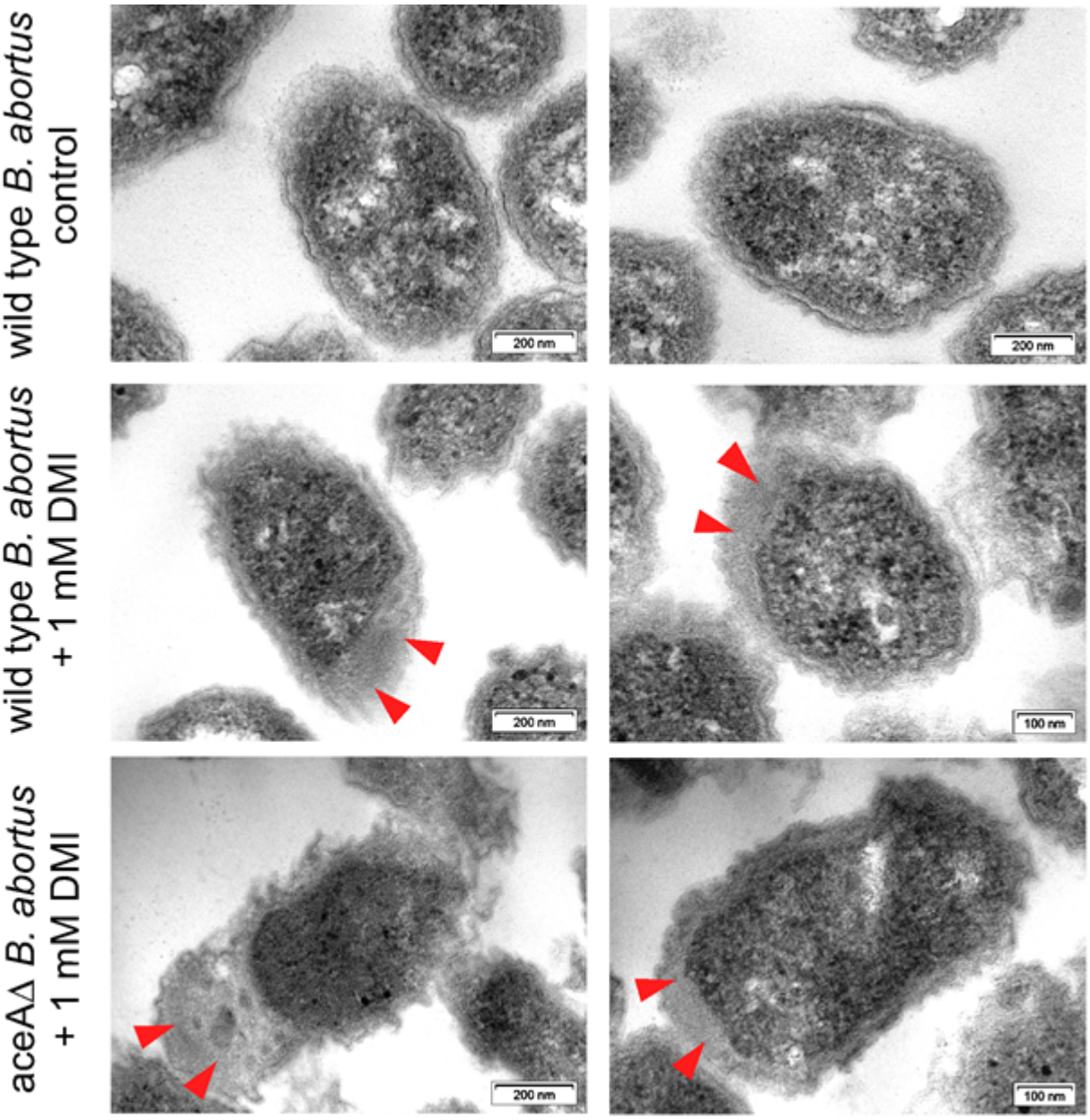

Supplementary Figure 7

Suppl. figure 7. Dimethyl-itaconate impacts *wild type and ΔaceA B. abortus* morphology *in vitro*. Transmission electronic microscopy images were performed as described in materials and methods section on wild type and *ΔaceA B. abortus,* cultured in poor medium (Plommet-Erythritol) overnight supplemented or not with 1 mM of dimethyl-itaconate. Red arrows indicate membrane alterations.

4 Discussion and perspectives

The immune response in mice after an intranasal *B. melitensis* infection has been previously characterized in our group (Hanot Mambres, Machelart et al. 2016). We showed that CD8 αβ T cells, γδ T cells and IL-17RA are indispensable in the control of primary infection in lungs at 5 days post infection and that IFN-γ secreting by CD4 αβ T cells is indispensable at 12, 28 and 50 days post infection (Hanot Mambres, Machelart et al. 2016). However, the earlier immune response (before 5 days) has never been characterized. After i.n. infection, alveolar macrophages (AMs) are the main infected cells (> 90 %) the first 48 hours p.i (Potemberg, Demars, in submission). We used RNA-seq, a without a priori high throughput technique, to identify upregulated genes in infected AMs. After a first selection based on the false discovery rate (FDR) and fold change (FC) (FDR < 0.05, and FC > 1.5), few (466) genes appear significantly upregulated at 24 hours p.i., probably due to the *Brucella* stealth. We used meta-analysis resource, Metascape, available freely online, to order these genes in different pathways. The "response to IFN-β" is the pathway the most represented.

4.1 The type I IFN response in bacterial infections

Even if IFN-β responses are often associated to viral responses and to a tissue damage control (Lee and Ashkar 2018), there are more and more studies about the role of type I IFN in bacterial diseases. The effect of type I IFN signaling upon bacterial infection can be protective as well as detrimental for the host (Perry, Chen et al. 2005, Boxx and Cheng 2016, Kovarik, Castiglia et al. 2016). In one hand, type I IFN induces a host susceptibility by promoting apoptosis of immune cells such as macrophages or lymphocytes, by inhibiting the expression of IL-17A by γδ T cells, or by leading to the inhibition of neutrophils recruitment. For examples, it has been demonstrated that IL-1 and TH1 responses are inhibited after lungs infection with *M. tuberculosis* in mice, leading to an immunosuppression (Mayer-Barber, Andrade et al. 2011). Another example is the inhibition of IL-17A in an i.n. infection model with *Francisella tularensis* (Henry, Brotcke et al. 2007). The deleterious impact of type I IFN can also coming from an exacerbated immune response, defined by an over production of inflammatory cytokines and immune cells recruitment, as demonstrated after an i.n. infection with *Staphylococcus aureus* (Parker, Planet et al. 2014). In the other hand, type I IFN can protect against bacterial infections by promoting hosts defenses by inducing interferon-stimulated

genes such as *Acod1* in *Legionella pneumophilia* model (Naujoks, Tabeling et al. 2016), but also by inducing CXCL10 in *Helicobacter pylori* model (Watanabe, Asano et al. 2010) for examples. In those models, IFN-β-deficient mice are more susceptible to the infection than wild type mice. Those contrasted responses triggered by IFN-β are not yet understood but suggest an incontestable role of type I IFN in some bacterial infections. Among the genes from "response to IFN-β" in our *Brucella* model, aconitate decarboxylase 1 (*Acod1*) (also called Immune responsive gene 1, *irg*1) is one of the most upregulated gene in AMs at 24 hours post intranasal infection with 10^7 bacteria, with a fold change of 1.92 in comparison to AMs from uninfected mice. We decided to work with this gene as *Acod1*-deficient C57BL/6 mice are available, and as more and more publications about the role of *Acod1* in bacterial infections emerged since 2016 (Lampropoulou, Sergushichev et al. 2016, Naujoks, Tabeling et al. 2016, Mills, Ryan et al. 2018, Nair, Huynh et al. 2018). We identified this gene only in AM at 24 hours p.i., not in total lung cells. As *Acod1* is a gene mainly expressed in mitochondria of myeloid cells, it is not surprising to do not detect it in RNA-seq performed on entire lungs. Of course, even if we detected *Acod1* by RNAseq, and that we confirmed the expression of *Acod1* mRNA by qRT-PCR, we did not check the production of ACOD1 at the protein level. However, as the inhibition of bacterial growth seems dependent on ICL, we could speculate that ACOD1 is produced, at least at a low level.

4.2 *Acod1* and inflammation

One of the well described role of *Acod1* gene (and of its product itaconate) is an anti-inflammatory role by decreasing pro-inflammatory cytokines production such as IL-1β or IL-6. In *in vitro* and *in vivo* infectious models with *Legionella* or *Mycobacterium*, it has been shown that the absence of *Acod1* leads to a loss of the infection control (Michelucci, Cordes et al. 2013, Nair, Huynh et al. 2018). In our model, we showed that the absence of *Acod1* in *Brucella* infected mice leads to an increase in CFU (of 0.5 - 1 log) compared to wt mice, but this increase was not due to a lack of inflammation. Indeed, we did not observe a different recruitment of neutrophils, a difference of pro-inflammatory cytokines expression, or a difference in total recruited cells in lungs of *Acod1*-KO mice.

One thing which seems quite obvious in this study is the difference of impact of the *Acod1* deficiency with *B. melitensis* or *B. abortus* in lungs after i.n. infection. Indeed, *Acod1*-KO mice

showed higher susceptibility to *B. abortus* infection than *Acod1*-KO mice infected with *B. melitensis*. However, *in vitro*, itaconate, the product of ACOD1 action, inhibits the growth of both bacteria species in a similar manner at 4 mM and 6 mM in rich medium, suggesting that both species are equally sensitive to itaconate. Hence, the difference observed *in vivo* could be due to the fact that *B. abortus* is present at higher levels and persists longer in lungs of infected wt mice, probably due to a more inflammatory character than *B. melitensis*. In the literature, high levels of *Acod1* expression are associated to highly pro-inflammatory bacteria such as *Mycobacterium tuberculosis, Legionella pneumonae* or *Acinetobacter baumannii*, suggesting that the trigger of inflammation is necessary for the expression of *Acod1* (Naujoks, Tabeling et al. 2016, Nair, Huynh et al. 2018). A possible hypothesis could be that once highly inflammatory bacteria are detected by the immune system, the induced inflammation allows the induction of *Acod1* expression allowing itaconate to play its anti-inflammatory role. Indeed, a too high inflammatory environment can be deleterious for the host. However, in the case of bacteria more stealth but enough inflammatory to induce *Acod1* expression, itaconate could play its anti-bacterial role to try to eliminate bacteria. It would be the case for *Brucella*, known for its stealth (see introduction) and being a model where no inflammation impacts have been observed (no difference in cytokines expression, in recruited cells, etc.). Even if it is also realistic to imagine that highly inflammatory bacteria actively induce *Acod1* gene to take advantage of the anti-inflammatory role of itaconate, this second hypothesis would not explain the expression of *Acod1* in infections with less inflammatory bacteria. In addition, as the *Acod1*-KO mice infected with *Mycobacterium tuberculosis* died at 21 d. p.i. of an important neutrophilia, the first hypothesis seems the most probable. This could explain why the impact of *Acod1* on the control of *Brucella* is weaker than another more inflammatory bacteria. The fact that DMI completely inhibits the growth of *B. melitensis* and *B. abortus in vitro*, where inflammation is absent, also suggests that the inflammatory environment seems important for the expression of *Acod1* and the itaconate role. In order to test this hypothesis, it would be interesting to infect wt and *Acod1*-KO mice with a more virulent mutant of *Brucella*. It is the case for example of the Δ*fliC*, a mutant for flagellin which presents CFU 2 logs higher than wt strain at 12 and 21 days post i.p. infection in spleen (Terwagne, Ferooz et al. 2013). Wild type *B. microti* could also be tested as this *Brucella* species is hyper-virulent in mice (Jiménez de Bagüés, Ouahrani-Bettache et al. 2010). Another experiment that we could test is to decrease the infectious dose (to 10^5 bacteria for example) and infect intranasally wt and *Acod1*-deficient mice in order to evaluate the bacterial level in kinetic in lungs. Indeed, it would be interesting

to test whether the immune system is not "saturated" by 10^7 bacteria as infectious dose. In addition, whether the hypothesis that inflammation is required to express *Acod1* is correct, this lower dose should decrease the difference of CFU between both mice groups.

Finally, lungs have been mainly studied as we did not observe expression of *Acod1* in spleen and no difference of CFU between wt and *Acod1*-KO mice after an intranasal infection. What we should try is to infect wt and *Acod1*-KO mice by intraperitoneal injection to better confirm the absence of *Acod1* expression in spleen. It would be also interesting to harvest the lungs after an i.p. and to study the infected cells in this organ to check if the route of infection impacts somehow the expression of *Acod1* in lungs.

4.3 Itaconate and its alkylation power

Itaconate is able to alkylate cystein residues of protein thanks to its electrophilic α,β-unsaturated carboxylic acid. The reaction is a Michael addition, forming a 2,3-dicarboxypropyl adduct between itaconate and the targeted protein. For example, itaconate alkylates KEAP1 protein on cysteine residues 151, 257, 288, 273 and 297 (Mills, Ryan et al. 2018). As shown in supplementary data, itaconate is able to modify the morphology of wild type and Δ*aceA* (deficient for ICL) *Brucella* in a same way, suggesting a non-specific and general action of itaconate on these bacteria. It is not really surprising as cysteine residues are abundant at the protein level. However, we showed that itaconate inhibits the growth of *Brucella* in an ICL-dependent mechanism, *in vitro* (dose-dependent) but also *in vivo* as the level of CFU between *Acod1*-KO mice infected with *B. abortus* wt or *B. abortus* Δ*aceA* are the same. To go further in the study of the possible link between itaconate and ICL, it would be interesting to incubate itaconate with purified ICL, and to perform mass spectrometry in order to identify the presence of a modification on cysteine residues by itaconate, but also to mutate the cysteine residues of ICL to observe if the inhibition of the *Brucella* growth in these conditions is still present.

4.4 *aceA* gene, towards a new potential role?

As Δ*aceA B. abortus* grows almost as well as the wt strain in poor medium, suggesting this gene to be non-essential, it seems that the link between itaconate and ICL does not lead to the inhibition of ICL activity but rather lead to consequences ICL-dependent. Therefore, the known

impacts such as the glyoxylate shunt inhibition, or the propionyl-CoA detoxification linked to the ICL inhibition do not seem involved in our conditions. It could suggest another role of ICL, or the existence of a homologous gene. One thing that seems obvious is the potential link between *Acod1* expression induced by inflammation and the effect of itaconate on metabolism.

4.5 Role of *Acod1* and itaconate at the cellular level

We found *Acod1* as being one of the most interesting upregulated gene in AMs at 24 hours post intranasal infection with *B. melitensis*, but its expression was absent in whole lungs in the same conditions. Even if this could suggest an expression of *Acod1* mainly in those AMs, it would be interesting to compare the CFU level in infected "classical" *Acod1*-KO mice and *Acod1*-KO mice where the gene is KO only in myeloid cells (Nair, Huynh et al. 2018). It could be possible also to study the level of expression of *Acod1* overtime, *in vitro* in BMDM infected with *B. abortus* and to link this expression with the virulence of *Brucella* in those cells. To be closer of the *in vivo* model, we purified AMs as described in material and methods and we tried to culture these cells in plates (data not shown) and to infect them *in vitro*. Unfortunately, we did not succeed to infect AMs *in vitro* in our conditions. What we did not try is to purify AMs from already infected mice. However, the addition of physiological itaconate and DMI on infected RAW 264.7 macrophages *in vitro* shows an impact on the morphology of RAW macrophages (data not shown), leading to a complicated interpretation about the *Brucella* control by DMI *in vitro*.

4.6 ACOD1 and its localization

We know that itaconate, the product of ACOD1 action, is mainly produced in mitochondria of macrophages. A recent study (Naujoks, Tabeling et al. 2016) showed that mitochondria and *Legionella*-containing vacuoles were in close associations, hypothesizing that either *Legionella* recruits mitochondria to take advantage of its nutritional and energetic resources, or mitochondria are recruited via a TLR-depending mechanism to phagosomes to bring the defense strategies closer to bacteria (Naujoks, Tabeling et al. 2016). Even if we observed sometimes close associations between mitochondria and BCV in our transmission electronic microscopy images, the number of these observations was extremely weak and probably random. However, we could quantify this *in vivo* by comparing the number of associations in samples from infected wt mice to infected *Acod1*-KO mice. Always in the idea to localize

ACOD1 in cells, we could also use ACOD1-antibody (in addition to other markers) to label histology slides of infected lungs.

The major difference between *in vivo* and *in vitro* conditions in terms of localization is the presence of *Brucella* in a phagosome in *in vivo* condition. It is hypothesized that physiological itaconate does not impact *Brucella in vitro* as it does not cross the bacterial membrane. But *in vivo*, *Brucella* could be already a bit weakened before to be in contact with itaconate, giving to the endogenous itaconate the possibility to enter into phagocytosed bacteria. To confirm this hypothesis, it would be interesting to weakly permeabilized bacteria before addition of itaconate for kinetic *in vitro* studies. Another idea would be to use a mutant of *Brucella* with a defect in its cell wall, such as Δ*per-Brucella* (a rough strain), to see if this strain is more susceptible to itaconate. If the growth of this mutant is attenuated by itaconate, that would suggest that the non-inhibition of *Brucella* by itaconate in neutral condition is due to an inability of itaconate to penetrate inside *Brucella*.

It is also possible that transporters for itaconate are only induced in *in vivo* conditions, allowing itaconate to penetrate *Brucella*. We could imagine that those transporters are not specific for itaconate, but that the molecule could be able to use them in certain conditions. These transporters could be completely absent or inactive in *in vitro* conditions, leading to a non-penetration of physiological itaconate *in vitro.* It would be interesting to incubate *Brucella in vitro* with other acidic molecules such as citric acid or acetic acid in order to study if the inhibition of *Brucella* growth in acidic condition is due to acidity it-self or to itaconate molecule.

4.7 Dimethyl-itaconate, a good substitute?

In our study, we used *in vitro* a modified permeable form of itaconate, the dimethyl-itaconate (DMI). We observed that DMI inhibits, in a dose-dependent manner, the growth of *B. abortus* in an isocitrate lyase-dependent way. Before to test this experiment, we tried to use the physiological itaconate. The solution of this suspend molecule has an acid pH, and completely inhibits the growth of *Brucella* (*B. melitensis* and *B. abortus*) at 10 mM, independently of isocitrate lyase, as *B. abortus* Δa*ceA* was inhibited in the same way with the same concentrations. To be sure that itaconate effect was not due to its acidity, we tried the same experiments but with neutralization of itaconate pH. In this case, no inhibition, in any conditions, was observed, suggesting that the impact previously observed was due to acidity

itself. In literature, when physiological itaconate is used and is shown to be a good inhibitor of bacterial growth, the neutralization of pH is never mentioned, letting the doubt about the real impact of itaconate molecule itself, *in vitro*. However, using the modified DMI, we observed an inhibition of *B. abortus* growth, depending on isocitrate lyase, in neutral pH conditions. To be sure that the addition of methyl groups does not impact the action of itaconate, we used the dimethyl-fumarate as control molecule, and we confirmed that the methyl groups themselves do not impact specifically ICL. In addition, the fact that we found that ICL is also the target *in vivo* suggest that DMI is able to mimic what happen *in vivo*. This was not the case using physiological itaconate, in neutral or acid conditions, probably because the neutral physiological itaconate was not able to cross the bacterial membrane, or the acid itaconate had a non-specific impact on bacteria, respectively.

IV. General conclusion

Our work highlights different elements that are very important to take into account when we are working on infection process. Of course, the real study subject should be the natural host, taken in its environmental conditions, with its immunologic past context, and using the natural routes of infection or vaccination. However, this is almost impossible to use those natural hosts for numerous practical and economic reasons. This is why a reductionist approach using animal and *in vitro* models has been developed and used for decade in order to study biological questions. But the choice of this experimental model is very important and our work demonstrates how it can affect the results. Indeed, in a context of selection of potential vaccine candidates or host-pathogen relationship study in a mouse model, we highlight the importance of the choice of this infection route. As the experimental model is already different from the natural host, we thought that the route of infection, at least, should the same than the natural route of vaccination. We hypothesized that working with different routes of infection could bias the results.

We used Brucella, an intracellular bacterium causing brucellosis mainly in mammals such as bovine and ovine but also in human, to test this hypothesis in three different mouse models of infection: intraperitoneal, intranasal and intradermic infection routes. We observed from our study that the dissemination of bacteria, the nature of the infected cells or of the infected organs as well as the nature of protective immune response are different depending on the route of infection, suggesting a different control of bacteria depending on the primary site of infection and the passage through the blood, mainly. We concluded that it is important to use a route of infection as close as the natural route of vaccination to decrease the failure rate when a vaccine candidate experimented in mouse is finally tested in the natural host.

From this study, we also concluded that the mucosal model, with intranasal infection, is one of the most physiological model that we studied. But this route of infection leads to more questions about the early effector mechanisms in the local site of infection. To answer this question, we used a RNA sequencing approach and identified *Acod1* gene which is known to be expressed exclusively in myeloid cells such as macrophages. In lungs of intranasally infected mice, *Acod1* plays a role in the early control of *Brucella* multiplication in alveolar macrophages. However,

even if various types of macrophages, such as red pulp macrophages and marginal zone macrophages, are also infected in the spleens, we did not detect the expression of *Acod1* or an impact of *Acod1* deficiency in this organ, suggesting a specific role of *Acod1* in the control of *Brucella* in mucosal environment only. This also suggests that some effectors could be discovered using a specific route of infection but not another one, confirming the importance of the choice of the experimental model.

In conclusion, the use of an appropriate route of infection is a first prerequisite towards a better discovery of candidate vaccines or effectors. However, independently of the choice of the more appropriate experimental model, another major and unsolved problem to study biological systems is the redundant and the complementary genes/proteins that frequently hide the impact of inactivating a single target. This could explain the weak impact that we observed when we compared the course of *Brucella* infection in wild type and *Acod1*-deficient mice. Our results demonstrate that ACOD1 (via itaconate) is one of the effectors controlling *Brucella* infection in lungs, but ACOD1 certainly acts with other effectors such as Guanylate Binding Proteins (GBP), Nitric Oxide (NO), etc. In addition, *Brucella* is a stealthy bacterium. Consequently, it is still more complicated to find new potential effectors in this infectious model because, by using a physiological route of infection such as i.n., almost none change is detected in terms of cells recruitment, inflammation, cytokines production, etc.

At this point, we must conclude that years of research will be still necessary to completely understand *Brucella* infection and eradicate brucellosis. However, this work constitutes a first step in understanding of the complex world of host-pathogen relationship, from which some conclusions are transposable to other infection models.

V. Personal bibliography

1 As first or second author: published articles

Jansen W, **Demars A**, (…), Al Dahouk S. Shedding of *Brucella melitensis* happens through milk macrophages in the murine model of infection, 2020, *Sci Rep.*

Demars A, Lison A, (…), Muraille E. Route of infection strongly impacts the host-pathogen relationship, 2019, *Front. Immunol*.

Machelart A, Khadrawi A, **Demars A,** (…), Muraille E. Chronic *Brucella* infection induces selective and persistent IFN-γ-dependent alterations of marginal zone macrophages in the spleen, 2017, *Infection and Immunity.*

2 As first author: in preparation

Potemberg G, **Demars A,** (…), Muraille E. Comprehensive essentiality analysis in mouse infection model of the *Brucella melitensis* genome via saturating transposon mutagenesis.

Demars A, (…), Muraille E. Characterization of a novel potential effector controlling the multiplication of *Brucella* after intranasal infection in mice.

3 As associated author : published articles

Machelart A, Potemberg G, Van Maele L, **Demars A**, (…), Muraille E. , Allergic Asthma Favors *Brucella* Growth in the Lungs of Infected Mice., 2018, *Front Immunol.*

Machelart A, Van Vyve M, Potemberg G, **Demars A,** (…), Muraille E. Trypanosoma Infection Favors *Brucella* Elimination via IL-12/IFNγ-Dependent Pathways, 2017, *Front. Immunol.*

Macharlart A. *et al.*. Intrinsic antibacterial activity of nanoparticles made of β-cyclodextrins potentiates their effects as drug nanocarriers against tuberculosis, 2019, *ACS nano.*

VI. Supplementary material and methods

Animals

Ethic statements

All the procedures and the mice handling complied with current European legislation (directive 86/609/EEC) and the corresponding Belgian law: Royal Decree on the protection of experimental animals of April 6, 2010. The Animal Welfare Committee of the Université de Namur (UNamur, Belgium) has reviewed and approved the protocols (Permit Numbers: 13-195 for the intradermal infection, 05-058 for the intraperitoneal infection and 18-309 for the intranasal infection and *Acod1*-KO mice).

Mouse strains

Wild-type C56BL/6 mice were acquired from Harlan (Biester, UK). *TCR-* $\delta^{-/-}$, *CD3*$\varepsilon^{-/-}$, *TCR-*$\beta^{-/-}$, *MuMT*$^{-/-}$, *CCR2*$^{-/-}$, and *CCR7*$^{-/-}$ C57BL/6 were all purchased from The Jackson Laboratory (Bar Harbor, ME). *IFN-*$\gamma R^{-/-}$ and *IL-12p35*$^{-/-}$ C57BL/6 mice were acquired from Dr. B. Ryffel (University of Orleans, France). *IL17RA*$^{-/-}$ C57BL/6 mice were acquired from Dr. K. Huygen (Belgian Scientific Institute for Public Health, Brussels, Belgium). *TNFR1*$^{-/-}$ C57BL/6 were acquired from Dr. C. De Trez (Université Libre de Bruxelles, Belgique). *TAP1*$^{-/-}$ C57BL/6 mice and *MHCII*$^{-/-}$ C57BL/6 mice were acquired from Jörg Reimann (University of Ulm, Germany). *Acod1*$^{-/-}$ C57BL/6 mice were acquired from Dr. E. Hoffmann (Institute Pasteur of Lille, France).

All the mice were bred in the animal facility of the Gosselies campus (Université Libre de Bruxelles, Belgique).

Mouse infection

Preparation of the infectious dose

- Cultivate the strains 5 days before the infection in 2 YT rich medium agar plates
- Prepare an overnight (ON) liquid culture the day before in 10 mL of 2 YT rich medium (in a Falcon 50 mL) to obtain an optical density ($OD_{600\ nm}$) between 0.7-0.9 (end of the exponential phase)

- The morning of the infection, wash the bacteria: centrifuge the Falcon at 3,500 g during 10 min at 20 °C, through the supernatant away, and add 10 mL of PBS
- Repeat this last step once to wash bacteria again
- Measure the OD to calculate and prepare the infectious dose ($3x10^9$ bacteria / mL at OD = 1)

$$\text{Dilution factor} = \frac{(OD * 3.10\text{^}9\ bacteria\ /\ mL)}{Infectious\ dose/m\ L}$$

$$\text{Initial volume} = \frac{final\ volume}{dilution\ factor}$$

- Do serial dilutions as control of the infectious dose, and then plate them to obtain a countable number of CFU

Naïve animals were injected with the same volume (see the different infection below) of PBS.

Intraperitoneal infection

For i.p. injection, 500 µL of infectious dose was administrated by mouse. $2x10^4$ bacteria / mouse (10^5 bacteria / mL) were prepared in RPMI.

Intradermal infection

The infectious dose was administrated in the footpad of mice, after a brief anesthesia with Isoflurane. Around 20 µL of infectious dose was administrated in the footpad. So, $2x10^6$ bacteria / mL was prepared in order to obtain around $2x10^4$ bacteria / mouse.

Intranasal infection

Even if the type of anesthesia is still debated, it has been published that lungs are more efficiently infected by bacteria (Miller, Stabenow et al. 2012) or other products (Southam, Dolovich et al. 2002) when instillation is performed under anesthesia. Therefore, animals were anesthetized by intraperitoneal injection of Ketamine (36 mg/ kg) / Xylazine (9 mg/ kg) in PBS before the infection and were then infected with 30 µL of infectious dose ($4x10^4$ bacteria / mL, $3.33x10^8$ bacteria / mL or $3.33x10^9$ bacteria / mL).

Bacterial strains and media

Growth conditions

The different strains of *Brucella* were grown in 2 Yeast-Extract rich medium (composed of Luria-Bertani (LB) mix (20 g/ L), yeast extract (5 g / L), peptone (6 g / L) and agar (13 g / L) when it was necessary) or in Plommet Erythritol minimal medium (composed of K_2HPO_4 (7 g / L), KH_2PO_4 (3 g / L), NaCl (5 g / L), $Na_2S_2O_3$ (0.1 g / L), Biotine (0.0001 mg / L), Nicotinate (0.2mg / L), Thiamine (0.2 mg / L), Pantothenate (0.04 mg / L), $(NH_4)_2SO_4$ (0.5 g / L), Erythritol (2 g / L), Tyrosine (0.25 g / L), $MgSO_4$ (10 mg / L), $MnSO_4$ (0.1 mg / L), $FeSO_4$ (0.1 mg / L).

Nalidixic acid (Nal) (25 ug / mL) was added in the agar medium when *Brucella* WT (naturally resistant to Nal) was used, and Kanamycin (Kan) (10 ug / mL) was added for all the other modified strains of *Brucella*.

Escherichia coli was grown in LB rich medium, composed of peptone (10 g / L), yeast extract (5 g / L), NaCl (5 g / L) (and agar 15 g / L when necessary). Kanamycin was added in the agar medium as the plasmids used are Kan^R.

Bacterial strains

Different strains of bacteria were used in the experiments:

- *Brucella melitensis* 16M WT (Nal^R)
- *Brucella melitensis* 16M mCherry was performed to constitutively expressed the mCherry gene under a strong translocase (SecE) promotor (Nal^R, Kan^R). The construction protocol was published in (Copin, Vitry et al. 2012)
- *Brucella abortus* 2308 mCherry (Nal^R, Kan^R) was performed following the same protocol that was described in Copin et al., 2012 (Barbier, Machelart et al. 2017)
- *Brucella abortus* 2308 Δ*aceA*, for which the construction was described in (Zúñiga-Ripa 2014)
- *Brucella abortus* 2308 Δ*aceA* was complemented with the pMR10 plasmid. Briefly, the *aceA* gene and its promoter was amplified with the Q5 High-Fidelity DNA polymerase (New England Biolabs). PCR products were purified (Macherey-Nagel Clean-up kit) and cloned into the EcoRV site of the pGemT in *E. coli* DH10B. This plasmid allows

the white/blue screening in *E. coli* DH10B strain (thermofisher / Invitrogen). White clones were PCR screened and sequenced with the universal M13 primers. *aceA* gene was then subcloned into the pMR10 plasmid (a kind gift from C.D. Mohr and R.C. Roberts, Stanford University) with the restriction enzymes BamHI and PstI. The resulting plasmid was introduced into *E. coli* S17.1 strain and into *B. abortus* 2308 Δ*aceA* by conjugation

- *Brucella melitensis* Δ*virB* strain was constructed in the *B. melitensis* mCherry strain as described in (Nijskens, Copin et al. 2008)
- The complemented strain of *B. melitensis* Δ*virB* was done using the plasmid pBBR-p_{virB}*virB* containing the complete *virB* operon, under the control of its own promoter (Nijskens, Copin et al. 2008)

Brucella staining with eFluor670

For some experiments, eFluor670 staining was used to stain the primary amines of the outer membrane of *Brucella*. Because *Brucella* has an unipolar growth and because primary amines (and so the eFluor670) do not move in the membrane, the staining allows to distinguish between the mother bacteria and the daughter bacteria.

Protocol:

- Calculate the infectious dose as describe above. Make sure that initial volume ~ 1 mL to put this volume in an Eppendorf
- Wash the bacteria in 1 mL of PBS: centrifuge (7,000 g, 2 min 30 at 20 °C), throw away the supernatant, add 1 mL of PBS, suspend the bacteria
- Centrifuge again and then incubate the bacteria in eFluor670 diluted in 1 mL of PBS (1/500) 20 min in the dark on a wheel.

The stocks of eFluor670 have a final concentration of 5 mM and are stocked at - 20 °C

- Wash 4 times the bacteria: centrifuge (7,000 g, 2 min 30 at 20 °C), throw away the supernatant, add 1 mL of PBS, suspend the bacteria (x4)
- Make a last wash after which the bacteria are suspended in RPMI and put at the final volume with RPMI (depending on the infectious dose calculation)
- Infect the mice (see the protocol above)

*Brucell*a growth curve and CFU

Growth curve (bioscreen)

The measurement of OD 600 nm in a well containing *Brucella* allows to monitor the multiplication rate of these bacteria overtime. WT *Brucella* usually reach the stationary phase ($OD_{600\ nm}$ = 2) after 72 h. Based on that, measurements were done every 30 min during 72 h in a Bioscreen C (Oy Growth Curves).

Protocol:

- Prepare an overnight culture in 2 YT rich medium the day before in order to reach $OD_{600\ nm}$ between 0.2 and 0.5 (exponential phase) the day after
- Wash 2 times the bacteria with PBS (centrifuge the Falcon at 3,500 g during 10 min at 20 °C)
- Measure the $OD_{600\ nm}$ again
- Dilute bacteria to obtain $OD_{600\ nm}$ = 0.05 and resuspend them in a final volume of 700 µL of fresh medium (2 YT or minimal medium, depending on the experiment)
- Add 200 µL of the culture / well in the specific plate for bioscreen
- Add 5 mL of PBS in the edge of the plate to avoid the evaporation of the liquid in the wells what will modify the OD

Colonies forming units (CFU) – *in vivo*

The evaluation of the colonies forming units allow to know the number of bacteria from an organ (in our case) still living and able to divide (by opposition with the PCR technique for example). Each colony is the consequence of one isolated bacterium that divided to form the colony.

Protocol:

- Once the mice are killed, harvest the organ, weight it and place it in a Falcon 15 mL containing 1 mL of Triton-X100 0.01 % / PBS.
- Homogenized with an Ultraturax (X120 from CAT-Ing).
- Plate 100 µL of this lysat on 2 YT agar plates

- Incubated for 4-5 days at 37 °C.

Serial dilutions were done when necessary to obtain a countable number of CFUs.

Fluorescent microscopy on mice tissues

The immunohistofluorescence techniques allow to stain a specific protein present in the cell using antibodies and fluorochromes via emission of fluorescence. Not very quantitative, this method mostly allows a qualitative study, locating the proteins present within a cell.

- Once the mice are killed, harvest the lungs and fixe it with paraformaldehyde 2 % (pH 7.4) for 30 min at RT
- Evacuate the organs to be sure that paraformaldehyde fixed correctly the entire lungs. After that, lungs were still fixed for 1h30 more at RT
- Wash 2 times with PBS
- Incubate the organs in 20 % sucrose / PBS solution overnight at 4°C
- Embedded them in Tissue-Tek OCT compound (Sakura)
- Froze them in liquid nitrogen and stocked them at -20 °C

- Prepare slides of 5 µM of thickness with a microtome (Leica CM1850 Cryostat) and stock the slide at -20 °C

- Before staining, rehydrate the slide in PBS for 5 min
- Draw a hydrophobic circle around the organs and incubate them in Blocking reagent 1 % / PBS solution (BR) (Boeringer) for 20 min at RT
- Draw a hydrophobic circle around the organs to maintain and incubate the slide in the antibodies (mAbs) or reagents diluted in BR solution overnight at 4 °C
  In this thesis, we used the following antibodies or reagents: DAPI nucleic acid stain Alexa Fluor 350 (1/1000), 488 phalloidin (MolecµLar Probes) (1/100), APC-coupled BM8 (anti-F4/80, Abcam) (1/200), Alexa Fluor 647-coupled M5/114.15.2 (anti-I-A/I-E, MHCII, BioLegend) (1/200), AlexaFluor 647-coupled HL3 (anti-CD11c, BD Biosciences) (1/200), biotin-coupled 1A8 (anti-Ly6G, BioLegend) (1/200), biotin-coupled APA5 (anti-CD140a/ PDGFRA, eBioscience) (1/200).
- Wash the slide by diving it several times in a bath of PBS

- Draw a hydrophobic circle around the organs

- If a secondary staining is necessary, incubate the slide with the secondary antibody for 2 h at 4°C and, then wash 2 times

In our experiment, we used the biotin-coupled Abs were incubated with streptavidin-coupled APC (1/400) for 2 h.

- Wash in PBS as described above
- Mount the slides in Fluoro-Gel medium (Electron Microscopy Sciences, Hatfield, PA)
- Visualize the labeled tissue sections with a microscope

For our experiments, we used an Axiovert M200 inverted microscope (Zeiss, Iena, Germany) equipped with a high-resolution monochrome camera (AxioCamHR, Zeiss). Images (1,384×1,036 pixels, 0.16µm/pixel) were acquired sequentially for each fluorochrome with A-Plan 10x/0.25 N.A. and LD-Plan-NeoFluar 63x/0.75 N.A. dry objectives and recorded as eight-bit gray-level∗.zvi files.

At least 3 slides were analyzed per organ from 3 different animals and the results are representative of 2 independent experiments.

Confocal microscopy

The confocal microscopy, as the fluorescence microscopy, is an optical imaging technique using antibodies and fluorochromes to detect light from labelled proteins in a sample. The confocal microscopy has the advantage to have a laser that concentrate the light in one point and a pinhole in front of the detector to eliminate the out-of-focus light. This system allows to increase the resolution and the contrast of images.

Protocol:

- The tissue sections were prepared as described above
- Visualize the labeled tissue sections with a microscope

Confocal analyses were performed using a LSM780 confocal system fitted on an Observer Z 1 inverted microscope equipped with an alpha Plan Apochromat 63x/1.46 NA oil immersion objective (Zeiss, Iena, Germany). DAPI was excited using a 405 nm blue diode, and emission

was detected using a band-pass filter (410–480 nm). The 488 nm excitation wave length of the Argon/2 laser was used in combination with a band-pass emission filter (BP500-535 nm) to detect Alexa Fluor 488 phalloidin. The 543 nm excitation wave length of the HeNe1 laser and a band-pass emission filter (BP580–640 nm) were used for the red fluorochrome mCherry. The 633 excitation wave length of the HeNe2 laser and a band-pass emission filter (BP660–695 nm) were used for far-red fluorochromes such as APC. To ensure optimal separation of the fluorochromes, blue & red signals were acquired simultaneously in one track and green & far red signals were acquired in a second track. The electronic zoom factor and stack depth were adjusted to the region of interest while keeping image scaling constant (x-y: 0.066 micron, z: 0.287micron). A line average of 4 was used and datasets were stored as 8-bit proprietary∗.czi files. The images were displayed using Zen2012 software (Zeiss) with linear manual contrast adjustment and exported as 8-bit uncompressed∗.TIF images. The figures, representing single optical sections across the region of interest, were prepared using the Canvas program.

Flow cytometry analyses

Flow cytometry is a technique used to measure different properties of a cell population (as the size and granularity) as well as the presence of proteins by using anti-proteins antibodies. By contrast with microscopic analyses, this one is well more quantitative as flow cytometry is able to analyze billions of cells in few seconds. The flow of labelled single cells passes in front of a laser that excites the fluorochromes. The emitted fluorescences are concentrated, detected and converted in numeric values.

Protocol:

- Kill the mice and harvest the lungs
- Place them in a 6-wells plate (one lung / well) with droplets of cold RPMI
- Homogenized with scissors, flush, and filtered through 72 µM filter on a Falcon 15 mL
- Wash the cells: centrifuge them at 500 g during 7 min at 4 °C and resuspend them in cold FACS buffer (0.2 % BSA, 0.02 % NaN3 in PBS)
- Incubate the cells in saturating doses of purified 2.4G2 (anti-mouse Fc receptor, ATCC) (1/200) diluted in for 20 min at 4 °C to prevent antibody (Abs) binding to the Fc receptor.
- Wash (once) the cells as describe above
- Incubate the cells were in the different Abs diluted in FACS buffer for 30 min at 4°C

In our experiments, we used: BV421-coupled E50-2440 (anti-SiglecF, BD Biosciences) (1/200), BV421-coupled T45-2342 (anti-F4/80, BD Bioscences) (1/200), BV421-coupled M1/70 (anti-CD11b, BD Bioscences) (1/200), fluorescein (FITC)-coupled 145-2C11 (anti-CD3ε, BD Bioscences) (1/200), FITC-coupled 30-F11 (anti-CD45n BD Biosciences) (1/200), FITC-coupled M1/70 (anti-CD11b, BD Biosciences) (1/200), FITC-coupled HL3 (anti-CD11c, BD Biosciences) (1/200), phycoerythrin (PE)-coupled HL3 (anti-CD11c, BD Biosciences) (1/200), PE-coupled 1A8 (anti-Ly6G, BD Biosciences) (1/200), allophycocyanin (APC)-coupled BM8 (anti-F4/80, BD Bioscences) (1/200), biotin-coupled 2G9 (anti-MHCII, I-A/I-E, BD Biosciences) (1/200). Biotin-coupled APA5 (anti-CD140a/ PDGFRA, eBiosciences) (1/400).

- Wash the cells 2 times as described above
- If a secondary staining is necessary, incubate the cells with the secondary antibody for 30 min at 4°C and, then wash 2 times
- Fix the cell by incubating them in PFA 2 % for 30 min at RT
- Wash the cells 2 times
- Incubate the cells in FACS Buffer, at 4 °C and in the dark until the analyze
- Analyze the cells on a flow cytometer

We used the BD FacsVerse flow cytometer. Dead cells and debris were eliminated from the analysis according to size and scatter.

Cells numeration

To calculate the absolute number of cells present in a sample, the Neubauer cell (Figure 17) can be used. This cell is composed of 9 big squares (number1 on Figure 17), each of 1 mm². The central square is itself composed of 16 smaller squares (number 3 on Figure 17) of 0.4 mm², squares that we used for the cells numeration in this project.

Protocol:

- Take a proportion of the sample *(of the filtrate of lungs, after 24G2 incubation in the flow cytometry analyses in our case)*
- Add 10 µL of this sample in the chamber of the cell
- Count the number of cells in the 16 big squares in the center of the chamber

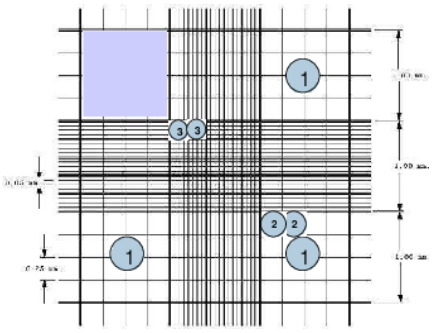

Figure 17: Image of a Neubauer cell

- Multiply the mean of counted cells by the dilution factor (depending on the proportion taken at the beginning) and by 250,000 (conversion factor of the small squares[5]) to obtain the number of cells / mL.

Detection of *Brucella* specific antibodies by Enzyme-Linked ImmunoSorbent Assay (ELISA)

The enzyme-linked immunosorbent assay technique is used to detect the presence of proteins in a sample by using antibodies. The antigen-antibody complex is revealed by the detection of color produced by the reaction between a substrate and an enzyme conjugated to an antibody. It exists different ELISA tests: the direct one, the indirect one, the "sandwich" one, and the competitive one. Even if in clinical research the sandwich one is the most use, in research the most common used ELISA test is the indirect one which is the one described below.

Protocol:

- Coat the polystyrene plate (269620 Nunc) with 50 µL / well of the antigen *(10^9 bacteria of heat-killed B. melitensis / mL diluted to obtain 10^7 bacteria / mL in each well)* and incubate the plate overnight at 4 °C with parafilm to avoid evaporation. Tap the edge of the plate before incubation to be sure that no air bubbles are present
- Flip the plate to eliminate all the liquid of the wells
- Block the non-specific sites with 200 µL of casein 3.35 % / PBS for 2 h at RT.
- Flip the plate
- Incubate the plate with 50 µL of plasma/ well in serial dilutions in casein 3.65 % / PBS during 1 h at RT.

[5] the superficy of counted squares is: 0.2 mm x 0.2 mm = 0.4 mm^2 = 0.0004 cm^2. The deeper of the cell is = 0.1 m = 0.01 cm. the volume of one square (nb 3) = 0.0004 cm^2 x 0.01 cm = 0.00004 cm^3 = 0.00004 mL. The conversion factor to calculate the number of cells / mL is so equal to 250,000.

- 6 dilutions of 3 in 3 (starting with a dilution 30x): take 4 µL of plasma, add 116 µL of casein 3.35 % / PBS; add these 120 µL in the first well. Add 80 µL of casein 3.35 % / PBS in the 5 other wells. Take 40 µL of the first well and dilute it in the second well. Start again from the second to the third well, with 40 µL and for the other wells

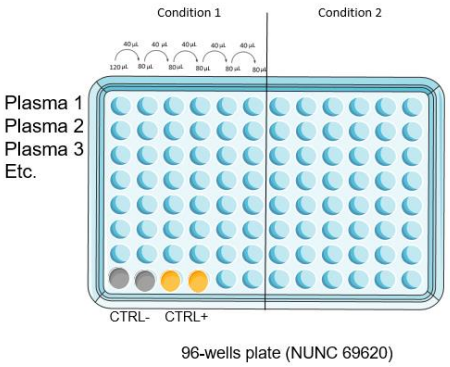

Figure 18: Example of the organization of a plate for ELISA

- The dilutions were prepared in another 96-wells plate and then transferred in the Nunc plate
- In our experiences, 12B12 (monoclonal antibody anti-smooth LPS of *Brucella*) and naïve mouse plasma were used as positive and negative controls, respectively

- Wash 4 times with PBS and flip between each wash
- Add 50 µL / well of antibody conjugated to an enzyme (ex. Horseradish Peroxidase - HRP) diluted in casein 3.35 % / PBS were added for 1h at RT.

We used isotype-specific to Brucella IgM, IgG1, IgG 2c, IgG3 (see the table below)

- Wash 4 times the plate and flip between each wash
- Add 100 µL / well of 3,3′,5,5′-Tetramethylbenzidine (TMB[6]) (the substrate of the enzyme HRP) and incubate the plate for 15 min in the dark at RT; a blue color appeared
- Stop the reaction by addition of 25 µL / well of H2SO4 2N; the blue color has to switch in yellow
- Measure the OD of each well at 450 nm with a spectrophotometer

We used the Bio-Rad xMark Microplate Spectrophotometer

[6] Kit BD OptEiA ref 555214. 2 solutions to mix together at equal volume just before ue. Take the reagents out of the frigde 30 min before use

Antibody	Reference	Dilution used
Anti-Mouse IgG Peroxydase antibody	A2554, Sigma-Aldrich	1/4000
Anti-Mouse IgM Peroxydase antibody	18786, Sigma-Aldrich	1/4000
Ant-mouse IgG1-Peroxydase	LO MG1-13	1/2000
Anti-mouse IgG2b - Peroxydase	LO MG2b-2	1/2000
Anti-mouse IgG2a et 2c)-Peroxydase	LO MG2a-9	1/2000
Anti-mouse IgG3 - Peroxydase	LO-MG3-13-HRP	1/2000

Immune memory study *in vivo*

As explained in the introduction, an immune memory developed after a first infection with a pathogenic agent, that will lead to a better and faster immune response during a second infection with the same pathogenic agent. To mimic this and evaluate the efficiency of a secondary infection, mice are first vaccinated then challenged with *Brucella,* and CFU are compared to those from mice infected only one time.

Protocol:

- Immunized C57BL/6 WT mice with *Brucella melitensis* WT ($2x10^4$ bacteria / mouse) during 1 month

- Give a double-antibiotics treatment (Streptomycin 450 mg/kg and Rifampycin 12 mg/kg) in water drink in order to eliminate *Brucella* from the first infection during 2 weeks
- Give 2 weeks of rest to in order to eliminate antibiotics from their organism (stop the antibiotics treatment by giving fresh water drink to mice)
- Challenge mice (by the same route of infection) with a dose of $2x10^4$ *B. melitensis* mCherry / mouse

The two different strains of bacteria that we used allowed us to control that no bacteria from the first infection were still present.

- Kill the mice and harvest the organs
- Make the CFUs (as describe above)

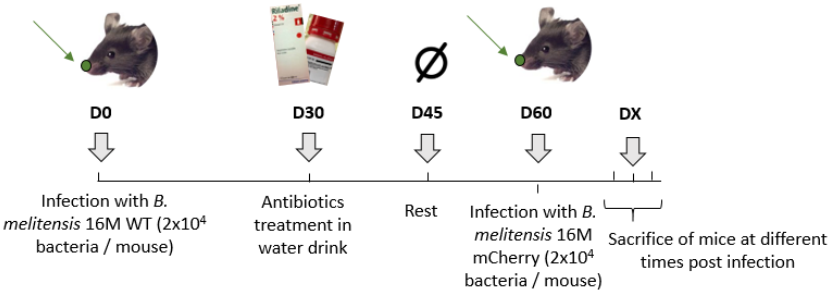

Figure 19: plan of the experiment to study the immune memory

Purification of lung alveolar macrophages (AM)

As we needed at least 10^6 AM for the transmission electronic microscopy (TEM – see below), the broncho-alveolar lavages (BAL) were not possible. To bypass this, we based our purification of alveolar macrophages (AM) on a protocol of dendritic cells purification from a spleen of rat.

Protocol:

- Sacrifice the mice
- Harvest the lungs
- Place the lung in a 6-wells plate (on ice) with 2, 3 drops of cold RPMI – 5 mM of EDTA)
- Homogenize the lungs with scissors

- Scratch the homogenate with the piston of a 1 mL syringe
- Add 4-5 mL of cold RPMI – 5 mM EDTA
- Filter the cells through a filter of 72 µM placed on a Falcon 15 mL
- Add 10 mL of cold complete medium[7] to wash the cells
- Centrifuge the cells at 1,400 g during 7 min at 4 °C
- Through the supernatant away and resuspend the cells in cold complete medium with 5 mM of EDTA + 24G2 (1/200) to block the non-specific site
- Incubate the cells 20 min at 4 °C
- Add 10 mL of cold complete medium to wash the cells
- Centrifuge the cells at 1400 g during 7 min at 4 °C
- Thought the supernatant away
- Add CD11c-coupled magnetic beads (Milteny) to the cells (in the liquid staying from the wash)
    - Fix the cells (if infected with *Brucella*)
    - Count the cells (with the Neubauer cells – see above)
    - Add 100 µL of beads for 10^8 cells
- Resuspend the cells and incubate in the dark during 15 min at 4 °C
- Place the MACS column (MS size) on the magnetic field
- Place a collector tube under the column to collect liquid
- Wet the MACS column: add 1 mL of cold complete medium and wait for the liquid is completely out of the column
- Add the cells into the column and wait for all liquid is completely out of the column
- Wash 3 times the column by adding 1 mL of cold complete medium with 5 mM of EDTA (between each wash, wait for all the liquid is completely out of the column
- Change your collector tube (Falcon 15)
- Remove the column of the magnetic field, and rapidly flush with the provided piston
- Add 10 mL of cold complete medium
- Centrifuge the cells at 1,400 g during 7 min at 4 °C
- Through the supernatant away
- Resuspend the cells in a medium depending on the next experiment

[7] Complete medium: 500 mL of RPMI + 50 mL of Fœtal Bovin Serum (FBS) + 5 mL of non-essential amino acids + 5 mL of L-Glutamate + 5 mL of pyruvate

RNA extraction, RNA-sequencing and qRT-PCR

RNA extraction and isolation

RNA was extracted with 2 different protocols depending on the samples: Trizol purification for entire lungs, and with a kit (RNeasy Mini kit (Qiagen[8])) for purified alveolar macrophages.

Trizol purification (total lung cells)

- Kill the mice and harvest the lungs (small piece, 50-100 mg, is sufficient) and place it in a Falcon 15 mL
- Add 1 mL of Tripure[9]
- Homogenized by using Ultraturax
- Transfer in Eppendorf
- Incubate 5 min at RT
- Add 0.2 mL of chloroform
- Mix vigorously during 15 sec
- Incubate 2 to 15 min at RT
- Centrifuge at 12,000 g fir 15 mon at 4 °C
- Transfer the aqueous phase in a new Eppendorf
- Add 500 µL of isopropanol to precipitate RNA
- Mix by inversion
- Incubate 5 to 10 min at RT
- Centrifuge at 12,000 d for 10 min at 4 °C
- Through the supernatant away
- Wash 2 times the pellet with 75 % ethanol
- Centrifuge at 7,500 g for 5 mon at 4 °C
- Through the supernatant away
- Quick spin and through the rest of ethanol away
- Resuspend in 30 µL of RNAse-free water

[8] Qiagen Online (Cat No./ID: 74104)

[9] TriPure Isolation Reagent (ref: 11667157001) from Merck

- Incubate for 10-15 min a 55-60 °C to completely resuspend RNA

After this technique, a DNAse I, RNase-free[10] treatment was done.

Protocol:

- In a new RNAse free Eppendorf, mix 1 µg of RNA with 1 µL of 10X reaction buffer (with MgCl2) and 1 µL (1U) of DNAse I, RNA-free, and fill up to 10 µL with DEPC water
- Incubate at 37 °C during 30 min
- Add 1 µL of 50 mM EDTA
- Incubate at 65 °C during 10 min

RNeasy Mini kit

- Purify the AMs (see protocol above), pellet the cells in an Eppendorf (in complete medium)
- Add 600 µL of Buffer RLT[11] and vortex
- Add 600 µL of 70 % ethanol and mix by pipetting
- Transfer 600 µL of the sample to a RNeasy Mini spin column placed on a 2 mL collection tube. Close the lid and centrifuge for 15 s at 8,000 g
- Discard the flow-through
- Do the same two previous steps in order to transfer all the sample in a column
- Add 700 µL of Buffer RW1[12] to the RNeasy spin column. Close the lid and centrifuge for 15 sec at 8,000 g
- Discard the flow-through
- Add 500 µL of Buffer RPE[13] to the RNeasy spin column, close the lid and centrifuge for 15 sec at 8,000 g

[10] Ref M0303S from New Englands BioLabs

[11] As we purified the RNA from tissues, we added 10 µL of β-mercaptoethanol to 1 mL of Buffer RLT. Buffer RLT contains guanidine isothiocycanate, which allows the binding of RNA to the silica membrane of the spin column.

[12] The Buffer RW1 contains a guanidine salt and ethanol. It is used to wash and remove biomolecules (carbohydrates, proteins, fatty acids etc.,) that are non-specifically bound to the silica membrane.

[13] The Buffer RPE contains ethanol. This washing buffer is used to remove the salts from the previous buffers.

- Discard the flow-through
- Add 500 µL of Buffer RPE to the RNeasy spin column, close the lid and centrifuge for 2 min at 8,000 g
- Place the RNeasy spin column in a new 2 mL collection tube and centrifuge at full speed for 1 min to dry the membrane
- Place the RNeasy spin column in a new 1.5 mL collection tube
- Add 30 µL of RNase-free water to elute RNA

Here, no DNAse I, RNAse-free treatment was done as the kit already process to a DNA elimination.

RNAsequencing

The RNAsequencing technique uses the next-generation sequencing in order to sequence the whole genome of an organism in order to quantify the RNAs present at one given moment. Different methods can be used to do RNA-Seq. one of the most common is the targeting of mRNA (poly-adenylated)[14] thanks to a poly-T queue binded to magnetic beads. The RNAs are then translated into cDNA, then fragmented and a library is prepared in function of the machine that will be use for the sequencing.

For this project, we did by ourself the RNA extraction (see protocol above), the DNAse I, RNAse-free treatment. The RNA samples were then send to the NGS service of ULB (F. Libert) where they transform the RNA into cDNA, prepared the library and did the Illumina RNA sequencing. They used the Novaseq 6000 Trueseq SBS reagents (25 millions reads paired-end) and Trueseq stranded RNA library preparation for the Illumina sequencing.

Analyse of the RNAsequencing

For the analyse, we collaborated with S. Goriely and A. Azouz (µLB). Briefly, genes with no raw read count were filtered out with an R script. Raw read counts were normalized and a

[14]These RNA are more stable and are often translated to proteins. The poly-T selection allows also to eliminate the ribosomal RNA, and the bacterial RNA (even if some bacteria possess poly-T tail)

differential expression analysis was performed with DESeq2 by applying an adjusted p-value < 0.05 and absolute log2-ratio larger than 0.5849.

Quantitative real-time polymerase chain reaction (qRT-PCR)

This technique provides quantitative information about the abundance of genes in a sample, in comparison to a reference gene, here called the housekeeping gene (HKG, *TBP for TATA binding protein in our case*). Briefly, a fluorescent dye – Takyon No ROX Syber 2x MasterMix blue dTTP[15] - *(in our case)* interlaces in any double-strand DNA formed during a polymerase chain reaction (in real-time). More DNA is present (correlated to RNA amount), more fluorescent signal is rapidly detected. Usually, the quantification DNA relies on a plotting of fluorescence depending on the number of cycle of PCR, on a logarithmic scale. A threshold is delimited by the background noise of fluorescence. Once the number of cycle at which the fluorescent signal exceeds this threshold, the threshold cycle (Ct) is reached and that corresponds to the value used to calculate the gene expression level. At each step of amplification during the PCR, the amount of DNA doubles. *In our case, we use the relative quantification, based on a reference condition, which was naive mice cDNA.*

Transformation of RNA into cDNA

One RNA extracted from lung (see protocol above) and treated with DNAse I RNAse-free treatment (see protocol above), RNA is transform into cDNA before doing qRT-PCR for different reasons: 1) RNAse are ubiquitous in nature, it is more preferable to work with cDNA, 2) RNA is chemically unstable due to their nucleophilic 2´ hydroxyl groups. 3) Amplification phase during PCR only work with DNA as material, and 4) most of sequencing protocol are designed to use DNA and not RNA (using DNA polymerase). *The kit that we used is High capacity cDNA Reverse Transciprtion kit from Applied BioSystems).*

Protocol:

[15] Ref UF-NSMT-B0101 from Eurogentec

- For the RT+ (with reverse transcriptase enzyme), add to a new RNAse-free Eppendorf 15 µL of treated RNA, 3 µL of Hexamer Random primer 10x, and 6.3 µL of RNase-free water
- Incubate 10 min at 65 °C
- Put on ice for 1 min
- Add 3 µL of RT Buffer 10x, 1.2 µL of dNTPs 25x, and 1.5 µL of Reverse Transcriptase
- Vortex for some seconds
- Quick spin
- Incubate for 10 min at 25 °C
- Incubate for 120 min at 37 °C
- Incubate for 5 min at 85 °C
- Dilute 10 times with RNAse-free water and freeze the cDNA until use

For the negative control (without Reverse Transcriptase – RT-), mix 5 µL of treated RNA, 1 µL of Hexamer Random Primer 10x, 2.1 µL of RNAse-free water. Follow the same incubation steps. The, add 1 µL of RT Buffer 10x, 0.4 µL of dNTPs 25x, and follow the same incubation steps.

qRT-PCR

- To calculate the efficacy of the PCR, we diluted the cDNA (3 in 3)
- Make duplicate for each condition
- Make a master mix; 5 µL of Takyon dye, 1 µL of reverse primer and 1 µL of forward primer
- Add 7 µL of this master mix in each well
- Add 3 µL of cDNA
- Cover the plate with the plastic sheet provided
- Centrifuge the plate at 200 rpm for 1 min
- Analyze is done on Roche machine[16] with the program provided with

For the analyze, mean of duplicates has been *calculate*d. Then, the slope, R^2, and the efficiency have been calculated on excel via the formulas "PENTE" for the slope,

[16] LightCycler® 96 System

"COEFFICIENT.DETERMINATION" for the R^2 and "=(10^(-1/slope)-1)*100" for the efficiency. Only the Ct with an efficiency included between 90 and 100 % were taken in count. These Ct were then transformed to have an efficiency of 100 %. At least 6 mice for each group have been tested. The mean of the Ct of each group has been *calculate*d.

For the calculation of the expression, we used the classical 2^{-ddCt}, with the Ct normalized to 100 %:

1) dCt= Mean of $Ct_{100\%}$ (Unknown gene – *Acod1*) – Mean of $Ct_{100\%}$ (Housekeeping gene – *tbp*)

2) ddCt= mean of $Ct_{100\,\%}$ (infected mice) – mean of $Ct_{100\,\%}$ (naïve mice)

3) 2^{-ddCt}

Transmission electronic microscopy (TEM)

The transmission electronic microscopy has the great advantage to have a resolution (0,2 nm) much higher than the fluorescent microscopy. This technique allows to observe very small and detailed structures thanks to electrons as source of illumination; more the wavelength is reduced, more the resolution is high. The source of electrons, *in the case of the microscope Tecnai 10 (Philips) of UNamur,* is emitted from an electron gun fitted with a tungsten filament. The electron beam is focused by 2 condenser lenses to one small spot. Then the electron beam passes through pairs of deflection coils and a final lens aperture. The spot of electron is deflected by this late lens and reaches the sample. The interaction between the sample and the electron beam results in an electrons exchange between the sample and the electron beam. The new secondary electrons produced can be detected by the secondary electron detector. Moreover, the energy absorbed by the sample can also be detected and used to create an image of the sample thanks to emitted signals from the samples and X-Ray detector.

This protocol was used for purified AMs (see protocol above), RAW macrophages (see protocol above), and bacteria from liquid culture. In this last case, 2 mL of liquid culture were used.

We work with a final volume of 400 µL for each steps.

- Suspend your cells in 50/50 Glutaraldehyde 4 % / Cacodylate buffer 0.2 M for 2 hours at RT or ON at 4 °C

- Transfer all the cells in a specific Eppendorf for TEM (ask to the TEM service from UNamur)
- Wash 3 times (centrifugation for cells: 1,000 g 2 min and for bacteria: 4,000 g for 5 min) with cacodylate 0.2 M
- Add 50/50 Osmium 4 % / Cacodylate 0.2 M during 1 h at RT
- Wash 1 time with sterile dH2O and centrifuge
- Wash 2 times with cacodylate 0.2 M and centrifuge
- Add EtOH 30 % and mix by inversing
- Incubate for 5 min, then centrifuge and through the supernatant away
- Add EtOH 30 % and mix by inversing
- Incubate for 10 min, then centrifuge and through the supernatant away
- Repeat the same steps for EtOH 50, 70 and 85 %
- Add EtOH 100 % and mix by inversing
- Incubate for 10 min
- Repeat the same step 2 more times
- Take the resin out of the freezer and let it at RT
- Add propylene oxide for 5 min and centrifuge
- Repeat this step 3 more times
- Add 75 % of propylene oxide / 25 % of resin and let your sample under agitation during 15 min
- Centrifuge and add 50 % of propylene oxide / 50 % of resin and let your sample under agitation during 20 min
- Centrifuge and add 25 % of propylene oxide / 75 % and let your sample under agitation during 20 min
- Centrifuge and add pure resin
- Place the sample at 37 °C for 1 day, then at 45 °C for 1 day and finally at 60 °C for 3 days. Let the cap open

The pellet has been cut and contrasted by the Service of electronic microscopy from UNamur). For the contrast, use small grids special for electronic microscopy. Place the bright side (with cells) on a drop (100 µL) of uranium acid and let them for 20 min. Rinse the grids with water and absorb water with a Tork paper. Do the same on a drop of lead citrate for 10 min. Rinse the grids with water and absorb water with a Tork paper.

Statistical analysis

We used a (Wilcoxon-)Mann-Whitney test provided by the GraphPad Prism software to statistically analyze our results. Each group of deficient mice was compared to the wild-type mice. We also compared each group with the other groups and displayed the results when required. Values of $p<0.05$ were considered to represent a significant difference. $*$, $**$, $***$ denote $p<0.05$, $p<0.01$, $p<0.001$, respectively.

VII. References

Acha, N. and B. Szyfres (2003). "Zoonoses and communicable diseases common to man and animals." Pan American Health Organization **1**: 42.

Ackermann, W. W. and V. R. Potter (1949). "Enzyme inhibition in relation to chemotherapy." Proc Soc Exp Biol Med **72**(1): 1-9.

Akira, S. and K. Takeda (2004). "Toll-like receptor signalling." Nat Rev Immunol **4**(7): 499-511.

Akira, S., S. Uematsu and O. Takeuchi (2006). "Pathogen Recognition and Innate Immunity." Cell **124**(783-801).

Akkaya, M., K. Kwak and S. K. Pierce (2020). "B cell memory: building two walls of protection against pathogens." Nat Rev Immunol **20**(4): 229-238.

Alder, J., S.-F. Wang and H. A. Lardy (1957). "The metabolism of itaconic acid by liver mitochondria." J. Biol. Chem. **229**(2): 865-879.

Alexander, B., P. R. Schnurrenberger and R. R. Brown (1981). "Numbers of *Brucella* abortus in the placenta, umbilicus and fetal fluid of two naturally infected cows." Vet Rec **108**(23): 500.

Alfani, G. and T. Murphy (2017). "Plague andlethal epidemics in the pre-industrial world." Journal of economic history **77**(1): 314-343.

Ali, S., S. Akhter, H. Neubauer, A. Scherag, M. Kesselmeier, F. Melzer, I. Khan, H. El-Adawy, A. Azam, S. Qadeer and Q. Ali (2016). "Brucellosis in pregnant women from Pakistan: an observational study." BMC Infect Dis **16**: 468.

Alsaif, M., K. Dabelah, H. Girim, R. Featherstone and J. L. Robinson (2018). "Congenital Brucellosis: A Systematic Review of the Literature." Vector Borne Zoonotic Dis **18**(8): 393-403.

Anderson, T. D., N. Cheville and V. Meador (1986). "Pathogenesis of Placentitis in the Goat Inoculated with *Brucella* abortus. 11. Ultrastructural Studie." Vet. Pathol. **23**: 227-239.

Anderson, T. D. and N. F. Cheville (1986). "Ultrastructural morphometric analysis of Brucella abortus-infected trophoblasts in experimental placentitis. Bacterial replication occurs in rough endoplasmic reticulum." Am J Pathol **124**(2): 226-237.

Angel, C. E., A. Lala, C. J. Chen, S. G. Edgar, L. L. Ostrovsky and P. R. Dunbar (2007). "CD14+ antigen-presenting cells in human dermis are less mature than their CD1a+ counterparts." Int Immunol **19**(11): 1271-1279.

Archambaud, C., S. P. Salcedo, H. Lelouard, E. Devilard, B. de Bovis, N. Van Rooijen, J. P. Gorvel and B. Malissen (2010). "Contrasting roles of macrophages and dendritic cells in controlling initial pulmonary *Brucella* infection." Eur J Immunol **40**(12): 3458-3471.

Arellano-Reynoso, B., N. Lapaque, S. Salcedo, G. Briones, A. Ciocchini, R. Ugalde and P. Gorvel (2005). "Cyclic b-1,2-glucan is a *brucella* virulence factor required for intracellular survival." Nature Immunology **6**(6): 618-625.

Artis, D. and H. Spits (2015). "The biology of innate lymphoid cells." Nature **517**: 293-301.

Asarnow, D. M., T. Goodman, L. LeFrancois and J. P. Allison (1989). "Distinct antigen receptor repertoires of two classes of murine epithelium-associated T cells." Nature **341**(6237): 60-62.

Ashford, D., J. di Pietra, J. Lingappa, C. Woods, H. Noll and B. Neville (2004). "Adverse events un humns associated with accidental exposure to the livestock burcellosis vaccine RB51." Vaccine **22**(25-26): 3435-3439.

Aver, G., V. Mottin, O. Kreutz and E. Suyenaga (2017). "Genesis of pharmaceuticals: from prontosil rubrum to antipsychotics - a history of sulfa drugs from the perspective of medicinal chemistry." International journal of research in pharmacy and chemistry **7**: 306-319.

Avila-Calderon, E. D., A. Lopez-Merino, N. Sriranganathan, S. M. Boyle and A. Contreras-Rodriguez (2013). "A history of the development of *Brucella* vaccines." Biomed Res Int **2013**: 743509.

Balloux, F. and L. van Dorp (2017). "Q&A: What are pathogens, and what have they done to and for us?" BMC Biology **15**(91).

Bambouskova, M., L. Gorvel, V. Lampropoulou, A. Sergushichev, E. Loginicheva, K. Johnson and M. Artyomov (2018). "Electrophilic properties of itaconate and derivatives regulate the IKBZ-ATF3 inflammatory axis." Nature **556**(7702): 501-504.

Bandara, A. B., A. Contreras, A. Contreras-Rodriguez, A. M. Martins, V. Dobrean, S. Poff-Reichow, P. Rajasekaran, N. Sriranganathan, G. G. Schurig and S. M. Boyle (2007). "*Brucella suis* urease encoded by ure1 but not ure2 is necessary for intestinal infection of BALB/c mice." BMC Microbiol **7**: 57.

Bang, B. (1897). "The etiology of epizootic abortions." Journal of Comparative Pathology and Therapeutics **10**: 125-149.

Barbier, T., A. Machelart, A. Zuniga-Ripa, H. Plovier, C. Hougardy, E. Lobet, K. Willemart, E. Muraille, X. De Bolle, E. Van Schaftingen, I. Moriyon and J. J. Letesson (2017). "Erythritol Availability in Bovine, Murine and Human Models Highlights a Potential Role for the Host Aldose Reductase during *Brucella* Infection." Front Microbiol **8**: 1088.

Barquero-Calvo, E., E. Chaves-Olarte, D. S. Weiss, C. Guzman-Verri, C. Chacon-Diaz, A. Rucavado, I. Moriyon and E. Moreno (2007). "*Brucella abortus* uses a stealthy strategy to avoid activation of the innate immune system during the onset of infection." PLoS One **2**(7): e631.

Barrio, M. B., M. J. Grillo, P. M. Munoz, I. Jacques, D. Gonzalez, M. J. de Miguel, C. M. Marin, M. Barberan, J. J. Letesson, J. P. Gorvel, I. Moriyon, J. M. Blasco and M. S. Zygmunt (2009). "Rough mutants defective in core and O-polysaccharide synthesis and export induce antibodies reacting in an indirect ELISA with smooth lipopolysaccharide and are less effective than Rev 1 vaccine against *Brucella melitensis* infection of sheep." Vaccine **27**(11): 1741-1749.

Basappa, G. M., S. B. Mallanagouda, C. B. Rajendra, S. M. Mallanna, K. Veerappa, P. Kariholu, B. P. Siddanagouda and S. M. Smita (2006). "Protean clinical manifestations and diagnosticchallenges of human brucellosis in adults:16 years' experience in an endemic area." Journal of Medical Microbiology **55**: 897-903.

Baup, S. (1836). "Ueber eine neue Pyrogen-Citronensäure, und über Benennung der Pyrogen-Säuren überhaupt." Annalen der Pharmacie **19**(1): 29-38.

Belser, J. A., K. M. Gustin, J. M. Katz, T. R. Maines and T. M. Tumpey (2015). "Comparison of traditional intranasal and aerosol inhalation inoculation of mice with influenza A viruses." Virology **481**: 107-112.

Bentley, R. and C. P. Thiessen (1955). "Cis-aconitatic decarboxylase." Science **122**(3164): 330.

Bentley, R. and C. P. Thiessen (1957). "Biosynthesis of itaconic acid in Aspergillus terreus. II. Early stages in glucose dissimilation and the role of citrate." J. Biol. Chem. **226**(2): 689-701.

Bentley, R. and C. P. Thiessen (1957). "Biosynthesis of itaconic acid in Aspergillus terreus. III. The properties and reaction mechanism of cis-aconitic acid decarboxylase." J. Biol. Chem. **226**(2): 703-720.

Bentley, R. and C. P. Thiessen (1957). "Biosynthesis of itaconic acid in Aspergiullus terreus. I. Tracer studies with C14-labelled substrates." J. Biol. Chem. **226**(2): 673-687.

Berger, T. G. (1981). "Cutaneous Lesions in Brucellosis." Archives of Dermatology **117**(1).

Billard, E., C. Cazevieille, J. Dornand and A. Gross (2005). "High susceptibility of human dendritic cells to invasion by the intracellular pathogens *Brucella suis*, *B. abortus*, and *B. melitensis*." Infect Immun **73**(12): 8418-8424.

Billard, E., J. Dornand and A. Gross (2007). "*Brucella suis* Prevents Human Dendritic Cell Maturation and Antigen Presentation through Regulation of Tumor Necrosis Factor Alpha Secretion." Infection and immunity **75**(10): 4980-4989.

Bizzell, E. (2018). "Microbial Ninja Warriors: bacterial immune evasion." american Society for microbiology.

Bonilla, F. A. and H. C. Oettgen (2010). "Adaptive immunity." J Allergy Clin Immunol **125**(2 Suppl 2): S33-40.

Boraschi, D. and P. Italiani (2018). "Innate Immune Memory: Time for Adopting a Correct Terminology." Front Immunol **9**: 799.

Boschiroli, M. L., S. Ouahrani-Bettache, V. Foulongne, S. Michaux-Charachon, G. Bourg, A. Allardet-Servent, C. Cazevieille, J. P. Liautard, M. Ramuz and D. O'Callaghan (2001). "The *Brucella suis* virB operon is induced intracellularly in macrophages." Proceedings of the National Academy of Sciences **99**(3): 1544-1549.

Bosseray, N. and V. Dufrenoy (1982). "Mother to young transmission of *Brucella* abortus infection in mouse model." Annales de Recherches Vétérinaires **13**: 341-349.

Bossi, P. (2004). "BICHAT GUIDELINES* FOR THE CLINICAL MANAGEMENT OF BRUCELLOSIS AND BIOTERRORISM-RELATED BRUCELLOSIS." Euro surveillance **9**(12).

Boxx, G. M. and G. Cheng (2016). "The Roles of Type I Interferon in Bacterial Infection." Cell Host Microbe **19**(6): 760-769.

Brambell, R. F. W. (1970). "The transmission of passive immunity from mother to young." Frontiers of Biology **18**: 102-105.

Brennan, M., M. Matos, B. Li, X. Hronowki, B. Gao and P. Juhassz (2015). "Dimethyl Fumarate and Monoethyl Fumarate Exhibit Differential Effectson KEAP1, NRF2 Activation, and Glutathione Depletion In Vitro. ." Plos One **10**(3).

Brinley Morgan, W. J., A. I. Littlejohn, D. J. MacKinnon and J. R. Lawson (1966). "The Degree of Protection Given by Living Vaccines against Experimental Infection

with *Brucella melitensis* in Goats." 34: 33-40.

Bruce, D. (1887). "Note on the discovery of a micro-organism in Malta fever." Practitioner **39**: 161.

Bruce, D. (1907). "Recent researches into the epidemiology of Malta fever." Trans Epidemiol Soc Lond. **26**: 78-98.

Bruns, H., F. Stegelmann, M. Fabri, K. Dohner, G. van Zandbergen, M. Wagner, M. Skinner, R. L. Modlin and S. Stenger (2012). "Abelson tyrosine kinase controls phagosomal acidification required for killing of *Mycobacterium tuberculosis* in human macrophages." J Immunol **189**(8): 4069-4078.

Buck, J. M. (1930). "STUDIES OF VACCINATION DURING CALFHOOD TO PREVENT BOVINEI NFECTIOUS ABORTION." J Agri Res **41**: 667-689.

Buck, J. M. (1930). "Studies on vaccination during calfhood to prevent bovine infectious abortion. ." Journal of Agricultural Research **41**(9): 667-690.

Burke, S. M., T. B. Issekutz, K. Mohan, P. W. Lee, M. Shmulevitz and J. S. Marshall (2008). "Human mast cell activation with virus-associated stimuli leads to the selective chemotaxis of natural killer cells by a CXCL8-dependent mechanism." Blood **111**(12): 5467-5476.

Calam, C. T., A. E. Oxford and H. Raistrick (1939). "Itacoic acid, a metabolic product of a strain of Aspergillus terreus thom."

Capasso, L. (2002). "Bacteria in two-millenia-old cheese, and related epizoonoses in Roman populations." The British Infection Society.

Carmichael, L. E. and R. M. Kenney (1968). "Canine abortion caused by *Brucella canis*." J Am Vet Med Assoc **152**(6): 605-616.

Carpenter, C. (1926). "Bacterium abortus invasion of the tissue of calves from ingestion of infected milk." Cornell Vet. **14**: 16.

Carvalho, T. (2016). "Meta-Analysis and Avancement of brucellosis vaccinology." PLoS One **11**.

Celli, J. (2015). "The changing nature of the *Brucella*-containing vacuole." Cell Microbiol **17**(7): 951-958.

Celli, J. (2019). "The Intracellular Life Cycle of Brucella spp." Microbiol Spectr **7**(2).

Celli, J., C. de Chastellier, D. M. Franchini, J. Pizarro-Cerda, E. Moreno and J. P. Gorvel (2003). "*Brucella* evades macrophage killing via VirB-dependent sustained interactions with the endoplasmic reticulum." J Exp Med **198**(4): 545-556.

Chairatana, P. and E. M. Nolan (2017). "Defensins, lectins, mucins, and secretory immunoglobulin A: microbe-binding biomolecules that contribute to mucosal immunity in the human gut." Crit Rev Biochem Mol Biol **52**(1): 45-56.

Cheville, N., D. Rogers, W. Deyoe, E. Krafsur and J. Cheville (1989). "Uptake and excretion of *Brucella* aobrtus in tissues of the face fly (Musca autumnalis)." AM J Vet Res. **50**(8): 1302-1306.

Cheville, N., M. Stevens, A. Jensen, F. Tatum and Halling (1993). "Immunes responses and protection Against Infection and Abortion in Cattle Experimentally Vaccinated With Mutant Strains of *Brucella Abortus*." Am J Vet Res **54**: 1591-1597.

Cheville, N. F., O. S.C., A. E. Jensen, M. G. Stevens, M. V. Palmer and A. M. Florance (1996). "Effects of age at vaccination on efficacy of *Brucella* abortus strain RB51 to protect cattle against brucellosis." Am. J. Vet. Res. **57**(8): 1153-1156.

Ciofani, M. and J. C. Zuniga-Pflucker (2010). "Determining gammadelta versus alphass T cell development." Nat Rev Immunol **10**(9): 657-663.

Comerci, D. J., M. J. Martinez-Lorenzo, R. Sieira, J. P. Gorvel and R. A. Ugalde (2001). "Essential role of the VirB machinery in the maturation of the *Brucella abortus*-containing vacuole." Cell Microbiol **3**(3): 159-168.

Conde-Alvarez, R., V. Arce-Gorvel, M. Iriate, M. Mancek-Keber, E. Barqyero-Calvo, L. Palacios-Chaves and J.-P. Gorvel (2012). "The Lipopolysaccharide Core of *Brucella abortus* Acts as a Shield Against Innate Immunity Recognition." PLoS Pathog **8**(5): e1002675.

Conlon, B. P., E. S. Nakayasu, L. E. Fleck, M. D. LaFleur, V. M. Isabella, K. Coleman, S. N. Leonard, R. D. Smith, J. N. Adkins and K. Lewis (2013). "Activated ClpP kills persisters and eradicates a chronic biofilm infection." Nature **503**(7476): 365-370.

Copin, R., P. De Baetselier, Y. Carlier, J. J. Letesson and E. Muraille (2007). MyD88-dependent activation of B220-CD11b+LY-6C+ dendritic cells during *Brucella melitensis* infection. 178.

Copin, R., M. A. Vitry, D. Hanot Mambres, A. Machelart, C. De Trez, J. M. Vanderwinden, S. Magez, S. Akira, B. Ryffel, Y. Carlier, J. J. Letesson and E. Muraille (2012). "In situ microscopy analysis reveals local innate immune response developed around Brucella infected cells in resistant and susceptible mice." PLoS Pathog **8**(3): e1002575.

Corbel (2006). "Brucellosis in humand and animals." World Health Organization.

Corsetti, P., L. de Almeida, N. Carvalho, V. Azevedo, T. M. Silva, H. Teixeira, A. Faria and S. C. Oliveira (2013). "Lack of endogenous IL-10 enhances production of proinflammatory cytokines and leads to *Brucella abortu*s clearance in mice." PLoS One **17**(8): 9.

Cruz, C. M., A. Rinna, H. J. Forman, A. L. Ventura, P. M. Persechini and D. M. Ojcius (2007). "ATP activates a reactive oxygen species-dependent oxidative stress response and secretion of proinflammatory cytokines in macrophages." J Biol Chem **282**(5): 2871-2879.

Czibener, C., F. Merwaiss, F. Guaimas, M. G. Del Giudice, D. A. Serantes, J. M. Spera and J. E. Ugalde (2016). "BigA is a novel adhesin of *Brucella* that mediates adhesion to epithelial cells." Cellular Microbiology **18**(4): 500-513.

D'Anastasio, R., B. Zipfel, J. Moggi-Cecchi, R. Stanyon and L. Capasso (2009). "Possible brucellosis in an early hominin skeleton from sterkfontein, South Africa." PLoS One **4**(7): e6439.

Dai, H., N. Wan, S. Zhang, Y. Moore, F. Wan and Z. Dai (2010). "Cutting edge: programmed death-1 defines CD8+CD122+ T cells as regulatory versus memory T cells." J Immunol **185**(2): 803-807.

Dawson, R., R. Condos, D. Tse, M. L. Huie, S. Ress, C. H. Tseng, C. Brauns, M. Weiden, Y. Hoshino, E. Bateman and W. N. Rom (2009). "Immunomodulation with recombinant interferon-gamma1b in pulmonary tuberculosis." PLoS One **4**(9): e6984.

de Barsy, M., A. Jamet, D. Filopon, C. Nicolas, G. Laloux, J.-F. Rual, A. Muller, J.-C. Twizere, B. Nkengfac, J. Vandenhaute, D. E. Hill, S. P. Salcedo, J.-P. Gorvel, J.-J. Letesson and X. De Bolle (2011). "Identification of a *Brucella* spp. secreted effector specifically interacting with human small GTPase Rab2." Cellular Microbiology **13**(7): 1044-1058.

Dean, A. S. (2012). "Global burden of human brucellosis: a systematic review of disease frequency." PLoS Negl Trop Dis **6**(10): e1865.

Deghelt, M., C. Mullier, J. F. Sternon, N. Francis, G. Laloux, D. Dotreppe, C. Van der Henst, C. Jacobs-Wagner, J. J. Letesson and X. De Bolle (2014). "G1-arrested newborn cells are the predominant infectious form of the pathogen *Brucella abortus*." Nat Commun **5**: 4366.

Delpino, M. V., M. I. Marchesini, S. M. Estein, D. J. Comerci, J. Cassataro, C. A. Fossati and P. C. Baldi (2007). "A bile salt hydrolase of *Brucella abortus* contributes to the establishment of a successful infection through the oral route in mice." Infect Immun **75**(1): 299-305.

Delrue, R. M., M. Martinez-Lorenzo, P. Lestrate, I. Danese, V. Bielarz, P. Mertens, X. De Bolle, A. Tibor, J. P. Gorvel and J. J. Letesson (2001). "Identification of *Brucella* spp. genes involved in intracellular trafficking." Cell Microbiol **3**(7): 487-497.

Demars, A., A. Lison, A. Machelart, M. Van Vyve, G. Potemberg, J. M. Vanderwinden, X. De Bolle, J. J. Letesson and E. Muraille (2019). "Route of Infection Strongly Impacts the Host-Pathogen Relationship." Front Immunol **10**: 1589.

Detilleux, P. G., B. L. Deyoe and N. F. Cheville (1990). "Entry and intracellular localization of *Brucella* spp. in Vero cells: fluorescence and electron microscopy." Vet Pathol **27**(5): 317-328.

Dhomer, P., E. Valguarnera, C. Czibener and J. Ugalde (2014). "Identification of a type IV secretion substrate of *Brucella abortus* that participates in the early stages of intracellular survival." Cell Microbiol. **16**(3): 396-410.

Diaz Aparicio, E. (2013). "Epidemiology of brucellosis in domestic animals caused by *Brucella melitensis*, *Brucella suis* and *Brucella abortus*." Rev Sci Tech **32**(1): 43-51, 53-60.

Dimijian, G. (2000). "Evolving together: the biology of symbiosis, part 1." Proc (Bayl Univ Med Cent.) **13**(3): 217-226.

Doganay, M. (2001). "Brucellosis due to blood transfusion." Journal of Hospital Infection **49**(2): 151-152.

Dorneles, E. M., N. Sriranganathan and A. P. Lage (2015). "Recent advances in *Brucella abortus* vaccines." Vet Res **46**: 76.

Dubois, B., J. M. Bridon, J. Fayette, C. Barthelemy, J. Banchereau, C. Caux and F. Briere (1999). "Dendritic cells directly modulate B cell growth and differentiation." J Leukoc Biol **66**(2): 224-230.

E., M., S. E., D. M., W. J., B. M. and H. Mayer (1990). "*Brucella* abortus 16S rRNA and lipid A reveal a phylogenetic relationship with members of the alpha-2 subdivision of the class Proteobacteria." J Bacteriol **172**(7): 3569-3576.

Eckman, M. R. (1975). "Brucellosis linked to Mexican cheese." JAMA **232**(6): 636-637.

El Idrissi, A., A. Benkirane, M. El Maadoudi, M. Bouslikhane, J. Berrada and A. Zerouali (2001). "Comparison of the efficacy if *Brucella* abortus strain RB51 and *Brucella* melitensis Rev1 live vaccines against experimental infection with *Brucella* malitensis in pregnant ewes." Rev. sci. tech. Off. int. Epiz. **20**: 741-747.

Elberg, S. S. and D. W. Henderson (1948). "Respiratory pathogenicity of *Brucella*." J Infect Dis **82**(3): 302-306.

Evans, A. (1918). "Further studies on bacterium abortus and related bacteria." The Journal of Infectious Disease **22**: 581-593.

Eyre, J. (1908). "Melitensis septicemi." Lancet **1**: 1747.

Eyre, M. S., D. P. H. Durh and Cantab (1908). "The Milroy Lectures ON MELITENSIS SEPTICÆMIA (MALTA OR MEDITERRANEAN FEVER)." The Lancet **171**(4426): 1826-1832.

Fekete, A., J. Bantle, S. Hallong and M. Sanborn (1990). "Preliminary development of a diagostic test for *Brucella* using polymerase chain reaction." Journal of Applied bacteriology **69**: 216-227.

Fensterbank, R., P. Pardon and J. Marly (1982). "Comparison Between Subcutaneous and Conjunctival Route of Vaccination With Rev. 1 Strain Against *Brucella* Melitensis Infection in Ewes " Annales de Recherches Vétérinaires **13**: 295-301

Fiori, P. L., S. Mastrandrea, P. Rappelli and P. Cappucinelli (2000). "*Brucella abortus* infection acquired in microbiology Laboratories." Journal of clinical microbiology **38**(5): 2005-2006.

Foster, G., B. S. Osterman, J. Godfroid, I. Jacques and A. Cloeckaert (2007). "*Brucella* ceti sp. nov. and *Brucella* pinnipedialis sp. nov. for *Brucella* strains with cetaceans and seals as their preferred hosts." Int J Syst Evol Microbiol **57**(Pt 11): 2688-2693.

Foulongne, V. (2000). "Identification of *Brucella suis* genes affecting intracellular suvival in an in vitro human macrophag infection model by signature-tagged transposon mutagenesis." Infection and immunity **68**(3): 1297-1303.

Fretin, D., M. Mori, G. Czaplicki, C. Quinet, B. Maquet, J. Godfroid and C. Saegerman (2013). "Unexpected *Brucella suis* biovar 2 Infection in a dairy cow, Belgium." Emerg Infect Dis **19**(12): 2053-2054.

Frevert, C., J. Felgenhauer, M. Wygrecka, M. Nastase and L. Schaefer (2018). "Danger-Associated Molecular Patterns Derived From the Extracellular Matrix Provide Temporal Control of Innate Immunity." J Histochem Cytochem. **66**(4): 213-227.

Ganchua, S. K. C., A. M. Cadena, P. Maiello, H. P. Gideon, A. J. Myers, B. F. Junecko, E. C. Klein, P. L. Lin, J. T. Mattila and J. L. Flynn (2018). "Lymph nodes are sites of prolonged bacterial persistence during *Mycobacterium tuberculosis* infection in macaques." PLoS Pathog **14**(11): e1007337.

Gaudino, S. J., and Kumar, P. (2019). "Cross-talk between antigen presenting cells and T cells impacts intestinal homeostasis, bacterial infections, and tumorigenesis." Front. Immunol. **10**(360).

Gershon, R. K. and K. Kondo (1970). "Cell interactions in the induction of tolerance: the role of thymic lymphocytes." Immunology **18**(5): 723-737.

Gilchrist, M., V. Thorsson, B. Li, A. G. Rust, M. Korb, J. C. Roach, K. Kennedy, T. Hai, H. Bolouri and A. Aderem (2006). "Systems biology approaches identify ATF3 as a negative regulator of Toll-like receptor 4." Nature **441**(7090): 173-178.

Godefroid, J. (2002). "Brucellosis in the european union and norway at the turn of the twenty-first century." Veterinary Microbiology **90**(1-4): 135-145.

Goossens, H. (1983). "*Brucella* melitensis: person-to-person transmission?" Lancet **1**(8327): 773.

Gotuzzo, E., C. Carrillo, J. Guerra and L. Llosa (1986). "An evaluation of diagnostic methods for brucellosis--the value of bone marrow culture." J Infect Dis **153**(1): 122-125.

Graham, J. E. and J. E. Clark-Curtiss (1999). "Identification of *Mycobacterium* tuberculosis RNAs synthesized in response to phagocytosis by human macrophages by selective capture of transcribed sequences (SCOTS)." Proc Natl Acad Sci U S A **96**(20): 11554-11559.

Graves, R. (1943). "The story of John M. Buck's and Matilda's contribution to the cattle industry." J Am Vet Med Assoc **102**: 193-195.

Gray, D. F. and P. A. Jennings (1955). "Allergy in experimental mouse tuberculosis." Am Rev Tuberc **72**(2): 171-195.

Greenberg, S., J. El Khoury, F. Di Virgilio, E. Kaplan and S. Silverstein (1991). "Ca2+-independent F-actin Assembly and Disassembly during Fc Recptor-mediated phagocytosis in mouse macrophages." The Journal of Cell Biology **113**(4): 757-767.

Grilló, M.-J., J. M. Blasco, J. P. Gorvel, I. Moriyón and E. Moreno (2012). "What have we learned from brucellosis in the mouse model?" Veterinary research **43**: 29.

Grillo, M. J., M. Barberan and J. M. Blasco (1997). "Transmission of *Brucella* melitensis from sheep to lambs." Vet Rec **140**(23): 602-605.

Grillo, M. J., J. M. Blasco, J. P. Gorvel, I. Moriyon and E. Moreno (2012). "What have we learned from brucellosis in the mouse model?" Vet Res **43**: 29.

Guzman-Verri, C., R. Gonzalez-Barrientos, G. Hernandez-Mora, J. A. Morales, E. Baquero-Calvo, E. Chaves-Olarte and E. Moreno (2012). "*Brucella ceti* and brucellosis in cetaceans." Front Cell Infect Microbiol **2**: 3.

Halling, S. M., B. D. Peterson-Burch, B. J. Bricker, R. L. Zuerner, Z. Qing, L. L. Li, V. Kapur, D. P. Alt and S. C. Olsen (2005). "Completion of the genome sequence of *Brucella abortus* and comparison to the highly similar genomes of *Brucella melitensis* and *Brucella suis*." J Bacteriol **187**(8): 2715-2726.

Hanot Mambres, D., A. Machelart, G. Potemberg, C. De Trez, B. Ryffel, J. J. Letesson and E. Muraille (2016). "Identification of Immune Effectors Essential to the Control of Primary and Secondary Intranasal Infection with *Brucella melitensis* in Mice." J Immunol **196**(9): 3780-3793.

Hendricks, S. L., I. H. Borts, R. H. Heeren, W. J. Hausler and J. R. Held (1962). "Brucellosis outbreak in an Iowa packing house." Am J Public Health Nations Health **52**: 1166-1178.

Henkart, P. (1994). "Lymphocyte-Mediated Cytotocicity: Two Pathways and Multiple Effector Molecules." Immunity **1**: 343-346.

Henning, M. W. (1956). "Animal diseases in South Africa."

Henry, T., A. Brotcke, D. S. Weiss, L. J. Thompson and D. M. Monack (2007). "Type I interferon signaling is required for activation of the inflammasome during Francisella infection." Journal of Experimental Medicine **204**(5): 987-994.

Herzberg, M. and S. Elberg (1953). "Immunization against *Brucella* infection." J Bacteriol **66**(5): 585-599.

Herzberg, M. and S. Elberg (1953). "Immunization against *Brucella* Infection I. Isolation and characterization of a streptomycin-dependent mutant." J. Bacteriol. **66**(5): 585-599.

Hielpos, M. S., A. G. Fernandez, J. Falivene, I. M. Alonso Paiva, F. Munoz Gonzalez, M. C. Ferrero, P. C. Campos, A. T. Vieira, S. C. Oliveira and P. C. Baldi (2018). "IL-1R and Inflammasomes Mediate Early Pulmonary Protective Mechanisms in Respiratory *Brucella Abortus* Infection." Front Cell Infect Microbiol **8**: 391.

Hill, A. V. (2012). "Evolution, revolution and heresy in the genetics of infectious disease susceptibility." Philos Trans R Soc Lond B Biol Sci **367**(1590): 840-849.

Hilleringmann, M., W. Pansegrau, M. Doyle, S. Kaufman, M. L. MacKichan, C. Gianfaldoni, P. Ruggiero and A. Covacci (2006). "Inhibitors of Helicobacter pylori ATPase Cagalpha block CagA transport and cag virulence." Microbiology (Reading) **152**(Pt 10): 2919-2930.

Honda, K., A. Takaoka and T. Taniguchi (2006). "Type I interferon [corrected] gene induction by the interferon regulatory factor family of transcription factors." Immunity **25**(3): 349-360.

Höner, Z. B., M. Kerstin, S. Andras, L. Dana and D. G. Russell (1999). "Characterization of Activity and Expression of Isocitrate Lyase in *Mycobacterium avium* and *Mycobacterium tuberculosis*." Journal of Bacteriology **181**(23): 7161-7167.

Hong, P. C., R. M. Tsolis and T. A. Ficht (2000). "Identification of genes required for chronic persistence of *Brucella abortus* in mice." Infect Immun **68**(7): 4102-4107.

Hooftman, A. and L. A. J. O'Neill (2019). "The Immunomodulatory Potential of the Metabolite Itaconate." Trends Immunol **40**(8): 687-698.

Horton, P., K.-J. Park, T. Obayashi and K. Nakai (2006). "Protein subcellular localization prediction with wolf psort." London: Imperial College Press: 39-48.

Hu, D., K. Ikizawa, L. Lu, M. E. Sanchirico, M. L. Shinohara and H. Cantor (2004). "Analysis of regulatory CD8 T cells in Qa-1-deficient mice." Nat Immunol **5**(5): 516-523.

Issa, M. N. and Y. Ashhab (2016). "Identification of *Brucella melitensis* Rev.1 vaccine-strain genetic markers: Towards understanding the molecular mechanism behind virulence attenuation." Vaccine **34**(41): 4884-4891.

Itoh, K., N. Wakabayashi, Y. Katoh, T. Ishii, K. Igarashi, J. D. Engel and M. Yamamoto (1999). "Keap1 represses nuclear activation of antioxidant responsive elements by Nrf2 through binding to the amino-terminal Neh2 domain." Genes Dev **13**(1): 76-86.

Jamaati, H., E. Mortaz, Z. Pajouhi, G. Folkerts, M. Movassaghi, M. Moloudizargari, I. M. Adcock and J. Garssen (2017). "Nitric Oxide in the Pathogenesis and Treatment of Tuberculosis." Front Microbiol **8**: 2008.

Jansen, W., A. Demars, C. Nicaise, J. Godfroid, X. De Bolle, A. Reboul and S. Al Dahouk (2020). "Shedding of *Brucella melitens* is happens through milk macrophages in the murine model of infection." Scientific Reports.

Jiménez de Bagüés, M., C. Marin, M. Barberan and J. Blasco (1989). "Responses of ewes to B. melitensis Rev1 vaccine administered by subcutaneous or conjunctival routes at different stages of pregnancy." Ann. Rech. Vét. **20**: 205-213.

Jiménez de Bagüés, María P., S. Ouahrani-Bettache, Juan F. Quintana, O. Mitjana, N. Hanna, S. Bessoles, F. Sanchez, Holger C. Scholz, V. Lafont, S. Köhler and A. Occhialini (2010). "The New Species *Brucella microti* Replicates in Macrophages and Causes Death in Murine Models of Infection." The Journal of Infectious Diseases **202**(1): 3-10.

Kamala, T. (2007). "Hock immunization: a humane alternative to mouse footpad injections." J Immunol Methods **328**(1-2): 204-214.

Karcaaltincaba, D. and S. Yalvac (2010). "Does brucellosis in human pregnancy increase abortion risk? Presentation of two cases and review of literature." J. Obstet. Gynecol. **36**: 418-423.

Kaufmann, S. and A. Dorhoi (2016). "Molecular determinants in phagocye-bacteria interactions." Cell Press.

Kawai, T. and S. Akira (2007). "Signaling to NF-kB by Toll-like receptors." Trends in Molecular Medicine **13**(11): 460-469.

Kawashima, Y., M. Sugimura, Y. Hwang and N. Kudo (1964). "The lymph system in mice." Jap. J. Vet. Res. **12**(4): 69-78.

Ke, Y., Y. Wang, W. Li and Z. Chen (2015). "Type IV secretion system of *Brucella* spp. and its effectors." Front Cell Infect Microbiol **5**: 72.

Kelly, B. and L. A. O'Neill (2015). "Metabolic reprogramming in macrophages and dendritic cells in innate immunity." Cell Res **25**(7): 771-784.

Khan, M. Z. and M. Zahoor (2018). "An Overview of Brucellosis in Cattle and Humans, and its Serological and Molecular Diagnosis in Control Strategies." Trop Med Infect Dis **3**(2).

Kim, S., M. Watarai, H. Suzuki, S. Makino, T. Kodama and T. Shirahata (2004). "Lipid raft microdomains mediate class A scavenger receptor-dependent infection of *Brucella* abortus." Microb Pathog **37**(1): 11-19.

Kinoshita (1931). "Aspergillus itaconicus." Botan. Mag. **45**: 60-61.

Kobayashi, E. H., T. Suzuki, R. Funayama, T. Nagashima, M. Hayashi, H. Sekine, N. Tanaka, T. Moriguchi, H. Motohashi, K. Nakayama and M. Yamamoto (2016). "Nrf2 suppresses macrophage inflammatory response by blocking proinflammatory cytokine transcription." Nat Commun **7**: 11624.

Kobayashi, K. S. and P. J. van den Elsen (2012). "NLRC5: a key regulator of MHC class I-dependent immune responses." Nat Rev Immunol **12**(12): 813-820.

Kolls, J. K., P. McCray and Y. Chan (2010). "Cytokine-mediated regulation of antimicrobial proteins." Nat Rev Immunol **8**(11): 829-835.

Kornberg, H. L. and H. A. Krebs (1957). "Synthesis of cell constituents from C2-units by a modified tricarboxylic acid cycle." Nature **179**(4568): 988-991.

Kovarik, P., V. Castiglia, M. Ivin and F. Ebner (2016). "Type I Interferons in Bacterial Infections: A Balancing Act." Front Immunol **7**: 652.

Kunda, N. K., D. N. Price and P. Muttil (2018). "Respiratory Tract Deposition and Distribution Pattern of Microparticles in Mice Using Different Pulmonary Delivery Techniques." Vaccines (Basel) **6**(3).

Kurtz, J. (2005). "Specific memory within innate immune system." Trends in Immunology **20**(4).

LA., C. and A. CG. (1981). "Persistence of *Brucella* abortus strain 19 infection in adult cattle vaccinated with reduced doses." Rest Vet Sci. **31**(3): 342-344.

Lalsiamthara, J. and J. H. Lee (2017). "Development and trial of vaccines against *Brucella*." J Vet Sci **18**(S1): 281-290.

Lampropoulou, V., A. Sergushichev, M. Bambouskova, S. Nair, E. E. Vincent, E. Loginicheva, L. Cervantes-Barragan, X. Ma, S. C. Huang, T. Griss, C. J. Weinheimer, S. Khader, G. J. Randolph, E. J. Pearce, R. G. Jones, A. Diwan, M. S. Diamond and M. N. Artyomov (2016). "Itaconate Links Inhibition of Succinate Dehydrogenase with Macrophage Metabolic Remodeling and Regulation of Inflammation." Cell Metab **24**(1): 158-166.

Larsen, H. and K. E. Eimhjellen (1955). "The mechanism of itaconic acid formation by Aspergillus terreus. 1. The effect of acidity." Biochem J **60**(1): 135-139.

Lawand, M., J. Dechanet-Merville and M. C. Dieu-Nosjean (2017). "Key Features of Gamma-Delta T-Cell Subsets in Human Diseases and Their Immunotherapeutic Implications." Front Immunol **8**: 761.

Lebre, M. C., A. M. van der Aar, L. van Baarsen, T. M. van Capel, J. H. Schuitemaker, M. L. Kapsenberg and E. C. de Jong (2007). "Human keratinocytes express functional Toll-like receptor 3, 4, 5, and 9." J Invest Dermatol **127**(2): 331-341.

Lee, A. J. and A. A. Ashkar (2018). "The Dual Nature of Type I and Type II Interferons." Front Immunol **9**: 2061.

Lee, C. G., N. A. Jenkins, D. J. Gilbert, N. G. Copeland and W. E. O'Brien (1995). "Cloning and analysis of gene regulation of a novel LPS-inducible cDNA." Immunogenetics **41**(5): 263-270.

Liu, J., D. Chen, G. D. Nie and Z. Dai (2015). "CD8(+)CD122(+) T-Cells: A Newly Emerging Regulator with Central Memory Cell Phenotypes." Front Immunol **6**: 494.

Lobet, E., K. Willemart, N. Ninane, C. Demazy, J. Sedzicki, C. Lelubre, X. De Bolle, P. Renard, M. Raes, C. Dehio, J. J. Letesson and T. Arnould (2018). "Mitochondrial fragmentation affects neither the sensitivity to TNFalpha-induced apoptosis of *Brucella*-infected cells nor the intracellular replication of the bacteria." Sci Rep **8**(1): 5173.

Lorenz, M. and G. Fink (2001). "The glyoxylate cycle is required forfungal virulence." Nature **412**(6842): 83-86.

Lucci, F., W. Tan, S. Krishnan, J. Hoeng, P. Vanscheeuwijck, R. Jaeger and A. Kuczaj (2020). "Experimental and computational investigation of a nose-only exposure chamber." Aerosolscience and technology **3**: 227-290.

Luo, X., X. Zhang, X. Wu, X. L. Yang, C. Han, Z. ang, Q. Du, X. Zhao, S. Liu, D. Tong and Y. Huang (2018). "*Brucella* downregulates Tumor Necrosis factor-a to promote Intracellular Survival via Omp25 regulation of different MicroRNAs in porcine and murine macrophages." Front Immunol **17**(8).

Machelart, A., A. Khadrawi, A. Demars, K. Willemart, C. De Trez, J. J. Letesson and E. Muraille (2017). "Chronic *Brucella* Infection Induces Selective and Persistent Interferon Gamma-Dependent Alterations of Marginal Zone Macrophages in the Spleen." Infect Immun **85**(11).

Maclean, W. C. (1875). "On "Malta fever": with a suggestion." The British Medcial Journal **2**: 224-225.

MacLennan, I. C., A. Gulbranson-Judge, K. M. Toellner, M. Casamayor-Palleja, E. Chan, D. M. Sze, S. A. Luther and H. A. Orbea (1997). "The changing preference of T and B cells for partners as T-dependent antibody responses develop." Immunol Rev **156**: 53-66.

MacNamara, K. C., K. Oduro, O. Martin, D. D. Jones, M. McLaughlin, K. Choi, D. L. Borjesson and G. M. Winslow (2011). "Infection-induced myelopoiesis during intracellular bacterial infection is critically dependent upon IFN-gamma signaling." J Immunol **186**(2): 1032-1043.

Mailles, A., B. Garin-Bastuji, J. Lavigne, M. Jay, A. Sotto, M. Maurin, I. Pelloux, D. O'Callaghan, V. Mick, V. Vaillant and H. De Valk (2016). "Human brucellosis in France in the 21st century: Results from national surveillance 2004–2013La brucellose humaine en France au 21e siècle : résultats de la surveillance nationale de 2004 à 2013." Med Mal Infect. **46**(8): 411-418.

Manthei, C., D. DE. and E. Goode (1950). "*Brucella* infection in bulls and the spread of brucellosis in cattle by artificial insimination." Proc.ss. Am. Med. Assoc. **87**: 177-184.

Manthei, C. A. (1960). "Summary of controlled research with Strain 19." Proceedings. United States Live Stock Sanitary Association, 1959 91-97.

Marston, J. A. (1861). "Report on fever (Malta)." Army Medical Department Reports **3**: 486-521.

Martin, F. F. and M. Kasahara (2010). "Origin and evolution of the adaptive immune system: genetic events and selective pressures." Nat Rev Genet **11**(1): 47-59.

Martin, W. R., F. Frigan and E. Bergman (1961). "Noninductive metabolism of itaconic acid by Pseudominas and Salminella species." J. Bacteriol. **82**: 905-908.

Martinez de Tejada, G., J. Pizarro-Cerda, E. Moreno and I. Moriyon (1995). "The outer membranes of *Brucella* spp. are resistant to bactericidal cationic peptides." Infect Immun **63**(8): 3054-3061.

Martinon, F., K. Burns and J. Tschopp (2002). "The inflammasome: a molecular platform triggering activation of inflammatory caspases and processing of proIL-beta." Mol Cell **10**(2): 417-426.

Matejuk, A. (2018). "Skin Immunity." Arch Immunol Ther Exp (Warsz) **66**(1): 45-54.

Matsumoto, A., H. Bessho, K. Uehira and T. Suda (1991). "Morphological Studies of the Association of Mitochondria with Chlamydial Inclusions and the Fusion of Chlamydial Inclusions." Journal of Electron Microscopy **40**: 356-363.

Mayer-Barber, Katrin D., Bruno B. Andrade, Daniel L. Barber, S. Hieny, Carl G. Feng, P. Caspar, S. Oland, S. Gordon and A. Sher (2011). "Innate and Adaptive Interferons Suppress IL-1α and IL-1β Production by Distinct Pulmonary Myeloid Subsets during *Mycobacterium tuberculosis* Infection." Immunity **35**(6): 1023-1034.

McCullough, B. (1951). "Growth and manometric studies on carbohydrate utilization of *Brucella* " Journal of Infectious Diseases **89**(3): 266-271.

McFadden, B. A. and S. Purohit (1977). "Itaconate, an isocitrate lyase-directed inihibior in Pseudomonas indigofera." Journal of Bacteriology **131**(1): 136-144.

McKinney, J. D., K. Honer zu Bentrup, E. J. Munoz-Elias, A. Miczak, B. Chen, W. T. Chan, D. Swenson, J. C. Sacchettini, W. R. Jacobs, Jr. and D. G. Russell (2000). "Persistence of *Mycobacterium tuberculosis* in macrophages and mice requires the glyoxylate shunt enzyme isocitrate lyase." Nature **406**(6797): 735-738.

Meador, V. P. and B. L. Deyoe (1989). "Intracellular localization of *Brucella* abortus in bovine placenta." Vet Pathol **26**(6): 513-515.

Medzhitov, R. (2007). "Recognition of microorganisms and activation of the immune response." Nature **449**(7164): 819-826.

Medzhitov, R. (2010). "Inflammation 2010: new adventures of an old flame." Cell **140**(6): 771-776.

Meiser, J., L. Kraemer, C. Jaeger, H. Mdry, A. Link, P. M. Lepper, K. Hiller and J. Schneider, G. (2018). "Itaconic acid indicates cellular but not systemic immune system activation." Oncotarget **9**: 32098-32107.

Memish, Z., M. W. Mah, S. Al Mahmoud, M. Al Shaalan and M. Y. Khan (2000). "*Brucella bacteraemia*: clinical and laboratory observations in 160 patients." J Infect **40**(1): 59-63.

Mense, M. G., L. L. Van De Verg, A. K. Bhattacharjee, J. L. Garrett, J. A. Hart, L. E. Lindler, T. L. Hadfield and D. L. Hoover (2001). "Bacteriologic and histologic features in mice after intranasal inoculation of *Brucella melitensis*." Am J Vet Res **62**(3): 398-405.

Meyer, K. F. and E. B. Shaw (1920). "A comparison of the morphological, cultural and bioschemical characteristics of B. abortus and B. melitensis: studies on the genus *Brucella*." Journal of Infectious Disease **27**(3): 173-184.

Michaux, S., J. Pailisson, M. Carles-Nurit, G. Bourg, A. Allardet-Servent and M. Ramuz (1993). "Presence of Two Independent Chromosomes in the *Brucella* melitensis 16M Genome." Journal of Bacteriology **175**(3): 701-705.

Michelucci, A., T. Cordes, J. Ghelfi, N. Reiling, O. Goldmann, T. Binz, A. Wegner, A. Tallam, A. Rausell, A. Pailot, M. Buttini, C. L. Linster, E. Medina, R. Balling and K. Hiller (2013). "Immune-responsive gene 1 protein links metabolism to immunity by catalyzing itaconic acid production." Proc Natl Acad Sci U S A **110**(19): 7820-7825.

Miller, L. S. (2008). "Toll-like receptors in skin." Adv Dermatol **24**: 71-87.

Miller, M. A., J. M. Stabenow, J. Parvathareddy, A. J. Wodowski, T. P. Fabrizio, X. R. Bina, L. Zalduondo and J. E. Bina (2012). "Visualization of murine intranasal dosing efficiency using luminescent Francisella tularensis: effect of instillation volume and form of anesthesia." PLoS One **7**(2): e31359.

Mills, E. L., D. G. Ryan, H. A. Prag, D. Dikovskaya, D. Menon, Z. Zaslona, M. P. Jedrychowski, A. S. H. Costa, M. Higgins, E. Hams, J. Szpyt, M. C. Runtsch, M. S. King, J. F. McGouran, R. Fischer, B. M. Kessler, A. F. McGettrick, M. M. Hughes, R. G. Carroll, L. M. Booty, E. V. Knatko, P. J. Meakin, M. L. J. Ashford, L. K. Modis, G. Brunori, D. C. Sevin, P. G. Fallon, S. T. Caldwell, E. R. S. Kunji, E. T.

Chouchani, C. Frezza, A. T. Dinkova-Kostova, R. C. Hartley, M. P. Murphy and L. A. O'Neill (2018). "Itaconate is an anti-inflammatory metabolite that activates Nrf2 via alkylation of KEAP1." Nature **556**(7699): 113-117.

Mogensen, T. H. (2009). "Pathogen recognition and inflammatory signaling in innate immune defenses." Clin Microbiol Rev **22**(2): 240-273, Table of Contents.

Molloy, M. J., W. Zhang and E. J. Usherwood (2011). "Suppressive CD8+ T cells arise in the absence of CD4 help and compromise control of persistent virus." J Immunol **186**(11): 6218-6226.

Mond, J. J., A. Lees and C. M. Snapper (1995). "T cell-independent antigens type 2." Annu Rev Immunol **13**: 655-692.

Moreno, E. (2014). "Retrospective and prospective perspectives on zoonotic brucellosis." Front Microbiol **5**: 213.

Moreno, E. and I. Moriyon (2002). "*Brucella melitensis*: a nasty bug with hidden credentials for virulence." Proc Natl Acad Sci U S A **99**(1): 1-3.

Morgan, W., MacKinnon, DJ (1979). "Fertility and infertility in domestic animals." ELBS **Chapter 9**: 171-198.

Muñoz González, F., G. Sycz, I. M. Alonso Paiva, D. Linke, A. Zorreguieta, P. C. Baldi and M. C. Ferrero (2019). "The BtaF Adhesin Is Necessary for Full Virulence During Respiratory Infection by *Brucella suis* and Is a Novel Immunogen for Nasal Vaccination Against *Brucella* Infection." Frontiers in Immunology **10**.

Mutolo, M. (2011). "Osteological and molecular identification of brucellelosisin ancient Butrint, Albania." American Journal of Physicak Anthopology **147**: 254-263.

Nair, S., J. P. Huynh, V. Lampropoulou, E. Loginicheva, E. Esaulova, A. P. Gounder, A. C. M. Boon, E. A. Schwarzkopf, T. R. Bradstreet, B. T. Edelson, M. N. Artyomov, C. L. Stallings and M. S. Diamond (2018). "Irg1 expression in myeloid cells prevents immunopathology during M. tuberculosis infection." J Exp Med **215**(4): 1035-1045.

Nakato, G., K. Hase, M. Suzuki, M. Kimura, M. Ato, M. Hanazato, M. Tobiume, M. Horiuchi, R. Atarashi, N. Nishida, M. Watarai, K. Imaoka and H. Ohno (2012). "Cutting Edge: *Brucella abortus* exploits a cellular prion protein on intestinal M cells as an invasive receptor." J. Immunol. **189**: 1540-1544.

Naparstek, E., C. S. Block and S. Slavin (1982). "Transmission of brucellosis by bone marrow transplantation." Lancet **1**(8271): 574-575.

Napier, R. J., W. Rafi, M. Cheruvu, K. R. Powell, M. A. Zaunbrecher, W. Bornmann, P. Salgame, T. M. Shinnick and D. Kalman (2011). "Imatinib-sensitive tyrosine kinases regulate mycobacterial pathogenesis and represent therapeutic targets against tuberculosis." Cell Host Microbe **10**(5): 475-485.

Naroeni, A. and F. Porte (2002). "Role of Cholesterol and the Ganglioside GM1in Entry andShort-Term Survival of *Brucella suis* in Murine Macrophages." Infection and immunity **70**(3): 1640-1644.

Naujoks, J., C. Tabeling, B. D. Dill, C. Hoffmann, A. S. Brown, M. Kunze, S. Kempa, A. Peter, H. J. Mollenkopf, A. Dorhoi, O. Kershaw, A. D. Gruber, L. E. Sander, M. Witzenrath, S. Herold, A. Nerlich, A. C. Hocke, I. van Driel, N. Suttorp, S. Bedoui, H. Hilbi, M. Trost and B. Opitz (2016). "IFNs Modify the Proteome of *Legionella*-Containing Vacuoles and Restrict Infection Via IRG1-Derived Itaconic Acid." PLoS Pathog **12**(2): e1005408.

Neupane, A. S., M. Willson, A. K. Chojnacki, E. S. C. F. Vargas, C. Morehouse, A. Carestia, A. E. Keller, M. Peiseler, A. DiGiandomenico, M. M. Kelly, M. Amrein, C. Jenne, A. Thanabalasuriar and P. Kubes (2020). "Patrolling Alveolar Macrophages Conceal Bacteria from the Immune System to Maintain Homeostasis." Cell.

Ni, K. and H. C. O'Neill (1997). "The role of dendritic cells in T cell activation." Immunol Cell Biol **75**(3): 223-230.

Nicoletti, P. (2013). "Brucellosis in Cattle (Contagious abortion, Bang's disease."

Nicolletti, P. (1981). "Prevalence and persistence of *Brucella* abortus strain 19infections and prevalence of other biotypes in vaccinated adult dairy cat." J Am Vet Med Assoc **178**: 1443-1145.

Nielsen, M. M., Lovato, P., MacLeod, A. S., Witherden, D. A., Skov, L., Dyring-Andersen, B., Dabelsteen, S., Woetmann, A., Odum, N., Havran, W. L., Geisler, C., Bonefeld, C. M. (2014). "IL-1beta-dependent activation of dendritic epidermal T cells in contact hypersensitivity." J Immunol **192**(7): 2975-2983.

Nijskens, C., R. Copin, X. De Bolle and J. J. Letesson (2008). "Intracellular rescuing of a B. melitensis 16M virB mutant by co-infection with a wild type strain." Microb Pathog **45**(2): 134-141.

O'Callaghan, D., C. Cazevieille, A. Allardet-Servent, M. L. Boschiroli, G. Bourg, V. Foulongne, P. Frutos, Y. Kulakov and M. Ramu (1999). "A homologue of the Agrobacterium tumefaciens VirB and Bordetella pertussis Ptl type IV secretion systems is essential for intracellular survival of *Brucella suis*." Molecular Microbiology **33**(6): 1210-1220.

O'Callaghan, D., C. Cazevieille, A. Allardet-Servent, M. L. Boschiroli, G. Bourg, V. Foulongne, P. Frutos, Y. Kulakov and M. Ramuz (1999). "A homologue of the Agrobacterium tumefaciens VirB and Bordetella pertussis Ptl type IV secretion systems is essential for intracellular survival of *Brucella suis*." Mol Microbiol **33**(6): 1210-1220.

Okabe, M., D. Lies, S. Kanamasa and E. Park (2009). "Biotechnological production of itaconic acid and its biosynthesis in Aspergillus terreus." Appl. Microbiol. Biotechnol **2009**(84): 597-606.

Ollé-Goig, J. E. and J. Canela-Soler (1987). "An outbreak of *Brucella* melitensis infection by airborne transmission among laboratory workers." Am. J. Public Health **77**: 335-338.

Olsen, S. (2013). "Recent developments in livestock and wildlife brucellosis vaccination." Rev Sci Tech **32**(1): 207-217.

Olsen, S. C., J. Boggiatto and J. Wilson-Welder (2017). "Immunogenicity and Efficacy of a Rough *Brucella suis* Vaccine Delivered Orally or Parenterally to Feral Swin."

Ouyang, W., J. K. Kolls and Y. Zheng (2008). "The biological functions of T helper 17 cell effector cytokines in inflammation." Immunity **28**(4): 454-467.

Pagan, A. J. and L. Ramakrishnan (2018). "The Formation and Function of Granulomas." Annu Rev Immunol **36**: 639-665.

Paixao, T. A., C. M. Roux, A. B. den Hartigh, S. Sankaran-Walters, S. Dandekar, R. L. Santos and R. M. Tsolis (2009). "Establishment of systemic *Brucella melitensis* infection through the digestive tract requires urease, the type IV secretion system, and lipopolysaccharide O antigen." Infect Immun **77**(10): 4197-4208.

Pappas, G. (2006). "The new global map of human brucellosis." Lancet Infect Dis **6**(2): 91-99.

Pardon, P. (1977). "Résistance de souris immunisées avec des *Brucella* tuées contre une épreuve intraveineuse, intrapéritonéale ou sous-cutanée e *Brucella abortus*." Bull. Acad. Vét. de France **50**: 335338.

Parker, D., P. J. Planet, G. Soong, A. Narechania and A. Prince (2014). "Induction of type I interferon signaling determines the relative pathogenicity of Staphylococcus aureus strains." PLoS Pathog **10**(2): e1003951.

Pasquali, P., A. Rosanna, C. Pistoia, P. Petrucci and F. Ciuchini (2003). "*Brucella abortus* RB51 induces protection in mice orally infected with the virulent strain B. abortus 2308." Infect Immun **71**(5): 2326-2330.

Paulsen, I. T., R. Seshadri, K. E. Nelson, J. A. Eisen, J. F. Heidelberg, T. D. Read, R. J. Dodson, L. Umayam, L. M. Brinkac, M. J. Beanan, S. C. Daugherty, R. T. Deboy, A. S. Durkin, J. F. Kolonay, R. Madupu, W. C. Nelson, B. Ayodeji, M. Kraul, J. Shetty, J. Malek, S. E. Van Aken, S. Riedmuller, H.

Tettelin, S. R. Gill, O. White, S. L. Salzberg, D. L. Hoover, L. E. Lindler, S. M. Halling, S. M. Boyle and C. M. Fraser (2002). "The *Brucella suis* genome reveals fundamental similarities between animal and plant pathogens and symbionts." Proc Natl Acad Sci U S A **99**(20): 13148-13153.

Payne, J. M. (1959). "The pathogenesis of experimental brucellosis in the pregnant cow." J Pathol Bacteriol **78**: 447-463.

Perez-Lopez, A., J. Behnsen, S. P. Nuccio and M. Raffatellu (2016). "Mucosal immunity to pathogenic intestinal bacteria." Nat Rev Immunol **16**(3): 135-148.

Perry, A. K., G. Chen, D. Zheng, H. Tang and G. Cheng (2005). "The host type I interferon response to viral and bacterial infections." Cell Res **15**(6): 407-422.

Pfeifer, V. F., C. Vojnovich and E. N. Heger (1952). "Itaconic Acid by Fermentation with Aspergillus Terreus." Industrial & Engineering Chemistry **44**(12): 2975-2980.

Philippon, A., G. Renouy, M. Plommet and N. Bosseray (1971). "Brucellose bovine expérimentale. V. – Excrétion de "*Brucella abortus*" par le colostrum et le lait."

Pizarro-Cerda, J., S. Meresse, R. G. Parton, G. Dergoot, A. Sola-Landa, I. Lopez-Goni, E. Moreno and A.-P. Gorvel (1998). "*Brucella abortus* Transits through the Autophagic Pathway and Replicates in the Endoplasmic Reticulum of Nonprofessional Phagocytes." Infection and immunity **66**(12): 5711-5724.

Plommet, M., R. Fensterbank, G. Renoux, J. Gestin, A. Philippon, G. Renouy, M. Plommet and N. Bosseray (1973). "Brucellose bovine expérimentale. XII. – Persistance à l'age adulte de l'infection congénitale de la génisse." Annales de Recherches Vétérinaires **4**(3): 419-435.

Plommet, M. and A. M. Plommet (1983). "Immune serum-mediated effects on brucellosis evolution in mice." Infect Immun **41**(1): 97-105.

Porte, F., J. Liautard and S. Kohler (1999). "Early Acidification of Phagosomes Containing *Brucella suis* Is Essential for Intracellular Survival in Murine Macrophages." Infection and immunity **67**(8): 4041-4047.

Radhakrishnan, G. K. and G. A. Splitter (2010). "Biochemical and functional analysis of TIR domain containing protein from *Brucella melitensis*." Biochem Biophys Res Commun **397**(1): 59-63.

Raetz, C. R., C. M. Reynolds, M. S. Trent and R. E. Bishop (2007). "Lipid A modification systems in gram-negative bacteria." Annu Rev Biochem **76**: 295-329.

Raju, I. T., R. Solanki, A. N. Patnaik, R. C. Barik, N. R. Kumari and A. S. Gulati (2013). "*Brucella* endocarditis - a series of five case reports." Indian Heart J **65**(1): 72-77.

Ratajczak, W. (2018). "Immunological memory cells." Centr Eur Immunol. **43**(2): 194-203.

Reddick, L. E. and M. A. Neal (2014). "Bacteria Fighting Back - How pathogens target and subvert the host innate immune system." Mol Cell. **54**(2): 321-328.

Renoux, G., G. G. Alton and A. Amarasinghe (1957). "Etudes sur la brucellose ovine et caprine. XI. Comparaison chez la chèvre suédoise de la valeur immunisante d'un vaccin tué en excipient irrésorbable et de deux vaccins vivants." Arch. Inst. Pasteur, Tunis. **34**: 3-17.

Rittenhouse, J. W. and B. A. McFadden (1974). "Inhibition of isocitrate lyase from Pseudomonas indigofera by itaconate." Archives of Biochemistry and Biophysics **163**(1): 79-86.

Rosales, C. and E. Uribe-Querol (2017). "Phagocytosis: A Fundamental Process in Immunity." Biomed Res Int **2017**: 9042851.

Rossetti, C. A., A. M. Arenas-Gamboa and E. Maurizio (2017). "Caprine brucellosis: A historically neglected disease with significant impact on public health." PLoS Negl Trop Dis **11**(8): e0005692.

Rubartelli, A. and M. Lotze (2007). "Inside, outside, upside down: damage-associated molecular-pattern molecules (DAMPs) and redox." Trends in Immunology **28**(10): 429-436.

Ruben, B. (1991). "Person-to-person transmission of *Brucella* melitensis." Lancet **337**(8732): 14-15.

Ruiz-Ranwez, V., D. M. Posadas, C. Van der Henst, S. M. Estein, G. M. Arocena, P. L. Abdian, F. A. Martín, R. Sieira, X. De Bolle, A. Zorreguieta and S. M. Payne (2013). "BtaE, an Adhesin That Belongs to the Trimeric Autotransporter Family, Is Required for Full Virulence and Defines a Specific Adhesive Pole of *Brucella suis*." Infection and Immunity **81**(3): 996-1007.

Sakaguchi, S., M. Toda, M. Asano, M. Itoh, S. S. Morse and N. Sakaguchi (1996). "T cell-mediated maintenance of natural self-tolerance: its breakdown as a possible cause of various autoimmune diseases." J Autoimmun **9**(2): 211-220.

Salcedo, S. P., N. Chevrier, T. L. Lacerda, A. Ben Amara, S. Gerart, V. A. Gorvel, C. de Chastellier, J. M. Blasco, J. L. Mege and J. P. Gorvel (2013). "Pathogenic brucellae replicate in human trophoblasts." J Infect Dis **207**(7): 1075-1083.

Sangari, F. J., A. Seoane, M. C. Rodriguez, J. Aguero and J. M. Garcia Lobo (2007). "Characterization of the urease operon of *Brucella abortus* and assessment of its role in virulence of the bacterium." Infect Immun **75**(2): 774-780.

Sasikaran, J., M. Ziemski, P. K. Zadora, A. Fleig and I. A. Berg (2014). "Bacterial itaconate degradation promotes pathogenicity." Nat Chem Biol **10**(5): 371-377.

Schatz, D. G., M. A. Oettinger and M. S. Schlissel (1992). "V(D)J recombination: molecular biology and regulation." Annu Rev Immunol **10**: 359-383.

Scholz, H. C., Z. Hubalek, I. Sedlacek, G. Vergnaud, H. Tomaso, S. Al Dahouk, F. Melzer, P. Kampfer, H. Neubauer, A. Cloeckaert, M. Maquart, M. S. Zygmunt, A. M. Whatmore, E. Falsen, P. Bahn, C. Gollner, M. Pfeffer, B. Huber, H. J. Busse and K. Nockler (2008). "*Brucella* microti sp. nov., isolated from the common vole Microtus arvalis." Int J Syst Evol Microbiol **58**(Pt 2): 375-382.

Scholz, H. C., K. Nockler, C. Gollner, P. Bahn, G. Vergnaud, H. Tomaso, S. Al Dahouk, P. Kampfer, A. Cloeckaert, M. Maquart, M. S. Zygmunt, A. M. Whatmore, M. Pfeffer, B. Huber, H. J. Busse and B. K. De (2010). "*Brucella* inopinata sp. nov., isolated from a breast implant infection." Int J Syst Evol Microbiol **60**(Pt 4): 801-808.

Scholz, H. C., S. Revilla-Fernandez, S. A. Dahouk, J. A. Hammerl, M. S. Zygmunt, A. Cloeckaert, M. Koylass, A. M. Whatmore, J. Blom, G. Vergnaud, A. Witte, K. Aistleitner and E. Hofer (2016). "*Brucella vulpis* sp. nov., isolated from mandibular lymph nodes of red foxes (Vulpes vulpes)." Int J Syst Evol Microbiol **66**(5): 2090-2098.

Schreyer, P., E. Caspi, Y. Leiba, Y. Eshchar and D. Sompolinsky (1980). "*Brucella* septicemia in pregnancy." Eur J Obstet Gynecol Reprod Biol **10**(2): 99-107.

Schurig, G. G., R. M. Roop, 2nd, T. Bagchi, S. Boyle, D. Buhrman and N. Sriranganathan (1991). "Biological properties of RB51; a stable rough strain of *Brucella* abortus." Vet Microbiol **28**(2): 171-188.

Schwebach, J., B. Chen, A. Glatman-Freedman, A. Casadevall, J. McKinney, J. Harb, P. McGuire, E. Barkley, B. Bloom and W. Jacobs (2002). "Infection of Mice with Aerosolized *Mycobacterium tuberculosis*: Use ofa Nose-Only Apparatus for Delivery of Low Doses of Inocula and Design of an Ultrasafe Facility." Applied and Envrionemental Microbiology **69**(9): 4646-4649.

Sedzicki, J., T. Tschon, S. H. Low, K. Willemart, K. N. Goldie, J. J. Letesson, H. Stahlberg and C. Dehio (2018). "3D correlative electron microscopy reveals continuity of *Brucella*-containing vacuoles with the endoplasmic reticulum." J Cell Sci **131**(4).

Sengupta, D., A. Koblansky, J. Gaines, T. Brown, A. Phillip West, T. Nishikawa, S. Park, M. Roop and S. Ghosh (2010). "Subversion of innate Immune Responses by *Brucella* through the targeter degradation of the TLR signaling adapter, MAL." the Journal of Immunology **184**: 956-964.

Sfeir, M. M. (2018). "Raw milk intake: beware of emerging brucellosis." J Med Microbiol **67**(5): 681-682.

Shin, J. H., J. Y. Yang, B. Y. Jeon, Y. J. Yoon, S. N. Cho, Y. H. Kang, D. H. Ryu and G. S. Hwang (2011). "(1)H NMR-based metabolomic profiling in mice infected with *Mycobacterium tuberculosis*." J Proteome Res **10**(5): 2238-2247.

Sieira, R. (2000). "A Homologue of an operon required for DNA transfer in agrobacterium is required in *brucella abortus* for virulence and intracellular multiplication." Journal of Bacteriology **182**(17): 4849-4855.

Silva, T. M., J. P. Mol, M. G. Winter, V. Atluri, M. N. Xavier, S. F. Pires, T. A. Paixao, H. M. Andrade, R. L. Santos and R. M. Tsolis (2014). "The predicted ABC transporter AbcEDCBA is required for type IV secretion system expression and lysosomal evasion by *Brucella ovis*." PLoS One **9**(12): e114532.

Sinai, A. P. and K. A. Joiner (2001). "The Toxoplasma gondii protein ROP2 mediates host organelle association with the parasitophorous vacuole membrane." J Cell Biol **154**(1): 95-108.

Smith, E. P., A. Cotto-Rosario, E. Borghesan, K. Held, C. N. Miller and J. Celli (2020). "Epistatic Interplay between Type IV Secretion Effectors Engages the Small GTPase Rab2 in the *Brucella* Intracellular Cycle." mBio **11**(2).

Smith, H., A. E. Williams, J. H. Pearce, J. Keppie, P. W. Harris-Smith, R. B. Fitz-George and K. Witt (1962). "Foetal erythritol: a cause of the localization of *Brucella abortus* in bovine contagious abortion." Nature **193**: 47-49.

Smith, L. D. and T. A. Ficht (1990). "Pathogenesis of *Brucella*." Crit Rev Microbiol **17**(3): 209-230.

Southam, D. S., M. Dolovich, P. M. O'Byrne and M. D. Inman (2002). "Distribution of intranasal instillations in mice: effects of volume, time, body position, and anesthesia." Am J Physiol Lung Cell Mol Physiol **282**(4): L833-839.

Spink, W. W., J. W. Hall, 3rd, J. Finstad and E. Mallet (1962). "Immunization with viable *Brucella* organisms. Results of a safety test in humans." Bull World Health Organ **26**: 409-419.

Starr, T., R. Child, T. D. Wehrly, B. Hansen, S. Hwang, C. Lopez-Otin, H. W. Virgin and J. Celli (2012). "Selective subversion of autophagy complexes facilitates completion of the *Brucella* intracellular cycle." Cell Host Microbe **11**(1): 33-45.

Staszkiewicz, J., C. M. Lewis, J. Colville, M. Zervos and J. Band (1991). "Outbreak of *Brucella* melitensis among microbiology laboratory workers in a community hospital." Journal of clinical microbiology **29**(2): 287-290.

Stoenner, H. G. and D. B. Lackman (1957). "A new species of *Brucella* isolated from the desert wood rat, Neotoma lepida Thomas." Am J Vet Res. **18**(69): 947-957.

Strelko, C. L., W. Lu, F. J. Dufort, T. N. Seyfried, T. C. Chiles, J. D. Rabinowitz and M. F. Roberts (2011). "Itaconic acid is a mammalian metabolite induced during macrophage activation." J Am Chem Soc **133**(41): 16386-16389.

Sturgill-Koszycki, S., P. L. Haddix and D. G. Russell (1997). "The interaction between *Mycobacterium* and the macrophage analyzed by two-dimensional polyacrylamide gel electrophoresis." Electrophoresis **18**(14): 2558-2565.

Sugimoto, M., H. Sakagami, Y. Yokote, H. Onuma, M. Kaneko, M. Mori and M. Tomita (2011). "Non-targeted metabolite profiling in activated macrophage secretion." Metabolomics **8**(4): 624-633.

Takemori, T. (2015). "B cell memory and plasma cell development." Molecular Biology: 227-249.

Tangye, S. G. (2015). "Thucydides and longer-lived plasma cells." Blood **125**(11): 1684-1685.

Tau, G. Z., S. N. Cowan, J. Weisburg, N. S. Braunstein and P. B. Rothman (2001). "Regulation of IFN-gamma signaling is essential for the cytotoxic activity of CD8(+) T cells." J Immunol **167**(10): 5574-5582.

Terwagne, M., J. Ferooz, H. G. Rolán, Y.-H. Sun, V. Atluri, M. N. Xavier, L. Franchi, G. Núñez, T. Legrand, R. A. Flavell, X. De Bolle, J.-J. Letesson and R. M. Tsolis (2013). "Innate immune recognition of flagellin limits systemic persistence of *Brucella*." Cellular Microbiology **15**(6): 942-960.

Thienpont, D., Vandervelden, F. M., P. and J. Mortelmans (1961). "L'hydroma brucellique: l'aspect clinique caractéristique de la brucellose bovine au Rwanda-Burundi."

Thieu, V. T., Q. Yu, H. C. Chang, N. Yeh, E. T. Nguyen, S. Sehra and M. H. Kaplan (2008). "Signal transducer and activator of transcription 4 is required for the transcription factor T-bet to promote T helper 1 cell-fate determination." Immunity **29**(5): 679-690.

Thomas, E., C. Bracewell and M. Corbel (1981). "Characterisation of *Brucella* abortus strain 19 cultures isolated from vaccinated cattle." Vet Rec **108**: 90-93

Tremblay, Y. D. N., S. Hathroubi and M. Jacques (2014). "Les biofilms bactériens: leur importance en santé animale et en santé publique." Can J Vet Res. **78**: 110-116.

Tsenova, L., A. Moreira, E. Party, V. Freedman and G. Kaplan (1997). "Aerosol infection of mice with mycobacteria using a nose-only exposure device." Journal of the American Biological Safety Association **2**(3): 20-31.

Tsolis, R. M. (2002). "The *Brucella* suis genome reveals fundamental similarities between animal and plant pathogens and symbionts." Proc Natl Acad Sci USA **99**: 12503-12505.

Turgut, M., A. T. Turgut and U. Kosar (2006). "Spinal brucellosis: Turkish experience based on 452 cases published during the last century." Acta Neurochir (Wien) **148**(10): 1033-1044; discussion 1044.

Turner, E. (1841). "Elements of Chemistry: Including the Actual State and Prevalent Doctrines of the Science." London.

Uribe-Querol, E. and C. Rosales (2017). "Control of Phagocytosis by Microbial Pathogens." Front Immunol **8**: 1368.

Usharauli, D. (2010). "Chronic infection and the origin of adaptive immune system." Med Hypotheses **75**(2): 241-243.

Valbon, S. F., S. A. Condotta and M. J. Richer (2016). "Regulation of effector and memory CD8+ T cell function by inflammatory cytokines." Cytokines **82**: 16-23.

Viana, D., M. Comos, P. R. McAdam, M. J. Ward, L. Selva, C. M. Guinane, B. M. Gonzalez-Munoz, A. Tristan, S. J. Foster, J. R. Fitzgerald and J. R. Penades (2016). "A signel natural nucleotide mutation alters bacterial pathogen host-tropism." Nat. Genet. **47**(4): 361-366.

Vitry, M., D. H. Mambres, M. Deghelt, K. Hack, A. Machelart, F. Lhomme, J.-M. Vanderwinden, M. Vermeersch, C. De Trez, D. Pérez-Morga, J. J. Letesson and E. Muraille (2014). "*Brucella melitensis* Invades Murine Erythrocytes during Infection." IAI **82**: 3927-2938.

Vitry, M. A., C. De Trez, S. Goriely, L. Dumoutier, S. Akira, B. Ryffel, Y. Carlier, J. J. Letesson and E. Muraille (2012). "Crucial role of gamma interferon-producing CD4+ Th1 cells but dispensable function of CD8+ T cell, B cell, Th2, and Th17 responses in the control of *Brucella melitensis* infection in mice." Infect Immun **80**(12): 4271-4280.

Vitry, M. A., D. Hanot Mambres, C. De Trez, S. Akira, B. Ryffel, J. J. Letesson and E. Muraille (2014). "Humoral immunity and CD4+ Th1 cells are both necessary for a fully protective immune response upon secondary infection with *Brucella melitensis*." J Immunol **192**(8): 3740-3752.

von Bargen, K., A. Gagnaire, V. Arce-Gorvel, B. de Bovis, F. Baudimont, L. Chasson, M. Bosilkovski, A. Papadopoulos, A. Martirosyan, S. Henri, J. L. Mege, B. Malissen and J. P. Gorvel (2014). "Cervical Lymph Nodes as a Selective Niche for *Brucella* during Oral Infections." PLoS One **10**(4): e0121790.

Vos, Q., A. Lees, Z. Q. Wu, C. M. Snapper and J. J. Mond (2000). "B-cell activation by T-cell-independent type 2 antigens as an integral part of the humoral immune response to pathogenic microorganisms." Immunol Rev **176**: 154-170.

Wallach, J. C., L. E. Samartino, A. Efron and P. C. Baldi (1997). "Human infection by *Brucella* melitensis: an outbreak attributed to contact with infected goats." FEMS Immunol Med Microbiol **19**(4): 315-321.

Walzer, T., C. Arpin, L. Beloil and J. Marvel (2001). "Phénotype et fonctions des lymphocytes T CD8* mémoire." Médecine/sciences **17**: 1105-1111.

Wang, S. F., J. Adler and H. A. Lardy (1961). "The pathway of itaconate metabolism by liver mitochondria." J Biol Chem **236**: 26-30.

Ward, J. E., D. E. Akiyoshi, D. Regier, A. Datta, M. P. Gordon and E. W. Nester (1988). "Characterization of the virB operon from an Agrobacterium tumefaciens Ti plasmid." J Biol Chem **263**(12): 5804-5814.

Watanabe, T., N. Asano, S. Fichtner-Feigl, P. L. Gorelick, Y. Tsuji, Y. Matsumoto, T. Chiba, I. J. Fuss, A. Kitani and W. Strober (2010). "NOD1 contributes to mouse host defense against Helicobacter pylori via induction of type I IFN and activation of the ISGF3 signaling pathway." J Clin Invest **120**(5): 1645-1662.

Watarai, M., S. Makino, Y. Fujii, K. Okamoto and T. Shirahata (2002). "Modulation of *Brucella*-induced macropinocytosis by lipid rafts mediates intracellular replication." Cell Microbiol **4**(6): 341-355.

Wegmann, T. G., H. Lin, L. Guilbert and T. R. Mosmann (1993). "Bidirectional cytokine interactions in the maternal-fetal relationship: is successful pregnancy a TH2 phenomenon?" Immunol Today **14**(7): 353-356.

Wellmann, G. (1951). "Blood sucking insects as mechanical vectors of *Brucella*." Zentralbl Bakteriol Orig. **156**(6): 414-426.

Whatmore, A. M., N. Davison, A. Cloeckaert, S. Al Dahouk, M. S. Zygmunt, S. D. Brew, L. L. Perrett, M. S. Koylass, G. Vergnaud, C. Quance, H. C. Scholz, E. J. Dick, Jr., G. Hubbard and N. E. Schlabritz-Loutsevitch (2014). "*Brucella papionis* sp. nov., isolated from baboons (Papio spp.)." Int J Syst Evol Microbiol **64**(Pt 12): 4120-4128.

WHO (1986). "Joint FAO/WHO expert committee on brucellosis." WHO Tech Rep Ser. **70**: 1-132.

WHO (1997). "Joint FAO/WHO Expert Com-mittee, The development of new improvedbrucellosis vaccine." WHO/EMC/ZDI **98**(14): 41.

WHO (2019). "World Malaria Report 2019; Switzerland: World Health Organization." pp. xii-xiii, 4-10.

WHO (2020). "WHO Coronavirus Disease (COVID-19) Dashboard."

WHO/EMC/ZDI/98.14 (1997). "The Development of New/Improved Brucellosis Vaccines:Report of WHO Meeting."

Wibom, C., I. Surowiec, L. Moren, P. Bergstrom, M. Johansson, H. Antti and A. T. Bergenheim (2010). "Metabolomic patterns in glioblastoma and changes during radiotherapy: a clinical microdialysis study." J Proteome Res **9**(6): 2909-2919.

Williams, J. O., T. E. Roche and B. A. McFadden (1971). "Mechanism of action of isocitrate lyase from Pseudomonas indigofera." Biochemistry **10**(8): 1384-1390.

Wood, E. E. (1955). "Brucellosis as a hazard of blood transfusion." British Medical Journal.

Woolhouse, M. E. and S. Gowtage-Sequeria (2005). "Host range and emerging and reemerging pathogens." Emerg Infect Dis **11**(12): 1842-1847.

Wright, A., C. H. Hawkins, E. E. Anggard and D. R. Harper (2009). "A controlled clinical trial of a therapeutic bacteriophage preparation in chronic otitis due to antibiotic-resistant Pseudomonas aeruginosa; a preliminary report of efficacy." Clin Otolaryngol **34**(4): 349-357.

Wright, A. E. and D. Semple (1897). "On the Employment of Dead Bacteria in the Serum Diagnosis of Typhoid and Malta Fever, and on an Easy Method of Extemporising a Blowpipe Flame for Making Capillary Sero-Sedimentation Tubes." Br Med J **1**(1898): 1214-1215.

Wu, R., F. Chen, N. Wang, D. Tang and R. Kang (2020). "ACOD1 in immunometabolism and disease." Cellular & Molecular Immunology **17**(8): 822-833.

Xavier, M. N., T. A. Paixa˜o, F. P. Poester, A. P. Lage and R. L. Santos (2009). "Pathological, Immunohistochemical and Bacteriological Study of Tissues and Milk of Cowsand Fetuses Experimentally Infected with *Brucella abortus*." J. Comp. Path. **140**: 149-157.

Young, E. (1975). "Brucellosis outbreak attributed to ingestion of unpasteruized goat cheese." Archives of internal medicine **135**(2): 240.

Yousuf Khan, M., M. W. Mah and Z. A. Memish (2001). "Brucellosis in Pregnant Women." Clinical Infectious Diseases **32**: 1172-1177.

Yu, Y., X. Ma, R. Gong, J. Zhu, L. Wei and J. Yao (2018). "Recent advances in CD8(+) regulatory T cell research." Oncol Lett **15**(6): 8187-8194.

Zammit, T. (1905). "A preliminary note on the susceptibility of goats to Malta fever." Proceedings of the Royal Society of London. Series B, Containing Papers of a Biological Character **76**(510): 377-378.

Zhen, Q., Y. Lu, X. Yuan, Y. Qiu, J. Xu, W. Li, Y. Ke, Y. Yu, L. Huang, Y. Wang and Z. Chen (2013). "Asymptomatic brucellosis infection inhumans: implications for diagnosis andprevention." Clin. Microbiol. Infect. **19**: 395-397.

Zhou, G., Q. Shi, X. Huang and X. Xie (2015). "The three bacterial lines of defense against antimicrobial agents." Int. J. Mol. Sci. **16**: 21711-21733.

Zhu, J., H. Yamane and W. E. Paul (2010). "Differentiation of effector CD4 T cell populations (*)." Annu Rev Immunol **28**: 445-489.

Zúñiga-Ripa, A. (2014). "*Brucella abortus* Depends on Pyruvate Phosphate Dikinase and Malic Enzyme but Not on Fbp and GlpX Fructose-1,6-Bisphosphatases for Full Virulence in Laboratory Models." Journal of Bacteriology.

Zuniga-Ripa, A., T. Barbier, R. Conde-Alvarez, E. Martinez-Gomez, L. Palacios-Chaves, Y. Gil-Ramirez, M. J. Grillo, J. J. Letesson, M. Iriarte and I. Moriyon (2014). "*Brucella abortus* depends on pyruvate phosphate dikinase and malic enzyme but not on Fbp and GlpX fructose-1,6-bisphosphatases for full virulence in laboratory models." J Bacteriol **196**(16): 3045-3057.